

**CHEMICAL RECYCLING OF WASTE PLASTICS VIA  
HYDROTHERMAL PROCESSING**

By

Eyup Yildirim

Submitted in accordance with the requirements for the degree of  
Doctor of Philosophy

The University of Leeds  
School of Chemical and Process Engineering  
Energy Research Institute

August 2015

The candidate confirms that the work submitted is his own, except where work which has formed part of jointly-authored publications has been included. The contribution of the candidate and the other authors to this work has been explicitly indicated below. The candidate confirms that appropriate credit has been given within the thesis where reference has been made to the work of others.

This copy has been supplied on the understanding that it is copyright material and that no quotation from the thesis may be published without proper acknowledgement.

### **Journal Papers**

Chapter 4 was based on the following published papers;

1. Onwudili, Jude A, Yildirim, Eyup, & Williams, Paul T. (2013). Catalytic hydrothermal degradation of carbon reinforced plastic wastes for carbon fibre and chemical feedstock recovery. *Waste and Biomass Valorization*, 4(1), 87-93.
2. Yildirim, Eyup, Onwudili, Jude A., & Williams, Paul T. (2014). Recovery of carbon fibres and production of high quality fuel gas from the chemical recycling of carbon fibre reinforced plastic wastes. *The Journal of Supercritical Fluids*, 92(0), 107-114.
3. Yildirim, E., Miskolczi, N., Onwudili, J. A., Németh, K. E., Williams, P. T., & Sója, J. (2015). Evaluating the mechanical properties of reinforced LDPE composites made with carbon fibres recovered via solvothermal processing. *Composites Part B: Engineering*, 78, 393-400.

Chapter 5 was based on the following published paper;

4. Yildirim, E., J.A. Onwudili, and P.T. Williams, Chemical Recycling of Printed Circuit Board Waste by Depolymerization in Sub-and Supercritical Solvents. *Waste and Biomass Valorization*: p. 1-7.

The co-authors, Professor P. T. Williams and Dr Jude Onwudili, supervised and supported the entire research work, proof read the drafts and made suggestions and corrections to the draft papers.

The right of Eyup Yildirim to be identified as Author of this work has been asserted by him in accordance with the Copyright, Designs and Patents Act 1988.

© 2015 The University of Leeds and Eyup Yildirim

## **Acknowledgements**

*In the name of Allah, most Gracious, most Merciful*

Foremost, I would like to gratefully acknowledge the Ministry of National Education, Republic of Turkey for the scholarship for funding this PhD, and also supporting for the two presentations (a poster and an oral) in international conferences in Porto and Rio de Janeiro. I also would like to thank for the support from Royal Society (UK) during my studies in University of Pannonia, Hungary.

I would like to thank to my supervisor Professor Paul T. Williams with my deepest and sincere gratitude for his excellent guidance, support, feedback, help, encouragement, caring, patience and his faith in me throughout this research. I have benefited from his great knowledge, and his aid has met any kind of problems I faced.

I want to especially thank to Dr. Jude A. Onwudili, for his great support during my PhD. I have been able to overcome all difficulties thanks to his feedback, advice on the laboratory work and analytical analyses, and knowledge. Also I would like to thank Dr. Norbert Miskoczi for his kind help and during the studies in University of Pannonia, Hungary. In addition, I would like to thank to my colleagues in my research group; Anas, Chika, Ramzi, Paula, Jonathan, Amal, Juniza and Ibrahim for their friendship and support. Working in this group has been a joyful experience for me.

Lastly, I would like to thank my family; my mom, dad and sister, for their love, support and prayers during the last for years. And most of all, my loving, supportive, patient and encouraging wife Fatma is so appreciated. Thank you.

## **Abstract**

Utilizing a simple, cost effective, feasible and efficient recycling process for waste plastics, which are largely produced from non-renewable sources, is strategically important for a sustainable environment and economy. In Europe, landfilling is still the major waste management method; therefore new routes for recycling are being researched to increase the recycling rates.

In this research, hydrothermal processing was used for recycling of waste carbon fibre reinforced plastics (CFRP) and printed circuit boards (PCB) in a batch reactor were investigated. Also, the applicability of the hydrothermal process was tested on refuse derived fuel (RDF), as it is a good representative of municipal solid waste which is a complex waste mixture consisting of plastics, other biodegradable materials and inorganic materials.

The ability of supercritical water to degrade the resins and plastics in the composite wastes was largely influenced by the presence of different additives and/or co-solvents. Water at supercritical conditions was able to remove 92.6% of the resin from the CFRP waste in the presence of KOH and 10 wt% H<sub>2</sub>O<sub>2</sub>. In the work with PCB, 94% of the resin removal was achieved with alkalis, at zero residence time. The carbon fibre was recovered by preserving 78 % of its tensile strength due to the loss in the mechanical properties as a result of oxidation on the carbon fibre surface. When mixtures of ethylene glycol and water were used as solvent, without any addition of a catalyst, 97.6 % resin removal was achieved at 400°C. The liquid obtained from hydrothermal processing of PCB mainly composed of phenol, and phenolic compounds, which are the precursors of the original thermosetting resin. The liquid effluent from the degradation of CFRP with water and ethylene glycol mixture became too complex for recovery and so was gasified under supercritical water conditions. In the presence of NaOH and ruthenium oxide as catalysts the produced fuel gas consisted of H<sub>2</sub>, CH<sub>4</sub>, CO<sub>2</sub>, CO and C<sub>2-4</sub> hydrocarbon gases. The carbon fibres recovered using ethylene glycol co-solvent preserved its mechanical properties and

used for the manufacture of new composite materials. The mechanical tests showed that the new composites with recovered carbon fibres had enhanced mechanical properties similar to those made from virgin carbon fibres. Finally RDF was subjected to hydrothermal gasification process to produce fuel gas. Up to 93% carbon gasification efficiency was achieved in the presence of 5 wt%  $\text{RuO}_2/\gamma\text{-Al}_2\text{O}_3$  catalyst, producing a fuel gas mostly consisting of  $\text{H}_2$ ,  $\text{CH}_4$ , and  $\text{CO}_2$  with a heating value of  $22.5 \text{ MJ/Nm}^3$ . The gross calorific value of the product gas increased to  $32.4 \text{ MJ/Nm}^3$  in the presence of NaOH, as a result of carbon dioxide fixation as sodium carbonate. Also, high yields of hydrogen were obtained in the presence of both the NaOH and ruthenium catalysts, as both promoted the water-gas shift reaction.

## Table of Contents

<b>Acknowledgements</b> .....	<b>iii</b>
<b>Abstract</b> .....	<b>iv</b>
<b>Table of Contents</b> .....	<b>vi</b>
<b>List of Tables</b> .....	<b>xi</b>
<b>List of Figures</b> .....	<b>xiv</b>
<b>Chapter 1 INTRODUCTION</b> .....	<b>1</b>
1.1 General Overview of Plastic Production .....	1
1.2 Recycling Routes .....	5
1.3 Waste Samples .....	7
1.3.1 Carbon Fibre Reinforced Plastics (CFRP).....	7
1.3.2 Printed Circuit Boards (PCB).....	12
1.3.3 Refuse Derived Fuel (RDF) .....	16
1.4 Aim and Objectives of this Research.....	18
1.5 Thesis Structure .....	24
<b>Chapter 2 Literature Review</b> .....	<b>31</b>
2.1 Hydrothermal Processing .....	31
2.1.1 Role of Water .....	32
2.2 Recycling of Waste Plastics via Hydrothermal Processes.....	35
2.2.1 Classification of the Waste Plastics.....	35
2.2.2 Primary Recycling .....	37
2.2.3 Mechanical (Secondary) Recycling .....	38
2.2.4 Chemical (Tertiary) Recycling .....	38
2.2.5 Energy (tertiary) Recycling .....	39
2.2.6 Hydrothermal Treatment for Recycling.....	39

2.3 Chemical Recycling of Common Plastic Wastes.....	40
2.3.1 Common Reactions of Organic Compounds in Hydrothermal Medium.....	40
2.3.1.1 Hydrolysis Reactions.....	42
2.3.1.2 Condensation Reactions .....	49
2.3.2 Application of Hydrothermal Organic Reactions for Plastics Recycling .....	51
2.3.2.1 Hydrolysis of Condensation Plastics .....	51
2.3.2.1.1 Polyethylene Terephthalate (PET) .....	51
2.3.2.1.2 Polycarbonates (PC).....	58
2.3.2.1.3 Nylons .....	60
2.3.3 Degradative Hydration of Addition Polymers.....	62
2.3.3.1 Polyethylene.....	62
2.3.3.2 Phenolic Resins .....	64
2.3.3.3 Fibre Reinforced Plastics .....	66
2.3.3.3.1 Glass Fibre Reinforced Plastics .....	66
2.3.3.3.2 Carbon Fibre Reinforced Plastics .....	67
2.3.4 Other Types of Plastics and Materials.....	71
2.3.4.1 Cross-Linked Polyethylene.....	71
2.3.4.2 Polyvinyl chloride (PVC).....	72
2.3.4.3 Refuse Derived Fuel (RDF).....	74
<b>References.....</b>	<b>76</b>
<b>Chapter 3 Materials and Methods .....</b>	<b>88</b>
3.1 Materials.....	88
3.1.1 Carbon Fibre Reinforced Plastic (CFRP) Waste .....	89
3.1.2 Printed Circuit Board Waste .....	91
3.1.3 Refuse Derived Fuel (RDF).....	94
3.2 Hydrothermal Reactor System .....	96



3.3 Experimental Procedure.....	100
3.3.1 Set up of the 500 ml Reactor.....	100
3.3.2 Setup of the 75 ml Reactor.....	101
3.4 Effluent Gas Analyses .....	102
3.4.1 Permanent Gas Chromatography Analyses .....	103
3.4.2 Hydrocarbons Gas Chromatography Analyses .....	105
3.4.3 Calculation of Gas Compositions .....	107
3.5 Liquid Effluent Analyses .....	110
3.5.1 Total Organic Carbon (TOC) and Total Inorganic Carbon (TIC) Analyses.....	111
3.5.2 Gas Chromatography/Mass Spectrometry (GC/MS) .....	112
3.6 Solid Residue Analyses.....	114
3.6.1 Thermogravimetric Analyses (TGA) and Differential Thermal Analyses (DTA).....	114
3.6.2 Scanning Electron Microscopy (SEM).....	115
3.6.3 Infrared Spectrometry (FTIR) .....	115
3.6.4 Mechanical Properties Analyses .....	116
<b>CHAPTER 4 RECYCLING OF CARBON FIBRE REINFORCED PLASTIC WASTES VIA HYDROTHERMAL PROCESSING .....</b>	<b>121</b>
4.1 Catalytic Hydrothermal Degradation of Carbon Fibre Reinforced Plastic Wastes .....	122
4.1.1 Effect of Temperature and Promoters (CaO, Na <sub>2</sub> CO <sub>3</sub> ).....	122
4.1.2 Effect of Alkalis (KOH, NaOH) and Residence Time .....	124
4.1.3 Analysis of Liquid Products .....	127
4.1.4 Analysis of Recovered Carbon Fibre.....	132
4.1.5 Summary.....	134

4.2 Recovery of Carbon Fibres and Production of High Quality Fuel Gas from the Chemical Recycling of Carbon Fibre Reinforced Plastic Wastes .....	136
4.2.1 Influence of Reaction Conditions on Carbon Fibre Recovery .....	136
4.2.2 Processing of the Residual Liquid Product.....	139
4.2.2.1 Liquid-Liquid Extraction Results .....	139
4.2.2.2 Catalytic Supercritical Water Gasification of Liquid Products .....	144
4.2.3 Mechanical Properties of the Recovered Carbon Fibre....	147
4.2.4 Summary.....	150
4.3 Evaluating the Mechanical Properties of Reinforced LDPE Composites Made With Carbon Fibres Recovered via Hydrothermal Processing.....	152
4.3.1 Properties of Recovered Carbon Fibres and Additives.....	152
4.3.2 Mechanical Properties of the Composites.....	155
4.3.2.1 Tensile and Flexural Strengths.....	155
4.3.2.2 Elongation at Break.....	159
4.3.2.3 Charpy Impact Strengths.....	160
4.3.2.4 LDPE-Additive-Carbon Fibre Ester Linkage Mechanism.....	161
4.3.3 Summary.....	166
<b>Chapter 5 Chemical Recycling of Printed Circuit Board Waste via Depolymerisation in Sub- and Supercritical Solvents .....</b>	<b>170</b>
5.1 The Effect of Solvent on Resin Removal.....	171
5.2 Product Distribution.....	174
5.3 Summary.....	181

**CHAPTER 6 HYDROTHERMAL PROCESSING OF REFUSE**

<b>DERIVED FUELS .....</b>	<b>185</b>
6.1 Low Temperature Hydrothermal Processing of RDF.....	187
6.2 Hydrothermal Gasification of RDF.....	191
6.4 Summary.....	207

**Chapter 7 Conclusions & Future Work..... 210**

7.1 Recycling of Carbon Fibre Reinforced Plastic Wastes via Hydrothermal Processing.....	210
7.1.1 Catalytic Hydrothermal Degradation of Carbon Fibre Reinforced Plastic Wastes .....	210
7.1.2 Recovery of Carbon Fibres and Production of High Quality Fuel Gas from the Chemical Recycling of Carbon Fibre Reinforced Plastic Wastes .....	212
7.1.3 Evaluating the Mechanical Properties of Reinforced LDPE Composites Made With Carbon Fibres Recovered via Hydrothermal Processing.....	213
7.1.4 Chemical Recycling of Printed Circuit Board Waste via Depolymerisation in Sub- and Supercritical Solvents.....	214
7.1.5 Hydrothermal Processing of Refuse Derived Fuels.....	215
7.1.6 General Summary .....	216
7.2 Future Work.....	217

## List of Tables

Table 1.3.1 Metals in printed circuit board by type .....	14
Table 1.3.2 Proximate analysis of different RDF samples.....	17
Table 1.3.3 Ultimate analysis of different RDF samples.....	17
Table 1.4.1 PCB and CFRP recycling facilities in the UK.....	22
Table 2.1.1 Properties of Water .....	32
Table 2.1.2 Properties of Water at Different Conditions .....	33
Table 2.2.1 Typical applications of common plastics .....	36
Table 2.3.1 Advantages and disadvantages of different recycling processes.....	69
Table 3.1.1 Characteristics of the ruthenium oxide-alumina catalysts.....	89
Table 3.1.2 Printed circuit waste ash analysis result.....	92
Table 3.4.1 GC results of the standard for permanent gases.....	104
Table 3.4.2 GC results of the standard for hydrocarbon gases (alkanes and alkenes).....	107
Table 3.4.3 Excel spreadsheet solution for the hydrothermal gasification of RDF with 5 wt% ruthenium catalyst at 500°C and zero minute residence time .....	109
Table 4.1.1 Resin removals and distribution of carbon during hydrothermal depolymerisation of CFRP waste .....	123
Table 4.1.2 Influence of alkalis on product distribution [wt%].....	124
Table 4.1.3 Resin removal and distribution of carbon during hydrothermal depolymerisation of CFRP waste at 420°C and zero reaction time.....	125
Table 4.1.4 Resin removal and distribution of carbon during hydrothermal depolymerisation of CFRP waste with KOH at 420°C .....	126

Table 4.1.5 Mechanical properties of virgin carbon fibre and recovered carbon fibre .....	133
Table 4.2.1 Resin removal during depolymerisation of carbon fibre reinforced plastics in ethylene glycol (EG) .....	137
Table 4.2.2 Resin removal during depolymerisation of carbon fibre reinforced plastics in ethylene glycol (EG)/water mixture.....	138
Table 4.2.2 The produced mol gas per kg CFRP waste and the higher heating value of the product gas from the gasification experiments.....	146
Table 4.2.3 The mechanical properties of virgin and recovered carbon fibre. ....	147
Table 4.3.1 The main properties of surface treating agents .....	153
Table 4.3.2 Tensile and flexural properties of composite materials.....	157
Table 4.3.3 Elongation at break, [%] .....	159
Table 4.3.4 Charpy Impact Strength, [kJ/m <sup>2</sup> ].....	160
Table 4.3.5 Saturated aliphatic group frequencies .....	162
Table 5.1.1 The effect of temperature on depolymerisation of printed circuit board in Ethanol.....	171
Table 5.1.2 The gas yield after depolymerisation of printed circuit board in Ethanol .....	172
Table 5.1.3 The effect of acetone as solvent on depolymerisation of printed circuit board in the absence of any addition .....	173
Table 5.1.4 The effect of water as solvent on depolymerisation of printed circuit board in the absence of any addition .....	173
Table 5.1.5 The effect of temperature on depolymerisation of printed circuit board in water in the absence of any addition.....	173
Table 5.1.6 The effect of additives on depolymerisation of printed circuit board in water .....	174

Table 5.2.2 Organic composition of the liquid produced from depolymerisation at 400 °C with water (a) in the presence of NaOH (b) in the presence of KOH as catalyst (c) without any additives .....	177
Table 6.1 The average of the sample property of MSW and RDF .....	186
Table 6.1.1 Product distribution after low temperature hydrothermal processing of RDF .....	187
Table 6.2.1 Distribution of RDF-carbon after catalytic hydrothermal gasification .....	203

## List of Figures

Figure 1.1.1 World plastics production in million tonnes.....	2
Figure 1.1.2 European plastics demand by industrial sector, 2013 .....	3
Figure 1.1.3 European plastic demand by polymer type, 2013 .....	3
Figure 1.1.4 Total plastic waste recycling and recovery in Europe 2006- 2012 .....	4
Figure 1.2.1 Waste Hierarchy.....	5
Figure 1.2.2 Recycling routes for plastic wastes .....	6
Figure 1.3.1 Process steps of Carbon Fibre production from PAN precursors .....	8
Figure 1.3.2 Global demand for Carbon Fibre [ x1,000 tonnes] .....	9
Figure 1.3.3 Global carbon fibre demand by application [1,000 tonnes] (2013).....	10
Figure 1.3.4 Global demand for CFRP [1,000 tonnes] .....	10
Figure 1.3.5 Life cycle for carbon reinforced plastic wastes .....	11
Figure 1.3.6 Typical components of a printed circuit board .....	13
Figure 1.3.7 Global municipal solid waste composition .....	16
Figure 1.4.1 The carbon fibre reinforced plastics lifecycle loop adapted from.....	20
Figure 1.4.2 Open air burning of waste PCB in Guiyu, Guandong province (a) the toxic gas release to the atmosphere (b) the residue after burning adapted from .....	21
Figure 2.1.1 Phase diagram of Water.....	34
Figure 2.2.1 Stages of mechanical recycling .....	38
Figure 2.3.1 Selectivity of guaiacol hydrolysis to methanol with respect to reduced density of water .....	44

Figure 2.3.3 Hydrothermal reaction mechanism of formaldehyde in supercritical water, adapted from ref .....	46
Figure 2.3.4 Hydrolysis of nitriles and amides to acids adapted from ref ....	47
Figure 2.3.5 Hydrolysis of butyronitrile adapted from ref.....	48
Figure 2.3.6 Friedel-Crafts alkylation.....	49
Figure 2.3.7 Aldol condensation reaction scheme.....	50
Figure 2.3.8 PET synthesis reactions (a) via trans-esterification (b) via condensation.....	51
Figure 2.3.9 The depolymerisation products of PET .....	52
Figure 2.3.10 Reaction scheme of decomposition of PET in methanol .....	53
Figure 2.3.11 PET depolymerisation in NaOH solution .....	56
Figure 2.3.12 Depolymerisation products of PET in supercritical water (400°C, 40 MPa).....	57
Figure 2.3.13 Decomposition reaction of PC .....	59
Figure 2.3.14 Decomposition of nylon 6 in subcritical water.....	61
Figure 2.3.1 The chemical structure of a typical phenolic resin.....	64
Figure 2.3.2 Overview of carbon fibre reinforced plastic recycling and remanufacturing processes adapted from.....	71
Figure 3.1.1 Waste CFRP sample.....	90
Figure 3.1.2 TGA and DTG curves of CFRP waste.....	91
Figure 3.1.3 The printed circuit board extracted from desktop computer LCD monitors .....	91
Figure 3.1.4 TGA and DTG curves of PCB waste .....	93
Figure 3.1.5 RDF sample (a) original pellets (b) shredded samples .....	94
Figure 3.1.6 TGA and DTG curves of RDF sample.....	96
Figure 3.2.1 The Schematic diagram of hydrothermal reactor .....	97
Figure 3.2.2 Photograph of (a) Hydrothermal reactor and (b) The furnace and the control unit.....	98



Figure 3.2.3 Schematic diagram of 75 ml reactor.....	99
Figure 3.4.1 Gas chromatography with the computer unit.....	103
Figure 3.4.2 Block diagram of a typical gas chromatograph.....	103
Figure 3.4.3 GC chromatogram of the standard for permanent gases .....	104
Figure 3.4.4 GC chromatogram of the standard for hydrocarbon gases (a) Alkanes and (b) Alkenes .....	106
Figure 3.5.1 Liquid-liquid extraction with DCM (a) after first addition of 20 ml DCM, (b) after second addition of 20 ml DCM and (c) the resulting organic phase after extraction.....	111
Figure 3.5.2 GC/MS analyzer used for the analyses of liquid effluent.....	112
Figure 3.5.3 Calibration curves for phenol and dibenzofuran .....	113
Figure 3.6.1 Labtech two roll mill.....	117
Figure 3.6.2 Press moulding machine .....	118
Figure 3.6.3 INSTRON 3345 universal tensile machine .....	119
Figure 3.6.4 CEAST Resil Impactor .....	119
Figure 4.1.1 Simplified reaction mechanism of hydrothermal decomposition path of cellulose .....	126
Figure 4.1.2 GC/MS chromatogram of DCM extracted depolymerisation products of CFRP at 420°C with KOH and 5 wt% H <sub>2</sub> O <sub>2</sub> .....	127
Figure 4.1.3 GS/MS chromatogram and spectrum of DCM extracted depolymerisation products of CFRP at 420°C with KOH and 5 wt% H <sub>2</sub> O <sub>2</sub> , after the addition of KOH into the liquid effluent .....	128
Figure 4.1.4 GS/MS chromatogram and spectrum of DCM extracted depolymerisation products of CFRP at 420°C with KOH and 5 wt% H <sub>2</sub> O <sub>2</sub> , after the addition of HCl into the liquid effluent .....	129
Figure 4.1.5 Effect of reaction media, temperature and H <sub>2</sub> O <sub>2</sub> on the yields of phenols and aniline during hydrothermal processing of CRFP .....	130

Figure 4.1.6 Effects of H <sub>2</sub> O <sub>2</sub> loading during hydrothermal processing of CRFP to different alkalis at 420°C and zero residence time.....	131
Figure 4.1.7 The degradation mechanism of monomer of polybenzoxazine resin.....	132
Figure 4.1.8 SEM images of (a) Virgin carbon fibres, (b) Recovered carbon fibres at different magnitudes .....	134
Figure 4.2.1 GC/MS/MS chromatograms of extracts from the residual liquid products obtained during carbon fibre reinforced plastics depolymerisation at 400°C with water only; (a) alkaline extraction (b) acidic extraction .....	140
Figure 4.2.2 GC/MS/MS chromatograms of extracts from liquid residuals obtained during carbon fibre reinforced plastics depolymerisation at 400 °C with ethylene glycol only; (a) alkaline extraction (b) acidic extraction.....	141
Table 4.2.1 Main organic compounds detected in the liquid obtained from carbon fibre reinforced plastics depolymerisation at 400 °C, using ethylene glycol and water as separate solvents. ....	143
Figure 4.2.3 Product distribution after gasification of a sample of the residual liquid product. ....	145
Figure 4.2.4 Gas composition after gasification of a sample of the residual liquid product. ....	145
Figure 4.2.5 SEM images of virgin and recovered carbon fibre samples in relation to treatment in ethylene glycol (EG) and EG/water mixtures.....	149
Figure 4.2.6 FTIR results (a) recovered carbon fibre at 400 °C in EG/water mixture (EG/water ratio = 5), (b) virgin carbon fibre. ....	150
Figure 4.3.1 SEM images of (A) Virgin, (B) Recovered, (C) Oxidized recovered carbon fibres.....	152
Figure 4.3.2 The carbon fibre reinforced LDPE composites, after press-moulding.....	155

Figure 4.3.3 FTIR spectra of manufactured composites (A: without additive, B: CA-1, C: MA-g-HDPE, D: CFA-1, E: CFA-2). .....	163
Figure 4.3.4 The proposed reaction scheme of coupling between carbon fibre and commercial LDPE matrix. ....	164
Figure 4.3.5 FTIR results of (a) Oxidized recovered carbon fibre, (b) Non-oxidized recovered carbon fibre and (c) virgin carbon fibre .....	165
Figure 5.1.1 The gas composition after degradation of printed circuit board at 400°C in Ethanol .....	172
Table 5.2.1 Gas Compositions during depolymerisation of printed circuit board in water, in the presence of (a) NaOH (b) KOH (c) no additives .....	175
Figure 5.2.1 GC/MS result of the liquid from the experiment with water when NaOH was used as the additive, at 400°C.....	176
Figure 5.2.2 The degradation mechanism of the resin [10] .....	180
Figure 5.2.3 Solid residues after drying, before and after oxidation; samples from depolymerisation (a) via ethanol at 400 °C (b) via water at 400 °C (c) via water and NaOH at 400°C .....	181
Figure 6.1.1 Gas composition after low temperature hydrothermal processing of RDF .....	189
Figure 6.1.2 GC/MS outline of liquid residuals showing important compounds at 400°C when water alone was used.....	190
Figure 6.1.3 GC/MS chromatograms of liquid residuals obtained at 400°C showing important compounds (a) sodium hydroxide (b) methanol were used.....	191
Figure 6.2.1 Carbon gasification efficiencies in relation to reaction time and catalysts .....	192
Figure 6.2.2 Gas composition after hydrothermal gasification of RDF with 5 wt% RuO <sub>2</sub> /γ-Al <sub>2</sub> O <sub>3</sub> at 500°C .....	193
Figure 6.2.3 Gas composition after hydrothermal gasification of RDF with 10 wt% RuO <sub>2</sub> /γ-Al <sub>2</sub> O <sub>3</sub> at 500°C .....	194

Figure 6.2.4 Gas composition after hydrothermal gasification of RDF with 20 wt% RuO <sub>2</sub> /γ-Al <sub>2</sub> O <sub>3</sub> at 500°C .....	195
Figure 6.2.5 Gas composition after hydrothermal gasification of RDF at 500°C and 60 minutes reaction time with various RuO <sub>2</sub> loadings.....	196
Figure 6.2.6 Gas compositions in vol. % after hydrothermal treatment of RDF at 500°C with 5 wt% RuO <sub>2</sub> /γ-Al <sub>2</sub> O <sub>3</sub> .....	197
Figure 6.2.7 Gas compositions in vol. % after hydrothermal treatment of RDF at 500°C with 10 wt% RuO <sub>2</sub> /γ-Al <sub>2</sub> O <sub>3</sub> .....	198
Figure 6.2.8 Gas compositions in vol. % after hydrothermal treatment of RDF at 500°C with 20 wt% RuO <sub>2</sub> /γ-Al <sub>2</sub> O <sub>3</sub> .....	198
Figure 6.2.9 Gas compositions and carbon gasification efficiency after hydrothermal gasification of RDF with NaOH at 500°C at different time variations .....	201
Figure 6.2.10 Gas composition (vol%) after hydrothermal gasification of RDF with different catalysts and catalyst loadings at 500°C and 60 minutes reaction time .....	204
Figure 6.2.11 Gross calorific values of gas products in relation with temperature and catalyst loading/type .....	205

## Abbreviations

PE	Polyethylene
LDPE	Low Density Polyethylene
HDPE	High Density Polyethylene
PET	Polyethylene Terephthalate
PP	Polypropylene
PVC	Polyvinylchloride
PS	Polystyrene
PF	Phenol-Formaldehyde
UP	Unsaturated Polyesters
PU	Polyurethane
EP	Epoxy
CFRP	Carbon Fibre Reinforced Plastic
PCB	Printed Circuit Board
RDF	Refuse Derived Fuel
PAN	Polyacrylonitrile
WEEE	Waste Electrical And Electronic Equipment
EU	European Union
BFR	Brominated Fire Retardant
MSW	Municipal Solid Waste
GC	Gas Chromatography
GC/MS	Gas Chromatography Coupled To A Mass Spectrometer
FID	Flame Ionisation Detector
TCD	Thermal Conductivity Detector
TGA	Thermogravimetric Analysis

DTG	Differential Thermogravimetry
SEM	Scanning Electron Microscopy
FTIR	Fourier Transform Infrared Spectrometry
DCM	Dichloromethane
TOC	Total Organic Carbon
IC	Inorganic Carbon

## **Chapter 1**

### **INTRODUCTION**

#### **1.1 General Overview of Plastic Production**

The waste recycling problem is one of the most challenging topics in today's world, as it has effects on both environment and economy. For a sustainable environment, it is crucial to recycle wastes especially plastics which are largely produced from non-renewable sources such as fossil fuels. Also, the developed countries are spending a great amount of their budget for waste management.

One of the wastes produced in great amounts is from plastics. They are, by definition, the materials produced from polymers via chemical processes with the help of additives and chemicals. Polymers are the long-chain molecules mainly produced from petroleum oil, constructed from small repeating chemical units, called monomers. They are categorized into two groups; thermoplastics and thermosets [1].

Thermoplastics can be produced by heating or applying pressure, and when it is cooled, they solidify. The most common thermoplastics are polyethylene (PE) (low density PE (LDPE), high density PE (HDPE)), polyethylene terephthalate (PET), polypropylene (PP), polyvinylchloride (PVC) and polystyrene (PS). Thermosets are 3-D cross-linked molecules, whose production is irreversible, so, they cannot be melted by heating. Some common thermosets are phenol-formaldehyde (PF), unsaturated polyesters (UP), polyurethane (PU) and epoxy (EP). Commercially, thermosets are usually reinforced by carbon or glass fibres to produce important engineering composite materials.

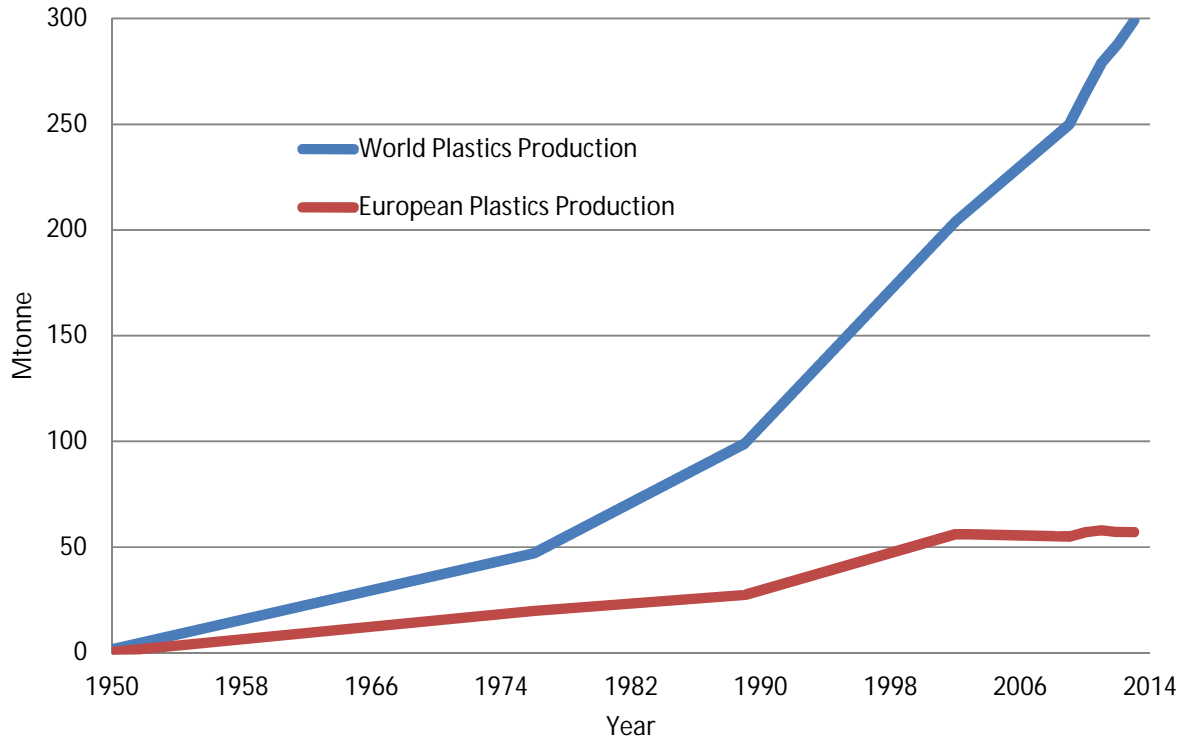


Figure 1.1.1 World plastics production in million tonnes [2]

Due to the wide usage areas of plastics such as the packaging industry, building & construction, automotive, electrical & electronic industries, etc., the plastics industry has grown continuously for the last 60 years, as shown by the global production rate which increased from 1.7 to 299 million tonnes from 1950 to 2013 (Figure 1.1.1). The difference between the years 2012 and 2013 in plastic production was 11 million tonnes, which means that a 3.9% increase was observed annually. In 2013, Europe had 20% of the total plastic production whereas China was the leading production country with a proportion of 24.8% of total worldwide plastic production [2].



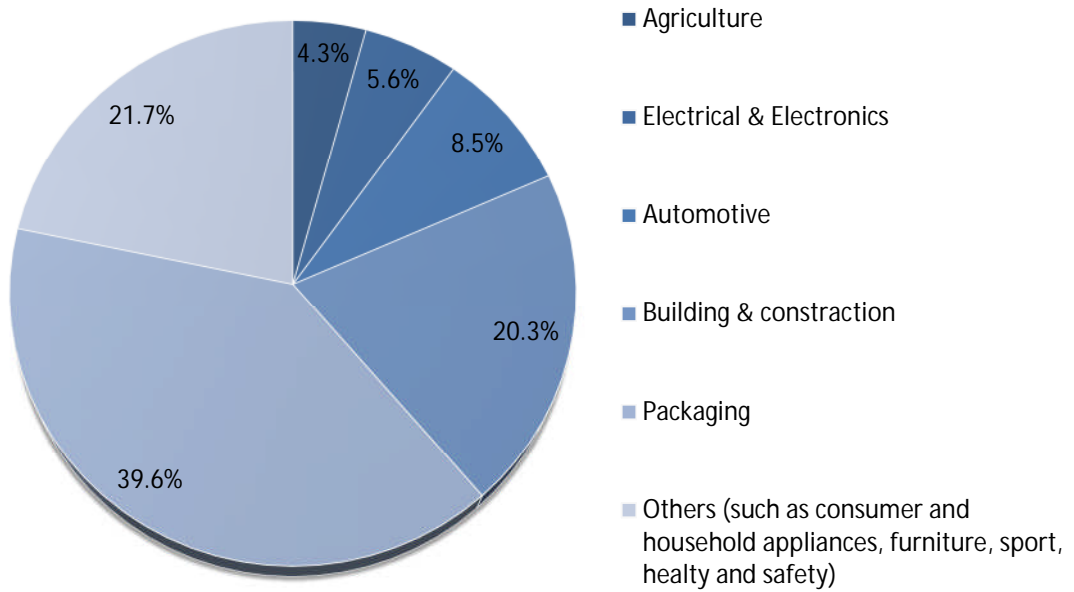


Figure 1.1.2 European plastics demand by industrial sector, 2013 [2]

The demand for plastics in Europe was 46.3 million tonnes in 2013 and the highest demand was for the packaging industry with a share of 39.6% of the total plastic demand. The building and construction, and automotive industries were the second and the third largest sectors for plastics demand, according to Figure 1.1.2 [2].

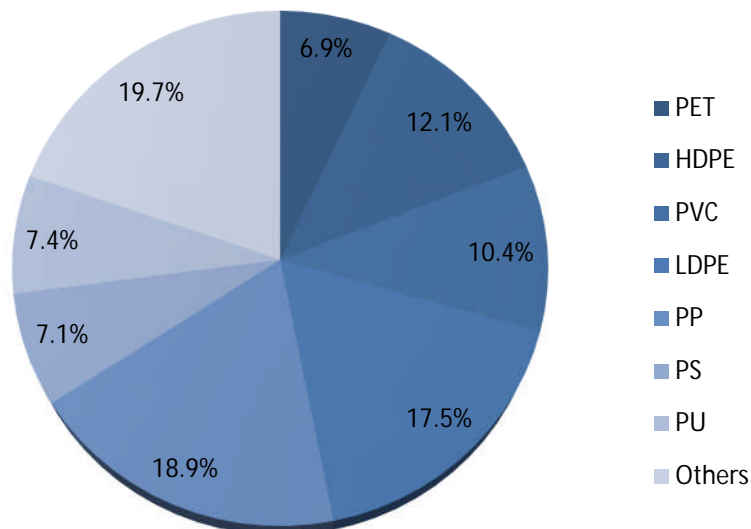


Figure 1.1.3 European plastic demand by polymer type, 2013 [2]

The main plastic wastes consist of polyethylene (high density polyethylene (HDPE) and low density polyethylene (LDPE)), polypropylene (PP) and polyvinylchloride (PVC), as they had a portion of 58.9% of the demand in 2013 in Europe. Figure 1.1.3 shows the proportions of each polymer type by demand as percentages in 2013 [2].

Between 2006 and 2012, 25 million tonnes of post-consumer plastics waste on average were generated in Europe. While 11.7 million tonnes of waste were recovered in 2006, this amount increased by 32.5% in 2012 to reach a value of 15.5 million tonnes. However, according to the figures in Europe, landfilling is still the major waste management method, as 38% of the waste plastics generated was sent to landfilling in 2012, while recycling and energy recovery options were 26% and 36% respectively [2]. From 2006 to 2012, energy recovery has increased by 27% and recycling by 40% as seen in Figure 1.1.4.

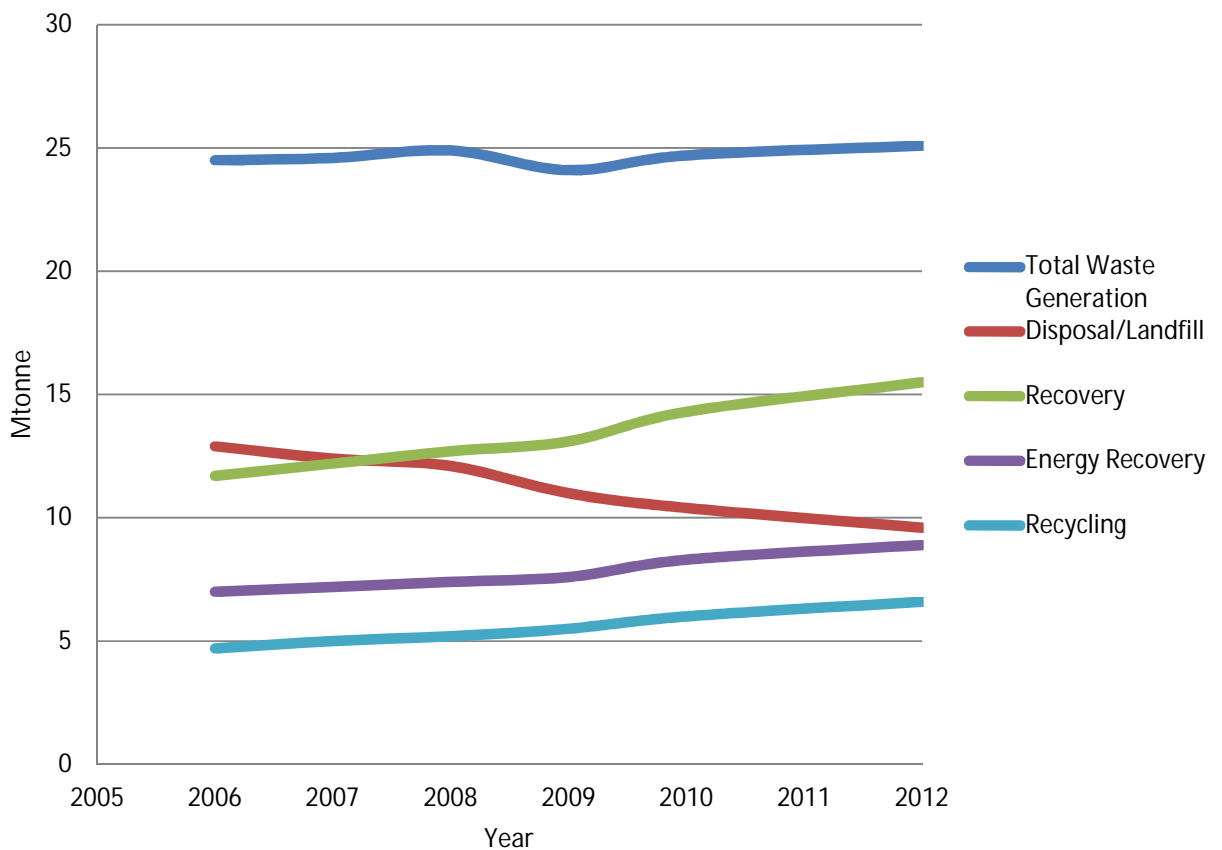


Figure 1.1.4 Total plastic waste recycling and recovery in Europe 2006-2012 [2]

## 1.2 Recycling Routes

With the increasing amount of plastic waste generated throughout the world, alternative routes for recycling are needed, as plastics are produced mostly from crude oil which is a very important natural resource to be conserved for a sustainable environment and economy. Therefore, combinations of legislation and governmental acts have been used to increase the rate of plastic waste recycling.

The high production rates of plastic and the growing plastics market has led to research to decrease the amount of the waste sent to landfilling or incineration, not only by recycling, but also by producing plastics with longer service life. Also the consumers are advised to reuse plastics, for example, PET bottles and nylon bags can be used over and over again once they are purchased from a store. This is proposed to be the first stage in the waste hierarchy, which was revised by European Union recently to become the EU Waste Framework Directive (Directive 2008/98/EC) as described in the Figure 1.2.1 [3].

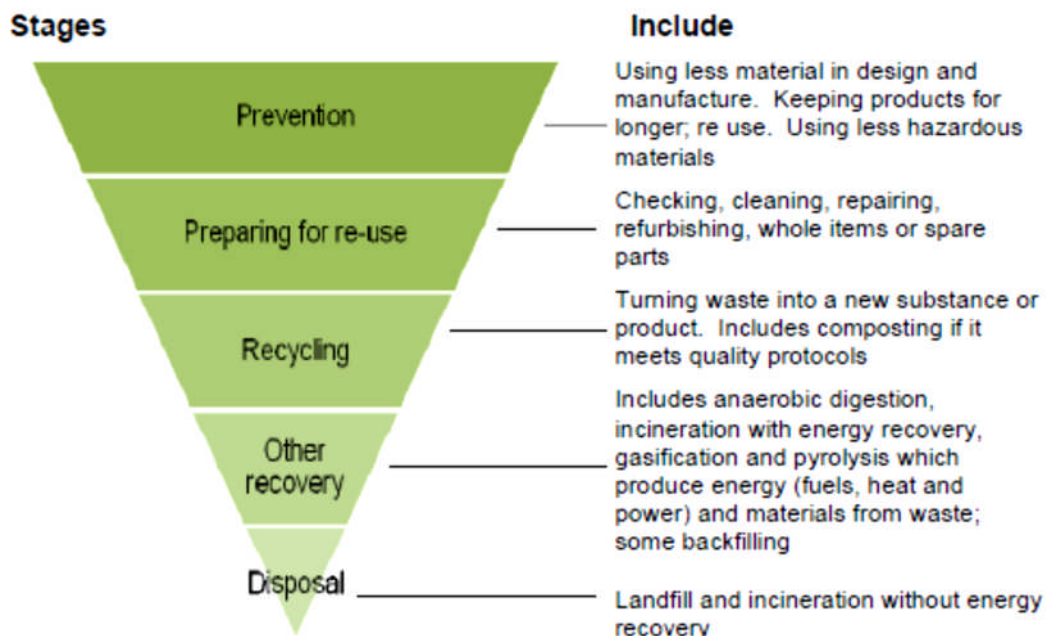


Figure 1.2.1 Waste Hierarchy

When it comes to recycling, the main routes for plastic waste recycling can be categorized into four major groups; primary recycling, mechanical

(secondary) recycling, chemical (tertiary) recycling and energy (quaternary recycling) recovery.

Primary recycling and mechanical recycling sometimes can be classified in the same group, as the concept is the same; recycling the waste via physical processes (milling or grinding, washing, separating, drying, etc..) to convert them to produce virgin plastics. It is applicable only to thermoplastics with high purity and homogeneity, which is a limitation for this method. Primary recycling is also referred to “in-plant” recycling, as shown in Figure 1.2.2 [1].

Chemical recycling is a process to degrade the plastic wastes via chemical processes to produce their precursors or to produce chemical feedstock as oil substitute. The research focus is to find processes with high energy efficiency and economically viable to install as large-scale plants.

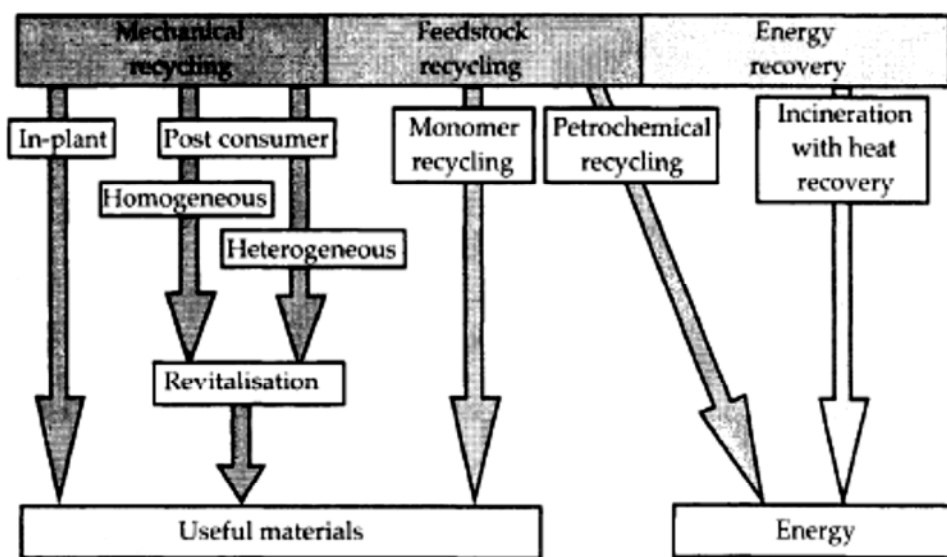


Figure 1.2.2 Recycling routes for plastic wastes [1]

Energy recovery uses the plastic wastes as a source of energy, so that via combustion district heating and/or electricity can be produced. However, producing pollutant gases and high cost are the challenges to be overcome which limit this process.

## **1.3 Waste Samples**

In this study, three different complex waste materials were selected for recovery and recycling. The initial work was carried out with waste carbon fibre reinforced plastic (CFRP) for the recovery of carbon fibre and degradation of the resin fraction to produce valuable organic compounds via a hydrothermal process. The same technique was applied to waste printed circuit boards (PCBs) to depolymerize the resin fraction to its monomers and to recover the valuable metals. Finally, refuse derived fuel (RDF) was subjected to hydrothermal gasification process, to produce a fuel mixture with a high heating value.

### **1.3.1 Carbon Fibre Reinforced Plastics (CFRP)**

Carbon fibres can be defined as fibres with at least 92 wt% carbon in their composition [4]. Since the beginning of the 1960s, firstly used for military aerospace applications, and with the developments in the properties, these strategically important engineering materials have found widespread commercial and industrial applications; such as in the automobile, housing, sport and leisure industries as well as airplane and space applications [5]. They are a viable replacement for steels and aluminium composite materials due to their high tensile strength, low density, high resistance to temperature and corrosion, and low thermal expansion [5, 6].

Currently the majority of the carbon fibres are being produced from non-renewable sources, as the commercial production is by the thermal decomposition of polyacrylonitrile (PAN) based precursor fibres. The process steps are described in Figure 1.3.1. The stabilization takes place at temperatures between 200-260 °C, whereas carbonization is at 1500 °C. The graphitization occurs at 2500 °C to obtain the final product [4, 5]

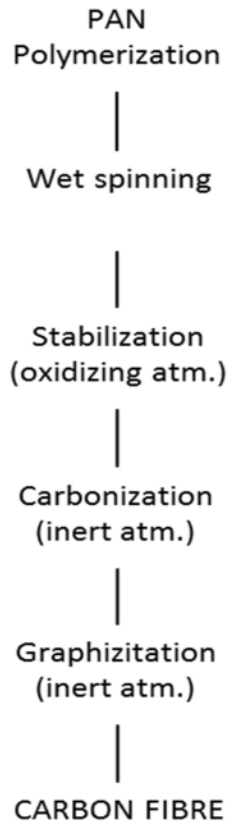


Figure 1.3.1 Process steps of Carbon Fibre production from PAN precursors [4]

Carbon fibres find widespread usage as reinforcement materials for composites. Composite materials consist of one or two fillers in a certain matrix. In carbon fibre reinforced materials, this matrix can be a polymer, or combinations of polymers, metals, ceramics etc.[4].

The matrix material can be a thermoplastic or more commonly a thermosetting resin such as polyester, epoxy, phenolic and polyamide resin as they offer much better properties compared to thermoplastic resins in terms of greater ductility and processing speed [4, 7]. It is reported that 76% of the carbon fibre reinforced plastics were manufactured by thermosetting resin curing in 2013, whereas thermoplastics account for 24% [8].

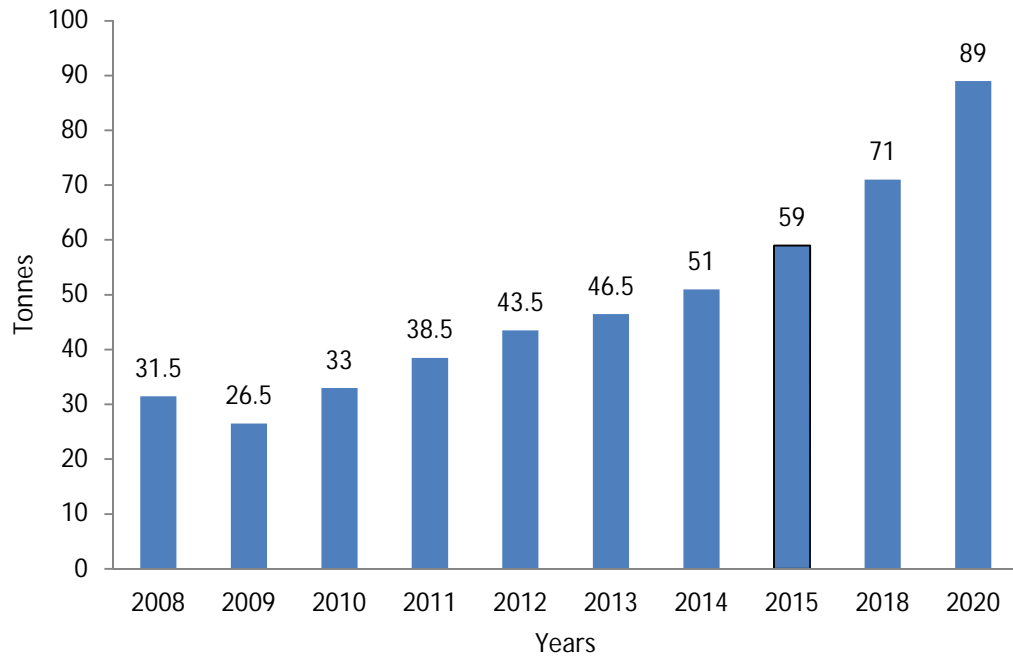


Figure 1.3.2 Global demand for Carbon Fibre [ x1,000 tonnes] [8]

The carbon fibre reinforced composites market has reached a high proportion in industry, as the figures suggest that the global sales of carbon fibre reinforced plastics was \$16.1 billion in 2011 and the projections show that it will rise to \$48.7 billion by 2020 [9]. According to Figure 1.3.2, the demand for Carbon fibre was 46,500 tonnes in 2013, and this number is expected to reach 89,000 tonnes in 2020 [8].

Currently, most of the carbon fibre produced is used in aerospace and defence applications, as it holds a 30% share of the total carbon fibre produced (Figure 1.3.3). The other major application areas are the sport/leisure sector, wind turbines and automotive industries.

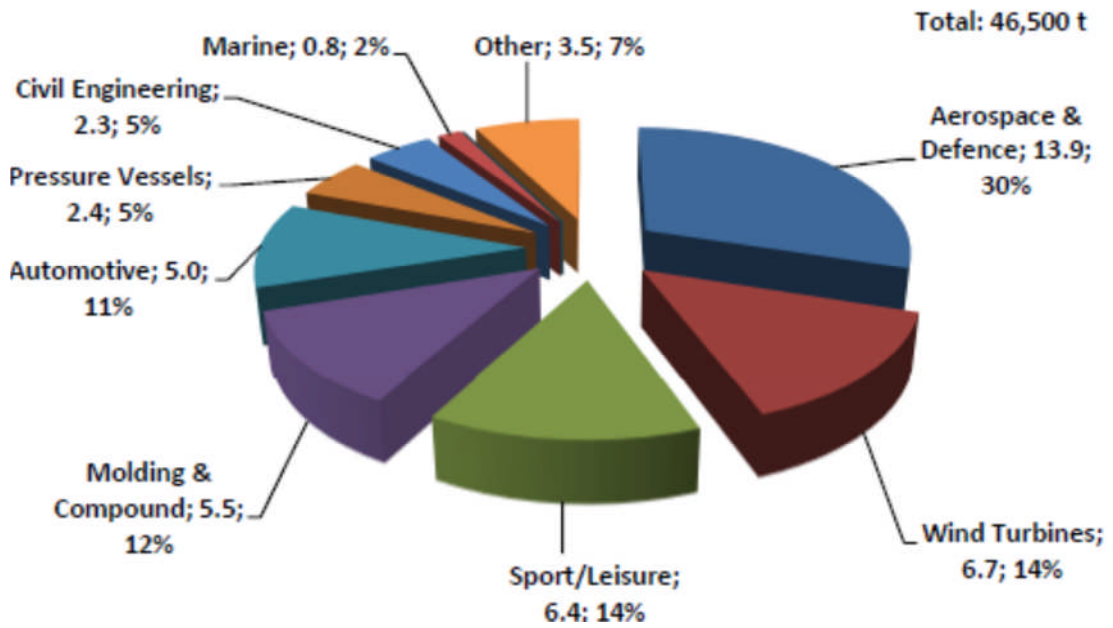


Figure 1.3.3 Global carbon fibre demand by application [1,000 tonnes] (2013) [8]

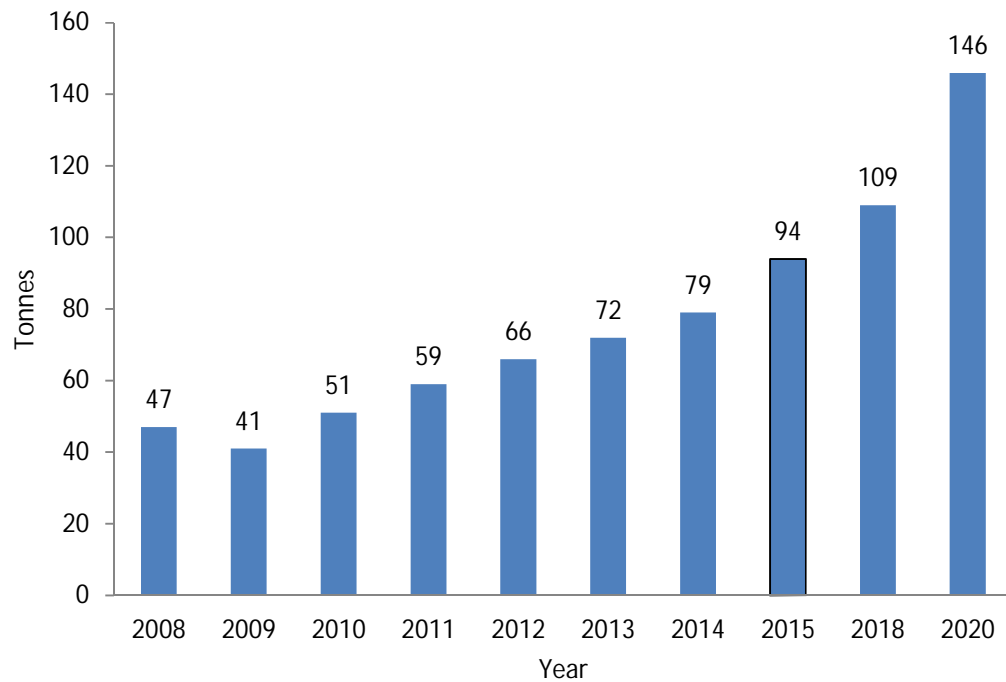


Figure 1.3.4 Global demand for CFRP [1,000 tonnes] [8]

The demand for carbon fibre reinforced plastics has the same trend with the carbon fibre sector. In 2013, the demand for carbon fibre reinforced



plastics was around 72,000 tonnes, and it will grow up to 146,000 tonnes by 2020, according to projections given in Figure 1.3.4 [8].

As the carbon fibre industry grows rapidly, the need for recycling carbon fibre reinforced plastics waste is gaining attention due to environmental and economic factors. In the USA and Europe, 3000 tonnes of carbon fibre reinforced plastics waste is generated every year, and this number is expected to rise dramatically as 6000 to 8000 airplanes will reach their end-of-service life by 2030 [10]. Also with the new regulations in relation to different types of wastes for example automobiles are to be 85% recyclable in the European Union, landfilling of carbon fibre reinforced plastics is limited. Another important issue is the price of the virgin carbon fibre, as in 2013, the costs were up to \$55 per kg carbon fibre and in general is around \$33 – 66 per kg, depending on the physical properties [11, 12].

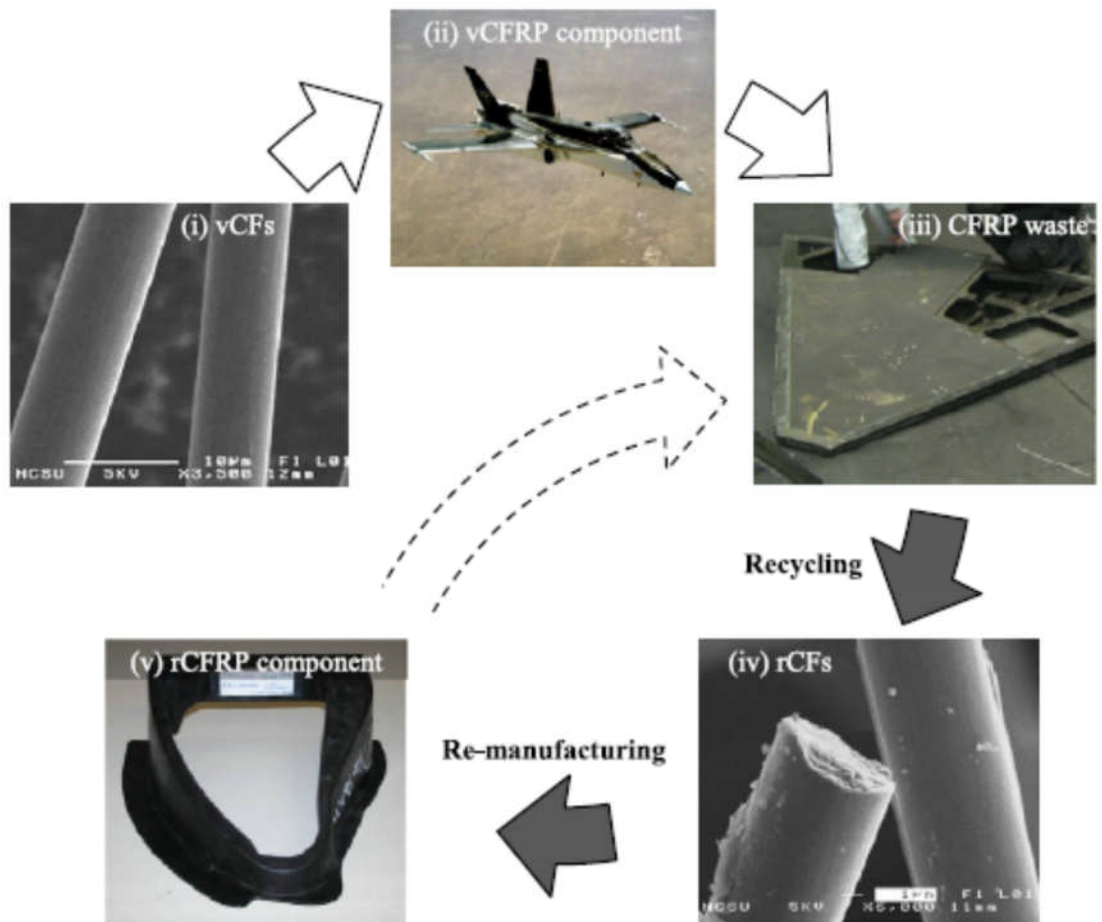


Figure 1.3.5 Life cycle for carbon reinforced plastic wastes [11]

Unfortunately, the current majority of carbon fibre reinforced plastic wastes are sent to landfill or incineration, which means the loss of the organic fraction produced from non-renewable sources. Therefore, it is crucial to develop a method to obtain a closed life cycle as suggested in Figure 1.3.5 for recycling carbon fibre reinforced plastics for a sustainable environment and economy.

### **1.3.2 Printed Circuit Boards (PCB)**

Electrical and electronic equipment have gained a very large worldwide usage area, with technological developments and intense marketing of new products; from cell phones to laptops, TVs to kitchen appliances. This increasing production and utilization result in waste generation, due to the fast replacement of the electronic devices. Currently waste electrical and electronic equipment (WEEE or E-waste) is one of the fastest growing wastes especially in the European Union, therefore stringent regulations were introduced by the EU under the WEEE Directive in 2002 (Directive 2002/96/EC) for its management. In 2008, this Directive was revised as the projections for 2020 showed more than 12 million tonnes of WEEE generation in the EU, so the new WEEE Directive 2012/19/EU was put into action [13] to give much more content to the issue of WEEE generation and disposal. The regulations' were revised to encourage the reuse and recycling of WEEE, as valuable metals and organic materials produced from non-renewable resources can be re-introduced to industry, for a sustainable environment and economy.

The estimation for worldwide WEEE generation is poor and insufficient due to lack of data available in terms of regional and global coverage. According to a United Nations report, annual waste generation is predicted to be around 40-50 million tonnes [14]. Between 1994 and 2003, 500 million computers reached the end of their service life [15]. The improvements in the technology and consumer behaviour affect this number such that very large amounts of waste electronic and equipment are produced annually. In other words, the short life span of electronic devices due to rapid changes in technology coupled with increasing affordability of consumers due to rapid economic developments mean that electronic devices are quick to become

obsolete, discarded or replaced leading to increasing annual WEEE generation.

Printed circuit boards (PCB) are the main waste stream in WEEE, as they are present almost in every electronic device. However, because of their heterogeneity, it is a complicated process to treat PCBs waste. Mainly, they consist of organic resins (polymer fraction), metals and glass fibre. Apart from those materials, there are larger components such as capacitors, resistors, transformers, etc., that can be dismantled. The resin is predominately a thermosetting polymer such as phenolic and creosol based epoxy resin, bisphenol A epoxy resin, or cyanate esters and polyamides. Generally the metal content is around 40 wt% and copper, iron, nickel, gold and palladium are the valuable metals which commonly exist in PCBs[16, 17].

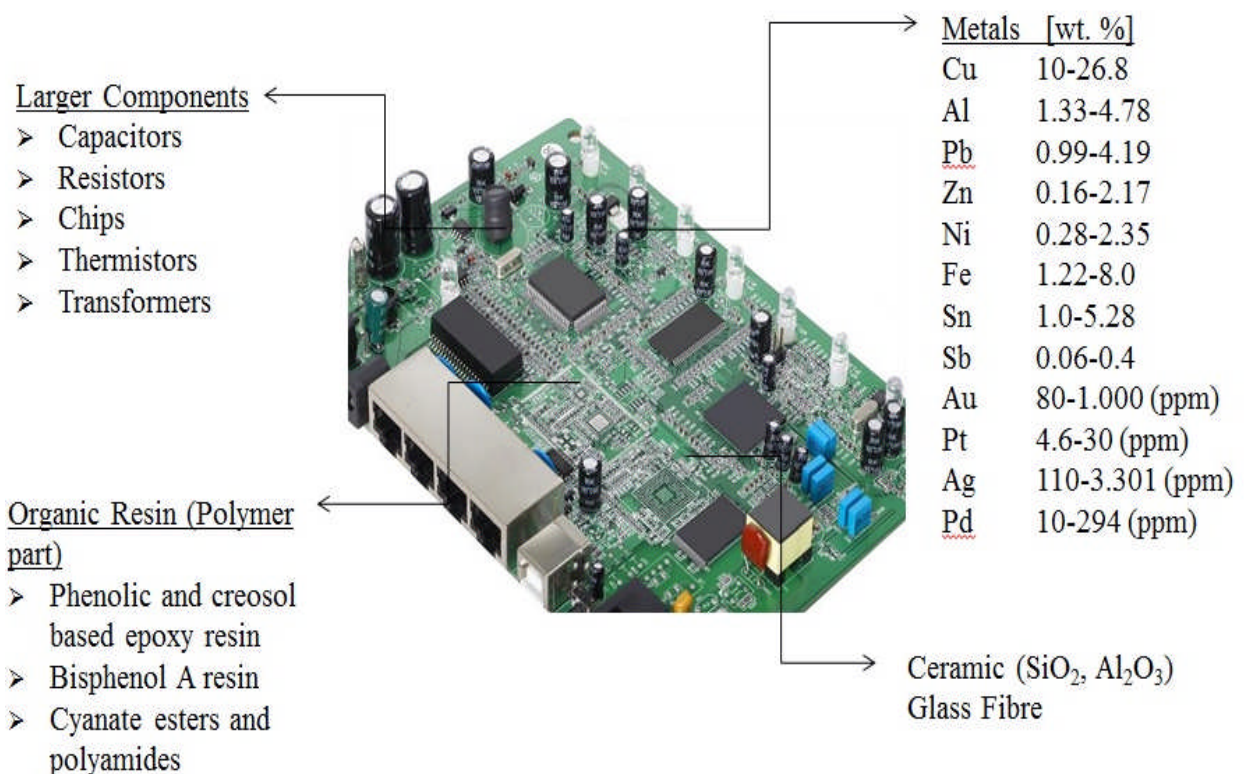


Figure 1.3.6 Typical components of a printed circuit board [17]

More detailed information in relation to the components in the printed circuit board is determined by the type of waste electronic and electrical equipment, as shown in Table 1.3.1 [18]. Copper, lead and tin are the major metals which exist in printed circuit boards. Apart from the metals, brominated fire retardants (BFRs) are also used in printed circuit boards, which are toxic and contain hazardous materials such as tetrabromobisphenol A, pentabromodiphenyl ethers, tetrabromodiphenyl ethers, tribromodiphenyl ethers and 4-bromophenyl ether. Their concentration range in the printed circuit boards are between 100 ppm and 1000 ppm, depending on the type of electronic and electrical equipment.

Table 1.3.1 Metals in printed circuit board by type (mg/kg) [18]

<i>Sample</i>	<i>Arsenic</i>	<i>Cadmium</i>	<i>Chromium</i>	<i>Copper</i>	<i>Lead</i>	<i>Mercury</i>	<i>Nickel</i>	<i>Zinc</i>
Microwave	13	173	57	168000	22300	3	279	6600
Vacuum cleaners	34	5	116	132000	31100	<0.5	1160	4700
Toasters	11	12	61	90600	34700	<0.5	478	3430
Printers	19	4	115	191000	12300	<0.5	6220	4210
Laptops	20	56	145	176000	90800	<0.5	10200	6910
Flat screen TV	27	9	107	313000	25200	0.8	4650	9770
Stereos VCR/DVD	25	3	72	137000	42900	3	3750	4240
Calculators	24	5	154	74200	13800	<0.5	5300	12900

The present technologies for treatment of waste PCBs are mechanical processing, combustion and hydrometallurgical methods. Before any of those treatments of the waste, a pre-treatment step is necessary to dismantle the large components such as resistors, capacitors, etc., which can be hazardous or reusable materials [19]. Mechanical recycling of PCBs is a physical separation process of the waste by grinding it into fine particles.

The final separation can be made via magnetic, electrostatic or density-based separation to produce a metal-rich fraction. The non-metallic fraction, which is the resin fraction, can find application areas as filler for thermosetting resin composites [20], a reinforcing filler for thermoplastic resin composite materials [21], as a raw material for concrete [22-24], or as a modifier for viscoelastic materials [25]. Although the mechanical separation process appears an environmentally friendly, convenient and relatively simple treatment option, the method is highly influenced and limited by the final properties of the recycled polymer, for example the clean separation of metals from the polymer should be achieved and the toxic and hazardous substances in the final product should be prevented. Also, for high recovery, very small particle sizes need to be achieved, which increases the cost.

Combustion of PCB is at temperatures of around 1200°C, aids recovery of the metals in the PCB. The polymer fraction of the waste is destroyed by the combustion process, and the residual metals are subjected to further separation methods. The precious metals, with copper as the most abundant amongst the non-precious metals, can be recovered by electro-refining. The main drawback of this process is the production of toxic and hazardous materials such as polychlorinated dibenzodioxins and polychlorinated dibenzofurans and polybrominated biphenyl ethers (PBDEs) [26].

The hydrometallurgical process involves the dissolution of the waste PCBs with an acid (or alkali) and to recover the metals from the solution via an electro-refining process or crystallization. In the studies conducted so far, the leaching of nickel and copper is carried out selectively and the gold can be recovered in high purity. However, the solutions are highly corrosive and hazardous, as concentrated nitric acid, hydrochloric acid and/or cyanide solutions are used for leaching for very long dissolution times [27-29]. Destruction of the resin by dissolution in acid/alkali also represents a waste of non-renewable organic resources, counteracting the EU zero waste policy.

Currently around 15% of the waste PCBs is being recycled in the UK, with the majority of the management of these wastes via landfilling and incineration. However, because of the formation of hazardous compounds such as polybrominated dibenzodioxins, dibenzofurans and toxic brominated compounds from incineration; and the leaching of toxic compounds and heavy metals to groundwater due to landfilling, recycling of waste PCBs are important to prevent the impact of such hazards to the environment [17].

### 1.3.3 Refuse Derived Fuel (RDF)

Municipal solid waste (MSW) generation is around 10% of the total waste produced in the world and the management of the waste collected has major environmental and economic issues [30]. The annual worldwide generation of municipal solid waste has been projected to be 2.2 billion tonnes by 2025, according to World Bank predictions [31].

Typically, paper/cardboard, plastics, glass, metal, textile and food/garden waste are the main components in the municipal solid waste. Around 46% of the municipal solid waste consists of organic wastes (Figure 1.3.7) which can be used for refuse derived fuel production [31, 32].

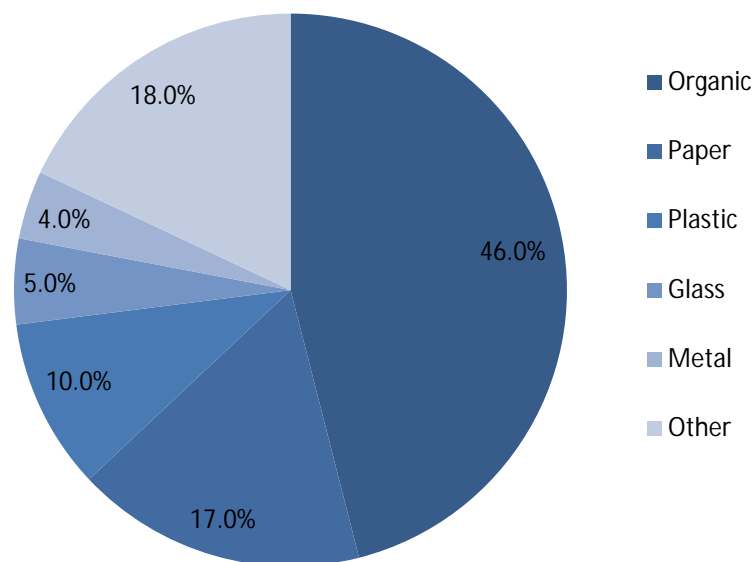


Figure 1.3.7 Global municipal solid waste composition [31]

Refuse derived fuel is a fuel produced from processing of municipal solid waste, by using mechanical treatment methods to remove materials such as glass and metals to obtain a combustible fraction. Then this fraction undergoes further processing to increase the energy density to achieve a high calorific value fuel with a uniform size and weight distribution. After these improvements in the properties with simple mechanical treatments, refuse derived fuels are ready to undergo processes such as combustion, pyrolysis or gasification to produce energy or energy fuel [33].

Table 1.3.2 Proximate analysis of different RDF samples

	<i>RDF<sup>1</sup> [wt%]</i>	<i>RDF<sup>2</sup> [wt%]</i>	<i>RDF<sup>3</sup> [wt%]</i>
Moisture Content	4.0	4.0	11.8
Ash Content	17.0	12.3	13.4
Volatile matter	64.0	77.8	71.0
Fixed Carbon	15.0	9.9	3.8

<sup>1</sup> Buah et. al., [34]; <sup>2</sup> Cozzani et. al., [33]; <sup>3</sup> Dou et. al., [35]

Table 1.3.3 Ultimate analysis of different RDF samples

	<i>RDF<sup>1</sup> [wt%]</i>	<i>RDF<sup>2</sup> [wt%]</i>	<i>RDF<sup>3</sup> [wt%]</i>
C	40.0	45.9	56.8
H	6.9	6.8	8.4
N	0.6	1.1	0.5
S	0.1	N/A**	N/A**
O*	52.4	33.7 <sup>a</sup>	3.0 <sup>a</sup>

<sup>1</sup> Buah et. al., [34]; <sup>2</sup> Cozzani et. al., [33]; <sup>3</sup> Dou et. al., [35]

\* obtained by difference \*\*not detected

<sup>a</sup> value as appeared in the cited reference

Generally, RDF is produced in pellet form, to obtain a better quality, high energy density fuel to be used in conventional boilers. The major advantage of RDF is the increasing calorific value as typically raw MSW has a calorific value of  $9 \text{ MJ kg}^{-1}$ , while this value increases up to  $18 \text{ MJ kg}^{-1}$  for RDF pellets [34]. Also the high content of volatile organic materials in RDF makes the production of oil with a thermal process such as pyrolysis favourable. According to the characterization studies in the literature, around 75 wt% of volatile matter is contained in the RDF. Although the composition of the RDF is highly dependent on the composition of the MSW collected, the proximate and ultimate analyses of different RDF samples that are shown in Table 1.3.2 and 1.3.3 indicate the range of the elemental composition of RDF in general [33-35].

#### **1.4 Aim and Objectives of this Research**

The objective of this research is to investigate the applicability of the hydrothermal processing for recycling of composite wastes. It is important to recover all the constituents of the waste and turn them into useful materials and/or fuel. For this purpose, three different kind of plastic waste samples were selected for this aim;

- (a) Carbon fibre reinforced plastic (CFRP)
- (b) Printed circuit board (PCB)
- (c) Refuse derived fuel (RDF)

The reason to choose carbon fibre reinforced plastic and printed circuit board is that both of them consist of a resin (polymer) fraction, and a material(s) that needs to be recovered. In the case of carbon fibre reinforced plastic, the polybenzoxazine type resin is to be recycled, and the carbon fibre is to be recovered. The printed circuit board has a phenolic resin, and the valuable metals are to be recovered. Both resin types are thermosetting, and it is not possible to recycle them with simple thermal processes, as in the case of thermoplastics. Finally, refuse derived fuel is the combustible waste that has been dehydrated and shredded from the municipal solid waste. RDF represents a good mixture of plastics and other kind of



biodegradable organic materials from where valuable chemicals and/or fuel gases consisting of  $\text{CH}_4$ ,  $\text{H}_2$  and  $\text{CO}$  can be produced.

Carbon fibre reinforced plastic waste was selected as one of the representative composite waste material in this research. Carbon fibres have a strategic importance, especially due to its military applications such as in protective helmets or in planes and missiles. They are a good replacement for steels and aluminium composite materials due to their high tensile strength, low density, high resistance to temperature and corrosion, and low thermal expansion [5, 6]. As mentioned in the previous sections, carbon fibres enhanced properties make them a good reinforcement material for the composite plastics. However, those great properties come with a cost, which is higher than steel. Also the pre-cursor for the carbon fibres are generally a fossil fuel based polymer (poly-acrylonitrile). Due to the large quantity of CFRP wastes expected within the next 10 to 20 years from projected end-of-life aeroplanes [10], it has become hugely important to develop efficient, clean and environmentally-friendly process for the recycling of this waste for the recovery of both resin and carbon fibre. Therefore, recycling of carbon fibre reinforced plastic wastes has crucial importance.

The aim is to recycle the resin fraction by depolymerizing it into monomers or useful chemicals, and at the same time to recover the carbon fibre by protecting its mechanical properties in order to use for re-manufacturing new composite materials as illustrated in Figure 1.4.1. For this aim, water and ethylene glycol, and also a mixture of both were used as solvents, and the effect of temperature, reaction time, additives such as  $\text{NaOH}$ ,  $\text{KOH}$  and oxidant ( $\text{H}_2\text{O}_2$ ) was investigated. The recovered carbon fibres were tested to find out if there is any reduction in the mechanical properties. In the last section, new composite material was produced with the recovered carbon fibre and the mechanical properties were tested and the results were compared with the one produced from virgin carbon fibre.

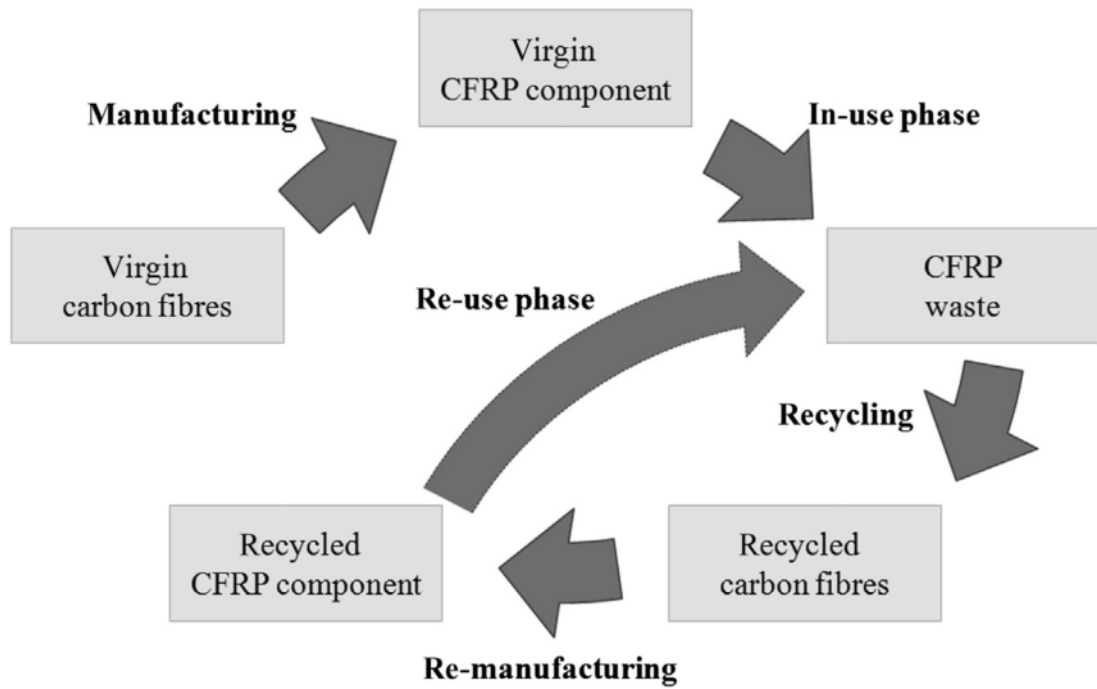


Figure 1.4.1 The carbon fibre reinforced plastics lifecycle loop adapted from [36]

Printed circuit boards are one of the main components in electronic devices, as they provide electrical interconnections between the components. The production rates of printed circuit boards have been increasing recently, as average worldwide production increased by 8.7% in 2009 [20]. This increase has been also reflected to the amount of the waste due to fast technological developments, high production and update rates, and consumer behaviours. Therefore much attention of public and scientists has been drawn because of the toxic materials such as heavy metals and brominated flame retardants in the waste printed circuit boards. Also the valuable metals such as gold, silver, titanium etc., in printed circuit boards, make their recycling strategically important for a sustainable economy and environment. Unfortunately, the existence of these valuable metals cause serious problems, as hazardous and primitive technologies are being used in the illegal recycling facilities running in poor areas [37]. For example, in Guandong province and Zhejiang province in China, serious environmental pollution was reported due to open dumping and burning, acid leaching and etc., of waste printed circuit boards as shown in Figure 1.4.2 [37]. As a result, likewise recycling of carbon fibre reinforced plastic wastes, it is

important to recycle waste printed circuit boards via a proper method without giving harm to environment.



(a)

(b)

Figure 1.4.2 Open air burning of waste PCB in Guiyu, Guandong province  
(a) the toxic gas release to the atmosphere (b) the residue after burning  
adapted from [37]

Currently in the UK pyrometallurgy and hydrometallurgy treatment processes are used for the waste management of PCBs. The main focus is on recovering the precious metals, while the resin part of the PCB waste is being used to supply energy to the process [38]. For carbon fibre recycling, pyrolysis and fluidised bed processes are being used as shown in Table 1.4.1.

Table 1.4.1 PCB and CFRP recycling facilities in the UK

<i>Company</i>	<i>Process</i>	<i>Outcomes</i>	<i>[ref]</i>
Johnson Matthey	Smelting/Chemical Leaching	Recovery of platinum, palladium and rhodium	[39]
GC Metals Ltd	Chemical, Electrical and Smelting Techniques	Recovery of gold, silver, platinum, palladium and rhodium	[40]
BASF Metals Recycling Ltd	Thermal Processing	Recovery of platinum, palladium, rhodium, iridium, ruthenium, gold, silver and rhenium	[41]
AWA Refiners	Melting/Chemical Leaching	Recovery of high value and precious metals	[42]
Milled Carbon Ltd	Continuous Pyrolysis and Fluidised Bed Process	Recovery of carbon fibres and precious metals	[43]
ELG Carbon Fibre Ltd	Pyrolysis	Staple Carbon Fibre	[44]

In this study, water, ethanol and acetone were used as solvents to depolymerise printed circuit board waste produced from desktop computer monitors. Alkalis (NaOH, KOH) and acetic acid were investigated as promoters to remove the resin part from the waste to recycle the polymer

fraction of the PCBs and to produce a chemical feedstock in addition to the recovery of the metals. The effect of temperature and reaction time were also studied, to construct a good method for recycling.

Refuse derived fuel is a good model to test the applicability of hydrothermal processing, as it represents a complex mixture of plastics, biodegradable materials and inorganic substances. In this study, refuse derived fuel samples underwent hydrothermal process to produce gas fuel, in the last section of the research. The effect of NaOH and Ru catalyst on the gas composition was investigated.

Utilizing a simple, cost effective, feasible and efficient process for waste recycling is strategically important. As summarised in this section, management of carbon fibre reinforced plastic and printed circuit board wastes have the bottom stage in the waste hierarchy, as most of the wastes are being disposed of by landfilling and/or incineration. To move to the recycling and recovery stages, many regulations and directives were adjusted by European Union. For example the EU Directive on End-of Life Vehicles (Directive 2000/53/EC places the responsibility of disposal of old vehicles on manufacturers. In addition, only 15 % by weight of car can be disposed of in landfill, while the remaining 85 wt% must be reused, recycled or treated for energy recovery with effect from 2006. By 2015, the proportion of a car allowed for landfill disposal will reduce further to 5 wt%. The current rise in the application of CFRPs will lead to increased generation and disposal of CFRP wastes in the next few years as aircrafts and other CRFP-associated equipment and utilities reach their end-of-life. Also the EU WEEE Directive in 2002 (Directive 2002/96/EC) was introduced for waste electronic and electrical equipment management. In 2008, this Directive was revised as the projections for 2020 showed that more than 12 million tonnes of waste electronic and electrical equipment generation in the EU, so the new WEEE Directive 2012/19/EU was put into action to better regulate waste electronic and electrical equipment generation and disposal.

Hydrothermal process offers a unique solution for complex waste recycling by utilizing water, and controlling the process parameters such as temperature and reaction time. Water is spread throughout the nature,

available in everywhere in the world and it is cheap, non-toxic and easy to utilize. It gains enhanced properties at its critical point, which enables to use water as a solvent, reactant and catalyst during the hydrothermal treatment of polymer wastes.

In this research, hydrothermal processing of waste carbon fibre reinforced plastics and printed circuit boards to degrade their resin (polymer) fraction into valuable chemicals and/or fuel gas for recycling and recovery of carbon fibres in CFRP waste and valuable metals in PCB waste were investigated. As a final step, the applicability of the hydrothermal process was tested on refuse derived fuel, as it is a good representative of municipal solid waste which is a complex waste mixture consisting of plastics, other biodegradable materials and inorganic materials.

## **1.5 Thesis Structure**

Hydrothermal processing of carbon fibre reinforced plastic, printed circuit board wastes and refuse derived fuels were investigated in this study. The thesis contains 7 chapters, and the contents are the chapters are as follows;

Chapter 2 contains a literature review about plastic recycling via hydrothermal processing. Firstly the change in the properties of water at critical point is discussed to explain the role of water during the hydrothermal processing. The current recycling routes were described briefly and hydrothermal treatment for recycling investigated in details to show the application of hydrothermal processing to thermoplastics and addition polymers.

Chapter 3 includes the materials and analytical methods used for the hydrothermal processing of carbon fibre reinforced plastic, printed circuit board wastes and refuse derived fuels. Also the characterisation of the waste samples was given in this chapter. The gas, liquid and solid residue analyses and analysis devices were described in detail.

Chapter 4 consists of three sections, each one focuses on the depolymerisation of carbon fibre reinforced plastic (CFRP) waste via hydrothermal processing via different types of solvents. Section 4.1 deals with the depolymerisation of CFRP waste in water, together with alkalis and oxidant agent. The effect of reaction temperature and time on the resin removal was investigated. Section 4.2 includes the results obtained from the depolymerisation of CFRP waste in ethylene glycol and ethylene glycol water mixture. Water and ethylene glycol was mixed in different proportions, and reacted with the resin at different temperatures and reaction times. The mechanical properties of the recovered carbon fibre were tested after the recovery. Section 4.3 contains results of the mechanical properties tests of fibre reinforced composites produced from recovered carbon fibres. The recovered carbon fibres were produced via hydrothermal depolymerisation in ethylene glycol and water mixture as described in section 4.2. The analysed mechanical properties were tensile, flexural and charpy impact strengths.

In chapter 5, the hydrothermal processing of printed circuit board waste was studied, and the results showed the applicability of this method on the thermosetting resins. Water, ethanol and acetone were used between 300 - 400°C to investigate the effect of the solvent type. Alkalis (NaOH, KOH) and acetic acid were used as additives to promote the removal of the resin fraction of the printed circuit board as recycled chemical feedstock from the waste.

Chapter 6 contains research carried out on refuse derived fuels (RDF). RDF represents a processed form of municipal solid waste (MSW) which is a highly heterogeneous mix of components. RDF comprises mostly the combustible fractions of MSW including paper, cardboards, textiles, wood and plastics. Arising from MSW, RDF also contains appreciable amounts of ash. Therefore, RDF was used to test applicability of hydrothermal processing to MSW.

Finally, Chapter 7 concludes the research on hydrothermal processing of carbon fibre reinforced plastic, printed circuit board wastes and refuse derived fuels. The outcomes of the research, and its contribution to the

literature were explained, and the future work was discussed to improve the outcomes of this research.



## References

1. Lundquist, L., et al., *Life Cycle Engineering of Plastics*. Materials & Mechanical. 2000: Elsevier Science Ltd. 1-220.
2. PlasticsEurope, *Plastics – the Facts 2014/2015: An analysis of European plastics production, demand and waste data*. [www.plasticseurope.org](http://www.plasticseurope.org), 2014.
3. 2008/98/EC, D. *Guidance on applying the waste hierarchy*. 2008; Available from: <https://www.gov.uk/government/publications/guidance-on-applying-the-waste-hierarchy>.
4. Chung, D.D.L., *Carbon Fiber Composites*, 1994, Elsevier.
5. Peters, S.T., *Handbook of Composites (2nd Edition)*, 1998, Springer - Verlag: London, UK.
6. Motoyuki, S., *Activated carbon fiber: Fundamentals and applications*. Carbon, 1994. **32**(4): p. 577-586.
7. Association, E.C.I. *Introduction to Composite Materials*. 2015; Available from: <http://www.eucia.eu/about-composites/intro/>.
8. Thomas Kraus, M.K., Dr. Elmar Witten, *Composites Market Report 2014: Market developments, trends, challenges and opportunities in Carbon Composites 2014*, European Composition Industry Association.
9. Tony, R., *THE CARBON FIBRE INDUSTRY WORLDWIDE 2011-2020: An Evaluation Of Current Markets And Future Supply And Demand*. Materials Technologies Publications, 2011.
10. Vicki P, M., *Launching the carbon fibre recycling industry*. Reinforced Plastics, 2010. **54**(2): p. 33-37.
11. Pimenta, S. and S.T. Pinho, *Recycling carbon fibre reinforced polymers for structural applications: Technology review and market outlook*. Waste Management, 2011. **31**(2): p. 378-392.
12. Oliveux, G., L.O. Dandy, and G.A. Leeke, *Current status of recycling of fibre reinforced polymers: Review of technologies, reuse and resulting properties*. Progress in Materials Science, 2015. **72**(0): p. 61-99.
13. European Parliament, C.o.t.E.U., *Directive 2012/19/EU of the European Parliament and of the Council of 4 July 2012 on waste electrical and electronic equipment (WEEE)*. Official Journal of the European Union, 2012.

14. UNEP, *Sustainable Innovation and Technology Transfer Industrial Sector Studies: RECYCLING – FROM E-WASTE TO RESOURCES*. 2009.
15. Widmer, R., et al., *Global perspectives on e-waste*. Environmental Impact Assessment Review, 2005. **25**(5): p. 436-458.
16. Hall, W.J. and P.T. Williams, *Separation and recovery of materials from scrap printed circuit boards*. Resources, Conservation and Recycling, 2007. **51**(3): p. 691-709.
17. Williams, P., *Valorization of Printed Circuit Boards from Waste Electrical and Electronic Equipment by Pyrolysis*. Waste and Biomass Valorization, 2010. **1**(1): p. 107-120.
18. Technology, A., *WEEE & Hazardous Waste Part 2*, in *A Report Produced for Defra2006*.
19. Jianzhi, L., et al., *Printed circuit board recycling: a state-of-the-art survey*. Electronics Packaging Manufacturing, IEEE Transactions on, 2004. **27**(1): p. 33-42.
20. Guo, J., J. Guo, and Z. Xu, *Recycling of non-metallic fractions from waste printed circuit boards: A review*. Journal of Hazardous Materials, 2009. **168**(2–3): p. 567-590.
21. Zheng, Y., et al., *The reuse of nonmetals recycled from waste printed circuit boards as reinforcing fillers in the polypropylene composites*. Journal of Hazardous Materials, 2009. **163**(2–3): p. 600-606.
22. Niu, X. and Y. Li, *Treatment of waste printed wire boards in electronic waste for safe disposal*. Journal of Hazardous Materials, 2007. **145**(3): p. 410-416.
23. Siddique, R., J. Khatib, and I. Kaur, *Use of recycled plastic in concrete: A review*. Waste Management, 2008. **28**(10): p. 1835-1852.
24. Panyakapo, P. and M. Panyakapo, *Reuse of thermosetting plastic waste for lightweight concrete*. Waste Management, 2008. **28**(9): p. 1581-1588.
25. Yokoyama, S. and M. Iji. *Recycling of thermosetting plastic waste from electronic component production processes*. in *Electronics and the Environment, 1995. ISEE., Proceedings of the 1995 IEEE International Symposium on*. 1995.
26. Leung, A.O.W., et al., *Spatial Distribution of Polybrominated Diphenyl Ethers and Polychlorinated Dibenzo-p-dioxins and Dibenzofurans in Soil and Combusted Residue at Guiyu, an Electronic Waste Recycling Site in Southeast China*. Environmental Science & Technology, 2007. **41**(8): p. 2730-2737.

27. Eswaraiah, C., et al., *Classification of metals and plastics from printed circuit boards (PCB) using air classifier*. Chemical Engineering and Processing: Process Intensification, 2008. **47**(4): p. 565-576.
28. Akita, S., et al., *Cloud-point extraction of gold(III) with nonionic surfactant-fundamental studies and application to gold recovery from printed substrate*. Separation Science and Technology, 1998. **33**(14): p. 2159-2177.
29. Kinoshita, T., et al., *Metal recovery from non-mounted printed wiring boards via hydrometallurgical processing*. Hydrometallurgy, 2003. **69**(1-3): p. 73-79.
30. Tammemagi, H.Y., *The waste crisis: landfills, incinerators, and the search for a sustainable future*. 1999: Oxford University Press.
31. Hoornweg, D. and P. Bhada-Tata, *What a waste: a global review of solid waste management*. 2012.
32. Blanco, P.H., et al., *Characterization of tar from the pyrolysis/gasification of refuse derived fuel: influence of process parameters and catalysis*. Energy & Fuels, 2012. **26**(4): p. 2107-2115.
33. Cozzani, V., et al., *A Fundamental Study on Conventional Pyrolysis of a Refuse-Derived Fuel*. Industrial & Engineering Chemistry Research, 1995. **34**(6): p. 2006-2020.
34. Buah, W., A. Cunliffe, and P. Williams, *Characterization of products from the pyrolysis of municipal solid waste*. Process Safety and Environmental Protection, 2007. **85**(5): p. 450-457.
35. Dou, B., et al., *Pyrolysis characteristics of refuse derived fuel in a pilot-scale unit*. Energy & Fuels, 2007. **21**(6): p. 3730-3734.
36. Pimenta, S. and S.T. Pinho, *Chapter 19 - Recycling of Carbon Fibers*, in *Handbook of Recycling*, E. Worrell and M.A. Reuter, Editors. 2014, Elsevier: Boston. p. 269-283.
37. Huang, K., J. Guo, and Z. Xu, *Recycling of waste printed circuit boards: A review of current technologies and treatment status in China*. Journal of Hazardous Materials, 2009. **164**(2-3): p. 399-408.
38. [www.wrap.org.uk](http://www.wrap.org.uk). *Demonstrating the economic benefits of different techniques for the recovery of printed circuit boards*. Techniques for Recovering Printed Circuit Boards (PCBs) 2014.
39. Matthey, J. *Precious Metal Refining*. 2015; Available from: <http://www.jmrefining.com/the-process>.
40. <http://www.refiningofpreciousmetals.com/servicesrefining.htm>. 2015; Available from: <http://www.refiningofpreciousmetals.com/servicesrefining.htm>.

41. *BASF Metals Recycling Ltd.* 2015.
42. Limited, A.R. 2015; Available from:  
<http://www.awarefiners.co.uk/about-us.php>.
43. Ltd, M.C.; Available from:  
<http://users.ox.ac.uk/~pgrant/Milled%20Carbon%20update.pdf>.
44. Ltd., E.C.F. *Recycled Carbon Fibre*. Available from:  
<http://www.elgcf.com/recycled-carbon-fibre/the-process>.

## **Chapter 2**

### **Literature Review**

#### **2.1 Hydrothermal Processing**

Hydrothermal technology has been used widely by many researchers and has many application areas in science and technology; from synthesis of chemicals to recycling processes. The first usage of the word 'hydrothermal' was by the British Geologist; Sir Roderick Murchison, to describe the role of water in the formation of rocks and minerals in the earth's crust [1]. After further developments, the 'Hydrothermal technique' was commercialized and used for the synthesis of inorganic compounds, especially metals from natural sources such as ilmenite, wolframite, cassiterite, laterites, etc. in the early 1900s [1].

Generally by definition, the hydrothermal technique is to dissolve (recrystallize) the materials that are insoluble under normal conditions with the help of aqueous solvents at high temperature and pressures, by means of heterogeneous reaction. However, introduction of solvents other than water to the reaction broadened the definition, so the solvent might be either aqueous or non-aqueous. This led to confusion in the name 'hydrothermal', so some of the scientists prefer calling the term 'solvothermal' [1].

With further improvements in the field, better understanding of the process was achieved and the technique has applied to many branches of science and technology. Today, the hydrothermal process is one of the best alternative techniques for recycling and/or energy production from wastes and biomass; as the waste polymers can be degraded into monomers and the organic compounds can be decomposed into fuel gas or liquid as chemical feedstock.

The main constituent in the hydrothermal process is water, due to the dramatic changes in its properties with the change in the temperature and pressure. Depending on the application area, the temperature and the

pressure can be over a wide range. In most cases, the pressure is higher than the atmospheric pressure (0.1 MPa), and the temperature is more than 100°C. However, the most radical changes in the properties of water are observed at its critical point, which highly affects its role during the hydrothermal reactions.

### 2.1.1 Role of Water

Water is the most abundant, non-hazardous and non-toxic substance in the world. Water is available in the liquid phase at standard ambient conditions (25°C, 0.1 MPa) with the properties given in Table 2.1.1 and Figure 2.1.1, to be used as processing fluid in industry especially hydropower plants, solvent for inorganic salts and natural compounds, cooking fluid for domestic purposes etc.. [2].

Table 2.1.1 Properties of Water [2]

<b><i>Properties</i></b>	<b><i>Values</i></b>
Molar mass	18.02 g/mol
Melting point	273.15 K
Boiling point	374.15 K
Density	997.1 kg m <sup>-3</sup>
Critical Pressure, P <sub>C</sub>	22.064 MPa
Critical Temperature, T <sub>C</sub>	647.096 K
Critical Density, ρ <sub>C</sub>	322 kg m <sup>-3</sup>
Viscosity	889.735 × 10 <sup>-6</sup> Pa s
Dielectric constant, ε	78.5

Those properties of water undergo phenomenal changes, when the temperature and pressure increase and reach values above the critical point. While water is a good solvent for ionic species at normal conditions, at supercritical conditions, it becomes a good solvent for organic substances as its dipole moment decreases to a value similar to organic solvents [2]. Another unique change is observed in its ionic product at near-critical

conditions, as more H<sup>+</sup> and OH<sup>-</sup> ions are released so the capability to catalyse reactions such as hydrolysis with its ions increases. Reactivity, the ionic product and the other properties (see Table 2.1.2) also change, and water becomes an ideal reactant, solvent and catalyst for hydrothermal treatment of hydrocarbons [3].

Table 2.1.2 Properties of Water at Different Conditions [2]

<i>Property</i>	<i>Ambient Conditions</i>	<i>Near-Critical Conditions</i>	<i>Supercritical Conditions</i>			<i>Superheated Steam</i>	
T (°C)	25	350	400	400	450	250	450
P (MPa)	0.1	25	25	50	25	2	1.5
$\rho$ (kg m <sup>-3</sup> )	997.45	625.45	166.54	577.79	108.98	8.9689	4.5624
$\eta$ (Pa s 10 <sup>-6</sup> )	890.45	72.81	29.18	68.02	28.96	17.85	26.51
$\epsilon$ (-)	78.5	14.865	3.8	12.16	1.745	1.03	1.03
pK <sub>w</sub> (-)	14.0	11.551	16.556	11.557	18.135	11.2	N/A

Water, with the molecular formula H<sub>2</sub>O, has a special structure, as each hydrogen atom is ordered between the oxygen atoms that covalently bonded (hydrogen bonds) to another molecule. This affects the boiling point and the critical point of the water, so that they are higher, compared to similarly structured substances such as H<sub>2</sub>S or NH<sub>3</sub> [2]. With increasing temperature, hydrogen bonds break and the water molecules aggregate to form clusters in a chain structure. The important changes in the water structure while reaching the critical conditions, such as the decrease in the viscosity and the dielectric constant are related to the changes in the structure [4].

As mentioned above, at ambient conditions, liquid water is poorly miscible with hydrocarbons and gases, while it can dissolve ionic species such as inorganic salts, due to its high dielectric constant (78.5) and the density (997.1 kg/m<sup>3</sup>). As the conditions of the water approach critical

conditions, those two properties decrease dramatically to a level which is similar to that of methylene chloride, so it becomes a good solvent for hydrocarbons [5]. Further increase in the temperature and the temperature yields higher values of the density and dielectric constant as shown in Table 2.1.2, as a result supercritical water becomes perfectly miscible with organic compounds.

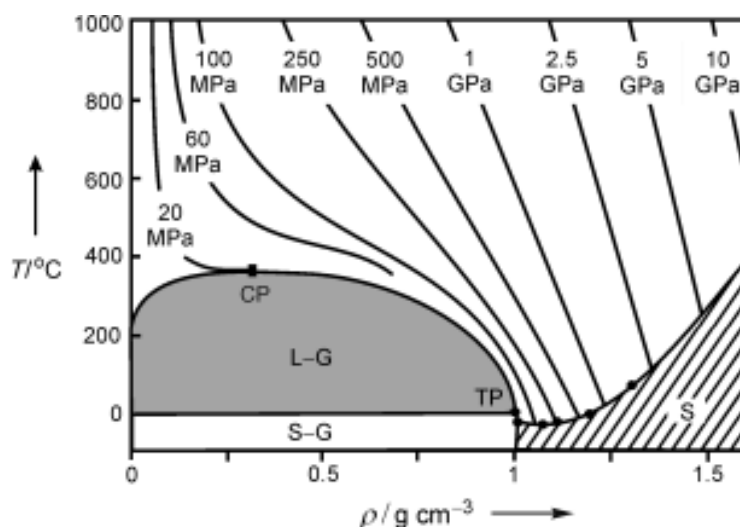


Figure 2.1.1 Phase diagram of Water [6]

Apart from being a good solvent for hydrocarbons, supercritical water is also a good reaction medium for homogeneous reactions due to having high diffusion rates and low viscosity. Also the high diffusion rates avoid the limitations in the mass transfer, the organic solvent properties of water prevent coke formation, and in the case of a heterogeneous catalyst usage, it prevents the poisoning of any catalysts used [5].

Because of the high pressure at critical conditions, the water medium has a higher collision frequency which promotes the reaction rates of small free radicals, however the reactions of high molecular mass free radicals are slowed down by a cage effect which means that the solvent surrounds the free radical molecule and prevents its contact with the other reactants, when these reactions occur during pyrolysis [2, 5].

Water also acts as a catalyst when its conditions approach near critical, due to the increase in the ionic product. Around temperatures of 200-300°C,



it catalyses acid-base catalysed reactions. Water is assumed to be involved in activated complexes during reaction, lowering the activation energy [2, 7].

All those changes in the water properties make it;

- a) A good solvent for organic compounds,
- b) A good reaction medium for homogeneous reactions,
- c) An acid (or base) catalyst.

So by making use of those important changes, water becomes the major constituent of the hydrothermal process. Numerous studies have been conducted among scientists to discover the applicability of the process to waste recycling or energy production from renewable sources.

All changes in the density, polarity and ionic product can be controlled by arranging the pressure and the temperature in supercritical water and thus in the hydrothermal process. So various reaction pathways may be created and controlled within the same solvent to react with different kinds of organic compounds. All those advantages make the hydrothermal process favourable by utilizing environmentally friendly, non-toxic, non-hazardous water.

## **2.2 Recycling of Waste Plastics via Hydrothermal Processes**

The application of hydrothermal processes to waste plastic recycling has great importance, as it offers a simple and environmentally friendly solution to recover the valuable organic materials by using water or other solvents..

### **2.2.1 Classification of the Waste Plastics**

The first step in plastic waste recycling is the identification of the plastic type, as the process parameters are highly dependent on the kind of the plastic. Plastic producers have used symbols to describe the material to help post consumers to be able to send the plastic wastes to the right route to be recycled. In Table 2.2.1, those symbols are represented and application areas of typical plastics are shown

Table 2.2.1 Typical applications of common plastics adapted from [8]








<i>Symbol</i>	<i>Abbreviation and Name</i>	<i>Typical Applications</i>
	PET: polyethylene terephthalate	Bottles and flasks for soft drinks, mineral water, detergents and pharmaceutical products; blister packs; packaging for ready meals
	HDPE: high-density polyethylene	Thick-walled applications such as bottles and flasks, barrels, jerry cans, crates and jalls; films for refuse bags; packaging for carpets and instruments
	PVC: polyvinyl chloride  PC: polycarbonate	Blister and press-through packs for medication; films for perishables  Refillable milk bottles; specific refillable packaging for liquids
	LDPE: low-density polyethylene  LLDPE: linear low-density polyethylene	Foil and film, such as shrink wraps, tubular film, sacks and covering wraps for bread, vegetables, fruit and carrier bags  Ultra-thin films: elastic wrap foil or stretch films
	PP: polypropylene	Buckets, crates, boxes, caps for bottles or flasks, transparent packaging for flowers, plants, confection products; yogurt and dairy product cups; industrial adhesive tapes

Table 2.2.1 Typical applications of common plastics (continued)

	<p><i>PS: polystyrene</i></p> <p><i>EPS: expanded polystyrene</i></p>	<p><i>Food service disposables; boxes and dishes for meat products and vegetables; boxes for ice; boxes for video tapes</i></p> <p><i>Buffer packaging for household devices, electronics and instruments; flasks and pipettes for the medical industry; egg packaging and fast food packaging</i></p>
	<p>Other</p>	<p>Other packaging</p>

The un-coded plastics are referred to plastic tarps, pipes, toys, computer keyboards, and other products that do not fit the numbering system [9]. By this way, the correct plastic waste can be sent to the recycling company. However, this research is more focused on the more complex situation, as those listed materials are only a part of the total plastic wastes. Thermosets and heterogeneous wastes are being investigated by many scientific groups, to find methods to recycle them.

### 2.2.2 Primary Recycling

Primary recycling is the simplest and most common type of recycling, as it is useful for recycling the off-specification scrap materials produced during the production in the plant. These easily identifiable materials can be mixed with the virgin material to give commercial products, instead of sending to landfill as wastes. This type of recycling can also be applied for single-type post-consumer plastic wastes, as it is feasible for unpolluted, relatively clean scrap [10].

### 2.2.3 Mechanical (Secondary) Recycling

Mechanical recycling was commercialized in the 1970s, as the treatment of plastic solid wastes using mechanical processes. It is feasible for the single-type polymers, but it is challenging to recycle wastes with more complexity and contamination via this method. It includes some pre-treatment and preparation steps. In most cases, initially the plastic wastes are processed for size reduction by grinding, milling or shredding in order to have the wastes in pulverized or pellet form. Then it is followed by a cleaning process, as contaminants can create heterogeneity which leads to different types of polymer formations during the process. The cleaning is done via washing with water for water-soluble impurities, however if there are contaminants such as glue, then chemical washing with caustic soda and surfactants takes place. After cleaning, the necessary additives and pigments are added and the waste is extruded in order to produce single-type polymer plastic [11, 12].

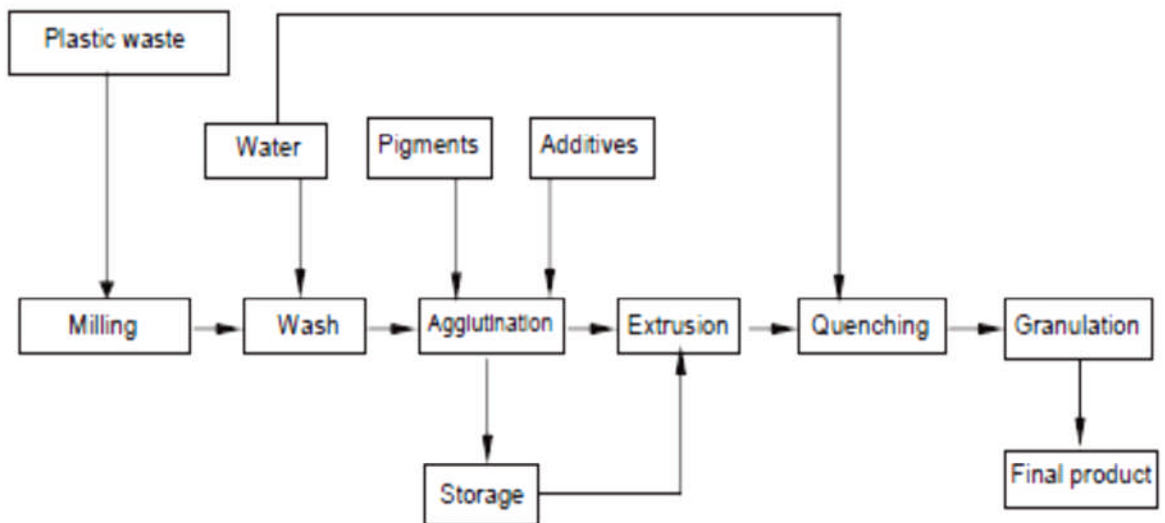


Figure 2.2.1 Stages of mechanical recycling [13]

### 2.2.4 Chemical (Tertiary) Recycling

Chemical recycling, also known as feedstock recycling, is treating the plastic wastes via chemical or thermal processes to produce their constituents, which are the monomers or petrochemical feedstock. Recent studies have shown that the products of chemical recycling are also useful

as fuel [12]. This type of recycling method is able to produce different types of petrochemicals. The main routes for recycling are thermal cracking (pyrolysis, gasification) and depolymerisation via hydrothermal processing.

Pyrolysis is a thermal cracking process which involves the degradation of the plastic waste at temperatures between 350 and 900 °C in the absence of oxygen. The products are usually char (solid residue) and a volatile fraction which mainly consists of condensable oil and non-condensable high calorific value gases [14]. The selectivity of thermal cracking reactions can be changed by adjusting the process temperature or the residence time, depending on the plastic wastes specifications. Although, increasing the temperature in most cases decreases the production rate of chars and increases the gas yield, it also increases the cost of the process. In that situation, a proper catalyst can be used to be able to depolymerize the waste at moderate temperatures.

Gasification is similar to pyrolysis, but since air is introduced to the process, the produced gas is rich in N<sub>2</sub>, which is an inert gas, and reduces the calorific value of the gas. The main gas products are CO<sub>2</sub> and H<sub>2</sub>, which can be used for the synthesis of important chemicals such as ammonia and methanol. But higher temperatures are necessary (typically 800°C) in gasification process compared to pyrolysis [10].

### **2.2.5 Energy (tertiary) Recycling**

Since they are petroleum derivatives; plastic wastes have high calorific values which make them a good energy source. However, when they are combusted in order to give energy, the produced gas mainly consisting of CO<sub>2</sub>, which increases the amount of the greenhouse gases in the atmosphere. Therefore, in many countries, the incinerations of plastic wastes are limited and only when other recycling methods are not feasible, energy recovery should be considered [10].

### **2.2.6 Hydrothermal Treatment for Recycling**

Hydrothermal processes are used for depolymerisation with the help of a suitable solvent to degrade the original polymer to recover the constituents of the plastic wastes. The most common solvent is water, while alcohols and

ethylene glycol might also be used. In the literature, the name of the process can be changed depending on the solvent utilized. For example, when water is used; hydrolysis, in case of alcohols, the name of the alcohol determines the name such as ethanolysis, methanolysis. Therefore, as a more common term, 'solvolysis' is used as the main term for this technique.

The hydrothermal process or solvolysis process can be listed under chemical recycling routes, as the waste is converted into its monomers and valuable chemicals. However, also depending on the reaction conditions and the feed type, fuel gas containing H<sub>2</sub> and CH<sub>4</sub> can be produced. In the following section, hydrothermal studies with common plastic waste types are reviewed to understand the applicability of the process.

## **2.3 Chemical Recycling of Common Plastic Wastes**

Chemical recycling via hydrothermal process is being researched by many scientists, as it enables the recovery the monomers from the plastic waste or to produce chemical feedstock which can be used as a fuel. In the literature, there are many studies with thermoplastics, as they can be degraded into their monomers relatively easily and selectively compared to thermosets even without catalysts, in water or alcohol [15]. On the other hand, the studies with thermosets and complex waste mixtures are still under investigation.

### **2.3.1 Common Reactions of Organic Compounds in Hydrothermal Medium**

The reactions of hydrocarbons in sub and supercritical water systems are important for polymer recycling. Water becomes a solvent, reactant and catalyst (via self-dissociation) at the same time. Also the quality of the products can be modified by preventing the undesired side reactions with the addition of catalysts (acids or bases) [5].

According to the literature data, it can be said that the reaction mechanism for aromatic and aliphatic hydrocarbons (without heteroatoms) are fundamentally the same during pyrolysis and in hydrothermal processing [2]. Water first acts as an inert solvent, then free radical chemistry may

involve [16]. The studies with bibenzyl [17], hexylbenzene and 1-decyl-naphthalene [18], and *n*-hexadecane [19] support this conclusion however there are also different reports in the literature showing that this behaviour can differ during the pyrolysis and hydrothermal processing [2].

At high temperatures (in supercritical water), aliphatic hydrocarbons can be reactive in hydrothermal systems. As mentioned above, the reaction chemistry is dominated by the free-radical mechanism. Watanabe et. al., [19] studied both the pyrolysis and hydrothermal processing of *n*-hexadecane and polyethylene. While the thermal pyrolysis was at 400-450°C and the inert gas was argon, hydrothermal processing was performed in supercritical water. They reported that the rates and the product distribution were almost the same for *n*-hexadecane. However, in case of polyethylene, the reactions were much faster in supercritical water and the product distribution differed compared to the products yielded during pyrolysis. This might be explained as the degradation products in supercritical water first dissolved in water and therefore were removed from the reacting molten polyethylene phase [16, 19].

The similar differences in the product distribution and reaction rates were observed in a study with *t*-butylbenzene. Ederer et. al., [20] stated that the reaction rate for *t*-butylbenzene decomposition in supercritical water was three times slower than in pyrolysis in argon atmosphere at the same temperature and ambient pressure. They used a flow reactor and the reaction conditions were 535°C, 25 MPa, and the reaction time was less than 1 minute. The differences between the two methods were explained as in water medium, the cage effects on decomposition reactions were observed and also the substitution reactions were promoted in supercritical water.

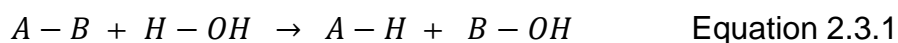
Aromatic hydrocarbons are stable in hot compressed water [2]. As the time approaches infinity, aromatic hydrocarbons remain stable at temperatures between 300 and 350°C in water and at 460°C. Hence aromatic hydrocarbons exhibit high stability for 1 hour under hydrothermal conditions as reported in the literature [18, 21]. The chemical reactions observed with aromatic compounds are limited to transformations of

substituent groups on the ring. Toluene and benzene are nonreactive at 300°C [18]. Ethylbenzene gives only 10 wt% decomposition at 450°C with a reaction time of 48 h, although it starts to decompose thermally at the same temperature [16, 22]. However, this behaviour is highly affected by addition of minerals, salts, alkalis etc., as their presence change the reactivity of hydrocarbons in hydrothermal medium [2, 16, 21, 23].

The experiments reported in the literature are generally carried out in a way that making comparison between the studies is very difficult. Also the hydrothermal studies are being conducted in batch systems, in which case it is difficult to interpret the results. To give an example, while studies for diphenylether were carried out for a residence time of 270 min in a batch reactor, the hydrothermal processing of *t*-butylbenzene was conducted in a flow reactor for 10-50 s reaction times. Therefore, the studies with batch reactors can be more useful to decide the parameters of the reactions, to construct or to design a process..

### 2.3.1.1 Hydrolysis Reactions

By definition, hydrolysis is the decomposition reaction of a compound by the action of the water as shown in Equation 2.3.1. Supercritical water medium is a proper reaction medium for the production of high value chemicals by the degradation of higher molecular weight compounds, such as the degradation of lignin (as a phenolic polymer) into phenols and phenolic compounds [2, 24].

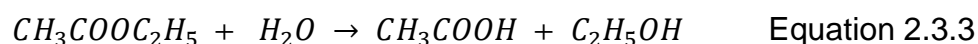


There are many application areas in which the hydrolysis processes take place such as in cleavage of fats and saccharose into glucose and fructose, the reactions of esters, in the cleavage of proteins into amino acids [2]. Water becomes a solvent and reactant during hydrolysis process, and also acts as a catalyst due to self-dissociation (Equation 2.3.2). The product selectivity can be managed with the addition of catalysts to prevent side reactions to take place [25]. In the literature, there are many studies related with the hydrolysis of esters, ethers, amines, amides, carbohydrates, proteins, etc. [2].





Hydrolysis of many esters such as acetates, phthalates, natural fats and others were investigated [2, 5]. Krammer and Vogel [26] studied the hydrolysis of ethyl acetate in a tubular reactor in sub and supercritical water. The reaction conditions were 250-400°C and 23-30 MPa and residence times of 4-230 s. According to Equation 2.3.3, ethyl acetate reacts with water to give ethanol and acetic acid:



As the temperature approached to 400°C, the conversion also increased but the selectivity for ethanol decreased. In this situation, the stability of ethanol and acetic acid gained an importance to decide the reaction conditions.

Ethanol and acetic acid were stable at temperatures around 250-400°C, at higher temperatures, ethanol dehydrated to ethene [2, 26]. However, it was reported in another study that ethanol was converted to ethylene at 400°C producing some gases such as H<sub>2</sub>, CO, CO<sub>2</sub>, CH<sub>4</sub>, C<sub>2</sub>H<sub>4</sub> and C<sub>2</sub>H<sub>6</sub> [27].

During hydrolysis of esters, carboxylic acids formation can occur which creates a potential for autocatalysis. Under hydrothermal conditions, decarboxylation of the acids might occur which forms carbonic acid due to production of CO<sub>2</sub>, which creates the autocatalytic effect [16]. Autocatalytic effects have been used in formation of glycols from hydrolysis of acetic acid diesters. Also formation of formic acid from hydrolysis of methyl formate and formation of glycerol from hydrolysis of glycerol triacetate with water are also with the help of autocatalytic effects [2].

The hydrolysis of ethers in sub and supercritical water has many similarities with the hydrolysis of esters [2, 5]. There are numerous studies with different ether compounds, such as guaiacol, phenylethyl phenyl ether, dibenzylether [28].

Klein et. al., [28] reported that while guaiacol decomposed to give methane, catechol, phenol and chars during pyrolysis, with the addition of water, the main products became methanol and catechol at supercritical water conditions (373 - 400°C). They stated that the selectivity of methanol as a product is highly dependent on the water's density. As shown in Figure 2.3.1, selectivity of methanol increased with the increasing density (or water concentration). The reduced density was referred as the initial water loading concentration [ $\text{g cm}^{-3}$ ] divided by the critical density of pure water.

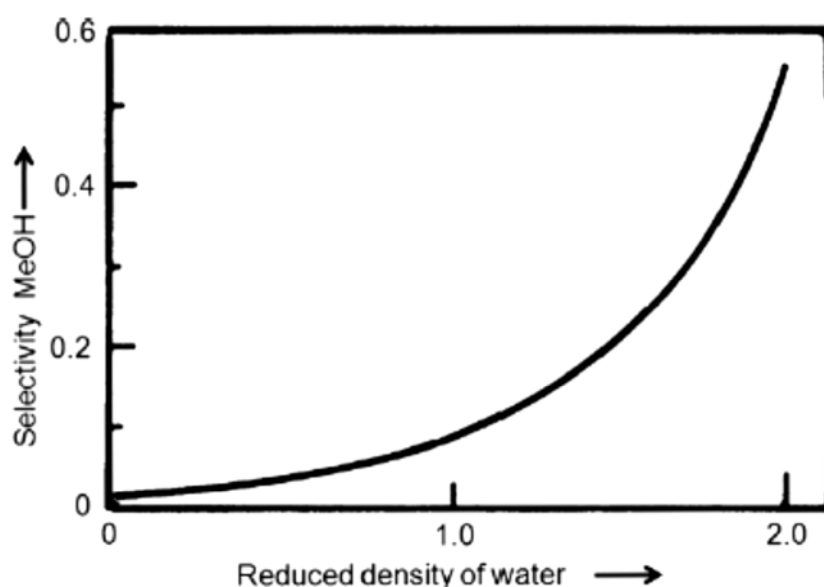


Figure 2.3.1 Selectivity of guaiacol hydrolysis to methanol with respect to reduced density of water [28]

In the same study, labelled water ( $\text{H}_2^{18}\text{O}$ ) was used to suggest a pathway for the hydrolysis reactions. According to their results, water molecules were incorporated into products by nucleophilic substitution which involves a saturated carbon with a heteroatom containing leaving group. The similar reaction mechanism was observed with dibenzylether, phenyl ethyl ether and esters (e.g. triacylglycerides) as shown in Figure 2.3.2 [28]. Also in the study with the ethylacetate, in subcritical water (350°C, 30 MPa, 170 s) the same mechanism occurred, i.e. the formation of a protonated ester is favoured in the subcritical range, because of the self-dissociation of water and the dissociation of the acid formed during the hydrolysis were increased [5, 26].



Figure 2.3.2 General reaction pathway for hydrolysis in supercritical water (LG: leaving group) adapted from ref [28]

Aromatic amines such as aniline, methylamine and benzylphenylamine are reactive in hydrothermal medium in the presence of catalysts, while aliphatic amines are less reactive [2, 5]. The hydrolysis of aniline was performed in a silver-lined tube reactor in the presence of phosphoric acid and its sodium salts as catalysts, at temperatures up to 450°C and between pressures of 40 and 70 MPa. The activation energy was lower when the reaction conditions are at subcritical water conditions, compared to the activation energy at supercritical water conditions. Also the reaction rate was increased, with the increasing pressure [5]. The hydrolysis of benzylphenylamine was carried out in a batch reactor at 385°C. The hydrolysis products were aniline, benzyl alcohol and toluene. The effect of pressure was tested between 22 and 100 MPa and it was concluded that the selectivity of hydrolysis increased with the increasing pressure, in the presence of NaCl [29, 30].

Methylamine was hydrolysed in supercritical water between the temperatures of 386 and 500°C. Ammonia and methanol were reported to be the main products of hydrolysis. When the water density was less than 0.28 g cm<sup>-3</sup> and the pressure was less than 25 MPa, the reaction rates were very low. With the increasing water density, the rate of conversion improved and the methanol yield increased [31].

The hydrolysis of alcohols also can be carried out in hydrothermal processing. Although the hydrolysis reaction is acid-catalysed, at supercritical conditions the concentration of H<sup>+</sup> ions increases due to the self-dissociation of water, and catalyses the reaction to some extent [2]. For example, ethanol decomposed only up to 7.4 wt% at temperatures between 433 and 494°C, and at a pressure about 25 MPa in the absence of any

catalyst. However, the hydrolysis of ethanol was performed rapidly when sulphuric acid at low concentration was added, to yield ethene mostly in supercritical water [32]. If an oxidant agent was added, ethanol decomposes to give acetaldehyde and formaldehyde in the liquid phase; with CO and CO<sub>2</sub> in the gas phase [33]. The hydrolysis rates and the decomposition path are highly dependent on the structure of the alcohol. Unlike ethanol, tertiary butanol totally decomposed in 30 s in subcritical water without and acid catalyse addition. For propanol, glycerol, glycol and cyclohexane, a mineral acid is necessary for hydrothermal processing [2].

Glycerol decomposed into liquid (methanol, acetaldehyde, propionaldehyde, acrolein, allyl alcohol, ethanol, formaldehyde) and gas (carbon monoxide, carbon dioxide, hydrogen) in supercritical water. At low temperatures, the ionic reactions took place at high pressures. As the temperature increased, free radical degradation dominated the reaction mechanism [34].

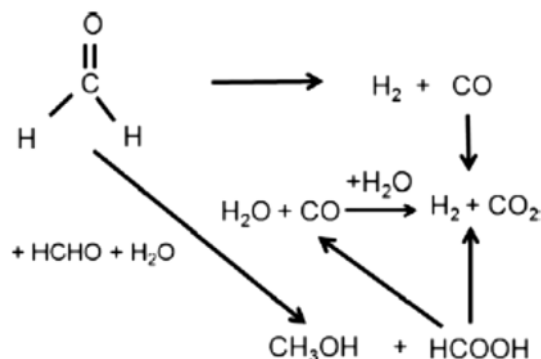


Figure 2.3.3 Hydrothermal reaction mechanism of formaldehyde in supercritical water, adapted from ref [2]

Aldehydes can be decomposed via hydrolysis. Formaldehyde was hydrolysed to give methanol, formic acid, hydrogen, carbon monoxide and carbon dioxide as shown in Figure 2.3.3. The yield of methanol increased with the increasing water density from 0.17 to 0.50 g cm<sup>-3</sup> at 400°C, while at low densities, CO yield was high due to monomolecular decomposition of formaldehyde. The main reaction pathway at higher water densities was

Cannizzaro reaction path, which is the disproportionation of an aldehyde into a carboxylic acid and an alcohol [35, 36].

Nitriles can decompose into amides and acids in hydrothermal medium as shown in Figure 2.3.4. Kramer et. al., [37] investigated the hydrolysis of acetamide acetonitrile, and benzonitrile at a temperature range of 350 – 450°C and a pressure range of 28 – 32 MPa in a tubular reactor in the absence of any additives. Acetonitrile and benzonitrile were decomposed into amides and carboxylic acid according to Equations 2.3.4 and 2.3.5, in where R stands for the methyl- or the benzyl group [2]. They reported that due to  $H_3O^+$  ions' catalytic effect, the activation energy of acetonitrile decreased with the increasing pressure.

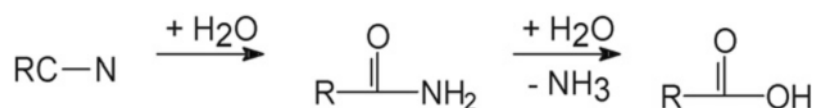
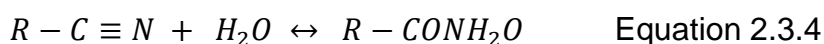


Figure 2.3.4 Hydrolysis of nitriles and amides to acids adapted from ref [5]



Acetamide is a product of the hydrothermal treatment of acetonitrile, and its hydrolysis yielded to acetic acid and a small amount of acetonitrile remained after the reaction. Acetic acid is stable up to 450°C in hydrothermal medium. Benzonitrile was decomposed into benzamide and then to benzoic acid [2, 37].

Hydrolysis of butyronitrile was carried out at 330°C at a pressure range of 12.8 – 260 MPa in a batch reactor. While a negligible amount of gas was produced, the main products were butyric acid, butanamide and ammonia as shown in Figure 2.3.5 [38].

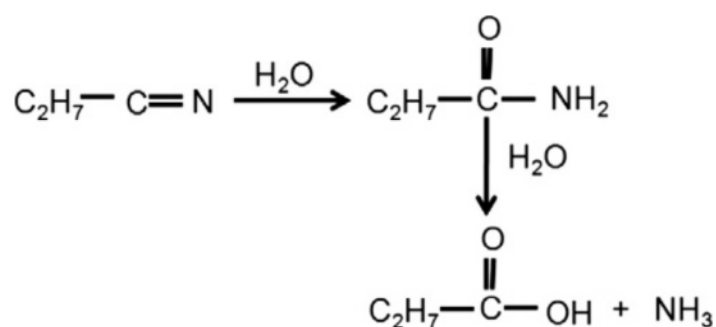
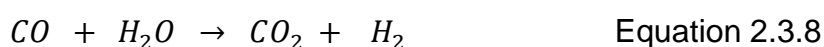


Figure 2.3.5 Hydrolysis of butyronitrile adapted from ref [38]

The hydrolysis of organic chlorides are important, as in hydrothermal medium,  $\text{Cl}^-$  ions from the organic chloride is eliminated by water, and because of the increasing concentration of chloride ions, corrosion problems occur. Due to these corrosive products, the reactions during hydrolysis may be affected [16]. During the hydrothermal treatment of aromatic and aliphatic chlorides, chloride (or in the form of HCl) is produced as a secondary product and attacks the metal walls of the reactor to form metal chlorides. The hydrolysis reactions are highly effected with the metal chloride presence, as it catalyses the reactions [16]. For example the decarboxylation of trichloroacetic acid under hydrothermal conditions was found to be influenced by the corrosion [39]. Hydrolysis of methylene chloride is an exception for this case, as no significant effect was observed during the hydrothermal treatment of methylene chloride in sub and supercritical water [40, 41].

Hydrolysis of methylene chloride in a tubular reactor at a temperature range of 450 – 600°C and at a pressure of 24.6 MPa yielded formaldehyde and HCl, and from formaldehyde to CO and  $\text{H}_2$ , as shown in the equations 2.3.16, 2.3.7 and 2.3.8 [41].



Also it was reported that the hydrolysis reaction of methylene chloride to form formaldehyde and HCl occurred fast under subcritical conditions of

water, while when the supercritical conditions reached, the reactions slowed down. This was due to reduction in the dielectric constant of water at supercritical conditions, as the reactions taking place during the hydrolysis involved polar species as reactants or intermediates, which decreased at high temperatures [16].

### 2.3.1.2 Condensation Reactions

By definitions, condensation reactions are the combination of two or more molecules to form a larger molecule and release a simple molecule such as  $\text{H}_2\text{O}$ ,  $\text{HCl}$  or  $\text{NH}_3$  [2]. Water can be the solvent, product and also the catalyst, due to its self-dissociation to release  $\text{H}^+$  ions [5]. Formation of esters can be a good example of condensation reactions, as in the cases of benzyl alcohol and phenethyl alcohol decomposition in aqueous acetic acid medium. They reacted to yield benzyl acetate and phenethyl acetate in hydrothermal conditions [18, 42]. Also formation of carbonyl groups, ethers and benzylether were carried out in sub and supercritical water without any acid catalysts [5].

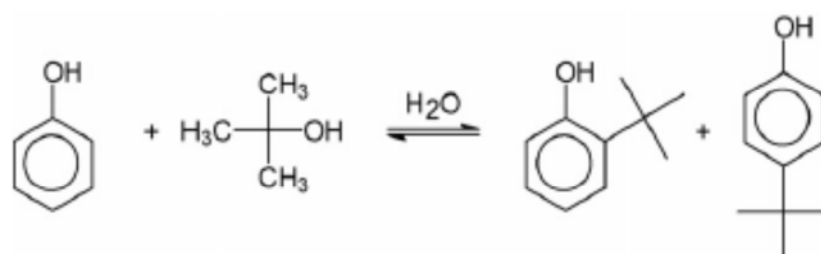


Figure 2.3.6 Friedel-Crafts alkylation

A special type of condensation reaction is the Friedel–Crafts alkylation, which is the alkylation of an aromatic ring with an alkyl halide using a strong Lewis acid catalyst, as shown in Figure 2.3.6 [5]. Friedel–Crafts alkylation of phenol and *p*-cresol with *tert*-butanol, isopropanol and *n*-propanol was investigated at  $275^\circ\text{C}$ . The fastest alkylation was observed when phenol was reacted with *tert*-butanol to form 2-*tert*-butylphenol. At this temperature, the  $\text{H}_3\text{O}^+$  and  $\text{OH}^-$  ions' concentration reach a maximum, so that the perfect medium for acid or base catalysed reactions was supplied [43].

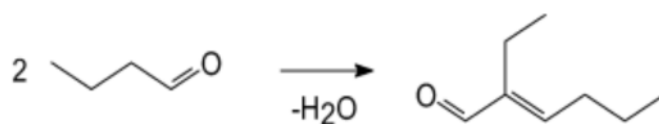


Figure 2.3.7 Aldol condensation reaction scheme

In general, aldol condensation reactions are base-catalysed reactions. In subcritical water, without any base catalysts, n-butyraldehyde reacted to give 2-ethyl-3-hexenal at 275°C, as the reaction scheme is shown in Figure 2.3.7 [44].



## 2.3.2 Application of Hydrothermal Organic Reactions for Plastics Recycling

### 2.3.2.1 Hydrolysis of Condensation Plastics

#### 2.3.2.1.1 Polyethylene Terephthalate (PET)

Polyethylene terephthalate (PET) is an important member of condensation plastics with its semi-crystalline thermoplastic polyester structure [2]. It is one of the major polymers used in the packaging industry.

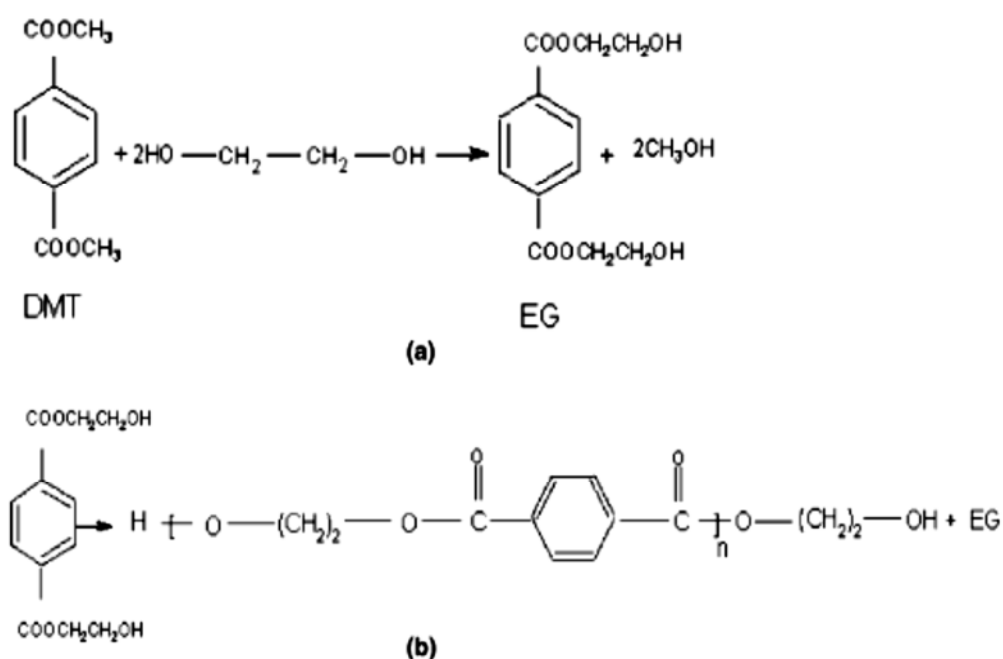


Figure 2.3.8 PET synthesis reactions (a) via trans-esterification (b) via condensation [45]

The demand for PET in the European Union (EU27) has increased rapidly as 1.9 m tonnes in 2001 were used for containers whereas 3.1 m tonnes were used in 2011; which means an average annual growth rate of about 6% in PET demand. About 1.6 million tonnes of PET were collected for recycling in Europe, in 2011 and this amount is likely to be increased as the new routes for recycling have been developed [46]. PET can be produced with the esterification reaction between terephthalic acid (TPA) and ethylene glycol (EG) at temperatures between 240 and 260 °C.

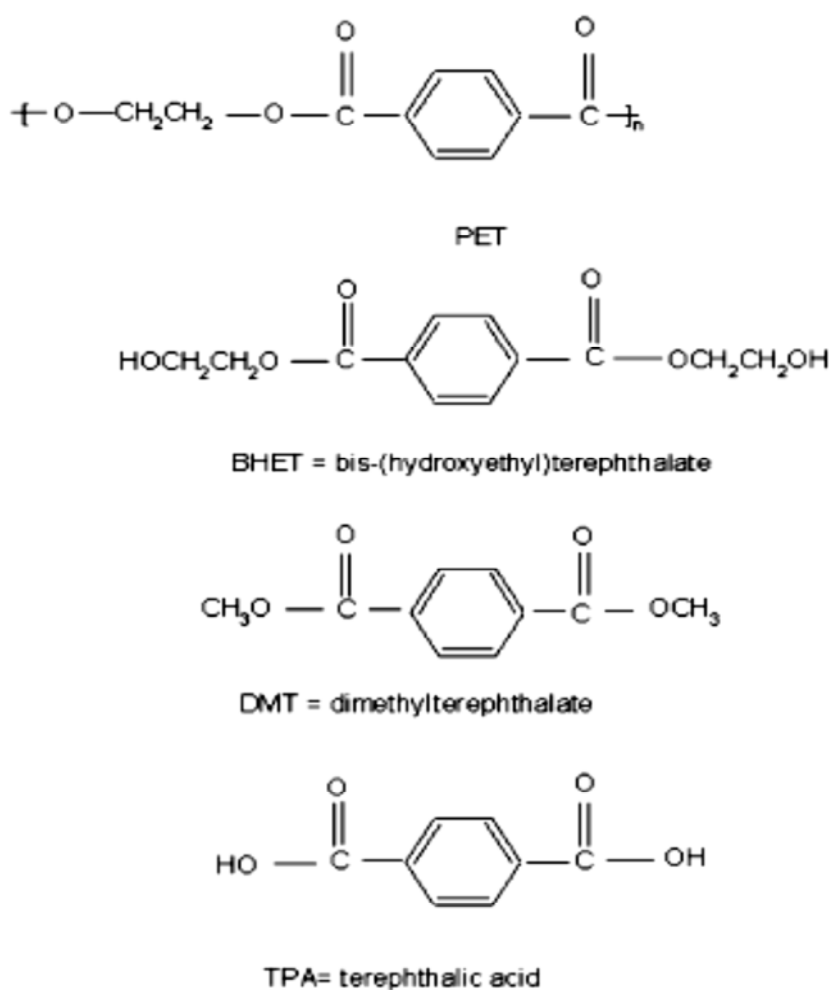


Figure 2.3.9 The depolymerisation products of PET [45]

PET can also be produced with the trans-esterification reaction of dimethyl terephthalate (DMT) and EG at temperatures between 150 and 240°C (see Figure 2.3.8) [45, 47]. Bis(hydroxyethyl) terephthalate (BHET) is produced after those reactions and to produce PET, pre-polymerisation applied to BHET up to a degree of polymerisation of 30. The final step is the polycondensation, in which the polymerisation occurs at around 285°C to increase the degree of polymerisation to 100 [48]. So the final product of PET has the properties such as the melting point of 260°C and a glass transition temperature between 70 and 115°C [49].

Depolymerisation of PET via methanolysis, glycolysis and hydrolysis has been studied widely, and the results were promising [50-52]. Depending

on the solvolysis process, the depolymerisation products of PET can be bis(hydroxyethyl) terephthalate, dimethyl terephthalate, terephthalic acid (see Figure 2.3.9) and ethylene glycol. Sako et. al., [53] reported that PET was totally decomposed in supercritical methanol to give its monomers with a reaction time of 30 min without a catalyst. Goto et. al., studied degradation of PET in supercritical methanol in a batch reactor for various reaction times. They found that PET was decomposed to its monomers; dimethyl terephthalate and ethylene glycol. Although no water was introduced to the process, some terephthalic acid monomethyl ester (TAMME) was found, which needs water to be produced. Therefore they concluded that water may be produced from either esterification or dimerization of ethylene glycol. Methyl-(2-hydroxyethyl) terephthalate (MHET), 2-methoxyethanol (ME), diethylene glycol (DEG) were the side products observed after the reaction. They also described the reaction mechanism of PET decomposition in methanol in Figure 2.3.10 [50, 54].

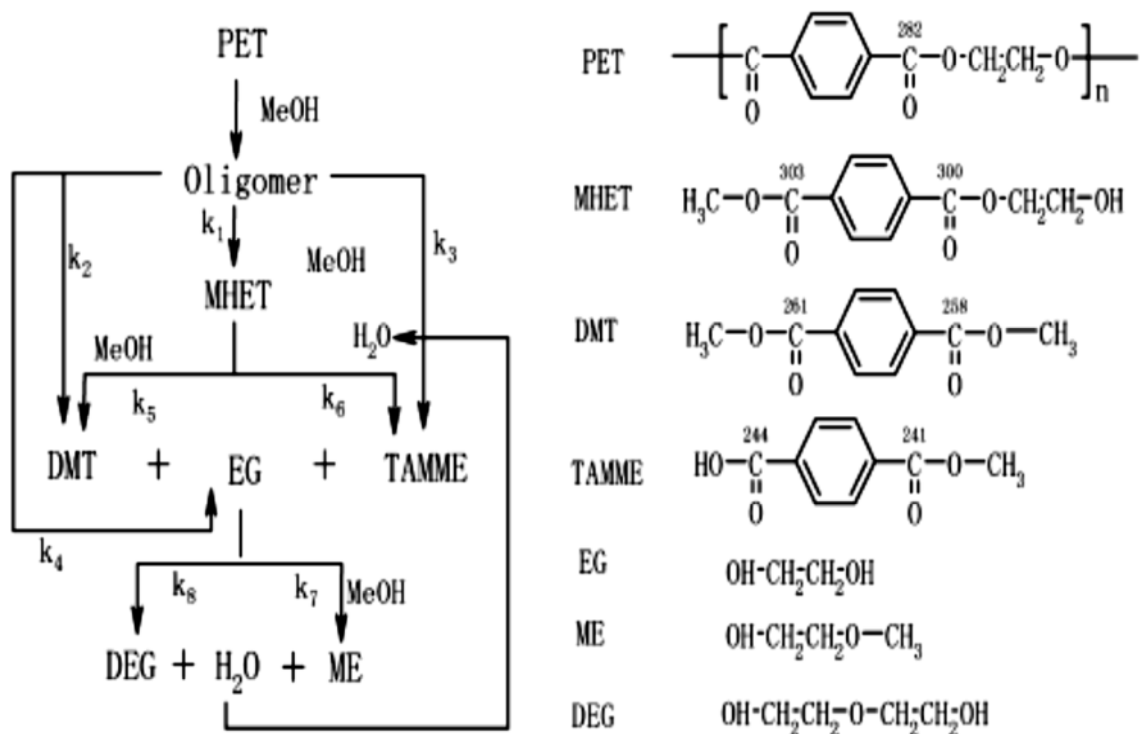


Figure 2.3.10 Reaction scheme of decomposition of PET in methanol [54]

Genta et. al., [55] ] studied the kinetics of PET depolymerisation in supercritical methanol to develop a chemical recycling process for postconsumer PET bottles. They also investigated PET with low molecular weight such as its oligomers, as they used bis(hydroxyethyl) terephthalate and methyl-(2-hydroxyethyl) terephthalate as reactants to describe the reaction kinetics and the routes of depolymerisation. They concluded that reactions from PET to its monomers were proceeding through methyl-(2-hydroxyethyl) terephthalate. They also researched the process in terms of reaction rate and energy demands, and found that usage of supercritical fluid decreased the reaction time without using a catalyst, as well as decreased the energy consumption [56].

Baliga et. al., [51] depolymerized PET by glycolysis in ethylene glycol at 190 °C with a metal (lead, zinc, cobalt and manganese) acetate catalyst. When the chemical equilibrium was reached after 8 h, they found that the main product was bis(hydroxyethyl) terephthalate. Lopez-Fonseca et. al., [57] carried out depolymerisation of PET by using an excess amount of ethylene glycol. At 196 °C, they obtained a yield of 70% of bis(hydroxyethyl) terephthalate by using zinc acetate as a catalyst. The other products were identified as oligomers. Abdelaal et. al., [58] glycolized PET via different glycols; propylene glycol, diethylene glycol, triethylene glycol and a mixture of them to get unsaturated polyester (UP). They treated the glycolysis products with maleic anhydride and after adding styrene, they obtained UP. They concluded that the results were promising as the produced UP had suitable properties for commercial purposes.

The yield of bis(hydroxyethyl) terephthalate, so the decomposition rate of PET even increased when ethylene glycol at its near and supercritical conditions was used. Imran et. al., [59] had 90% yield for bis(hydroxyethyl) terephthalate when they conducted the experiments at 450°C and 15.3 MPa which represents supercritical conditions for ethylene glycol. Also with the usage of sub- and supercritical ethylene glycol, the reaction time was shortened.

PET can be decomposed by hydrolysis; it decomposes into its monomers; terephthalic acid and ethylene glycol. Campanelli et al. [60]

studied the hydrolytic depolymerisation of molten PET in water medium, using a 2 L stirred pressure reactor at temperatures of 250, 265, and 280°C. They found that as water/PET (w/w) increased to 5:1 and greater values, complete depolymerisation to monomers was observed at 265°C. They also investigated the effects of zinc catalyst; the addition of catalyst increased the reaction rate constant slightly [52, 60].

Mishra et. al., [61] investigated the pressure effect in the hydrolysis of PET, as they performed experiments at temperatures of 100, 150, 200 and 250°C and a variation of pressures from 1.4 to 5.5 MPa. They had the maximum yield in depolymerisation of PET at 250°C and 5.5 MPa. However, the maximum rate of reaction was observed at 200°C and 3.4 MPa. Below 200°C, depolymerisation of PET was negligible. For constant temperature, there was a little effect of pressure on depolymerisation.

De Castro et. al., [62] investigated the depolymerisation of PET in supercritical ethanol (above 243°C and 6.4 MPa). PET samples decomposed to form diethyl terephthalate (DET) and either ethylene glycol or bis(hydroxyethyl) terephthalate as the main products. The maximum terephthalic acid recovery was 98.5% at 255°C and 5 h reaction time. They also used water in their experiments as an additive to see the effect of ethanol/water mixture. It was recorded that the addition of small amounts of water accelerated the depolymerisation of PET.

Karayannidis and Achilias [63] studied the depolymerisation of PET flakes in NaOH solution (5-15 wt%). The reaction temperature was between 75 and 95°C and the reaction time was 5 to 6 h. Trioctyl methyl ammonium bromide (TOMAB) was used as a catalyst to increase the reaction rate. They described the depolymerisation path as; PET rapidly degrades due to the attraction from OH<sup>-</sup> groups. The terephthalate anion reacts with Na<sup>+</sup> ions to form disodium terephthalate (TPA-Na<sub>2</sub>) and EG (see Figure 2.3.11).

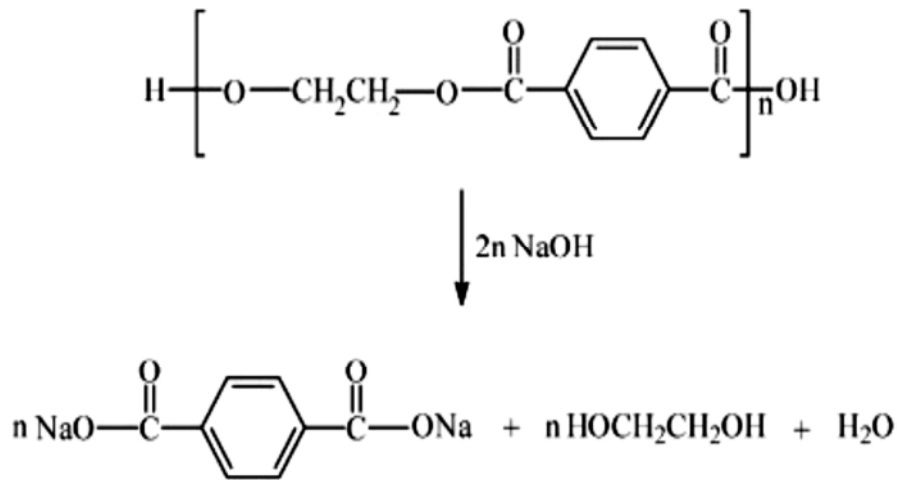


Figure 2.3.11 PET depolymerisation in NaOH solution [63]

The presence of trioctyl methyl ammonium bromide (TOMAB) as catalyst increased the production of terephthalic acid, as without TOMAB, the terephthalic acid yield was only 7 wt% while with the addition of 0.01 mol of it increased the yield to 90 wt% [64]. They also investigated the acidic depolymerisation of PET by using a 70-83 wt%  $\text{H}_2\text{SO}_4$  solution as the reaction media. PET was totally decomposed at  $90^\circ\text{C}$  after 3 h of reaction time. However, in terms of cost, acidic depolymerisation with  $\text{H}_2\text{SO}_4$  was not considered as an efficient process [65].

When water at its critical condition is used, the reaction time needed for total decomposition decreases. Sato et. al., [66] studied depolymerisation of PET using water at high temperatures to yield terephthalic acid and ethylene glycol. They conducted experiments at a temperature range of  $250 - 420^\circ\text{C}$ , pressures up to 48 MPa and residence time range of 10-60 minutes. At  $250^\circ\text{C}$ , TPA yield increased to 80 mol% with a residence time of 60 min whereas the yield of ethylene glycol was lower than that of terephthalic acid. The yields of terephthalic acid and ethylene glycol increased to 90 mol% and 70 mol% respectively at  $300^\circ\text{C}$  with 10 min residence time. As the reaction time increased, the yield of ethylene glycol decreased. Also at higher temperatures, TPA yield decreased to 80 mol% and ethylene glycol yield to 10 mol%. The secondary products were acetaldehyde, diethylene glycol and triethylene glycol.

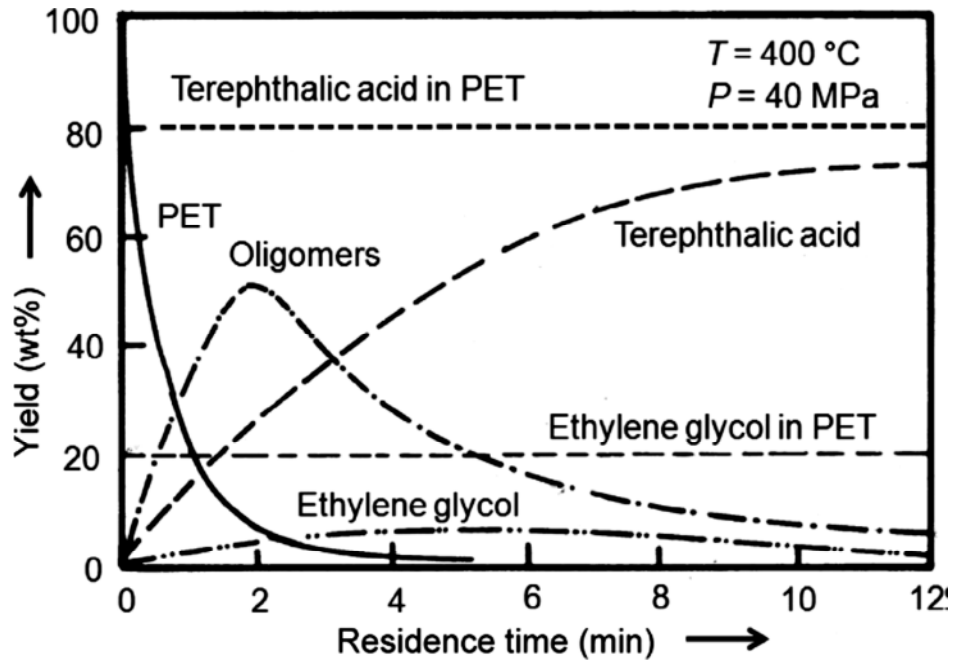


Figure 2.3.12 Depolymerisation products of PET in supercritical water (400°C, 40 MPa) [2]

In an another study, with a reaction time of 12.5 min the PET decomposed to terephthalic acid with a yield of 91 wt%, and ethylene glycol at 400°C and 40 MPa. The reaction rate was highly influenced with the temperature, as a decrease in the temperature to 300°C, slowed the reaction. The influence of pressure effect was also investigated, the char and carbon dioxide formation decreased with the increasing pressure. The results of PET depolymerisation with supercritical water are shown in Figure 2.3.12 with respect to residence time [2, 67].

Fang et. al., [68] investigated the phase behaviour of the PET-water mixture during hydrothermal treatment. The PET concentration range was between 12 to 59% in their study, and they showed that the mixtures became mostly homogeneous, when the temperature reached 240°C which is the melting point of PET when the heating rate was slow. With the increasing heating rate, the temperature where homogenous mixture occurs was also increased. PET particles that were rapidly heated to supercritical conditions underwent crystallization and surface hydrolysis which means that simultaneous dissolution and reaction occurred during the melting of the crystalline oligomers.

Hydrothermal processing of PET for recycling in supercritical water has advantageous, compared to methanolysis and glycolysis, because the reaction time decreases. Recently a supercritical water depolymerisation process was developed in Japan, which has an efficiency for PET recycling of about 99% [69].

#### **2.3.2.1.2 Polycarbonates (PC)**

Polycarbonates (PC) are also one of the widely used plastics in both engineering and commodity applications, as they provide resistance to temperature, resistance to impact and optical properties. Polycarbonate wastes can be depolymerized by solvolysis to yield bisphenol A (BPA) (Figure 2.3.13), which is the precursor of Polycarbonates [15].

Hu et. al., [70] studied alkali catalysed methanolysis of PC by using a mixture of methanol and toluene or dioxane as a solvent and NaOH as catalyst. PC was totally decomposed after being treated for 70 min at 60°C to yield bisphenol A in the solid phase and dimethyl carbonate (DMC) as a liquid product. Pinero R. et. al., [71] studied PC depolymerisation in methanol at subcritical conditions. As an outcome of their experiments, the optimal reaction conditions were found to be 120–140°C and 10 MPa, in which an optimal yield of bisphenol A and dimethyl carbonate was reached. Negligible formation of undesired by-products was reported, with a catalytic reaction medium of 1.5–2 kg m<sup>-3</sup> of NaOH in pure methanol. Reaction rate was considerably improved by temperature and NaOH concentration, although a high catalyst concentration affects the mechanism of the reaction and makes dimethyl carbonate yield decrease. Reaction time increased with the ratio of H<sub>2</sub>O/methanol, and selectivity was lower due to the formation of other aromatic products, while pressure had no significant influence on reaction rate.



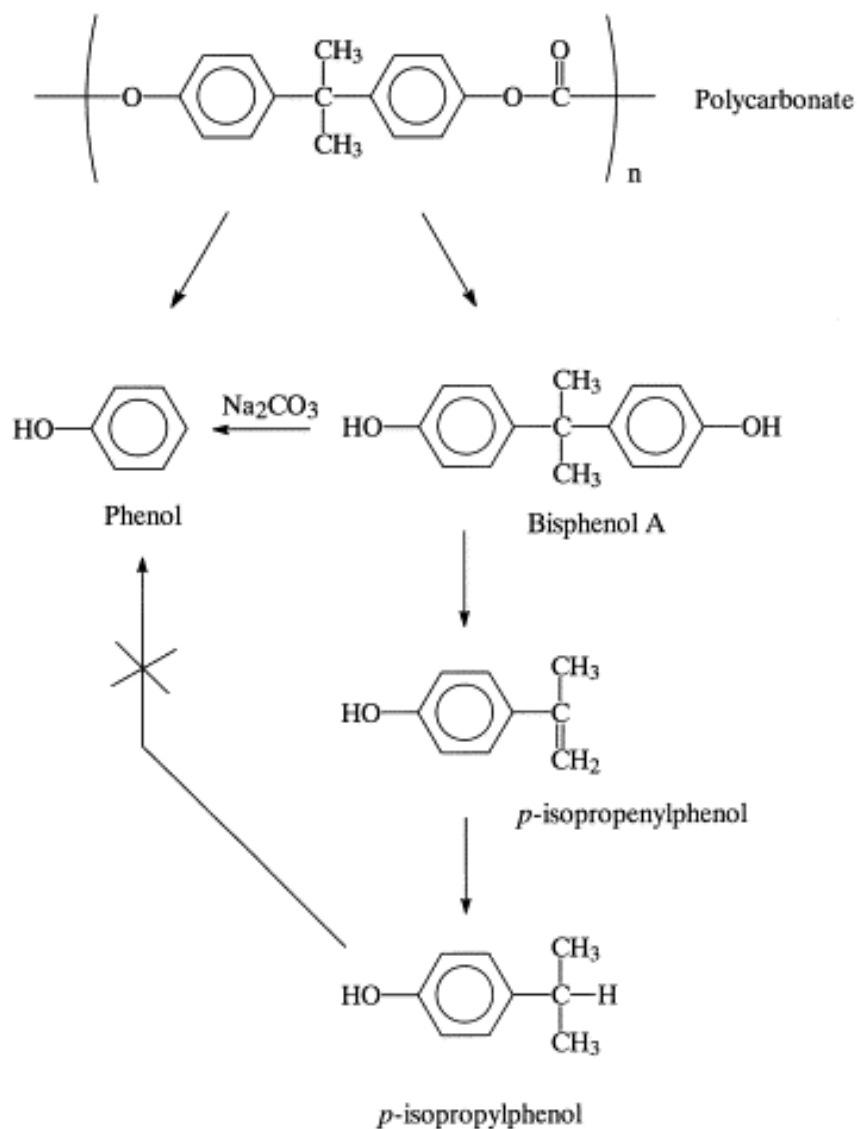


Figure 2.3.13 Decomposition reaction of PC [72]

Ikeda et. al., [73] found that PC was decomposed into phenol, bisphenol A and p-isopropenylphenol by the reaction at 130–300°C in water. The decomposition reaction was accelerated by the addition of  $\text{Na}_2\text{CO}_3$ , and the yield of identified products reached 68% in the reaction at 250°C for 1 h. By using the decomposed products, the pre-polymer of phenol resin was synthesized. Watanabe et. al. [74] found that PC can be hydrolysed in high pressure and temperature steam near the saturation pressure of water at 300°C. For 5 min reaction time, polycarbonate completely decomposed into bisphenol A with a maximum yield of 80%. In the liquid water phase at 300°C, PC could not be depolymerised even for 50 min reaction time. They concluded that; the high yield of bisphenol A in high pressure steam was due

to its high stability. The amount of water required for PC degradation was reduced, so the high pressure and temperature steam process was found to be feasible.

Grause et. al., [75] studied the hydrolysis of waste electrical and electronic (WEE) equipment, which mainly consisted of PC, in a steam atmosphere between the temperatures of 300 to 500°C with the addition of MgO and CaO as catalysts. The maximum bisphenol A yield was 91% at 300°C and as the temperature increased, bisphenol A decomposed further to give degradation products such as phenol, 4-isopropenyl phenol. Although pure PC was depolymerized in 15 min, hydrolysis of WEE waste took 30-60 min, since it contained other polymers like polystyrene and triphenylphosphate whose presence reduced the rate of the reaction by preventing steam from interacting with the surface of the PC.

Tagaya et. al., [72] depolymerized PC into phenol, bisphenol A, p-isopropenylphenol, and p-isopropylphenol by reaction at 230°C to 430°C in water. The decomposition reactions were accelerated by the addition of Na<sub>2</sub>CO<sub>3</sub>, and the yields of identified products reached 67% even at the reaction at 300°C for 24 h. In supercritical water, the production of p-isopropylphenol was confirmed and the yield of phenol, bisphenol A, p-isopropenylphenol and p-isopropylphenol reached 88.9% for the reaction at 430°C for 1 h.

#### **2.3.2.1.3 Nylons**

Nylon 6, as polyamide, has a large usage, as it is used for clothing, fibre and packaging. Commercially it has been produced by polymerization with ring-opening reaction of  $\epsilon$ -caprolactam [76]. Decomposition of nylon 6 via solvolysis has been investigated for chemical recycling. Kamimura et. al., [77] investigated the decomposition of nylon 6 using supercritical methanol. The main product was the precursor of nylon 6, which is  $\epsilon$ -caprolactam and the intermediates were N-methylcaprolactam and methy 6-(N,N-dimethylamino)caprolactam.

Iwaya et. al., [76] searched the effects of temperature, reaction time and water density for the depolymerisation of nylon 6 in sub- and supercritical water,  $\epsilon$ -caprolactam and  $\epsilon$ -aminocaproic acid were the chief products (see Figure 2.3.14). The highest yield of  $\epsilon$ -caprolactam was 85%. At high temperatures (above 360°C); the yield of  $\epsilon$ -caprolactam decreased as the reaction time increased since secondary reactions took place. At supercritical temperature, the  $\epsilon$ -caprolactam production rate was increased with water density.

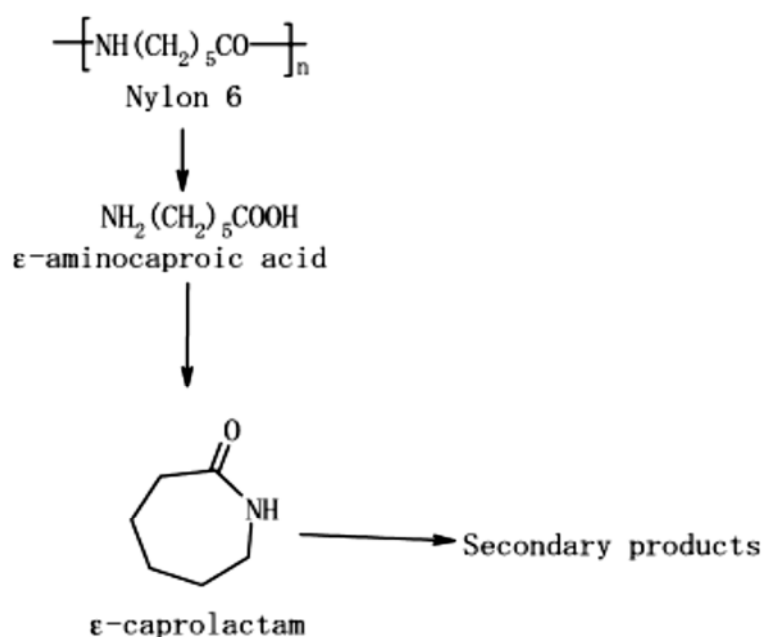


Figure 2.3.14 Decomposition of nylon 6 in subcritical water [15]

Kaiso et. al., [78] examined different types of hydrocarbon solvents to depolymerize nylon 6 with the addition of water at its critical point. Treatment at 370°C for 1 h, showed effective decomposition when supercritical toluene in the presence of a small amount of water was used. In the absence of water, the depolymerisation failed, as they reported.

Polyurethanes have been used in many applications such as foam as insulation in walls, roofs; in medical devices, footwear, coatings and automotive interiors as they provide long life due to their durability [79]. They can be depolymerized via solvolysis. The hydrolysis products of polyurethane (PU) are polyols which can be used as fuels and amine

intermediates which can be re-used to produce different PU components. Dai et. al., [80] used superheated water to degrade PU foam at temperatures between 250°C and 450°C. The optimum conditions were stated as 350°C reaction temperature and 30 min reaction time, in which they obtained 72% diaminotoluene by the end of the experiment.

Glycolysis of PU is the most common method for recycling. Gerlock et. al., [81] researched glycolysis with the addition of a small amount of water (hydroglycolysis). They found that the process was feasible, as they were able to depolymerize contaminated water-blown polyurethane wastes.

### **2.3.3 Degradative Hydration of Addition Polymers**

#### **2.3.3.1 Polyethylene**

Polyethylene (PE) is a thermoplastic polymer consisting of long hydrocarbon chains, and has a wide range of application especially in the packaging industry with an annual production rate of 60 million tonnes [15]. Depending on its density, polyethylene has a melting point in the temperature range between 105 and 130°C.

Polyethylene can be degraded via hydrothermal treatment. Moriya et. al., [82] degraded polyethylene in supercritical water and they obtained alcohols (2-propanol and 2-butanol) and ketones (2-propanone and 2-butanone) as the main products. The product distribution was 90% of liquid and 6% of gas after 2 hours reaction time at 425°C.

High density polyethylene (HDPE) is produced from ethene, and the polymer has a chain length of 500000 to 1000000 carbon units. It has a melting point of 130°C and a density of 0.941 g/cm<sup>3</sup> [83]. The uses of HDPE are generally for the packaging industry and the annual production rate is 5.5 million tonnes [84]. The main research for recycling has been carried out on pyrolysis of HDPE in different types of reactors such as in a reactive extruder or in a fluidized sand bed reactor [85, 86].

Usage of catalyst creates better reaction conditions for the pyrolysis of HDPE. There are a number of studies with catalysts, showing that there are

improvements in the process conditions. Beltrame et. al., [87] tested the catalysts silica, alumina, silica-alumina and zeolites to see their effects on pyrolysis of HDPE in a Pyrex vessel reactor. In their experiments, silica-alumina gave better results at temperatures higher than 400°C. Bagri et. al., [88] studied the effect of zeolite in a fixed bed reactor. PE waste was degraded to mainly aliphatic compounds; alkene and alkanes, at 500°C. The usage of zeolite increased the gas yield while it decreased the oil yield.

The similar results observed when HZSM-5 zeolite was used as a catalyst as Sharratt et. al., reported [89]. In a fluidized bed reactor, at 360°C, more than 90 wt% of the feed was converted into volatile hydrocarbons at 60 min reaction time. HZSM-5 as a catalyst reduced the reaction temperature, improved the yield of volatile products and provided selectivity in the product distribution.

Lee et. al., [90, 91] studied the degradation of a plastic waste mixture consisting of HDPE, LDPE and PP via spent fluid catalytic cracking (FCC) catalyst. They found that the temperature had a greater effect than the other parameters such as plastic type, weight ratio of the plastics and catalyst amount. Also they found that as the amount of the catalyst increased, the yield of degradation increased linearly, whereas it increased exponentially with the increasing temperature. They also pointed out that the addition of spent FCC increased the liquid product yield while it decreased the solid yield, as the heavy hydrocarbons were decomposed into lighter hydrocarbons with the help of catalyst.

Different types of zeolites have been used by many researchers, for catalytic degradation of HDPE [92, 93]. The high acid strength, high stability, large pore size, etc., make zeolites a good catalyst, as they have found application in cracking of hydrocarbons in industry. In the case of plastics, the pores are a limiting variable as the large molecules fill the pores and the rate of degradation decreases. Using zeolites in powder form may be a solution as well as impregnating active carbons with zeolites [83].

### 2.3.3.2 Phenolic Resins

Thermosets in composite materials have a broad usage area such as in petrochemistry, construction, aerospace industry and automotive industry as polyester resins in glass fibre reinforced plastics (GFRP) and phenolic or cresol based epoxy resins in printed circuit boards and carbon fibre reinforced plastics (CFRP) [94]. The most important advantages they offer are high thermal stability, good rigidity and hardness [95].

Since the thermosetting resin production is irreversible, meaning that once they are cured, the new material cannot undergo a chemical process to re-produce them, which makes thermosetting resin recycling more challenging. So far, researchers have focused on grinding the resin waste into smaller particles to use it as a filler in cement [96].

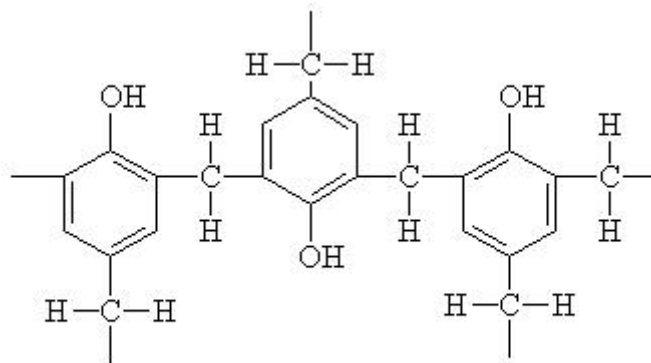


Figure 2.3.1 The chemical structure of a typical phenolic resin [97]

Phenolic epoxy resin is one of the major thermosetting resins, especially used in printed circuit boards. The methylene bond exists in phenolic resin which connects the aryl groups, as shown in Figure 2.3.1, and is not easy to decompose. Suzuki et. al., [97] used a hydrothermal method to degrade the phenolic resin into its precursors such as phenol, cresols and *p*-isopropylphenol at temperatures of 523 – 703 K (250 – 430°C). They reached 78% conversion of the waste into oil, at 703 K, in 0.5 h reaction time. They also reported that the addition of Na<sub>2</sub>CO<sub>3</sub> improved the rate of the reaction. Also in another study by Suzuki et. al., the moulding material from phenol resin was degraded to give phenol and cresols in supercritical water [97]. Goto et. al., [98] studied the decomposition of the phenolic resin in

printed circuit boards in near critical water. About 80% of the feed, which was printed circuit board after the removal of copper coating, was converted into gas and liquid. The major organic compounds detected in the liquid phase were phenol, *o*-cresol and *p*-cresol. The yield of those monomers increased when the reaction time and the temperature were increased. Oliveux G. et. al., [99] investigated the degradation of a bisphenol A based epoxy resin in water with carbon dioxide in a batch reactor. They concluded that the addition of CO<sub>2</sub> improved the mass transfer and diffusion, and also CO<sub>2</sub> acted as a catalyst with the phenol that was produced during the degradation. The epoxy resin was mainly decomposed to phenol and phenolic compounds.

Recovery of organic compounds from waste printed circuit board is even more complex, due to many toxic and hazardous additives such as brominated or chlorinated flame retardants. In 2002, around 15% of the waste PCBs is being recycled in the UK, as the conventional methods for management of these wastes are landfilling and incineration. However, because of the formation of hazardous compounds such as polybrominated dibenzodioxins, dibenzofurans and toxic brominated compounds from incineration; and the leaching of toxic compounds and heavy metals to groundwater due to landfilling, recycling of waste PCBs are crucial to prevent the hazards impacting to the environment [86]. Currently studies on thermochemical methods to recycle waste PCBs are being investigated to convert the resin part into its monomers. Pyrolysis process has been applied to PCBs, where the polymer can be broken down to its precursors and monomers. However, the char formation is high and the liquid phase contains bromine, which contaminates the oil [85].

When hydrothermal processes are applied, the fate of bromine dramatically changes, and the liquid products can be recovered bromine-free. According to Yin et. al., [100] at lower temperatures (300°C), when brominated epoxy resin decomposed by hydrolysis, some brominated organics were detected in the produced is oil, such as bromophenols and bromobenzenes. However when the temperature was increased to 400°C, no brominated compounds were detected in the oil phase. Onwudili et. al.,

[101] explained the disappearance of the brominated compounds in high temperature hydrolysis as they investigated the decomposition of brominated flame retarded plastics (Br-ABS and Br-HIPS) in supercritical water. They found that after the reaction, the bromines were collected in the aqueous phase, which results in almost bromine free oil phase.

### **2.3.3.3 Fibre Reinforced Plastics**

Fibre reinforced plastics are very important engineering composite materials that contain high strength fibre reinforcements supported by a matrix material. The matrix material is the adhesive binder which can be metallic, ceramic and an organic resin. For high performance composites, carbon or glass fibres are supported by a thermosetting resin to offer combinations of good engineering properties such as low density, the strength-weight and modulus-weight ratios which cannot be produced by using homogenous metallic alloys; such as steel, titanium and aluminium [102, 103]. Fibre reinforced composites find a very wide usage area, from aircraft to space applications, automotive to sporting goods, marine to infrastructure; also in electronics, furniture, building construction etc. [103].

#### **2.3.3.3.1 Glass Fibre Reinforced Plastics**

Glass fibre reinforced plastics are one of the important engineering composite materials due to the useful properties such as high tensile strength, high chemical resistance and excellent insulating properties, and low cost. The use of glass fibre reinforced plastics has been widening and the production rates reached 1.2 million tons in 2007 in Europe and about 1.6 million tons in the United States [103, 104]. Although mechanical recycling of glass fibre reinforced plastics currently has industrial applications, with the increasing production rates, researchers have focused on finding a sustainable recycling method [104].

Pyrolysis of glass fibre reinforced plastics has been studied at low temperatures and in the presence of steam and complete degradation of the resin was achieved which enables easy recovery of the fibres. However when the temperature reaches around 400°C, the recovered glass fibres lost



50% of the mechanical properties of that of the virgin glass fibre [94, 104]. When oxidation took place in a fluidised bed at 550°C, the glass fibre reinforced plastics lost 80% of their mechanical properties [105].

Hydrothermal treatment of waste glass fibre reinforced plastics at lower temperatures is a promising method to recover the glass fibres with good mechanical properties and recycle the resin. Oliveux et. al., [106] used hydrolysis in a batch reactor for recycling of glass fibres reinforced by unsaturated polyester resin cross-linked with styrene. At subcritical conditions of water, the resin was degraded to give its monomers mostly glycols and phthalic acid. Kamimura et. al., [107] depolymerized glass fibre reinforced plastics in supercritical methanol with the addition of N,N-dimethylaminopyridine. The experiments took place at 275°C and 11 MPa for 6 h of reaction time. The recovered glass fibre kept its mechanical properties after this process. Sugeta et. al., [108] decomposed glass fibre reinforced by unsaturated polyester matrix, using supercritical water. After treating the glass fibre reinforced plastic sample at 380°C for 5 min, they detected the products as CO<sub>2</sub> and CO in the gas phase and styrene derivatives and phthalic acid in the liquid phase.

#### **2.3.3.3.2 Carbon Fibre Reinforced Plastics**

Since the beginning of the 1960s, carbon fibres have become one of the most important engineering materials, as they offer excellent physical and chemical properties. They are a good replacement for steels and aluminium composite materials due to their high tensile strength, low density, high resistance to temperature and corrosion, and low thermal expansion [102, 109]. Carbon fibres have been used widely as reinforcements in composite materials such as carbon fibre reinforced plastics (polymers), carbon-carbon composite and carbon fibre reinforced cement in many areas; automobile, housing, sport and leisure industries as well as airplane and space applications due to this unique properties [109, 110].

With the widening of the usage of carbon fibre reinforced plastics (CFRP), the production rate of carbon fibre has also increased recently. In the early 1990s, the global annual production rate of carbon fibre was 6000

tons [109]. The worldwide demand for carbon fibre is reported to be 46000 tons in 2011 and according to projections, it is expected to rise to 140000 tons by 2020 [111]. The production of carbon fibre reinforced plastic scrap in Europe and the USA was reported as 3000 tonnes per annum. This number will increase as 6000 to 8000 airplanes will reach their end of service life by 2030 [112]. As the carbon fibre industry grows rapidly, the need for recycling carbon fibre reinforced plastic waste is gaining great attention due to the environmental and economic aspects.

Currently, various mechanical and chemical recycling processes of carbon fibre reinforced plastic waste are proposed and their advantages and disadvantages are shown in Table 2.3.1. Mechanical recycling processes consist of reducing the size of waste materials into small pieces by crushing, milling etc. and segregation of these pieces into powdered products (mainly resin) and fibre products. Without using any hazardous solvents or producing toxic materials, recovery of both fibres and resin can be achieved. However, due to the dramatic reduction in the mechanical properties, limited usage can be found for the mechanically recycled carbon fibre reinforced plastic waste such as reinforcement materials in the cement industry as mineral source or in asphalt as filler [113].

Chemical recycling methods are used to recover the carbon fibre part from the waste and convert the resin part into the monomers or to useful chemicals as a fuel or as a feedstock by means of a chemical process such as pyrolysis or gasification. In pyrolysis, thermal decomposition of the resin fraction into low molecular weight organic substances takes place at temperatures between 300 - 800°C, to recover the carbon fibres and recycle the organic resin [114]. Although pyrolysis has been used to recover carbon fibre and recycle the organic resin part, the main disadvantage is that after pyrolysis, an oxidization process is needed in order to get rid of the char deposited on the fibre surface [115].

Table 2.3.1 Advantages and disadvantages of different recycling processes adapted from [8]

	<i>Advantages</i>	<i>Disadvantages</i>
Mechanical	<ul style="list-style-type: none"> <li>• Simple Process</li> <li>• Recovery of both fibres and resin</li> <li>• no hazardous or toxic production</li> </ul>	<ul style="list-style-type: none"> <li>• Low mechanical performance</li> <li>• Unstructured, coarse and variable fibre architecture</li> <li>• Limited re-manufacturing possibilities</li> </ul>
Pyrolysis	<ul style="list-style-type: none"> <li>• High retention of fibre properties</li> <li>• Energy recovery from the resin</li> <li>• Good adhesion between recovered fibres and epoxy</li> </ul>	<ul style="list-style-type: none"> <li>• Possible deposition of char on fibre surface</li> <li>• Quality of fibres is sensitive to processing parameters</li> <li>• Need for off-gases treatment unit</li> </ul>
Chemical	<ul style="list-style-type: none"> <li>• Very high retention of fibre properties</li> <li>• potential for recovering valuable matrix products</li> </ul>	<ul style="list-style-type: none"> <li>• Fibre adhesion to epoxy resins is commonly reduced</li> <li>• Low tolerance to contamination</li> <li>• Environmental impact if using hazardous solvents</li> </ul>
Oxidation	<ul style="list-style-type: none"> <li>• High tolerance to contamination</li> <li>• No residual products on the recovered fibre surface</li> <li>• Well established and documented process</li> </ul>	<ul style="list-style-type: none"> <li>• Large fibre strength degradation</li> <li>• Fibre length degradation</li> <li>• Unstructured Fibre architecture</li> <li>• No material recovery</li> </ul>

To overcome those disadvantages, hydrothermal treatment of carbon fibre reinforced plastic in a suitable reaction media can be a solution as it is possible to recover carbon fibre by protecting the mechanical properties and

recycling the resin fraction as useful chemicals. Sub- and supercritical fluids like alcohols and water are perfect solvents for this process [15].

Pinero et. al., [116, 117] studied the chemical recycling of carbon fibre reinforced plastic waste in both sub- and supercritical alcohols (methanol, ethanol, 1 –propanol and acetone) and water. They investigated the effect of temperature, reaction time, addition of oxidant ( $H_2O_2$ ) and catalyst concentration in relation to resin removal efficiency. The experiments were conducted at temperatures between  $250^\circ C$  to  $400^\circ C$  and at pressures from 4.0 to 27.0 MPa in a batch reactor with a volume of 10 ml. In supercritical water, resin removal efficiency reached 79.3 wt% and was improved to 95.3 wt% by using KOH as catalyst in supercritical water. Between 10% and 2% loss in the tensile strength of the recovered fibres compared to that of virgin fibres were observed.

Liu et. al., [118] used subcritical water for the decomposition of carbon fibre reinforced plastic waste. The experiments were performed at temperatures between  $250^\circ C$  and  $290^\circ C$ ; the matrix of carbon fibre reinforced plastic waste totally decomposed at  $260^\circ C$  for reaction conditions of 105 min with 1.5 g/mL feedstock ratio, and at  $290^\circ C$  for 75 min with the same feedstock ratio. They also concluded that addition of 1 M of sulphuric acid could increase the rate of degradation of the epoxy resins. The recovered fibre had a reduction of 1.8% in tensile strength.

Bai et. al., [119] investigated the effect of  $O_2$  in the chemical recycling of carbon fibre reinforced epoxy resin composites in supercritical water. The carbon fibres were recovered in an oxygen medium at 30 MPa and  $440^\circ C$  for 30 min reaction time. According to the results of their research, the clean carbon fibres recovered had higher tensile strength relative to the virgin fibres when the decomposition yield was between 85% and 96%. Above 96%, the tensile strength decreased rapidly.

After carbon fibre recovery, it is important to find an application area for recovered carbon fibres. Therefore, it is crucial to preserve the mechanical strength of the original fibre. Depending on the recovery method, recovered carbon fibres (rCF) can find themselves an application area. An overview of

the recycling and re-manufacturing processes of carbon fibre reinforced plastics and recovered carbon fibres are shown in Figure 2.3.2.

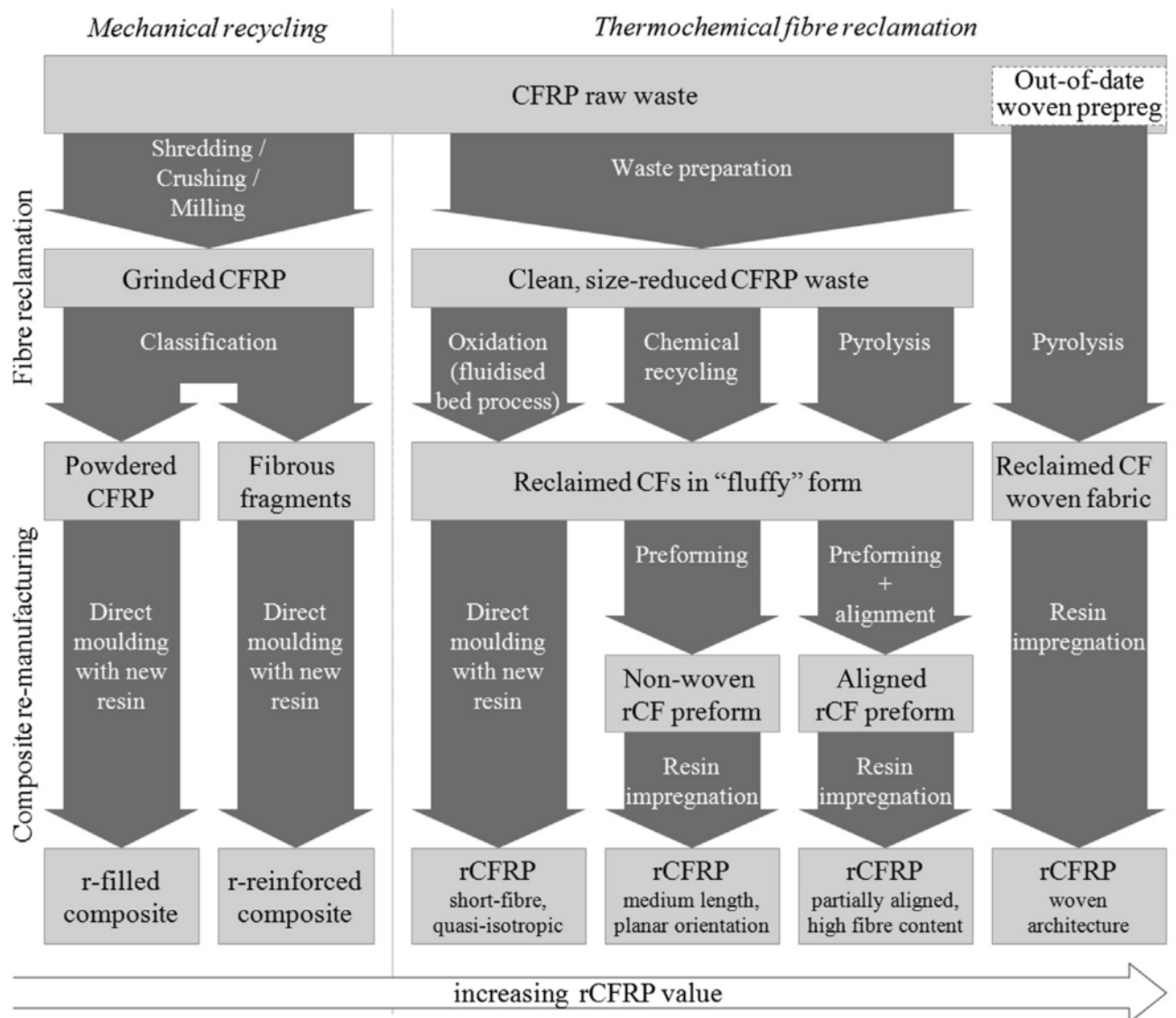


Figure 2.3.2 Overview of carbon fibre reinforced plastic recycling and re-manufacturing processes adapted from [8]

## 2.3.4 Other Types of Plastics and Materials

### 2.3.4.1 Cross-Linked Polyethylene

Crosslinked polyethylene (XLPE) is a thermosetting resin with poor conductivity, and has been used as an insulating material for electrical equipment, especially in cables and wires. Since it is a thermosetting plastic, recycling is a challenging problem. Watanabe et. al., [120] used supercritical water to remove the crosslinking fraction from XLPE waste. The recovered

thermoplastic polyethylene then was recrosslinked with the resin obtained from the original waste XLPE and the properties were compared with the original XLPE. They reported that the recovered XLPE had the same characteristics after recrosslinking.

Goto et. al., [121] used supercritical alcohols for chemical recycling of silane XLPE. They recovered the raw polyethylene by preserving its properties to be used as an insulation material in cables and wires. Lee et. al., [122] investigated the decrosslinking of XLPE in methanol at supercritical conditions. At 360°C and 15 MPa for 10 min, the resin fraction was removed and 100% raw polyethylene was obtained.

#### **2.3.4.2 Polyvinyl chloride (PVC)**

Polyvinyl chloride (PVC) is one of the thermoplastics that have a huge usage as the annual worldwide production rate is more than 35 million tonnes, which makes it the third most common plastic after polyethylene (PE) and polypropylene (PP). Construction, packaging industry, textile, pipes, window frames and electrical cables are the most common usage areas of PVC [123]. However, most of the PVC wastes are sent to landfilling, as it is difficult to recycle the wastes contain many additives and stabilizers to make PVC suitable for the corresponding application. 2.5% of PVC produced in Europe was recycled in 2008, but it is expected to increase in the following years as new routes of recycling are being investigated [123]. Chemical recycling of PVC is taking much of the attention among the methods of recycling. The benefit of chemical recycling is that, it is less sensitive to the heterogeneity of the waste. The main processes of chemical recycling for PVC are thermal cracking via hydrogenation, pyrolysis and gasification.

The pyrolysis of PVC includes a dechlorination step, which is the treatment of PVC at temperatures between 250 and 320°C, to remove chlorine by producing HCl. This step is followed by pyrolysis of chlorine free PVC. Also it is possible to recycle PVC via a one-step pyrolysis, by adding adsorbents to the waste to capture the HCl with chemical or physical adsorption [124]. Slapak et. al., [125] studied pyrolysis of PVC waste in a bench-scale bubbling fluidized bed with porous alumina powder as bed

material. They found that the temperature was the main parameter affecting the products and conversion. At 877°C, the carbon conversion from waste to gas products was 69%, whereas when they used inactive solid quartz as bed material the resulting products were mostly tar and char. When the temperature was increased to 977°C, the conversion increased to 98%.

Matsuda et. al., [126] decomposed PVC thermally with the help of metal oxides such as ZnO, Fe<sub>2</sub>O<sub>3</sub>, Al<sub>2</sub>O<sub>3</sub>, PbO, CaO and rare earth oxides. They reported that while the addition of metal oxides decreased the liquid product yield, it didn't have a major effect on gas yield, except Fe<sub>2</sub>O<sub>3</sub> and Al<sub>2</sub>O<sub>3</sub>, as there was a significant increase in gas production. On the other hand, the HCl emission changed significantly with the addition of oxides, and they concluded that this was due to the oxides chlorine fixing capacity.

In the studies of recycling of PVC via pyrolysis, in most cases, instead of recycling of pure PVC, the feeds containing a mixture of plastics have been used, as recycling of PVC itself is a difficult process due to the heterogeneity of the waste's character. The pyrolysis of PVC-rich plastic waste mixture yields hydrocarbons (oil), HCl and chlorinated hydrocarbons, in which HCl must be removed from the gas stream since it may cause production of toxic dioxins. However, the corrosive effect of HCl gas, is a problem which limits the PVC content to less than 30% in the plastic waste mixture [123]. To solve this issue, an attempt was made by Tongamp et. al. [127]. They ground oyster shell waste and PVC waste together to form CaCl<sub>2</sub> by mechanically induced reactions. After milling, they washed the mixed sample by water to remove Cl in the waste, as CaCl<sub>2</sub> is soluble in water. Also other metal-alloys can be used to remove Cl content from the waste as metal chlorides via the same process [128].

Duangchan et. al., [129] investigated the co-pyrolysis of PVC with cattle manure, to prevent the corrosion arising from the Cl content in PVC waste. The HCl production from PVC waste was reduced and the maximum yield was reached at 450°C in a tubular pyrolysis reactor. The chlorinated hydrocarbon amount produced was decreased by 45% when cattle manure and PVC waste was mixed in a proportion of 5:1 respectively.

Besides the pyrolysis, degradation of PVC via chemical treatment is also a suitable method for recycling. Generally the idea is dehydrochlorination of PVC in alkaline media. One method is degradative extrusion, which is based on the degradation of PVC in the presence of oxygen with the help of catalysts, in steam in an extruder. The main product is HCl and the remaining polymer is too viscous for direct application [130].

Another method is degradation in alkali media, in the presence of oxygen. Yoshioka et. al., oxidized PVC waste in NaOH solution at temperatures between 150 and 260°C. Oxalic acid and CO<sub>2</sub> were determined as the major products and their concentration increased with the increasing temperature, increasing the partial pressure of oxygen while it decreased with the increasing NaOH concentration. The yield of oxalic acid was 45% and 42% of the chlorine was recovered from the waste as HCl [131, 132].

Shin et. al., [133] treated PVC pellets at temperatures between 150 and 250°C in NaOH solution for reaction times of 0 to 12 h. They reached 100% dehydrochlorination of PVC pellets at 250°C for 3 h reaction time. Wu et. al., [134] investigated the effect of Poly(ethylene glycol) (PEG) on dehydrochlorination of PVC, and they found that polyethylene glycol accelerated the process. For 1 h reaction time at 210°C, while the yield of dechlorination of PVC was 50%, the addition of polyethylene glycol increased this recovery to 74.2%. They concluded that polyethylene glycol served as an environmentally-friendly reaction medium, as there was no need to add any base catalyst which produces toxic by-products.

#### **2.3.4.3 Refuse Derived Fuel (RDF)**

Refuse derived fuel is a fuel produced from processing of municipal solid waste (MSW), by using mechanical treatment methods to remove materials such as glass and metals to obtain a combustible fraction. Then this fraction undergoes further processing to increase the energy density to achieve a high calorific value fuel with a uniform size and weight distribution. Normally, the calorific value of a typical MSW sample is around 9 MJ/kg, while this amount increases in RDF around 18 MJ/kg. After these improvements in the properties with simple mechanical treatments, refuse



derived fuels are ready to undergo processes such as combustion, pyrolysis or gasification to produce energy or energy fuel [135, 136].

Pyrolysis of RDF was performed at a temperature range of 400 – 700°C and fuel gas with high calorific values were yielded at high pyrolysis temperatures. The gases mainly composed of CO<sub>2</sub>, CO, H<sub>2</sub>, CH<sub>4</sub>, C<sub>2</sub>H<sub>6</sub> and C<sub>3</sub>H<sub>8</sub>. The oil obtained was analysed by FT-IR and carboxylic acids and their derivatives, alkanes, alkenes, mono and polycyclic and substituted aromatic groups were detected. Also it was reported that with the increasing pyrolysis temperature, the organic compounds in the oil shifted from aliphatic groups to aromatic groups [136].

Dalai et. al., [137] researched the steam gasification of RDF in a fixed bed reactor at atmospheric pressure. The optimum gasification temperature was determined as 725°C, as the optimum selectivity for H<sub>2</sub> and CO was obtained at this temperature. The further increase in the temperature resulted in a gas product with a lower caloric value. Also they reported that the hydrogen and carbon ratio of raw RDF highly affects the selectivity of CO and H<sub>2</sub>, as higher ratio resulted in high amounts of CO and H<sub>2</sub>.

Hydrothermal gasification of RDF in the presence of sodium hydroxide was investigated at a temperature range of 300 – 375°C. The product gas was hydrogen rich, containing carbon dioxide and carbon monoxide, and also small amounts of C<sub>1</sub>-C<sub>4</sub> hydrocarbons. The hydrogen composition in the gas was increased with the increasing sodium hydroxide concentrations. It was reported that sodium hydroxide catalysed the gasification reactions by fixing carbon dioxide as carbonate salts [138].

The water, plastics and cellulosic content of RDF makes hydrothermal process as a good solution to convert the valuable organic materials into oil or fuel gas [136]. By utilizing its own water content, RDF can undergo hydrothermal process to produce useful chemicals or fuel gases.

## References

1. Byrappa, K. and M. Yoshimura, *Handbook of hydrothermal technology*. 2002: William Andrew.
2. Brunner, G., *Hydrothermal and Supercritical Water Processes*. Vol. 5. 2014: Elsevier.
3. Brunner, G., *Near critical and supercritical water. Part I. Hydrolytic and hydrothermal processes*. The Journal of Supercritical Fluids, 2009. **47**(3): p. 373-381.
4. Seward, T.M. and T. Driesner, *Chapter 5 - Hydrothermal solution structure: Experiments and computer simulations*, in *Aqueous Systems at Elevated Temperatures and Pressures*, D.A.P.F.-P.H. Harvey, Editor. 2004, Academic Press: London. p. 149-182.
5. Kruse, A. and E. Dinjus, *Hot compressed water as reaction medium and reactant: Properties and synthesis reactions*. The Journal of Supercritical Fluids, 2007. **39**(3): p. 362-380.
6. Weingärtner, H. and E.U. Franck, *Supercritical Water as a Solvent*. Angewandte Chemie International Edition, 2005. **44**(18): p. 2672-2692.
7. Akiya, N. and P.E. Savage, *Effect of Water Density on Hydrogen Peroxide Dissociation in Supercritical Water. 2. Reaction Kinetics*. The Journal of Physical Chemistry A, 2000. **104**(19): p. 4441-4448.
8. Pimenta, S. and S.T. Pinho, *Chapter 19 - Recycling of Carbon Fibers*, in *Handbook of Recycling*, E. Worrell and M.A. Reuter, Editors. 2014, Elsevier: Boston. p. 269-283.
9. Nikles, D.E. and M.S. Farahat, *New Motivation for the Depolymerization Products Derived from Poly(Ethylene Terephthalate) (PET) Waste: a Review*. Macromolecular Materials and Engineering, 2005. **290**(1): p. 13-30.
10. Lundquist, L., et al., *Life Cycle Engineering of Plastics*. Materials & Mechanical. 2000: Elsevier Science Ltd. 1-220.
11. Al-Salem, S.M., P. Lettieri, and J. Baeyens, *Recycling and recovery routes of plastic solid waste (PSW): A review*. Waste Management, 2009. **29**(10): p. 2625-2643.
12. Al-Salem, S.M., P. Lettieri, and J. Baeyens, *The valorization of plastic solid waste (PSW) by primary to quaternary routes: From re-use to energy and chemicals*. Progress in Energy and Combustion Science, 2010. **36**(1): p. 103-129.

13. Aznar, M.P., et al., *Plastic waste elimination by co-gasification with coal and biomass in fluidized bed with air in pilot plant*. Fuel Processing Technology, 2006. **87**(5): p. 409-420.
14. Panda, A.K., R.K. Singh, and D.K. Mishra, *Thermolysis of waste plastics to liquid fuel: A suitable method for plastic waste management and manufacture of value added products—A world prospective*. Renewable and Sustainable Energy Reviews, 2010. **14**(1): p. 233-248.
15. Motonobu, G., *Chemical recycling of plastics using sub- and supercritical fluids*. The Journal of Supercritical Fluids, 2009. **47**(3): p. 500-507.
16. Brill, T.B. and P.E. Savage, *Chapter 16 - Kinetics and mechanisms of hydrothermal organic reactions*, in *Aqueous Systems at Elevated Temperatures and Pressures*, D.A.P.F.-P.H. Harvey, Editor. 2004, Academic Press: London. p. 643-675.
17. Houser, T.J., et al., *The reactivity of tetrahydroquinoline, benzylamine and bibenzyl with supercritical water*. Fuel, 1989. **68**(3): p. 323-327.
18. Katritzky, A.R., et al., *Aqueous High-Temperature Chemistry of Carbo- and Heterocycles. 20. Reactions of Some Benzenoid Hydrocarbons and Oxygen-Containing Derivatives in Supercritical Water at 460 .degree.C*. Energy & Fuels, 1994. **8**(2): p. 487-497.
19. Watanabe, M., et al., *Polyethylene conversion in supercritical water*. The Journal of Supercritical Fluids, 1998. **13**(1–3): p. 247-252.
20. Ederer, H.J., et al., *Modelling of the pyrolysis of tert-butylbenzene in supercritical water*. The Journal of Supercritical Fluids, 1999. **15**(3): p. 191-204.
21. McCollom, T.M., J.S. Seewald, and B.R.T. Simoneit, *Reactivity of monocyclic aromatic compounds under hydrothermal conditions*. Geochimica et Cosmochimica Acta, 2001. **65**(3): p. 455-468.
22. Houser, T.J., et al., *Reactivity of some organic compounds with supercritical water*. Fuel, 1986. **65**(6): p. 827-832.
23. Katritzky, A.R., et al., *Reactions in High-Temperature Aqueous Media*. Chemical Reviews, 2001. **101**(4): p. 837-892.
24. Ikushima, Y. and M. Arai, *Stoichiometric Organic Reactions*, in *Chemical Synthesis Using Supercritical Fluids*. 2007, Wiley-VCH Verlag GmbH. p. 259-279.
25. Dinjus, E. and A. Kruse, *Applications of Supercritical Water*, in *High Pressure Chemistry*. 2007, Wiley-VCH Verlag GmbH. p. 422-446.

26. Krammer, P. and H. Vogel, *Hydrolysis of esters in subcritical and supercritical water*. The Journal of Supercritical Fluids, 2000. **16**(3): p. 189-206.
27. Antal Jr, M.J., et al., *Heterolysis and homolysis in supercritical water*. Supercritical Fluids: Chemical and Engineering Principles and Applications, 1987: p. 77-86.
28. Klein, M.T., et al., *Hydrolysis in supercritical water: Solvent effects as a probe of the reaction mechanism*. The Journal of Supercritical Fluids, 1990. **3**(4): p. 222-227.
29. Abraham, M.A. and M.T. Klein, *Pyrolysis of benzylphenylamine neat and with tetralin, methanol, and water solvents*. Industrial & Engineering Chemistry Product Research and Development, 1985. **24**(2): p. 300-306.
30. Townsend, S.H., et al., *Solvent effects during reactions in supercritical water*. Industrial & Engineering Chemistry Research, 1988. **27**(1): p. 143-149.
31. Benjamin, K.M. and P.E. Savage, *Hydrothermal reactions of methylamine*. The Journal of Supercritical Fluids, 2004. **31**(3): p. 301-311.
32. Xu, X., C.D. Almeida, and M.J. Antal Jr, *Mechanism and kinetics of the acid-catalyzed dehydration of ethanol in supercritical water*. The Journal of Supercritical Fluids, 1990. **3**(4): p. 228-232.
33. Schanzenbächer, J., J.D. Taylor, and J.W. Tester, *Ethanol oxidation and hydrolysis rates in supercritical water*. The Journal of Supercritical Fluids, 2002. **22**(2): p. 139-147.
34. Bühler, W., et al., *Ionic reactions and pyrolysis of glycerol as competing reaction pathways in near- and supercritical water*. The Journal of Supercritical Fluids, 2002. **22**(1): p. 37-53.
35. Geissman, T.A., *The Cannizzaro Reaction*, in *Organic Reactions*. 2004, John Wiley & Sons, Inc.
36. Osada, M., et al., *Water density dependence of formaldehyde reaction in supercritical water*. The Journal of Supercritical Fluids, 2004. **28**(2-3): p. 219-224.
37. Krämer, A., S. Mittelstädt, and H. Vogel, *Hydrolysis of Nitriles in Supercritical Water*. Chemical Engineering & Technology, 1999. **22**(6): p. 494-500.
38. Iyer, S.D. and M.T. Klein, *Effect of pressure on the rate of butyronitrile hydrolysis in high-temperature water*. The Journal of Supercritical Fluids, 1997. **10**(3): p. 191-200.

39. Belsky, A.J., P.G. Maiella, and T.B. Brill, *Spectroscopy of Hydrothermal Reactions 13. Kinetics and Mechanisms of Decarboxylation of Acetic Acid Derivatives at 100–260 °C under 275 bar*. The Journal of Physical Chemistry A, 1999. **103**(21): p. 4253-4260.
40. Salvatierra, D., et al., *Kinetic Study of Hydrolysis of Methylene Chloride from 100 to 500 °C*. Industrial & Engineering Chemistry Research, 1999. **38**(11): p. 4169-4174.
41. Marrone, P.A., et al., *Solvation Effects on Kinetics of Methylene Chloride Reactions in Sub- and Supercritical Water: Theory, Experiment, and Ab Initio Calculations*. The Journal of Physical Chemistry A, 1998. **102**(35): p. 7013-7028.
42. Katritzky, A.R., M. Balasubramanian, and M. Siskin, *Aqueous high-temperature chemistry of carbo- and heterocycles. 2. Monosubstituted benzenes: benzyl alcohol, benzaldehyde and benzoic acid*. Energy & Fuels, 1990. **4**(5): p. 499-505.
43. Chandler, K., et al., *Tuning alkylation reactions with temperature in near-critical water*. AIChE journal, 1998. **44**(9): p. 2080-2087.
44. Nolen, S.A., et al., *The catalytic opportunities of near-critical water: a benign medium for conventionally acid and base catalyzed condensations for organic synthesis*. Green Chemistry, 2003. **5**(5): p. 663-669.
45. Awaja, F. and D. Pavel, *Recycling of PET*. European Polymer Journal, 2005. **41**(7): p. 1453-1477.
46. Petcore, *Petcore Fact sheet on Poly Ethylene Terephthalate*, in [http://www.petcore.org/files/pet\\_profile\\_-\\_english\\_1.pdf](http://www.petcore.org/files/pet_profile_-_english_1.pdf)2012.
47. Ravindranath, K. and R.A. Mashelkar, *Polyethylene terephthalate—I. Chemistry, thermodynamics and transport properties*. Chemical Engineering Science, 1986. **41**(9): p. 2197-2214.
48. Carraher, C.E. and C.U. Pittman, *Inorganic Polymers*, in *Ullmann's Encyclopedia of Industrial Chemistry*. 2000, Wiley-VCH Verlag GmbH & Co. KGaA.
49. Kong, Y. and J.N. Hay, *Multiple melting behaviour of poly(ethylene terephthalate)*. Polymer, 2003. **44**(3): p. 623-633.
50. Motonobu, G. and et al., *Depolymerization of polyethylene terephthalate in supercritical methanol*. Journal of Physics: Condensed Matter, 2002. **14**(44): p. 11427.
51. Baliga, S. and W.T. Wong, *Depolymerization of poly(ethylene terephthalate) recycled from post-consumer soft-drink bottles*. Journal of Polymer Science Part A: Polymer Chemistry, 1989. **27**(6): p. 2071-2082.

52. Campanelli, J.R., M.R. Kamal, and D.G. Cooper, *A kinetic study of the hydrolytic degradation of polyethylene terephthalate at high temperatures*. Journal of Applied Polymer Science, 1993. **48**(3): p. 443-451.
53. Sako, T., et al., *Depolymerization of polyethylene terephthalate to monomers with supercritical methanol*. Journal of Chemical Engineering of Japan, 1997. **30**(2): p. 342-346.
54. Goto, M., et al., *Degradation kinetics of polyethylene terephthalate in supercritical methanol*. AIChE Journal, 2002. **48**(1): p. 136-144.
55. Genta, M., et al., *Depolymerization Mechanism of Poly(ethylene terephthalate) in Supercritical Methanol*. Industrial & Engineering Chemistry Research, 2005. **44**(11): p. 3894-3900.
56. Genta, M., et al., *Supercritical methanol for polyethylene terephthalate depolymerization: Observation using simulator*. Waste Management, 2007. **27**(9): p. 1167-1177.
57. Lopez-Fonseca, R., et al., *Chemical recycling of post-consumer PET wastes by glycolysis in the presence of metal salts*. Polymer Degradation and Stability, 2010. **95**(6): p. 1022-1028.
58. Abdelaal, M.Y., T.R. Sobahi, and M.S.I. Makki, *Chemical transformation of pet waste through glycolysis*. Construction and Building Materials, 2011. **25**(8): p. 3267-3271.
59. Imran, M., et al., *Sub- and supercritical glycolysis of polyethylene terephthalate (PET) into the monomer bis(2-hydroxyethyl) terephthalate (BHET)*. Polymer Degradation and Stability, 2010. **95**(9): p. 1686-1693.
60. Campanelli, J.R., D.G. Cooper, and M.R. Kamal, *Catalyzed hydrolysis of polyethylene terephthalate melts*. Journal of Applied Polymer Science, 1994. **53**(8): p. 985-991.
61. Mishra, S., V.S. Zope, and A.S. Goje, *Kinetics and thermodynamics of hydrolytic depolymerization of poly(ethylene terephthalate) at high pressure and temperature*. Journal of Applied Polymer Science, 2003. **90**(12): p. 3305-3309.
62. de Castro, R.E.N., et al., *Depolymerization of poly(ethylene terephthalate) wastes using ethanol and ethanol/water in supercritical conditions*. Journal of Applied Polymer Science, 2006. **101**(3): p. 2009-2016.
63. Karayannidis, G.P., A.P. Chatziavgoustis, and D.S. Achilias, *Poly(ethylene terephthalate) recycling and recovery of pure terephthalic acid by alkaline hydrolysis*. Advances in Polymer Technology, 2002. **21**(4): p. 250-259.

64. Karayannidis, G.P. and D.S. Achilias, *Chemical Recycling of Poly(ethylene terephthalate)*. *Macromolecular Materials and Engineering*, 2007. **292**(2): p. 128-146.
65. Achilias, D. and G. Karayannidis, *The Chemical Recycling of PET in the Framework of Sustainable Development*. *Water, Air, & Soil Pollution: Focus*, 2004. **4**(4): p. 385-396.
66. Sato, O., K. Arai, and M. Shirai, *Hydrolysis of poly(ethylene terephthalate) and poly(ethylene 2,6-naphthalene dicarboxylate) using water at high temperature: Effect of proton on low ethylene glycol yield*. *Catalysis Today*, 2006. **111**(3-4): p. 297-301.
67. Arai, K., R.L. Smith Jr, and T.M. Aida, *Decentralized chemical processes with supercritical fluid technology for sustainable society*. *The Journal of Supercritical Fluids*, 2009. **47**(3): p. 628-636.
68. Fang, Z., et al., *Phase behavior and reaction of polyethylene terephthalate–water systems at pressures up to 173 MPa and temperatures up to 490°C*. *The Journal of Supercritical Fluids*, 1999. **15**(3): p. 229-243.
69. Nagase, Y., M. Yamagata, and R. Fukuzato, *Development of a chemical recycling process for waste plastics using supercritical water*. *KOBELCO Technology Review*, 1999(22): p. 11-14.
70. Hu, L.-C., et al., *Alkali-Decomposition of Poly(ethylene terephthalate) in Mixed Media of Nonaqueous Alcohol and Ether. Study on Recycling of Poly(ethylene terephthalate)*. *Polym J*, 1997. **29**(9): p. 708-712.
71. Pinero, R., J. Garcia, and M.J. Cocero, *Chemical recycling of polycarbonate in a semi-continuous lab-plant. A green route with methanol and methanol-water mixtures*. *Green Chemistry*, 2005. **7**(5): p. 380-387.
72. Tagaya, H., et al., *Decomposition of polycarbonate in subcritical and supercritical water*. *Polymer Degradation and Stability*, 1999. **64**(2): p. 289-292.
73. Ikeda, A., K. Katoh, and H. Tagaya, *Monomer recovery of waste plastics by liquid phase decomposition and polymer synthesis*. *Journal of Materials Science*, 2008. **43**(7): p. 2437-2441.
74. Watanabe, M., et al., *Chemical recycling of polycarbonate in high pressure high temperature steam at 573 K*. *Polymer Degradation and Stability*, 2009. **94**(12): p. 2157-2162.
75. Grause, G., et al., *High-value products from the catalytic hydrolysis of polycarbonate waste*. *Polym J*, 2010. **42**(6): p. 438-442.

76. Iwaya, T., M. Sasaki, and M. Goto, *Kinetic analysis for hydrothermal depolymerization of nylon 6*. *Polymer Degradation and Stability*, 2006. **91**(9): p. 1989-1995.
77. Kamimura, A., et al., *Direct conversion of polyamides to [small omega]-hydroxyalkanoic acid derivatives by using supercritical MeOH*. *Green Chemistry*, 2011. **13**(8): p. 2055-2061.
78. Kaiso, K., et al., *Effective Depolymerization of Nylon-6 in Wet Supercritical Hydrocarbons*. *Chemistry Letters*, 2011. **40**(4): p. 370-371.
79. Zia, K.M., H.N. Bhatti, and I. Ahmad Bhatti, *Methods for polyurethane and polyurethane composites, recycling and recovery: A review*. *Reactive and Functional Polymers*, 2007. **67**(8): p. 675-692.
80. Dai, Z., et al., *Effect of diaminotoluene on the decomposition of polyurethane foam waste in superheated water*. *Polymer Degradation and Stability*, 2002. **76**(2): p. 179-184.
81. Gerlock, J., J. Braslaw, and M. Zinbo, *Polyurethane waste recycling. 1. Glycolysis and hydroglycolysis of water-blown foams*. *Industrial & Engineering Chemistry Process Design and Development*, 1984. **23**(3): p. 545-552.
82. Moriya, T. and H. Enomoto, *Characteristics of polyethylene cracking in supercritical water compared to thermal cracking*. *Polymer Degradation and Stability*, 1999. **65**(3): p. 373-386.
83. Kumar, S., A.K. Panda, and R.K. Singh, *A review on tertiary recycling of high-density polyethylene to fuel*. *Resources, Conservation and Recycling*, 2011. **55**(11): p. 893-910.
84. PlasticsEurope, *Plastics - the Facts 2011: An analysis of European plastics production, demand and recovery for 2010*. [www.plasticseurope.org](http://www.plasticseurope.org), 2011.
85. Hall, W.J. and P.T. Williams, *Separation and recovery of materials from scrap printed circuit boards*. *Resources, Conservation and Recycling*, 2007. **51**(3): p. 691-709.
86. Williams, P., *Valorization of Printed Circuit Boards from Waste Electrical and Electronic Equipment by Pyrolysis*. *Waste and Biomass Valorization*, 2010. **1**(1): p. 107-120.
87. Beltrame, P.L., et al., *Catalytic degradation of polymers: Part II—Degradation of polyethylene*. *Polymer Degradation and Stability*, 1989. **26**(3): p. 209-220.
88. Bagri, R. and P.T. Williams, *Catalytic pyrolysis of polyethylene*. *Journal of Analytical and Applied Pyrolysis*, 2002. **63**(1): p. 29-41.



89. Huelsman, C.M. and P.E. Savage, *Intermediates and kinetics for phenol gasification in supercritical water*. Physical Chemistry Chemical Physics, 2012. **14**(8): p. 2900-2910.
90. Lee, K.-H., et al., *Thermal and catalytic degradation of waste high-density polyethylene (HDPE) using spent FCC catalyst*. Korean Journal of Chemical Engineering, 2003. **20**(4): p. 693-697.
91. Lee, K.-H. and D.-H. Shin, *Catalytic degradation of waste polyolefinic polymers using spent FCC catalyst with various experimental variables*. Korean Journal of Chemical Engineering, 2003. **20**(1): p. 89-92.
92. Hafner, S., et al., *A detailed chemical kinetic model of high-temperature ethylene glycol gasification*. Combustion Theory and Modelling, 2011. **15**(4): p. 517-535.
93. Morin, C., et al., *Near- and supercritical solvolysis of carbon fibre reinforced polymers (CFRPs) for recycling carbon fibers as a valuable resource: State of the art*. The Journal of Supercritical Fluids, 2012. **66**(0): p. 232-240.
94. Pickering, S.J., *Recycling technologies for thermoset composite materials—current status*. Composites Part A: Applied Science and Manufacturing, 2006. **37**(8): p. 1206-1215.
95. <http://www.reinforcedplastics.com/view/28086/thermosetting-resins-an-introduction/>.
96. Guo, J., J. Guo, and Z. Xu, *Recycling of non-metallic fractions from waste printed circuit boards: A review*. Journal of Hazardous Materials, 2009. **168**(2–3): p. 567-590.
97. Suzuki, Y.-i., et al., *Decomposition of Prepolymers and Molding Materials of Phenol Resin in Subcritical and Supercritical Water under an Ar Atmosphere*. Industrial & Engineering Chemistry Research, 1999. **38**(4): p. 1391-1395.
98. Goto, M., et al., *Depolymerization of printed circuit board in near-critical water*. Hydrothermal Reactions and Techniques, World Scientific, New Jersey, 2003: p. 201-208.
99. Oliveux, G., L.O. Dandy, and G.A. Leeke, *Degradation of a model epoxy resin by solvolysis routes*. Polymer Degradation and Stability, 2015. **118**: p. 96-103.
100. Yin, J., et al., *Hydrothermal decomposition of brominated epoxy resin in waste printed circuit boards*. Journal of Analytical and Applied Pyrolysis, 2011. **92**(1): p. 131-136.
101. Onwudili, J.A. and P.T. Williams, *Degradation of brominated flame-retarded plastics (Br-ABS and Br-HIPS) in supercritical water*. The Journal of Supercritical Fluids, 2009. **49**(3): p. 356-368.

102. Peters, S.T., *Handbook of Composites (2nd Edition)*, 1998, Springer - Verlag: London, UK.
103. Mallick, P.K., *Fiber-reinforced composites: materials, manufacturing, and design*. 2010: CRC press.
104. Oliveux, G., L.O. Dandy, and G.A. Leeke, *Current status of recycling of fibre reinforced polymers: Review of technologies, reuse and resulting properties*. *Progress in Materials Science*, 2015. **72**(0): p. 61-99.
105. Pickering, S.J., et al., *A fluidised-bed process for the recovery of glass fibres from scrap thermoset composites*. *Composites Science and Technology*, 2000. **60**(4): p. 509-523.
106. Oliveux, G., et al., *Recycling of glass fibre reinforced composites using subcritical hydrolysis: Reaction mechanisms and kinetics, influence of the chemical structure of the resin*. *Polymer Degradation and Stability*, 2013. **98**(3): p. 785-800.
107. Kamimura, A., et al., *Effective depolymerization waste FRPs by treatment with DMAP and supercritical alcohol*. *Chemistry Letters*, 2006. **35**(6): p. 586-587.
108. Sugeta, T., et al., *Decomposition of fiber reinforced plastics using fluid at high temperature and pressure*. *Kobunshi Ronbunshu*, 2001. **58**(10): p. 557-563.
109. Motoyuki, S., *Activated carbon fiber: Fundamentals and applications*. *Carbon*, 1994. **32**(4): p. 577-586.
110. Chand, S., *Review Carbon fibers for composites*. *Journal of Materials Science*, 2000. **35**(6): p. 1303-1313.
111. Tony, R., *THE CARBON FIBRE INDUSTRY WORLDWIDE 2011-2020: An Evaluation Of Current Markets And Future Supply And Demand*. *Materials Technologies Publications*, 2011.
112. Vicki P, M., *Launching the carbon fibre recycling industry*. *Reinforced Plastics*, 2010. **54**(2): p. 33-37.
113. Ogi, K., T. Shinoda, and M. Mizui, *Strength in concrete reinforced with recycled CFRP pieces*. *Composites Part A: Applied Science and Manufacturing*, 2005. **36**(7): p. 893-902.
114. Yang, Y., et al., *Recycling of composite materials*. *Chemical Engineering and Processing: Process Intensification*, 2012. **51**(0): p. 53-68.
115. Pimenta, S. and S.T. Pinho, *Recycling carbon fibre reinforced polymers for structural applications: Technology review and market outlook*. *Waste Management*, 2011. **31**(2): p. 378-392.

116. Piñero-Hernanz, R., et al., *Chemical recycling of carbon fibre reinforced composites in nearcritical and supercritical water*. Composites Part A: Applied Science and Manufacturing, 2008. **39**(3): p. 454-461.
117. Pinero-Hernanz, R., et al., *Chemical recycling of carbon fibre composites using alcohols under subcritical and supercritical conditions*. Journal of Supercritical Fluids, 2008. **46**(1): p. 83-92.
118. Liu, Y., G. Shan, and L. Meng, *Recycling of carbon fibre reinforced composites using water in subcritical conditions*. Materials Science and Engineering a-Structural Materials Properties Microstructure and Processing, 2009. **520**(1-2): p. 179-183.
119. Bai, Y., Z. Wang, and L. Feng, *Chemical recycling of carbon fibers reinforced epoxy resin composites in oxygen in supercritical water*. Materials & Design, 2010. **31**(2): p. 999-1002.
120. Watanabe, S., et al. *Development of cross-linked polymer material recycling technology by supercritical water*. in *Properties and Applications of Dielectric Materials, 2003. Proceedings of the 7th International Conference on*. 2003.
121. Goto, T., et al. *Recycling of silane cross-linked polyethylene for insulation of cables by supercritical alcohol*. in *Properties and Applications of Dielectric Materials, 2003. Proceedings of the 7th International Conference on*. 2003.
122. Lee, H.-s., et al., *A kinetic study of the decross-linking of cross-linked polyethylene in supercritical methanol*. Polymer Degradation and Stability, 2008. **93**(12): p. 2084-2088.
123. Sadat-Shojai, M. and G.-R. Bakhshandeh, *Recycling of PVC wastes*. Polymer Degradation and Stability, 2011. **96**(4): p. 404-415.
124. Lopez-Urionabarrenechea, A., et al., *Catalytic stepwise pyrolysis of packaging plastic waste*. Journal of Analytical and Applied Pyrolysis, 2012. **96**: p. 54-62.
125. Slapak, M.J., J. van Kasteren, and B.A. Drinkenburg, *Hydrothermal recycling of PVC in a bubbling fluidized bed reactor: the influence of bed material and temperature*. Polymers for Advanced Technologies, 1999. **10**(10): p. 596-602.
126. Masuda, Y., et al., *Pyrolysis study of poly (vinyl chloride)–metal oxide mixtures: quantitative product analysis and the chlorine fixing ability of metal oxides*. Journal of analytical and applied pyrolysis, 2006. **77**(2): p. 159-168.
127. Tongamp, W., et al., *Simultaneous treatment of PVC and oyster-shell wastes by mechanochemical means*. Waste management, 2008. **28**(3): p. 484-488.

128. Zhang, Q., et al., *A soft-solution process for recovering rare metals from metal/alloy-wastes by grinding and washing with water*. Journal of hazardous materials, 2007. **139**(3): p. 438-442.
129. Duangchan, A. and C. Samart, *Tertiary recycling of PVC-containing plastic waste by copyrolysis with cattle manure*. Waste management, 2008. **28**(11): p. 2415-2421.
130. Dietrich, B., *Recycling of PVC*. Progress in Polymer Science, 2002. **27**(10): p. 2171-2195.
131. Yoshioka, T., et al., *Oxidation of poly (vinyl chloride) powder by molecular oxygen in alkaline solutions at high temperatures*. Nippon Kagaku Kaishi(Japan), 1992(5): p. 534-541.
132. Yoshioka, T., et al., *Chemical recycling of flexible PVC by oxygen oxidation in NaOH solutions at elevated temperatures*. Journal of applied polymer science, 1998. **70**(1): p. 129-135.
133. Shin, S.-M., T. Yoshioka, and A. Okuwaki, *Dehydrochlorination behavior of rigid PVC pellet in NaOH solutions at elevated temperature*. Polymer degradation and stability, 1998. **61**(2): p. 349-353.
134. Wu, Y.-H., et al., *Poly (ethylene glycol) enhanced dehydrochlorination of poly (vinyl chloride)*. Journal of hazardous materials, 2009. **163**(2): p. 1408-1411.
135. Cozzani, V., et al., *A Fundamental Study on Conventional Pyrolysis of a Refuse-Derived Fuel*. Industrial & Engineering Chemistry Research, 1995. **34**(6): p. 2006-2020.
136. Buah, W.K., A.M. Cunliffe, and P.T. Williams, *Characterization of Products from the Pyrolysis of Municipal Solid Waste*. Process Safety and Environmental Protection, 2007. **85**(5): p. 450-457.
137. Dalai, A.K., et al., *Gasification of refuse derived fuel in a fixed bed reactor for syngas production*. Waste Management, 2009. **29**(1): p. 252-258.
138. Onwudili, J.A. and P.T. Williams, *Hydrothermal Catalytic Gasification of Municipal Solid Waste*. Energy & Fuels, 2007. **21**(6): p. 3676-3683.



## Chapter 3

### Materials and Methods

This chapter describes characteristics of the samples used, the experimental procedures for the hydrothermal depolymerisation and the preparation of the composites produced with the recovered carbon fibres. Also the equipment and materials used during the experimental work were presented.

#### 3.1 Materials

Sodium hydroxide (pellets, purity 99.999%), potassium hydroxide (pellets, purity 99.999%) and 30 wt% hydrogen peroxide ( $\text{H}_2\text{O}_2$ ) solution and other additives and catalysts such as calcium oxide (CaO, powder form, purity 99.99%), sodium carbonate ( $\text{Na}_2\text{CO}_3$ , powder form, purity 99.99%) and acetic acid were all purchased from Sigma-Aldrich, UK. Dichloromethane (purity 99.99%) for the extraction of organic compounds in the liquid effluent was also obtained from Sigma-Aldrich, UK.

Ruthenium oxide-gamma alumina ( $\text{Ru}/\text{Al}_2\text{O}_3$ ) catalyst containing 5 wt%, 10 wt% and 20 wt% of the ruthenium oxide was supplied by Catal Limited, a UK-based SME. The catalysts were in the form of 1 mm pellets but were pulverized and sieved to a particle size of less than 125  $\mu\text{m}$  before use. XRD analysis confirmed that the ruthenium was present as ruthenium (IV) oxide ( $\text{RuO}_2$ ). The characteristics of the catalysts are presented in Table 3.1.1.

The Low density polyethylene (LDPE) was obtained from Bralen RB 2-62, Tisza Chemical Group Publil Limited Company, Hungary. The LDPE has 11.4 MPa, 7.5 MPa and 18.2  $\text{kJ m}^{-2}$  tensile strength, and flexural strength and Charpy impact strength, respectively. The melt-flow index was 2.2 g per 10 min (at 190 °C, 2160 N), while the tensile and flexural modulus were 348 MPa and 495 MPa, respectively. The tensile extension at break of matrix material was 155% without reinforcement.

Table 3.1.1 Characteristics of the ruthenium oxide-alumina catalysts

<i>Properties</i>	<i>Catalyst Loading</i>		
	5 wt%	10 wt%	20 wt%
BET surface area [m <sup>2</sup> /g]	8.54	8.06	7.97
Pore Volume [cm <sup>3</sup> /g]	0.027	0.023	0.025
Pore adsorption diameter [nm]	12.7	11.2	12.4
Pore desorption diameter [nm]	15.4	15.3	16.5
% Ruthenium metal	4.05	7.48	15.1

The virgin carbon fibre has 3800 MPa tensile strength, 228 GPa tensile modulus, 1.81 g cm<sup>-3</sup> density and approximately 7.2 µm diameter. In addition, the mechanical properties of the recovered carbon fibre were measured. The recovered carbon fibre had tensile strength, tensile modulus and density of 3904 MPa, 211 GPa and 1.75 g cm<sup>-3</sup>, respectively.

### 3.1.1 Carbon Fibre Reinforced Plastic (CFRP) Waste

The samples used in this study were real-world wastes. The waste carbon fibre reinforced plastic sample was made of woven carbon fibre on a resin, which is used for making vehicle interiors. The CFRP sample (Figure 3.1.1) used in this study was obtained from Milled Carbon Ltd, UK who recovers carbon fibres from end-of-life vehicles including automobiles and aircrafts. Thermogravimetric analysis (TGA) of the CFRP sample revealed that it consisted of 58-63 wt% carbon fibre and 37-42 wt% resin. The resin was found to be of a polybenzoxazine backbone (a phenolic-type thermoset). The elemental (CHNSO) composition of the CFRP was; 80.3% carbon, 2.05% hydrogen, 5.9% oxygen, 4.15% nitrogen and 1.65% sulphur. In addition, proximate analyses showed 33% volatile matter, 66.6%

fixed carbon and 0.4% ash. The CFRP waste sample was cut into strips of approximately 1 cm x 3 cm, to fit into reactor.



Figure 3.1.1 Waste CFRP sample

Figure 3.1.2 shows the TGA thermograph of the sample and the differential weight loss (DTG). The heating rate was  $5^{\circ}\text{C min}^{-1}$  and the final temperature was  $500^{\circ}\text{C}$ . The inert gas was  $\text{N}_2$ , and when the final temperature reached, it was kept constant for 1 h, and then air was introduced for 3 h to oxidize the char in the solid residue. According to the TGA thermograph, the first weight loss was observed at around  $100^{\circ}\text{C}$ , which was due to the moisture content of the sample. The major weight loss was observed when the temperature reached  $280^{\circ}\text{C}$ , and because of the decomposition of the resin, it continued until the temperature was  $500^{\circ}\text{C}$ . After holding the sample at  $500^{\circ}\text{C}$  for 1 h, 72 wt% of the sample consisting of carbon fibres with char remained. When the air was introduced, in total 41 wt% of sample was lost, the remaining 59 wt% were carbon fibres. There were two major peaks in the DTG thermograph, in which the first one at a temperature of  $380^{\circ}\text{C}$  represents the volatile matter in the waste that decomposed thermally. The other peak at  $500^{\circ}\text{C}$  represents the char combustion, as the air was introduced at that temperature. These results agree with the work of Lorjai et. al., [1] stating that during the TGA analysis, polybenzoxazine resin started to decompose at  $250^{\circ}\text{C}$ , and the largest weight loss was occurred at temperatures between 250 and  $600^{\circ}\text{C}$ . Similar results were observed when pure phenolic resin was analysed with TGA,



where the resin started to lose weight at 290 °C and was totally decomposed by the time a temperature of 600°C was reached [2].

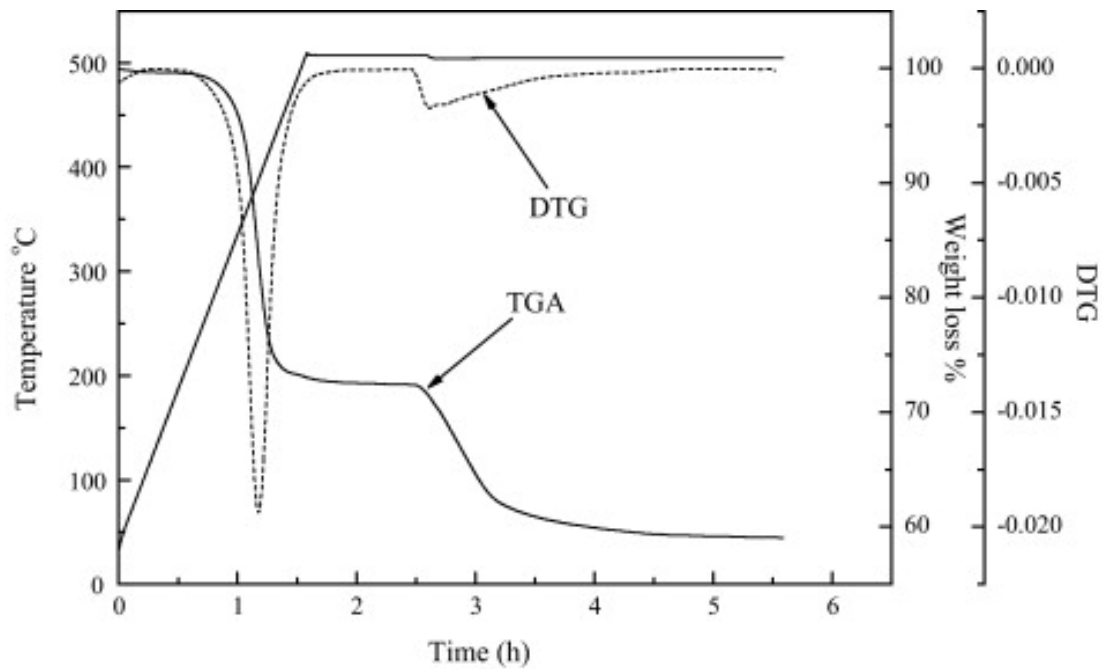


Figure 3.1.2 TGA and DTG curves of CFRP waste

### 3.1.2 Printed Circuit Board Waste

The printed circuit board of a desktop computer liquid crystal display (LCD) monitor was recovered from an LG computer. The capacitors, conductors, resistors and all removable materials were dismantled, and the boards were crushed into smaller particles as shown in the Figure 3.1.3



Figure 3.1.3 The printed circuit board extracted from desktop computer LCD monitors

A further grinding process was applied to decrease the particle size below 2 mm to produce a more homogenous mixture. The sample with particle size of <2 mm was characterized and used for the hydrothermal depolymerisation experiments. Ash analysis was carried out to determine the volatile (resin) fraction. Four samples of 1 g waste were oxidized at 500°C for 2 hours, and the results are shown in Table 3.1.2. These results suggested that approximately 38% of the dismantled waste composed of metals and ash, and the remaining part (~62) was the resin.

Table 3.1.2 Printed circuit waste ash analysis result

<i>Sample</i>	<i>Weight loss, %</i>	<i>Standard Deviation, %</i>
1	64.1	1.4
2	58.6	2.5
3	65.8	2.6
4	59.9	1.6
Average	62.1	2.4

Apart from ash analysis, thermogravimetric analysis (TGA) was performed to confirm the amount of the volatiles, and to characterize the thermal decomposition of the sample. The thermal analysis was carried out using a Mettler Toledo TGA/DSC 1 analyser. For this purpose, three samples were prepared in a way that each one had a weight about 15 mg and placed into the sample crucibles. A computer system recorded the time, temperature and the changes in the weight with the help of the microbalance. Nitrogen was the carrier gas with a flow rate of 50 ml min<sup>-1</sup> the temperature was increased from 25°C to 105°C with a heating rate of 25°C min<sup>-1</sup>, and held at this temperature for 10 minutes. Then the temperature was increased to 900°C with a heating rate of 25°C min<sup>-1</sup>. After holding the temperature constant for 10 minutes, air was introduced with a flow rate of 50 ml min<sup>-1</sup> for 15 minutes. The results of their average with a standard deviation less than 10% were displayed as TGA thermographs and the first derivative of the TGA thermograph (DTG curve) as shown for example in Figure 3.1.4.

The first weight loss was observed at 100°C, which was due to possible moisture content of the sample. The main weight loss occurred at temperatures between 280 and 600°C which is associated with the major peak in the DTG curve, where the thermal decomposition of the resin took place. Between these temperatures, weight loss was recorded as 60.4 wt%.

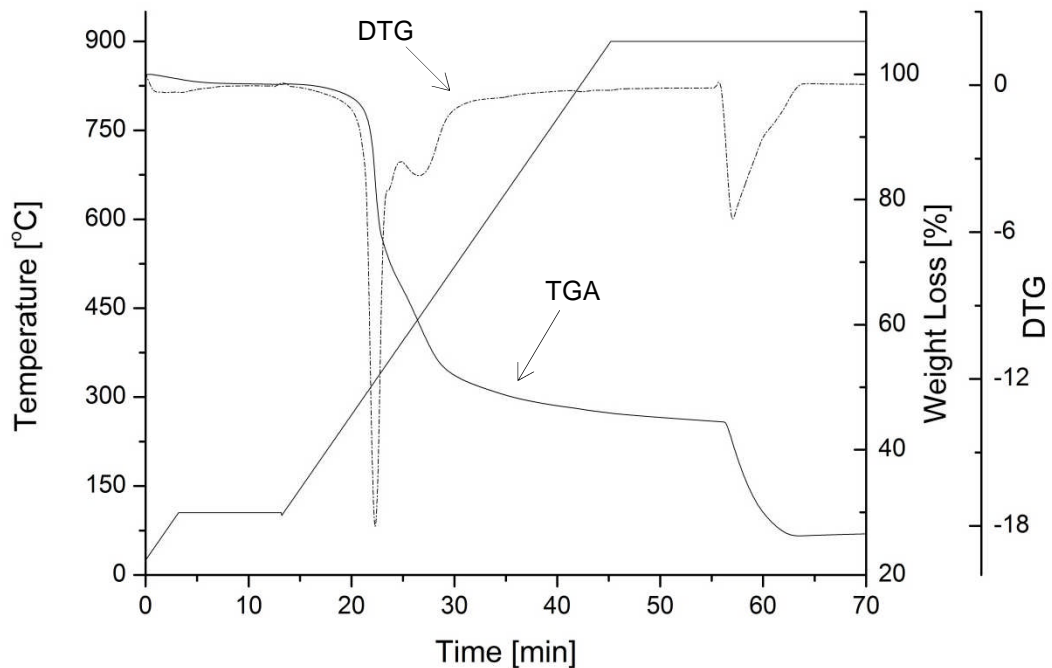


Figure 3.1.4 TGA and DTG curves of PCB waste

With the introduction of air, and at a temperature of 900°C another peak was observed in the DTG thermogram. This might be due to oxidation of the remaining chars and oxidation of some metals. These results confirm the work of others, such as Quan et. al., [3] who studied the thermogravimetric analysis of printed circuit boards and reported that the thermal decomposition started at a temperature range 295-309°C, depending on the heating rates of 10, 15, 20 and 40°C min<sup>-1</sup>. Barontini et. al., [4] studied the thermal decomposition of printed circuit boards containing brominated epoxy resin. They reported that the printed circuit board started decomposing at 280°C and the main weight loss occurred between 280 and 350°C when the heating rate was 10°C min<sup>-1</sup>.

### 3.1.3 Refuse Derived Fuel (RDF)

Refuse derived fuel (RDF) gathered from municipal solid waste (MSW) from a United Kingdom municipal waste treatment plant was used in the experiments in the hydrothermal treatment of RDF. The original sample was in pellet form with dimensions of 40 mm of length and 20 mm of diameter. The RDF in pellet form was shredded and ground to obtain a homogenous mixture of particle sizes between 0.25 mm and 1.0 mm as shown in Figure 3.1.5.



Figure 3.1.5 RDF sample (a) original pellets (b) shredded samples

The elemental analysis of the RDF sample was carried out to determine the amounts of carbon, hydrogen, nitrogen and sulphur. The amount of the oxygen was calculated by difference. According to the results of elemental analysis, the RDF sample consists of 44.5 wt% carbon, 5.8 wt% hydrogen, 49.0 wt% oxygen, 0.69 wt% nitrogen and 0.03 wt% sulphur. The gross calorific value of the RDF sample was determined as 22 MJ/kg, and net calorific value was 21 MJ/kg.

The thermal degradation behaviour of RDF sample was investigated to gather information about its thermal stability and the fraction of volatile components. For this aim, thermogravimetric analysis was carried out using a TGA Shimadzu, Stanton Redcroft 280 analyser. Approximately 15 mg of RDF sample was placed into an alumina crucible, which at the same time was held by a holder made of platinum acting also as a thermocouple. Under

a nitrogen atmosphere with a flow rate of  $50 \text{ ml min}^{-1}$ , the temperature was increased from  $15^{\circ}\text{C}$  to  $110^{\circ}\text{C}$  with a heating rate of  $25^{\circ}\text{C min}^{-1}$  and held constant for 10 minutes. Then, with the same heating rate, the temperature was increased up to  $900^{\circ}\text{C}$ . After holding for 10 minutes at this temperature, air was introduced and the temperature was increased to  $910^{\circ}\text{C}$ . After 10 minutes holding time, the analysis was finalized and the resulting thermograph is shown in Figure 3.1.6.

The first weight loss was 3.8 wt% and observed at around  $100^{\circ}\text{C}$ , which was due to the loss of moisture content of the sample. The decomposition of volatiles started at around  $240^{\circ}\text{C}$  and at  $300^{\circ}\text{C}$ , a major peak was observed in the DTG curve representing the decomposition of lighter volatile compounds.

According to Buah et. al., [5] the thermal degradation of plastics such as polystyrene, polypropylene, low density polyethylene and high density polyethylene occurs at a temperature range of  $350 - 500^{\circ}\text{C}$ , while polyvinyl chloride degradation is observed at around  $200 - 380^{\circ}\text{C}$ . Also, biogenic components of RDF, cellulose or hemicellulose are known to start degrading around  $240 - 380^{\circ}\text{C}$ . However, significant effort is made during MSW processing into RDF to remove PVC, hence the first peak observed was unlikely be related to the PVC content of RDF. Therefore it can be concluded that the weight loss between  $240-380^{\circ}\text{C}$  might be due to the decomposition of the cellulosic content of RDF [6].

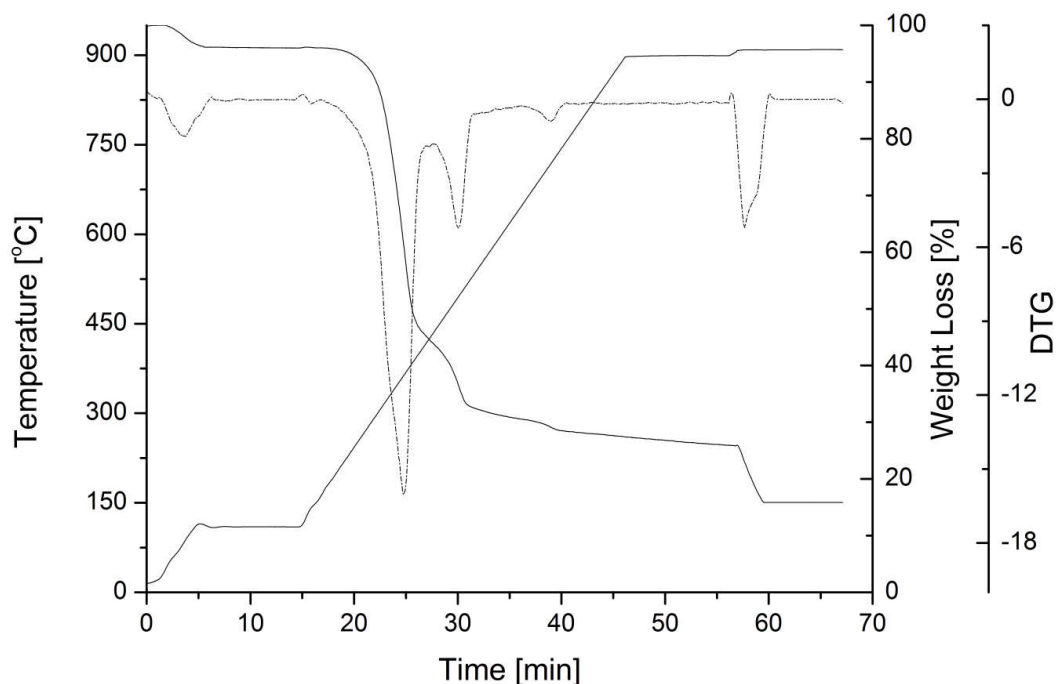


Figure 3.1.6 TGA and DTG curves of RDF sample

Two small peaks were observed at temperatures around 500°C and 670°C, showing that hydrocarbons with higher molecular weight could also exist in the RDF. This could possibly be due to the decomposition of the plastic fractions of the RDF [7]. The total weight loss between the temperatures of 110°C and 900°C was determined as 70 wt%. Finally, with the introduction of air, oxidation of the fixed carbon took place leaving only the ash content of the RDF which was around 15 wt%.

### 3.2 Hydrothermal Reactor System

In this study, a batch type reactor with a volumetric capacity of 500 ml was used for the hydrothermal processing of the carbon fibre reinforced plastic waste and printed circuit board waste samples. For the gasification of the liquid effluent produced from the hydrothermal depolymerisation of carbon fibre reinforced plastic waste samples in an ethylene glycol and water mixture, another batch type reactor with a volumetric capacity of 75 ml was used. The reason for using a different reactor for the gasification experiments was due to its limitations to high pressure at high temperatures.

The 500 ml batch reactor was obtained from the Parr Instrument Co., USA. A schematic diagram and a photograph of the reactor, furnace and the control unit are shown in Figure 3.2.1 and Figure 3.2.2 respectively. The reactor was made of stainless steel (SS316) with an inner diameter of 63.5 mm and a wall thickness of 15.9 mm. The maximum operation temperature and pressure of the reactor was 500°C and 35 MPa, respectively.

Heat to the reactor was supplied by an insulated ceramic furnace (3 kW, 240 volts) which was obtained from Elmatic Limited, Cardiff, UK. The process control of the furnace was carried out with the help of a temperature monitoring unit and a series of thermocouples. The thermocouples were connected to a controller which was installed in a switchbox connected to the main electricity supply.

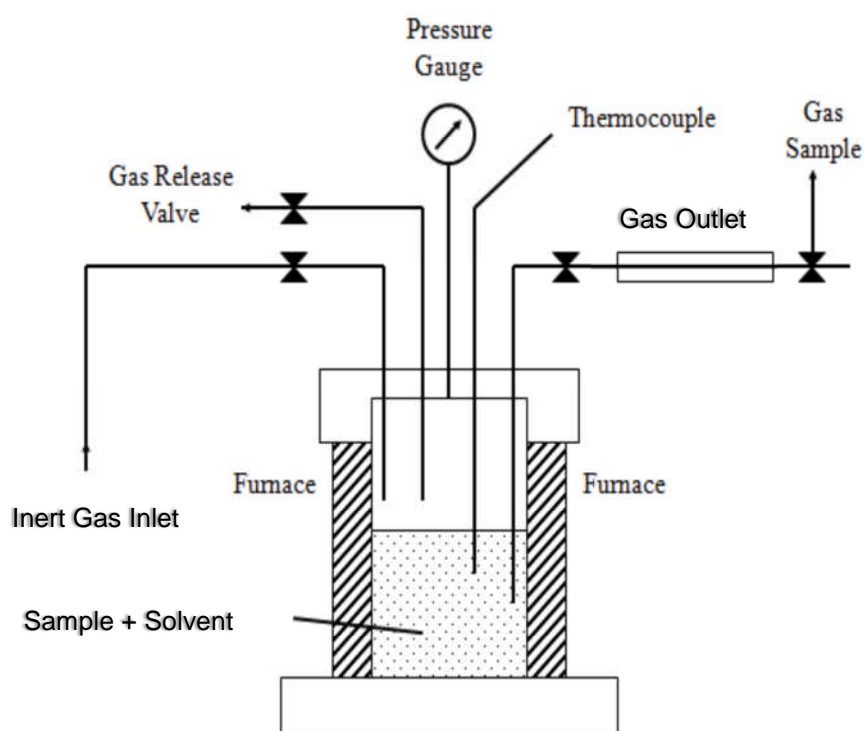


Figure 3.2.1 The Schematic diagram of hydrothermal reactor

There was also a thermowell installed on the top of the reactor extending to the interior vessel, to enable insert of another series of thermocouples to monitor the temperature of the reactor. The internal pressure of the reactor was measured with a pressure gauge with the accuracy of  $\pm 0.5$  bars that was fitted to the top of the reactor with a T316

Bourdon tube. The pressure gauge was calibrated in the range of 0 to 35 MPa.

The inert gas inlet was attached to the reactor to be used to introduce gases into the reactor for the purpose of gas purging. The gas outlet valve was attached to the reactor, to take gas samples from the experiments.

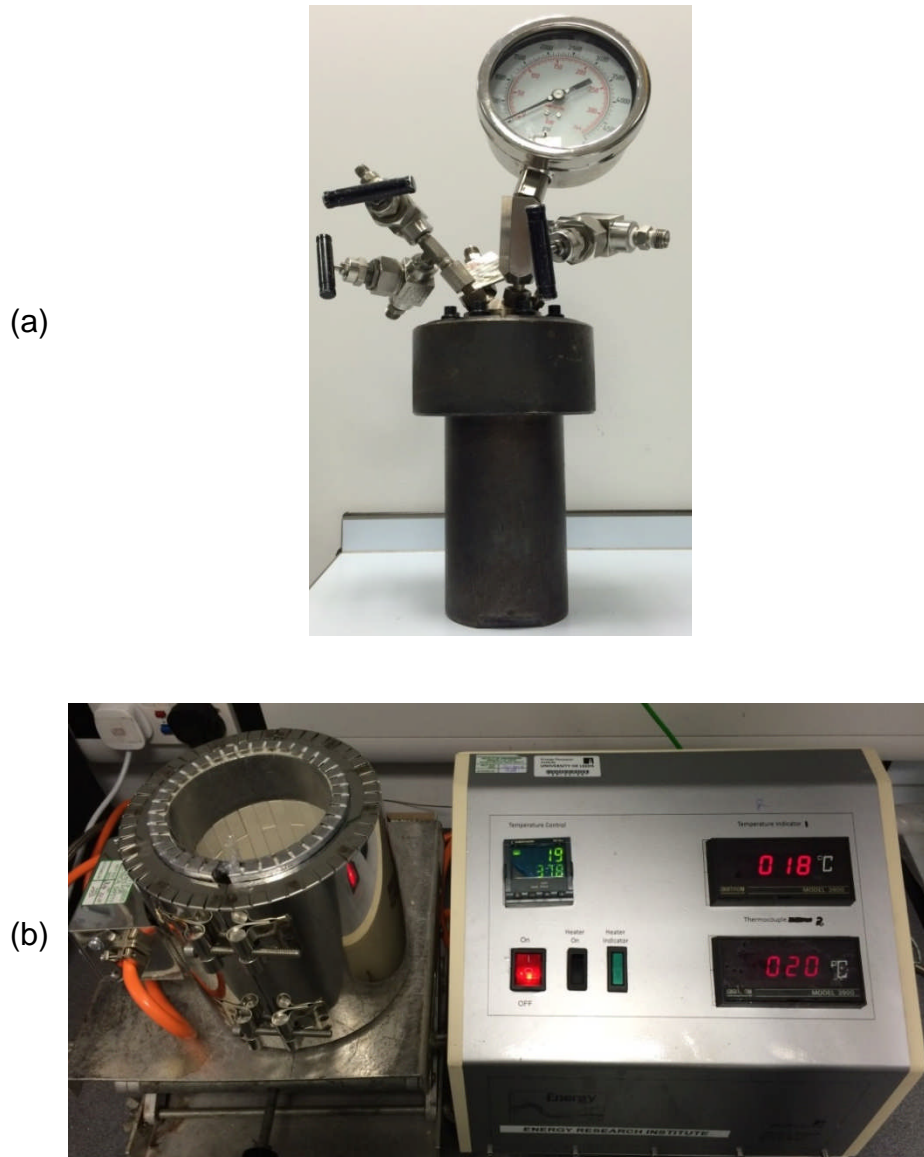


Figure 3.2.2 Photograph of (a) Hydrothermal reactor and (b) The furnace and the control unit

The internal temperature of the reactor was monitored with a type K thermocouple with an accuracy of  $\pm 1$  °C fitted into a stainless steel thermowell. Another type K thermocouple was used to monitor and control



the temperature of the furnace. A safety rupture disc was fitted to the chamber of the reactor, to limit the internal pressure up to 25 MPa, for safety reasons. Additionally, pressure safety tests were performed annually as part of the safety regime of the reactor.

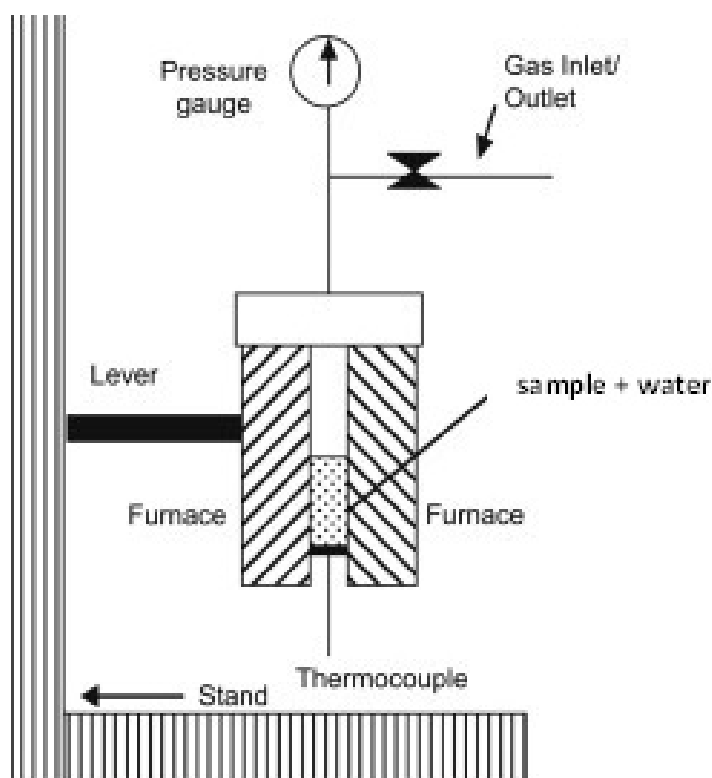


Figure 3.2.3 Schematic diagram of 75 ml reactor

The 75 ml reactor that was used for the gasification experiments was a small non-stirred Hastelloy-C reactor, obtained from the Parr Instrument Co., Moline, Illinois, USA. The reactor with an inner diameter of 25 mm and a wall thickness of 9.53 mm is shown in Figure 3.2.3 as a schematic diagram. The maximum operating temperature and pressure was 600°C and 45 MPa, respectively.

The reactor was fitted with a 1 kW Carbolite ceramic furnace, equipped with a lever which can move the furnace up and down horizontally. The temperature of the furnace was measured with by a series of thermocouples, connected to the display and control unit (Digitron Instrumentation Limited, UK, Model 3900). A portable type K thermocouple was located at the bottom of the reactor to measure the reactor temperature. A pressure gauge with an

accuracy of  $\pm 0.5$  bars together with the gas outlet and sampling valve were installed in the top of the reactor to display the pressure and to take gas samples for analysis.

### **3.3 Experimental Procedure**

#### **3.3.1 Set up of the 500 ml Reactor**

For the hydrothermal depolymerisation experiments, 2.5 g of sample (carbon fibre reinforced plastic waste, printed circuit board waste or refuse derived fuel) was added to the reactor. The total liquid volume to add was 60 ml for each experiment, as the pressure could only be adjusted with the temperature and the solvent volume, through auto-generation of pressure related to the temperature of the added liquid. Therefore for the experiments with water alone or with any solvent alone, 60 ml of solvent was added; for the experiments with oxidant agent ( $\text{H}_2\text{O}_2$ ), with any additives (acetic acid, methanol, etc.) or with any mixtures of the solvents (ethylene glycol-water) a known volume to be 5, 7.5 or 10 wt%  $\text{H}_2\text{O}_2$  or with a known volume of the additive and the volume of liquid made up to 60 mL with distilled water was added to the reactor. The amount of alkali (NaOH or KOH) and other additives such as CaO and  $\text{Na}_2\text{CO}_3$  were 1.0 g.

Then the reactor was sealed, and with the help of the inert gas inlet and gas outlet valves, the reactor was purged with nitrogen. The purging time was kept constant (5 min) and after purging, the gas outlet valve was closed so that the pressure inside of the reactor reached an equilibrium with the nitrogen pressure which was around 0.5 MPa. Therefore, for each experiment, the reactor was pressurized with nitrogen. The reason for this procedure was for gas analysis, as the gas production might be low in low temperature hydrothermal processing of the samples; therefore in order to be able to take gas samples after the experiments, the reactor was pressurized before the experiments.

After the purging and sealing, the reactor was placed inside of the ceramic furnace and with a constant heating rate of  $\sim 12^\circ\text{C min}^{-1}$  heated to the designated temperature and corresponding autogenerated pressure. The

reactor was quickly withdrawn from the furnace as soon as the designated conditions were reached, for the experiments having a reaction time more than zero minutes, when the designated temperature was reached, the time was started to be measured by stopwatch and as soon as the designated reaction time was reached, the reactor was quickly withdrawn from the furnace.

When the experiment ended, the reactor was taken out of the furnace, and cooled to room temperature with a cooler fan. This usually took 2 h, as the reactor wall thickness is very large. When the ambient temperature was reached, the internal pressure and temperature were recorded to calculate the number of moles of the gas product inside the reactor. The gas sampling valve was then opened to allow the gas effluent to flow into a gas-tight plastic syringe and the gaseous effluent was injected into a series of gas chromatographs for the identification and quantification of the gases. After gas sample collection, the reactor was opened and the liquid and solid samples were collected into a beaker and separated by filtration. Then the reactor was rinsed with a known amount of DCM to recover any remaining organic compounds, and the solution was stored in a separate container.

### **3.3.2 Setup of the 75 ml Reactor**

The 75 ml reactor was used for hydrothermal gasification experiments. For each experiment, the liquid volume in the reactor was no more than 15 ml, as the pressure could only be adjusted with the temperature and the liquid volume. When hydrothermal gasification of RDF was carried out, 1.0 g of RDF sample was added to the reactor. The amount of catalyst (5 wt%, 10 wt%, 20 wt%  $\text{RuO}_2/\gamma\text{-Al}_2\text{O}_3$  and NaOH) was 0.5 g. For the hydrothermal gasification of residual liquid obtained from hydrothermal depolymerisation of carbon fibre reinforced plastic waste with water and ethylene glycol mixture, 15 ml was added to the reactor with the same amount of catalysts that were used in the experiments with RDF. After adding the samples and catalysts into the reactor, the same procedures with the 500 ml reactor were carried out; the reactor was purged with nitrogen and sealed. However no pressurizing with nitrogen was carried out as after the gasification experiments, the gas production was high.

After the sealing and purging, the reactor was heated with a constant heating rate of  $\sim 12^{\circ}\text{C min}^{-1}$  to the designated temperature. When the set point was reached, the temperature was held constant depending on the reaction time. After the reaction time was completed, the reactor was taken out of the furnace and was cooled with the help of a cooling fan. This usually took 45 minutes for the reactor to reach the ambient temperature. The internal pressure and temperature were recorded after reaching ambient conditions, to calculate the number of moles of the gas product inside the reactor. Just as in the case of 500 ml reactor, the gas sampling valve was then opened to allow the gas effluent to flow into a gas-tight plastic syringe and the gaseous effluent was injected into the gas chromatographic analytical system for the identification and quantification of the gases. After gas sample collection, the reactor was opened and the liquid and solid samples were collected into a beaker and separated by filtration. Then the reactor was rinsed with a known amount of DCM for any remaining organic compounds, and the solution was kept in a separate container.

### **3.4 Effluent Gas Analyses**

The gas product was collected in a gas-tight syringe for injections to the gas chromatography (GC) equipment; an example of one of the gas chromatographs with the associated computer data handling system used in this study is shown in Figure 3.4.1. The aim of this analytical technique is to determine the gas composition qualitatively and quantitatively. The injected gas is carried with an inert gas (e.g. helium, nitrogen or argon) through the oven and then through the analytical column packed with a mesh of specific characteristics. The sample reaches the detection system which in this work was either can be a flame ionization (FID) or thermal conductivity detector (TCD) as described in Figure 3.4.2 [8].

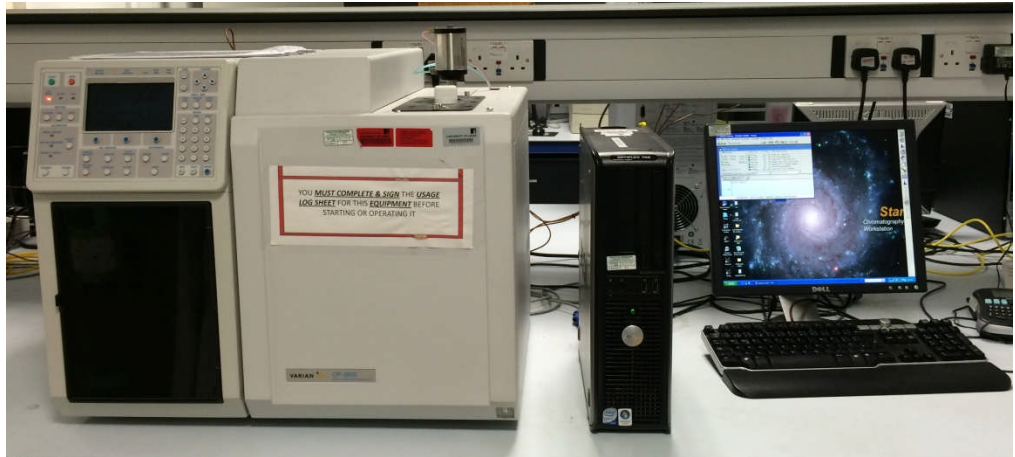


Figure 3.4.1 Gas chromatography with the computer unit

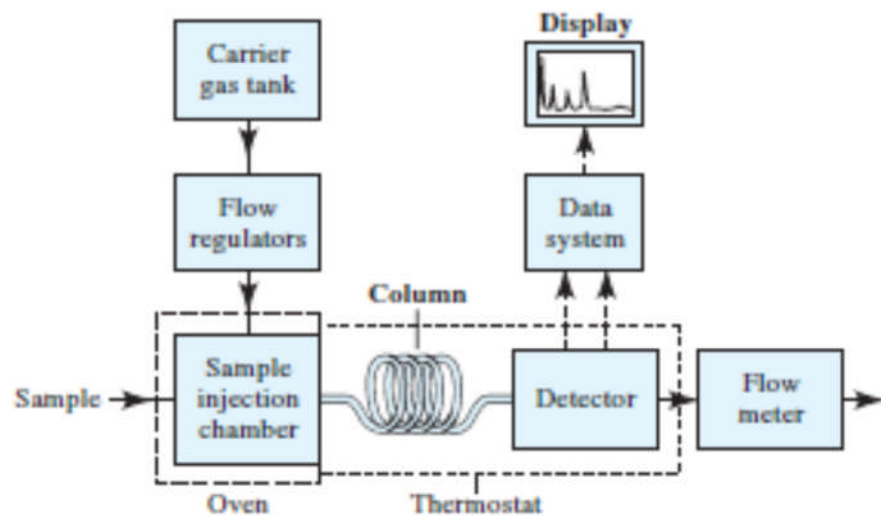


Figure 3.4.2 Block diagram of a typical gas chromatograph [8]

### 3.4.1 Permanent Gas Chromatography Analyses

For permanent gases, the analyses were carried out using a Varian CP-3380 gas chromatograph with a thermal conductivity detector (GC/TCD) equipped with a 2 m long by a 2 mm diameter column packed with a 60-80 mesh molecular sieve. The carrier gas for this GC was Argon. The column oven was held at a constant temperature of 40 °C during the analysis and the temperature of the injector was 120 °C. The temperatures of the detector and the filament were 120 °C and 160 °C respectively. Carbon dioxide was analysed by a Varian CP-3380 (GC/TCD), a column with 2 m length by 2

mm diameter was packed with a Hysep 80-100 molecular mesh, and argon was used as the carrier gas. Regularly, the GCs were calibrated by using a standard gas mixture obtained from Supelco, UK. The mixture contained 1 % of H<sub>2</sub>, O<sub>2</sub>, CO, CO<sub>2</sub> and 96 % of N<sub>2</sub> in volume percentages. Examples of the resulting chromatograph and the corresponding areas are shown in Figure 3.4.3 and Table 3.4.1.

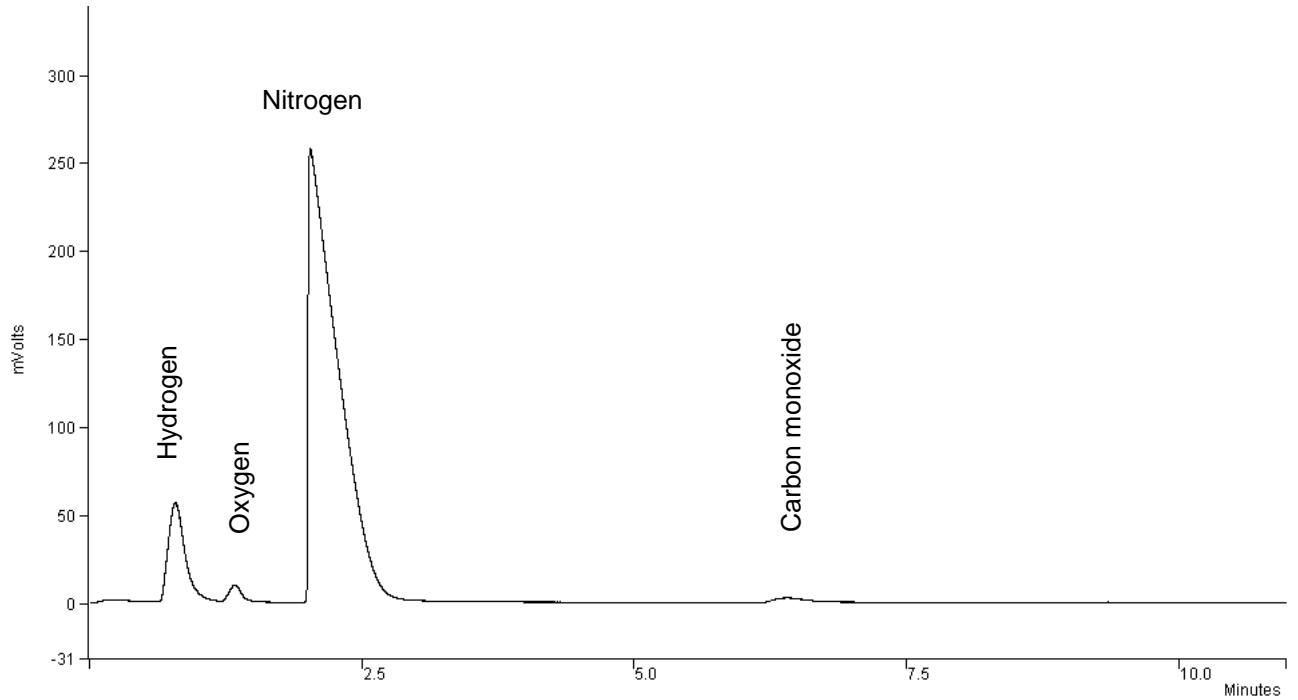


Figure 3.4.3 GC chromatogram of the standard for permanent gases

Table 3.4.1 GC results of the standard for permanent gases

<i>Gas Component</i>	<i>Retention time [min]</i>	<i>Area</i>	<i>Composition [vol.%]</i>
Hydrogen	0.784	607933	1
Oxygen	1.329	79458	1
Nitrogen	2.028	4872050	96
Carbon monoxide	6.400	49671	1

### 3.4.2 Hydrocarbons Gas Chromatography Analyses

For the analysis of hydrocarbon gases, a different Varian CP-3380 GC with a flame ionization detector (GC/FID) equipped with a 2 m long by 2 mm diameter column packed with 80-100 mesh Haysep was used. Nitrogen was the carrier gas. The injector was held at 150°C while the detector temperature was 200 °C. The oven temperature program was initially held at 60°C for 3 min, then heating up till 100°C with a rate of 10°C min<sup>-1</sup>, held for 3 min and finally ramped to 120°C at 20°C min<sup>-1</sup>.

Regularly, the GC was calibrated by using a standard gas mixture containing 1% of CH<sub>4</sub>, C<sub>2</sub>H<sub>6</sub>; 1% of C<sub>3</sub>H<sub>8</sub>; 1% of C<sub>4</sub>H<sub>10</sub> and remaining N<sub>2</sub> in volume percentages for the alkanes. And for the alkenes, a mixture of hydrocarbon gases containing 1% of C<sub>2</sub>H<sub>4</sub>, C<sub>3</sub>H<sub>6</sub>, C<sub>4</sub>H<sub>8</sub> & C<sub>4</sub>H<sub>10</sub>, and N<sub>2</sub> as make-up gas was used for calibration. Examples of GC chromatograms for the analyses for both alkanes and alkenes and the resulting corresponding areas are shown in Figure 3.4.4 and Table 3.4.2.

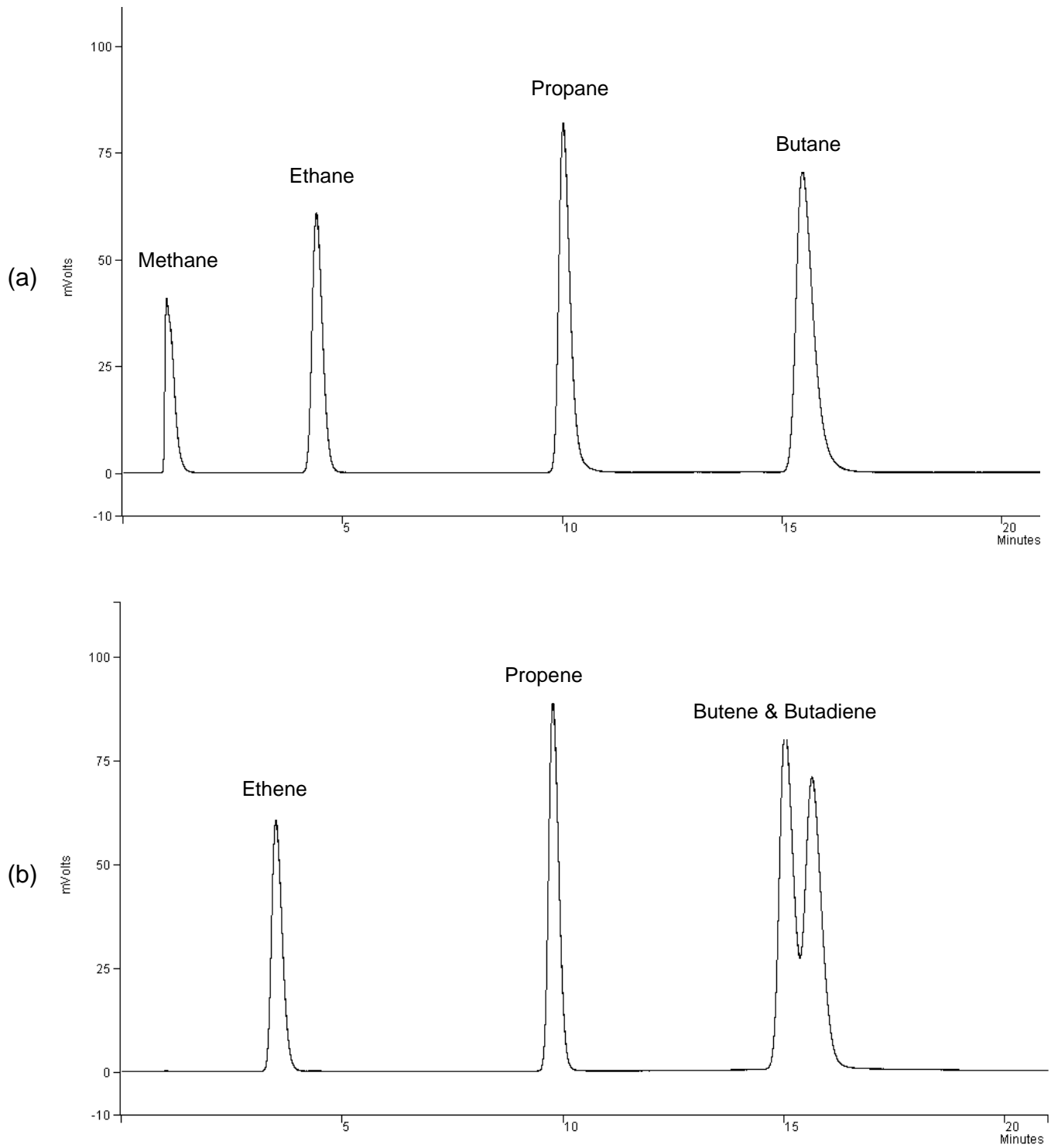


Figure 3.4.4 GC chromatogram of the standard for hydrocarbon gases (a) Alkanes and (b) Alkenes



Table 3.4.2 GC results of the standard for hydrocarbon gases (alkanes and alkenes)

<i>Gas Component</i>	<i>Retention time [min]</i>	<i>Area</i>	<i>Composition [vol.%]</i>
Methane	0.983	548695	1
Ethane	4.393	1007224	1
Propane	10.010	1469676	1
Butane	15.455	1950716	1
Ethene	3.491	1017571	1
Propene	9.762	1433275	1
Butene	15.021	1829362	1
Butadiene	15.628	1886543	1

### 3.4.3 Calculation of Gas Compositions

The calculation of the volume percentages contained in the product gas effluents from experiments were made in relation to the results produced from the analysis with the standard gases. The area values recognised by the digital integrator by converting the electrical signal from the detector were used to obtain response factors (RFs) for each species in the standard gases. The following equation was used to calculate response factors;

$$RF = \frac{\text{peak area of standard gas}}{\text{vol \% of standard gas}} \quad \text{Equation 3.4.1}$$

Since for almost all the gas compounds in the standard gases the gas composition was 1 vol%, the corresponding RF value was equal to the area produced in the chromatogram. After obtaining RF values for all gases, the

volume percentages of each species in the gas effluent obtained from the experiments can be calculated as;

$$\text{vol \%} = \frac{\text{peak area of each analytical gas sample}}{\text{RF of the standard gas}} \quad \text{Equation 3.4.2}$$

Since the mole fraction and the volume fraction are equal to each other for the ideal gases [9], once the volume percentages of each species are known, by using the Ideal Gas Law (Equation 3.4.3), the mole numbers of each gas individually can be calculated and the yield calculations in the unit of moles of gas per kg feed can be made. By using Excel 2010 spreadsheet, the yields of the gas product were calculated via this method.

$$n = \frac{PV}{RT} \quad \text{Equation 3.4.3}$$

Where  $n$  is the mole number (mol);  $V$  is the volume [ $\text{m}^3$ ];  $P$  is the pressure [Pa];  $T$  is the temperature [K] and  $R$  is the universal gas constant [ $8.314 \text{ J K}^{-1} \text{ mol}^{-1}$ ] [10].

A sample of the Excel spreadsheet solution for the hydrothermal gasification of RDF with 5 wt% ruthenium catalyst at  $500^\circ\text{C}$  and zero minute residence time is shown in Table 3.4.3. The relative standard deviation (RSTDV) was 0.75 for the total which was very low indicating that the analysis results are very accurate. After determining the volume compositions of each gas, the composition without nitrogen was calculated, and then the weight of each gas was calculated according to Equation 3.4.4.

Table 3.4.3 Excel spreadsheet solution for the hydrothermal gasification of RDF with 5 wt% ruthenium catalyst at 500°C and zero minute residence time

Gas	RF	PA of Sample 1	Con [vol%]	PA of Sample 2	Con [vol%]	Average Con [vol%]	Deviation [%]
H <sub>2</sub>	613016	8549426	13.95	8648308	14.11	14.03	0.81
O <sub>2</sub>	76316	60180	0.79	53626	0.70	0.75	8.14
N <sub>2</sub>	50751	2771600	54.61	27993464	55.04	54.83	0.56
CO	46671	43282	0.93	43612	0.93	0.93	0.54
CO <sub>2</sub>	1	25.30	25.30	24	24.00	24.65	3.73
CH <sub>4</sub>	566989	2013203	3.55	1883482	3.32	3.44	4.71
C <sub>2</sub> H <sub>4</sub>	1017571	1883482	0.03	30317	0.03	0.03	4.07
C <sub>2</sub> H <sub>6</sub>	1008230	32112	0.42	397495	0.39	0.41	4.30
C <sub>3</sub> H <sub>6</sub>	1433275	0	0	0	0	0	0
C <sub>3</sub> H <sub>8</sub>	1503720	422436	0.28	395000	0.26	0.27	4.50
C <sub>4</sub> H <sub>6</sub>	1829362	0	0	0	0	0	0
C <sub>4</sub> H <sub>8</sub>	1886543	37941	0.02	49874	0.03	0.02	19.22
C <sub>4</sub> H <sub>10</sub>	2085566	159757	0.08	183487	0.09	0.08	9.78
Total			100.0		98.9	99	0.75

$$X_{gas} = \sum_{i=1}^n X_i \quad \text{Equation 3.4.4}$$

$X_i$  stands for the calculated weight of each gas compound [g] and  $X_{gas}$  the total weight in grams.

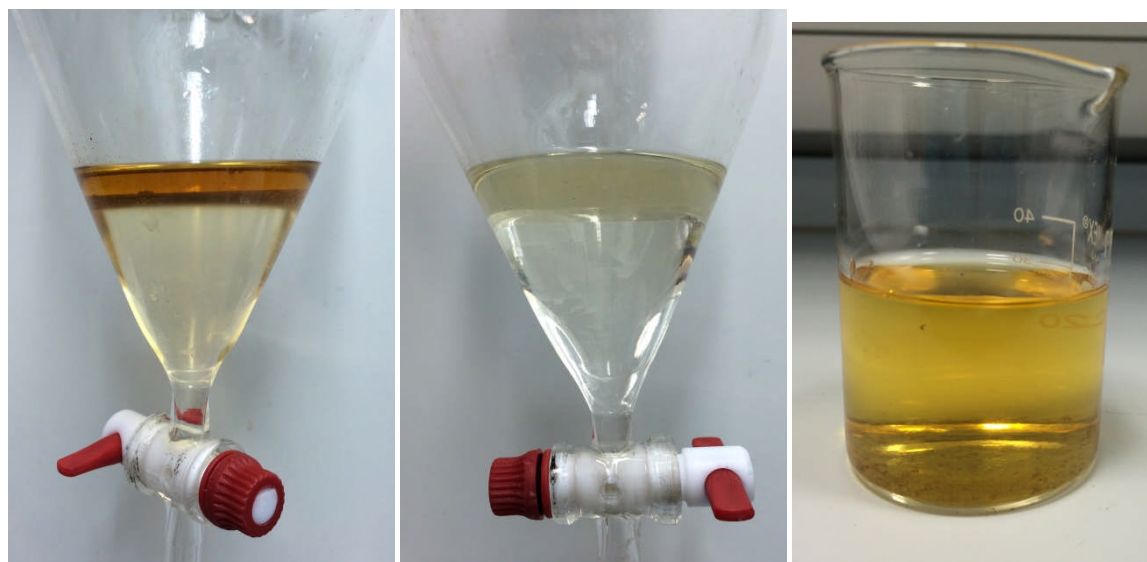
### 3.5 Liquid Effluent Analyses

After collecting the gas products, the remaining reactor contents including liquid and solid residues were collected into a beaker and separated by filtration by washing with distilled water. Also the reactor was washed with a known amount of DCM, to ensure that no char remained in the reactor, and the solution was stored in a separate container. The liquid effluent was analysed with TOC and GC/MS to determine the carbon content and to enable detection of the organic compounds present.

For GC/MS analyses, liquid-liquid extraction with DCM was carried out, to separate the water content from the organic phase. The purpose for determining the organic content of the liquid effluent was to determine whether the liquid could be used as a source of chemicals, either to recover the degraded polymer monomer or other high concentration/high value compounds. 20 ml of liquid sample was pipetted into a separating funnel for each sample, and 40 ml of DCM was added for the extraction, in a way that first 20 ml was added, the funnel was well shaken then after the two phases (aqueous and organic phases) separated, the organic phase was taken out. Then 20 ml of DCM was added again and the same procedure was applied to separate the organic phase. An example of the separation and the colours of the phases in this two stage liquid-liquid extraction with DCM are shown in Figure 3.5.1. The extracted phase was then passed through a column filled with sodium sulphate ( $\text{Na}_2\text{SO}_4$ ) for any remaining water content to be removed.

In some cases, a basification and acidification process was applied prior to the extraction process, since without any acid or base addition, some chemical compounds such as phenol and aniline created a single analysis

peak in the gas chromatogram. Therefore, for complete separation of such compounds, basification with 90% KOH was used to produce a pH value that was higher than 12 or acidification with 98% HCl to have a pH value that is lower than 3 was carried out.



(a)

(b)

(c)

Figure 3.5.1 Liquid-liquid extraction with DCM (a) after first addition of 20 ml DCM, (b) after second addition of 20 ml DCM and (c) the resulting organic phase after extraction

### 3.5.1 Total Organic Carbon (TOC) and Total Inorganic Carbon (TIC) Analyses

The liquid effluent was taken and analysed for total organic carbon (TOC) and total inorganic carbon (IC) using a TOC analyser (IL550 TOC-TN analyser Hach-Lange Co., UK) to determine the carbon balance.

The TOC analysis gave the results in units of mg/L, and the volume of the liquid was known; so the amount of carbon in grams was calculated according to the following formula;

*Organic carbon [g]*

$$= \text{TOC value of the sample}[\text{mg/L}] \times \text{Volume of the liquid effluent [L]}$$

In the same manner, inorganic carbon and total carbon in grams were calculated;

*Inorganic carbon [g]*

$$= IC \text{ value of the sample [mg/L]} \times \text{Volume of the liquid effluent [L]}$$

*Total carbon [g]*

$$= TC \text{ value of the sample [mg/L]} \times \text{Volume of the liquid effluent [L]}$$

### 3.5.2 Gas Chromatography/Mass Spectrometry (GC/MS)

For identification of organic compounds in the product, the liquid effluent was also analysed using a GC-MS analyser. The working principle of GC/MS is to combine the benefits of the separation of components from the GC with the selective and sensitive detection of the MS [11]. The mass spectrometer measures the relation of mass and charge ratio from the produced ions of the sample [12].



Figure 3.5.2 GC/MS analyzer used for the analyses of liquid effluent

The GC/MS analyses were carried out using a Varian 3800-GC coupled to a Varian Saturn 2200 ion trap MS/MS system as shown in Figure 3.5.2. The column used was a 30 m long x 0.25 mm inner diameter Varian VF-5ms (DB-5 equivalent) capillary column with helium carrier gas, at a constant flow rate of 1 ml min<sup>-1</sup>. The GC injector was held at 290°C. The oven temperature program was as follows; 40°C held for 2 min and ramped to 280°C at a rate of 5°C min<sup>-1</sup> and then held at 280°C for 10 min. The transfer line temperature was 280°C, manifold was at 120°C and the trap temperature was held at 200°C.

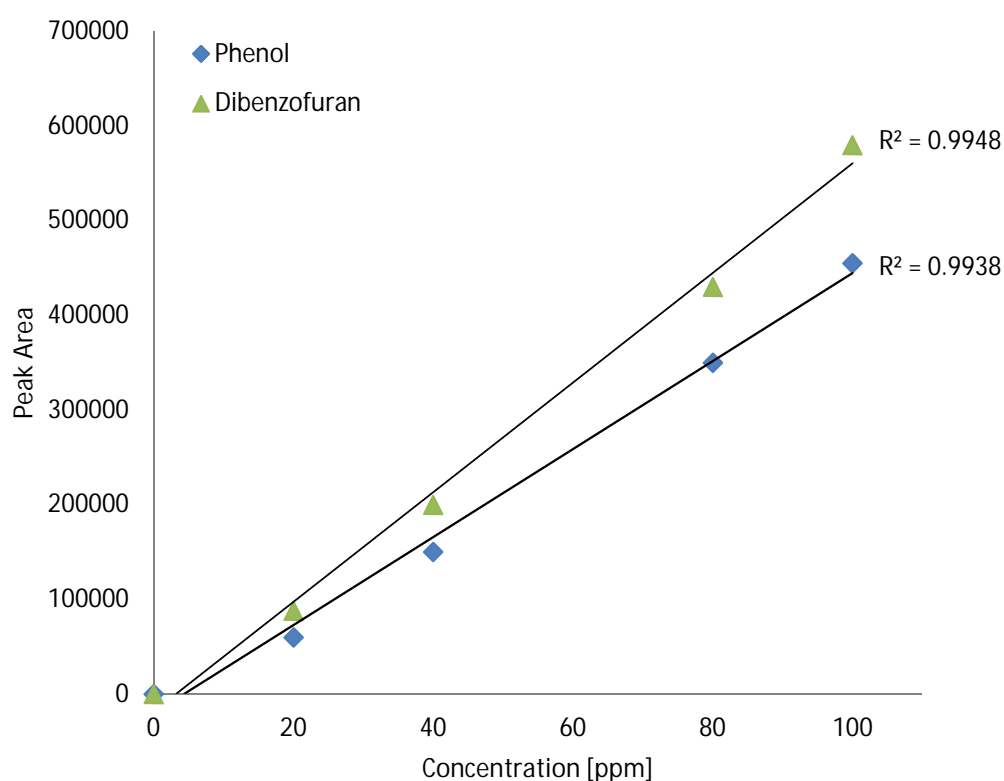


Figure 3.5.3 Calibration curves for phenol and dibenzofuran

Appropriate dilutions of the prepared fractions were made prior to GC/MS analysis. Quantitative analyses of the components in the oil products were carried out using different external standard methods for aromatics, heterocyclic and aliphatic compounds where applicable. For the aliphatic compounds a calibration curve was developed using a standard mixture of C<sub>8</sub> – C<sub>40</sub> compounds obtained from Sigma-Aldrich UK. In addition, a standard solution of 36 aromatic compounds was prepared and used to create 4-point calibration curves for their analysis at concentrations of 20,

40, 60 and 80 p.p.m. in DCM. The calibration curves gave  $R^2$  values close to 1, as seen in Figure 3.5.3 which represents the calibration curves for phenol and dibenzofuran. Results of oil analyses were obtained within the linear working range of the GC/MS/MS in p.p.m. and converted to reporting units based on the yields of oil products. In some case, spectral searches on the installed NIST2008 Library were used to qualitatively identify the major 'unknown' compounds in the oil products.

### **3.6 Solid Residue Analyses**

The solid residue collected after the filtration was dried to a constant weight in an oven at 105 °C to determine its weight. Also the raw samples of carbon fibre reinforced plastic waste, printed circuit board waste and refuse derived fuel sample were analysed for characterisation.

#### **3.6.1 Thermogravimetric Analyses (TGA) and Differential Thermal Analyses (DTA)**

Thermogravimetric analyses and differential thermal analyses were carried out to determine the thermal degradation behaviour of the carbon fibre reinforced plastic waste, printed circuit board waste and refuse derived fuel samples. For this purpose, two different kinds of TGA device were used. Also the amount of the volatile matter and the moisture content of the samples were determined by this method.

The thermal analysis was carried out using a Mattler Toledo TGA/DSC 1 analyser. The weight of sample was around 15 mg and was placed into the sample crucible. A computer system recorded the time, temperature and the changes in the weight using a microbalance. Nitrogen was the carrier gas with a flow rate of 50 ml min<sup>-1</sup> the temperature was increased from 25°C to 105°C with a heating rate of 25°C min<sup>-1</sup>, and held at this temperature for 10 minutes. Then the temperature was increased to 900°C with a heating rate of 25°C min<sup>-1</sup>. After holding the temperature constant for 10 minutes, air was introduced with a flow rate of 50 ml min<sup>-1</sup> for 15 minutes. Also a TGA Shimadzu, Stanton Redcroft 280 analyser was used for thermal analysis. Approximately 15 mg of sample was placed into an alumina crucible, which



at the same time was held by a holder made of platinum acting also as a thermocouple. Under helium atmosphere with a flow rate of  $50 \text{ ml min}^{-1}$ , the temperature was increased from  $15^{\circ}\text{C}$  to  $110^{\circ}\text{C}$  with a heating rate of  $25^{\circ}\text{C min}^{-1}$  and held constant for 10 minutes. Then, with the same heating rate, the temperature was increased up to  $900^{\circ}\text{C}$ . After holding for 10 minutes at this temperature, air was introduced and the temperature was increased to  $910^{\circ}\text{C}$ . After 10 minutes holding time, the analysis was finalized.

### **3.6.2 Scanning Electron Microscopy (SEM)**

The microscopic technique was used to characterise and examine the surface of the carbon fibres (both recovered and virgin). The surface rigidity and char deposition on the fibre were investigated. For this purpose a high resolution SEM (LEO 1530 FEG) coupled to an energy dispersive X-ray spectrometer (EDXS) was used to carry out the analysis. The carbon fibre samples were processed to reduce the size less than 1 mm. In order to observe the surface of the carbon fibre samples, a metallic coating was applied with Pt/Pi to produce a 5.0 nm layer to improve the charge dissipation.

### **3.6.3 Infrared Spectrometry (FTIR)**

Fourier Transform Infrared Spectrometry (FTIR) is a technique which is absorbing infrared spectra light across a wide range of wave lengths to determine the different functional groups in an organic liquid or solid sample. An IR spectrum consisting of the wave number [ $\text{cm}^{-1}$ ] versus intensity [%], transmittance or absorbance], can be obtained as those parameters can be converted by using Fourier-transformation.

FTIR analyses were carried out by using a TENSOR 27-type FTIR fitted with an Attenuated Total Reflectance (ATR) accessory (Ge crystal) at a frequency range of  $4000 - 650 \text{ cm}^{-1}$  to determine the interactions between the carbon fibres and the coupling agents and the matrix.

### **3.6.4 Mechanical Properties Analyses**

Mechanical tests were performed in the Department of Hydrocarbon and Coal Processing Chemical Engineering and Process Engineering Institute, University of Pannonia, Veszprém, Hungary to determine the quality of the recovered carbon fibres. For this purpose, the breaking force, tensile strength, elongation and young modulus of virgin and recovered individual carbon fibres were determined using an adaptation of the ISO BS EN ISO 5079 test method for textile fibres. The tests were carried out using an Instron 1123 which was calibrated by means of a 100 g mass. Single fibres were glued to both ends of hollow square pieces of cardboard 2 cm long, preferably in the middle and parallel to either side for the strongest position. For each result, a total of 50 individual fibres were tested in order to obtain the mean value for the recovered fibres.

Also for testing the mechanical properties of composites produced with virgin and recovered carbon fibre (Chapter 4) were conducted. For the preparation of the composites, a laboratory two-roll mill (LabTech LRM-S-110/T3E, Labtech Ltd, Thailand) as shown in Figure 3.6.1 was used. 15% carbon fibre was added into the virgin LDPE in each case. The temperatures of the rolls were 180°C (first roll,  $n = 20$  rpm) and 150°C (second roll,  $n = 8$  rpm). Firstly, the LDPE was placed on the heated rolls and then the reinforcement was added together with additives to the molten polymer.



Figure 3.6.1 Labtech two roll mill

Following the composite preparation, the manufactured composites were ground into particles with dimensions up to 5 mm using a laboratory grinder. Then 100 mm × 10 mm sheets were press-moulded at 180 °C using 5000 psi pressure by using the press moulding machine (Figure 3.6.2) and then specimens with dimension of 1 mm × 10 mm × 100 mm were cut from the carbon fibre reinforced LDPE composite sheets for further testing.



Figure 3.6.2 Press moulding machine

Standard tensile properties investigations (according to MSZ EN ISO 527-1-4:199 standard) were carried out on an INSTRON 3345 universal tensile testing machine (Figure 3.6.3) at a crosshead displacement rate of  $90 \text{ mm/min}^{-1}$ . During the tests, the ambient temperature was  $23 \text{ }^{\circ}\text{C}$ , and the relative humidity was 35% in all cases. Preloading was not applied. The three point flexural tests were performed also with a crosshead displacement rate of  $20 \text{ mm min}^{-1}$ .



Figure 3.6.3 INSTRON 3345 universal tensile machine

Charpy impact strength tests were carried out on a CEAST Resil Impactor (Figure 3.6.4) according to MSZ EN ISO 179-2:2000 standard method. The machine was equipped with a 4J hammer, while the specimens were not notched.



Figure 3.6.4 CEAST Resil Impactor

## References

1. Lorjai, P., T. Chaisuwan, and S. Wongkasemjit, *Porous structure of polybenzoxazine-based organic aerogel prepared by sol-gel process and their carbon aerogels*. Journal of Sol-Gel Science and Technology, 2009. **52**(1): p. 56-64.
2. Hung, A.Y.C., et al., *Preparation and characterization of novolac type phenolic resin blended with poly(dimethylsiloxane adipamide)*. Journal of Applied Polymer Science, 2002. **86**(4): p. 984-992.
3. Quan, C., A. Li, and N. Gao, *Thermogravimetric analysis and kinetic study on large particles of printed circuit board wastes*. Waste Management, 2009. **29**(8): p. 2353-2360.
4. Barontini, F., et al., *Thermal Degradation and Decomposition Products of Electronic Boards Containing BFRs*. Industrial & Engineering Chemistry Research, 2005. **44**(12): p. 4186-4199.
5. Buah, W.K., A.M. Cunliffe, and P.T. Williams, *Characterization of Products from the Pyrolysis of Municipal Solid Waste*. Process Safety and Environmental Protection, 2007. **85**(5): p. 450-457.
6. Williams, P.T. and S. Besler, *The influence of temperature and heating rate on the slow pyrolysis of biomass*. Renewable Energy, 1996. **7**(3): p. 233-250.
7. Cozzani, V., L. Petarca, and L. Tognotti, *Devolatilization and pyrolysis of refuse derived fuels: characterization and kinetic modelling by a thermogravimetric and calorimetric approach*. Fuel, 1995. **74**(6): p. 903-912.
8. Skoog, D., et al., *Fundamentals of analytical chemistry*. 2013: Cengage Learning.
9. Dahm, K. and D. Visco, *Fundamentals of Chemical Engineering Thermodynamics*. 2014: Cengage Learning.
10. Green, D.W., *Perry's chemical engineers' handbook*. Vol. 796. 2008: McGraw-hill New York.
11. Grob, R.L. and E.F. Barry, *Modern practice of gas chromatography*. 2004: John Wiley & Sons.
12. Poole, C.F., *The essence of chromatography*. 2003: Elsevier.

## **CHAPTER 4**

### **RECYCLING OF CARBON FIBRE REINFORCED PLASTIC WASTES VIA HYDROTHERMAL PROCESSING**

This chapter consists of three sections, each one focuses on the depolymerisation of carbon fibre reinforced plastic (CFRP) waste via hydrothermal processing via different types of solvents.

Section 4.1 deals with the depolymerisation of CFRP waste in water, together with alkalis and oxidant agent. The effect of reaction temperature and time on the resin removal was investigated. The composition of the liquid effluent was found with the help of GC/MS/MS analyses to propose a degradation mechanism. The mechanical properties of the recovered carbon fibre were tested, to determine if it could be utilized in order to remanufacture new composites.

Section 4.2 includes the results obtained from the depolymerisation of CFRP waste in ethylene glycol and ethylene glycol water mixture. Water and ethylene glycol was mixed in different proportions, and reacted with the resin at different temperatures and reaction times. The recovered carbon fibre was tested to see any change in the mechanical properties. The liquid effluent was analysed by GC/MS/MS and the depolymerisation products were compared with these in Section 4.1

Section 4.3 contains results of the mechanical properties tests of fibre reinforced composites produced from recovered carbon fibres. The recovered carbon fibres were produced via hydrothermal depolymerisation in ethylene glycol and water mixture as described in section 4.2. The analysed mechanical properties were tensile, flexural and charpy impact strengths. The interactions between the matrix and the additives were described with the help of the Fourier Transform Infrared Spectrometry (FTIR) analyses.

## 4.1 Catalytic Hydrothermal Degradation of Carbon Fibre Reinforced Plastic Wastes

This section contains the results and the discussions of experiments carried out on the hydrothermal degradation of carbon fibre reinforced plastic (CFRP) wastes in sub and supercritical water, with the addition of H<sub>2</sub>O<sub>2</sub> as oxidant, CaO and Na<sub>2</sub>CO<sub>3</sub> as promoters, and alkalis KOH and NaOH as catalyst additives. The resin removals were calculated according to the equation 4.1.1 as shown below;

$$R = \frac{F-X}{F_R} * 100 \quad \text{Equation 4.1.1}$$

R stands for resin removal [%]; F is the amount of the waste carbon fibre reinforced plastic added to the reactor. F<sub>R</sub> defines the amount of the resin in the raw waste carbon fibre reinforced plastic, which was found to be 38 wt% according to the thermogravimetric and ash analyses as described in Section 3.1.1. X is the amount of the solid residue, after the hydrothermal depolymerisation.

### 4.1.1 Effect of Temperature and Promoters (CaO, Na<sub>2</sub>CO<sub>3</sub>)

The experiments with CFRP waste were carried out between the temperatures of 300°C and 420°C and the reaction time was held at zero minutes. The results shown are in terms carbon balance of the waste CFRP as solid, gaseous and liquid products after the hydrothermal treatment (table 4.1.1). In general, 100 % carbon balances were obtained which shows the good accountability of the reaction products.

Below the subcritical point of water, less than 40% of the resin was removed during the hydrothermal degradation of the waste CFRP. When the temperature was 350°C, the resin removal was improved and reached its maximum value when the supercritical conditions were satisfied at 420°C and 230 MPa. However, with only water, no more than 55% of the resin was removed from the waste CFRP. To increase the resin removal efficiency,



H<sub>2</sub>O<sub>2</sub> as oxidant agent was used and the resin removal increased up to 63 %.

Table 4.1.1 Resin removals and distribution of carbon during hydrothermal depolymerisation of CFRP waste

<i>Additive</i>	<i>H<sub>2</sub>O<sub>2</sub> [wt%]</i>	<i>T [°C]</i>	<i>TOC [g]</i>	<i>IC [g]</i>	<i>Gas [g Carbon]</i>	<i>Solid Residue [g Carbon]</i>	<i>Balance [%]</i>	<i>Resin Removal [%]</i>
-	-	300	0.11	-	0	4.38	98.6	37.9
-	-	325	0.13	-	0.09	4.35	100.5	39.2
-	-	350	0.16	-	0.10	4.19	94.5	47.2
-	-	400	0.16	-	0.19	4.20	100.0	49.0
-	-	420	0.32	-	0.29	4.05	102.5	54.5
-	5	400	0.18	-	0.46	4.08	98.3	56.3
-	5	420	0.25	-	0.67	3.96	95.0	62.7
CaO	-	400	0.37	0.05	0.11	3.90	97.2	60.9
CaO	-	420	0.28	0.04	0.23	3.81	96.0	65.3
Na <sub>2</sub> CO <sub>3</sub>	-	400	0.28	0.13	0.24	3.71	95.7	70.1
Na <sub>2</sub> CO <sub>3</sub>	-	420	0.37	0.14	0.28	3.88	102.4	62.2

To enhance the depolymerisation rate and improve the resin removal, CaO was introduced to the reaction medium at temperatures of 400°C and 420°C. The addition of CaO increased the resin removal by 10% for each reaction conditions and this might be due to its ability to capture carbon by fixing CO<sub>2</sub>. While at 420°C, 44.5% CO<sub>2</sub> was detected in the gas products,

this amount reduced to 4.5% when CaO was added. Also the increase in the hydrogen composition in the gas from 19.1% to 41.1% suggests that CaO catalysed the steam reforming of the hydrocarbons [1].

Na<sub>2</sub>CO<sub>3</sub> was used to improve the depolymerisation rate and reduce the char formation. Although the resin removal reached 70% at 400°C, it decreased when the reaction conditions reached supercritical conditions.

#### 4.1.2 Effect of Alkalis (KOH, NaOH) and Residence Time

Alkalis can promote the reaction rates during the depolymerisation under hydrothermal conditions as reported in the literature. Especially they can improve the depolymerisation kinetics if transesterification reactions are involved [1, 2]. The degradation of this polybenzoxazine (phenolic-type thermosetting) resin was increased with the addition of KOH and NaOH..

Table 4.1.2 Influence of alkalis on product distribution [wt%]

	<i>No alkali</i>		<i>NaOH</i>		<i>KOH</i>	
	400°C	420°C	400°C	420°C	400°C	420°C
Solid Residue	81.5	78.5	68.0	67.6	77.6	75.6
Gas	3.70	5.64	2.52	3.48	4.32	4.76
Liquid	14.8	15.9	29.4	29.0	18.0	19.6

Among the alkali catalysts, NaOH was more effective than KOH as 84.2% of resin was removed from the carbon fibre composite at supercritical conditions of water. In Table 4.1.2, the product distribution in those experiments is shown.

In three different proportions, hydrogen peroxide (H<sub>2</sub>O<sub>2</sub>) as oxidant agent was added to the feed to further increase the resin removal. 5.0, 7.5 and 10 wt% H<sub>2</sub>O<sub>2</sub> was added to the reactor with NaOH or KOH at 420°C, and zero residence time (0 minutes). For those experiments, high carbon balance (around 100%) was reached (Table 4.1.3).

The resin removals increased for each experiment and reached its maximum value of 92.6% when KOH and 10 wt% H<sub>2</sub>O<sub>2</sub> were used. At the same conditions, more carbon was detected in the gas phase when KOH was used compared to experiments with NaOH. Also the amount of inorganic carbon was higher in the presence of NaOH. This might be due to sodium carbonate salt production, as NaOH reacts with CO<sub>2</sub>, which yielded low carbon dioxide composition in the gas. Also the increase in the amount of H<sub>2</sub>O<sub>2</sub>, increased the resin removals to give more carbon in the gas products.

Table 4.1.3 Resin removal and distribution of carbon during hydrothermal depolymerisation of CFRP waste at 420°C and zero reaction time

<i>Additive</i>	<i>H<sub>2</sub>O<sub>2</sub> [wt%]</i>	<i>TOC [g]</i>	<i>IC [g]</i>	<i>Gas [g Carbon]</i>	<i>Solid Residue [g Carbon]</i>	<i>Balance [%]</i>	<i>Resin Removal [%]</i>
NaOH	5.0	0.35	0.16	0.33	3.01	95.9	84.5
NaOH	7.5	0.29	0.17	0.35	2.94	93.4	88.5
NaOH	10	0.31	0.20	0.72	2.92	103.5	89.4
KOH	5.0	0.43	0.10	0.41	2.91	95.3	91.0
KOH	7.5	0.29	0.09	0.64	2.90	97.0	92.0
KOH	10	0.35	0.11	0.80	2.87	102.7	92.6

The effect of reaction time was investigated with experiments with KOH and 5 wt% H<sub>2</sub>O<sub>2</sub> loading at 10 and 30 minutes. The resin removal dramatically decreased with the increasing reaction time, from 91.0% to 83.7% as shown in Table 4.1.4. However the amount of carbon in the gas phase increased, which suggested that more resin decomposed to give

higher resin removal. The apparent decrease in the resin removal might be a result of re-polymerization reactions occurring. Also gasification reactions result in char production. According to the studies on cellulose by Kruse and Dinjus [3], the decomposition path in supercritical water is from phenols to different short chain polymers due to poly-condensation reactions as shown in Figure 4.1.1. From these intermediates, gases and coke formation occurs. The carbon fibre reinforced plastic waste sample used in this study has a phenolic resin, re-polymerization of phenolic degradation products could produce char at elongated reaction times that remained on the recovered carbon fibre surface after cooling.

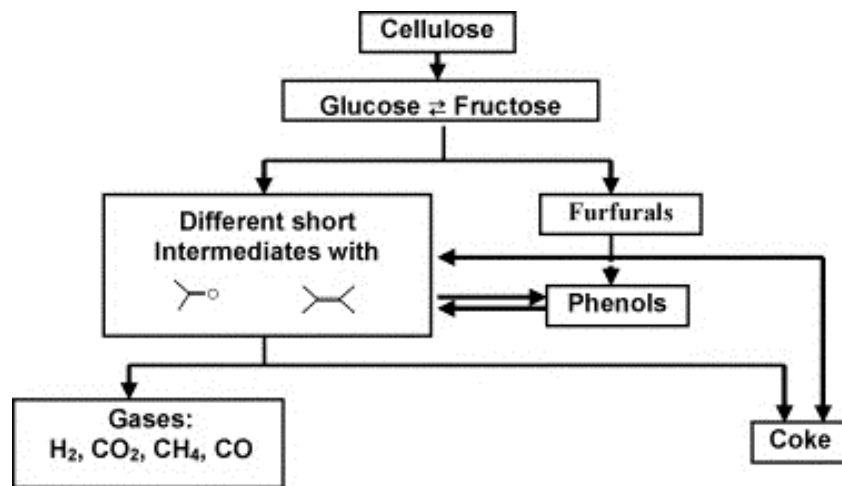


Figure 4.1.1 Simplified reaction mechanism of hydrothermal decomposition path of cellulose, adapted from [3]

Table 4.1.4 Resin removal and distribution of carbon during hydrothermal depolymerisation of CFRP waste with KOH at 420°C

<i>Time [min]</i>	<i>H<sub>2</sub>O<sub>2</sub> [wt%]</i>	<i>TOC [g]</i>	<i>IC [g]</i>	<i>Gas [g Carbon]</i>	<i>Solid Residue [g Carbon]</i>	<i>Balance [%]</i>	<i>Resin Removal [%]</i>
0	5.0	0.43	0.10	0.41	2.91	95.3	91.0
10	5.0	0.36	0.11	0.47	2.99	97.5	86.2
30	5.0	0.44	0.13	0.59	3.04	104.1	83.7

With the addition of KOH and 10 wt% H<sub>2</sub>O<sub>2</sub>, the resin removal increased from 55% to 93%, compared to water only. KOH improved the depolymerisation rate and H<sub>2</sub>O<sub>2</sub> decomposed more resin to produce gas by oxidation.

#### 4.1.3 Analysis of Liquid Products

The liquid effluent collected after the experiments were first extracted with DCM to separate the water phase and then analysed with the help of GC/MS/MS to identify the organic compounds as described in the previous chapter. As the CFRP waste has a polybenzoxazine resin (phenolic type), after the hydrothermal processing, it decomposed to give phenol and phenolic compounds. Apart from the phenol, the second major depolymerisation product was aniline. Since the molecular weights of phenol and aniline (94 and 93 g mol<sup>-1</sup>, respectively) are very close, they created a single peak in the chromatogram as in the analysis of the liquid produced from depolymerisation of CFRP at 420°C with the addition of KOH as catalyst and 10 ml of H<sub>2</sub>O<sub>2</sub> as oxidant agent. In Figure 4.1.2, the peak at 12.60 min is corresponding to both aniline and phenol.

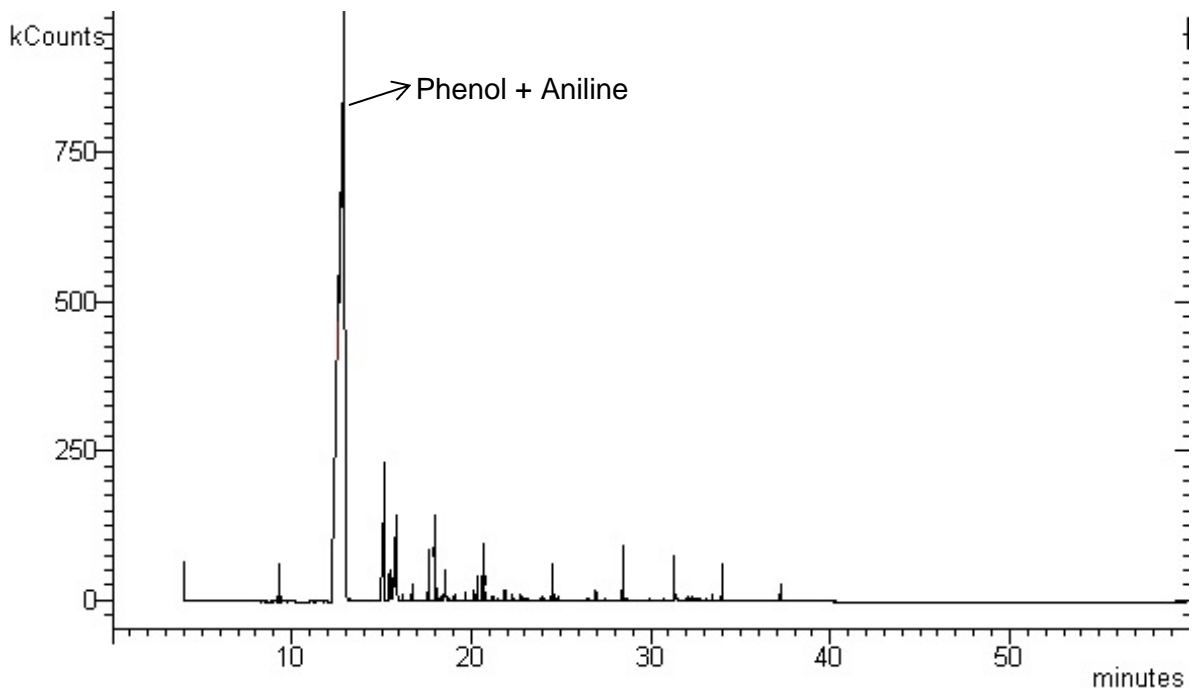


Figure 4.1.2 GC/MS chromatogram of DCM extracted depolymerisation products of CFRP at 420°C with KOH and 5 wt% H<sub>2</sub>O<sub>2</sub>

Therefore, to separate phenol from the liquid effluent, before extraction with DCM, 90% KOH solution was added until the pH of the effluent became higher than 12 to produce phenol salts which can dissolve in water. After that, DCM was added for extraction, so the organic compounds other than phenol were dissolved and create an organic phase, which was collected after extraction. When this basic organic solution was analysed, the aniline gave a single peak as shown in the Figure 4.1.3. The alkaline extract contained aniline, methyl aniline and quinoline, apparently from the decomposition of the polybenzoxazine resin.

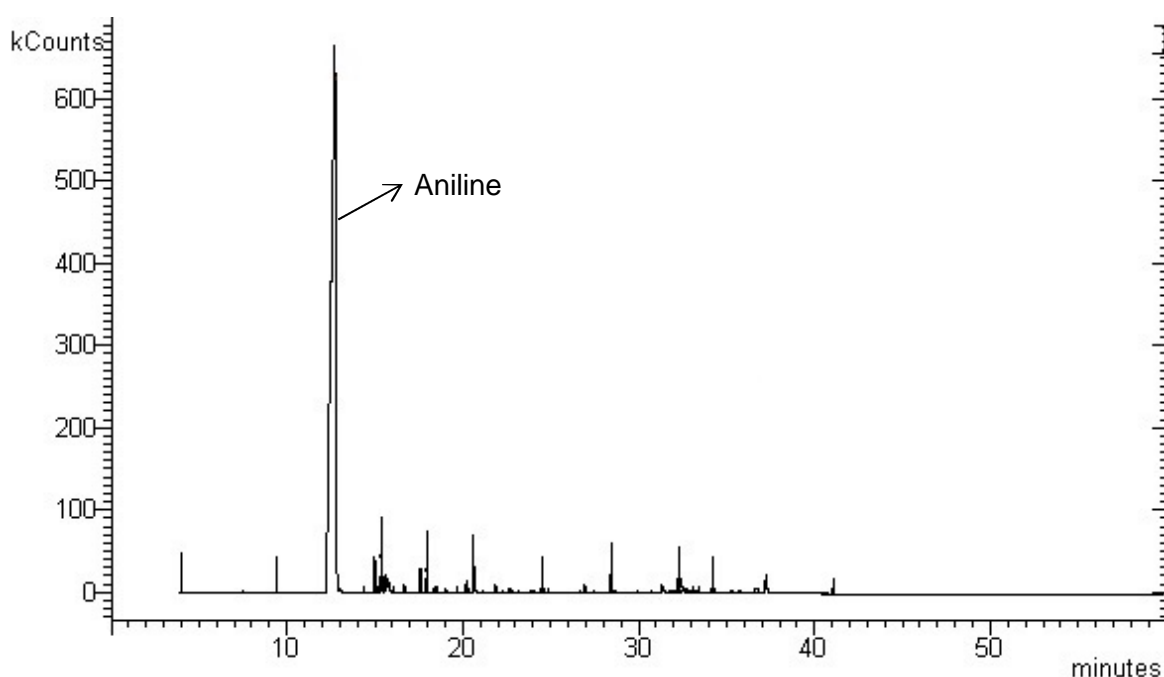


Figure 4.1.3 GS/MS chromatogram and spectrum of DCM extracted depolymerisation products of CFRP at 420°C with KOH and 5 wt% H<sub>2</sub>O<sub>2</sub>, after the addition of KOH into the liquid effluent

After decanting the organic phase from the aqueous phase which contained phenol salts, 98% HCl solution added, until the pH value become lower than 3, so that, phenol salts reacted with HCl to produce phenol again. Than DCM was added for extraction, and the organic phase was separated. The chromatogram gave a single peak for phenol as expected (Figure 4.1.4). Apart from the phenol, some methyl phenols were detected as well. However, the major products were found to be phenol and aniline, as they

were around 30 wt% of the total organic compounds detected in the liquid effluent.

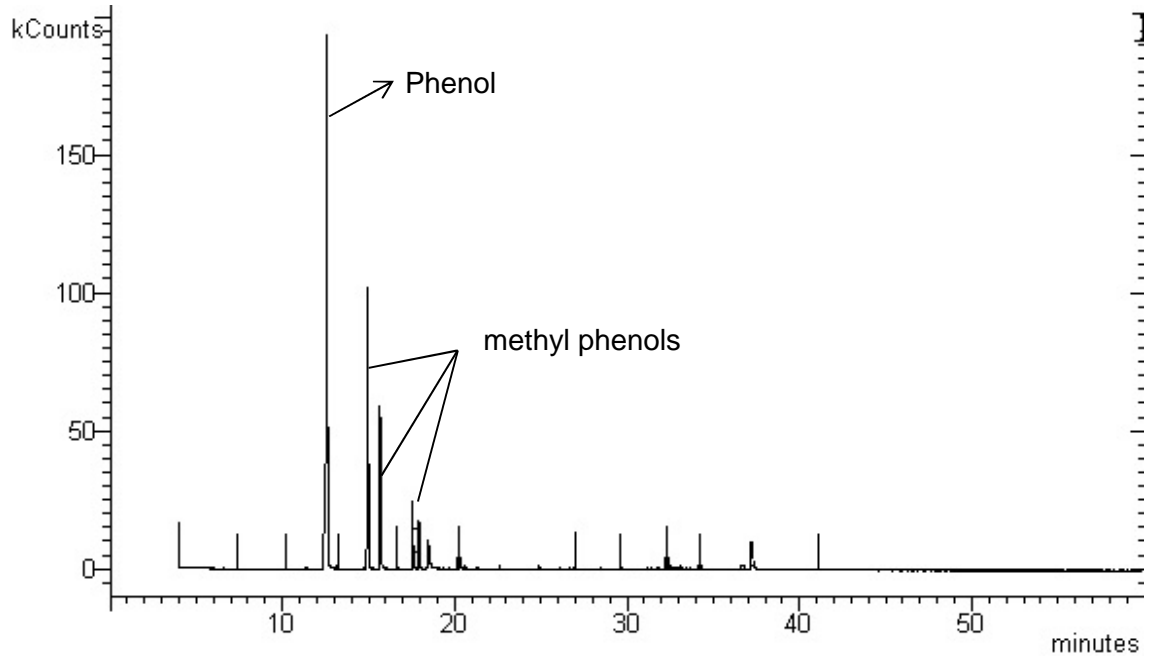


Figure 4.1.4 GS/MS chromatogram and spectrum of DCM extracted depolymerisation products of CFRP at 420°C with KOH and 5 wt% H<sub>2</sub>O<sub>2</sub>, after the addition of HCl into the liquid effluent

The amount of monomers, phenol and aniline were highly affected with the changing reaction conditions. Around 5 mg of phenol and 1 mg of aniline per gram resin were detected in the liquid effluent when water alone reacted with CFRP waste at 400°C. These amounts were doubled at 420°C and 230 MPa, as the supercritical conditions achieved. However, the rapid increase was observed when the alkalis were present in the reaction medium. 37 mg phenol and 33 mg aniline per gram resin were decomposed from the resin fraction when KOH was used as the catalyst; 45 mg phenol and 61.5 mg aniline per gram resin were decomposed when NaOH was the catalyst, as shown in Figure 4.1.5.

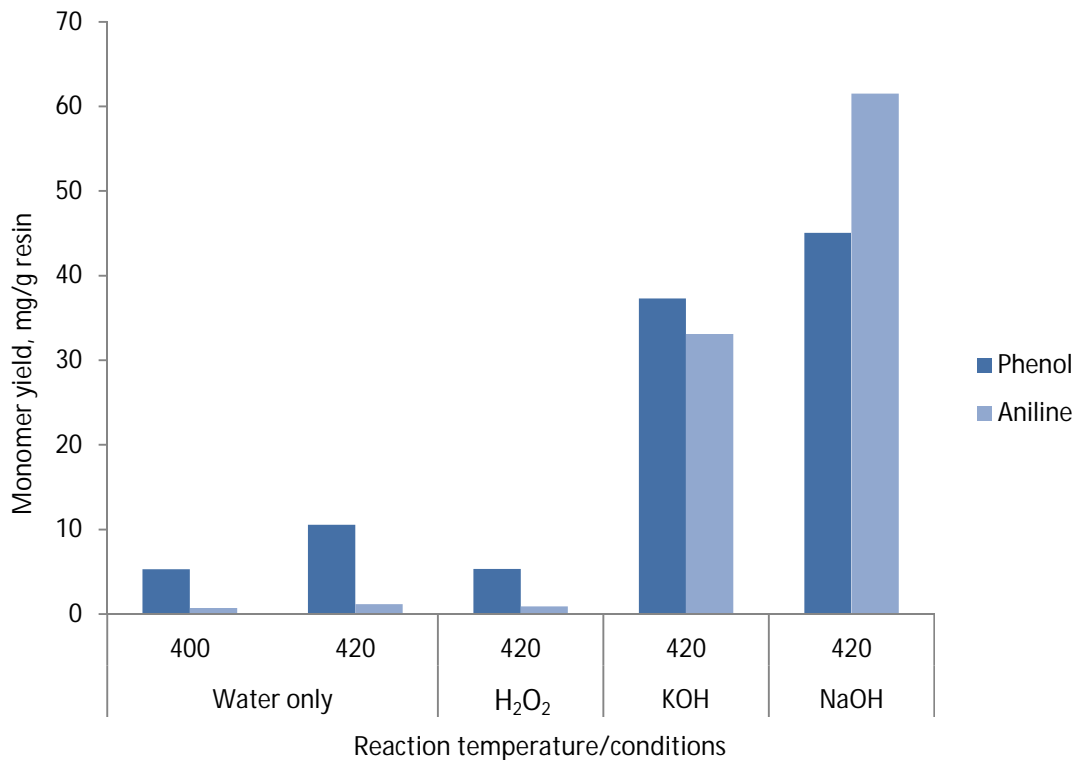


Figure 4.1.5 Effect of reaction media, temperature and H<sub>2</sub>O<sub>2</sub> on the yields of phenols and aniline during hydrothermal processing of CRFP

The hydrogen peroxide addition also changed the phenol and aniline amounts in the liquid effluent. With the increasing H<sub>2</sub>O<sub>2</sub> amount, the phenol and aniline yields decreased. In Figure 4.1.6, it can be clearly seen that the amount of phenol decreased from 35.5 mg to 10 mg per gram resin when the H<sub>2</sub>O<sub>2</sub> amount increased from 5.0 wt% to 10 wt%, when KOH was used as catalyst at 420°C and zero residence time.

At 420°C, in the presence of NaOH, more phenol and aniline were detected in the liquid effluent, compared to that with KOH. However, when 7.5 wt% H<sub>2</sub>O<sub>2</sub> was added, the phenol and aniline amounts in both KOH and NaOH were almost the same. In the case of NaOH, more phenol and aniline were oxidized to give more gas products, which might lead to char formation on the carbon fibre surface as mentioned in the previous section. This might be the reason for the lower resin removals when NaOH and H<sub>2</sub>O<sub>2</sub> were used to improve depolymerisation rate, compared to that with KOH and H<sub>2</sub>O<sub>2</sub>.



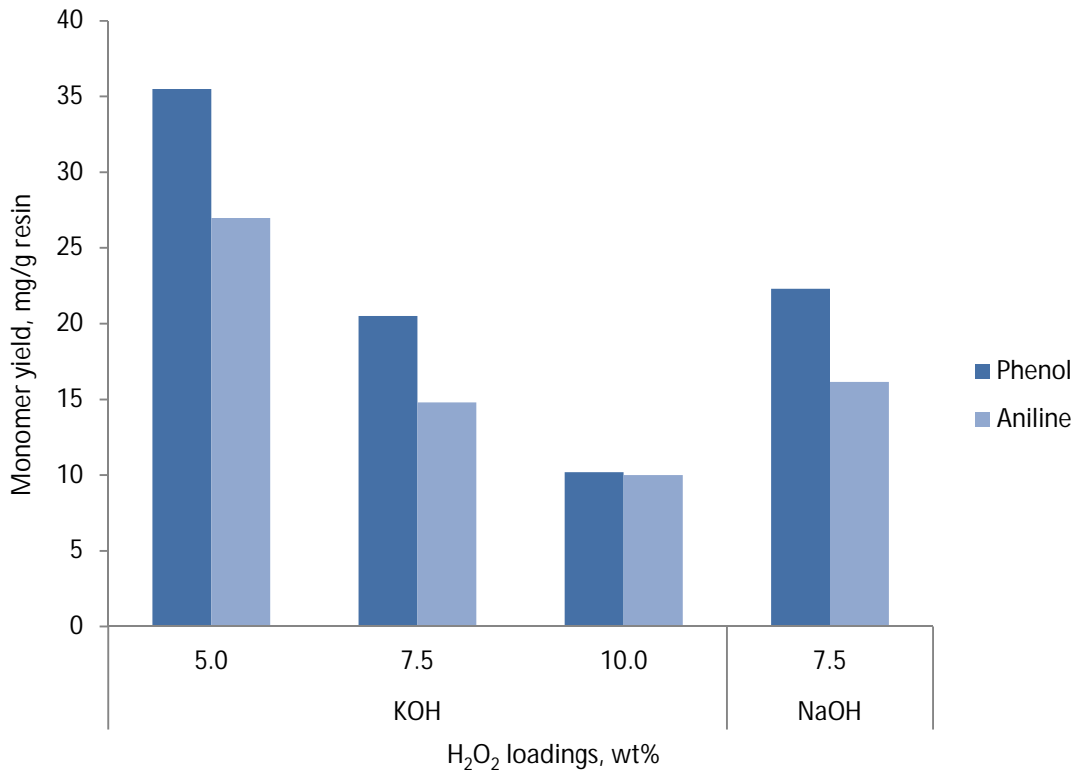


Figure 4.1.6 Effects of H<sub>2</sub>O<sub>2</sub> loading during hydrothermal processing of CRFP to different alkalis at 420°C and zero residence time

Polybenzoxazines can be synthesized from phenols, amines or formaldehyde. Depending on the final properties required, phenols and amines from different structures can be combined during the production [4]. The polybenzoxazine resin in the CFRP waste was a phenolic type, synthesized from phenols aniline and amines, as it can be seen from the organic compounds detected such as methyl phenol, methyl aniline, quinolone, dimethyl benzenamine apart from the phenol and aniline themselves.

Benzoxazine monomers in the polybenzoxazine resin contain oxazine rings which open into a phenolic structure during the polymerization process to manufacture the resin. The main difference between with the phenolic resins and the polybenzoxazine resin is the linkage of the phenolic moieties. In phenolic resins, linkage of the phenolic groups is with the methylene bridges while in polybenzoxazines, the linkage is by the C-N-C bridges (Mannich base) [5]. Therefore, apart from phenols and aniline, organic compounds containing oxazolidine rings such as 5-methyl-3-phenyl-1,3-

oxazolidine and 1,3-diphenyl-2-propyl imidazolidine were detected, which confirms the resin type as polybenzoxazine based on aniline and phenols.

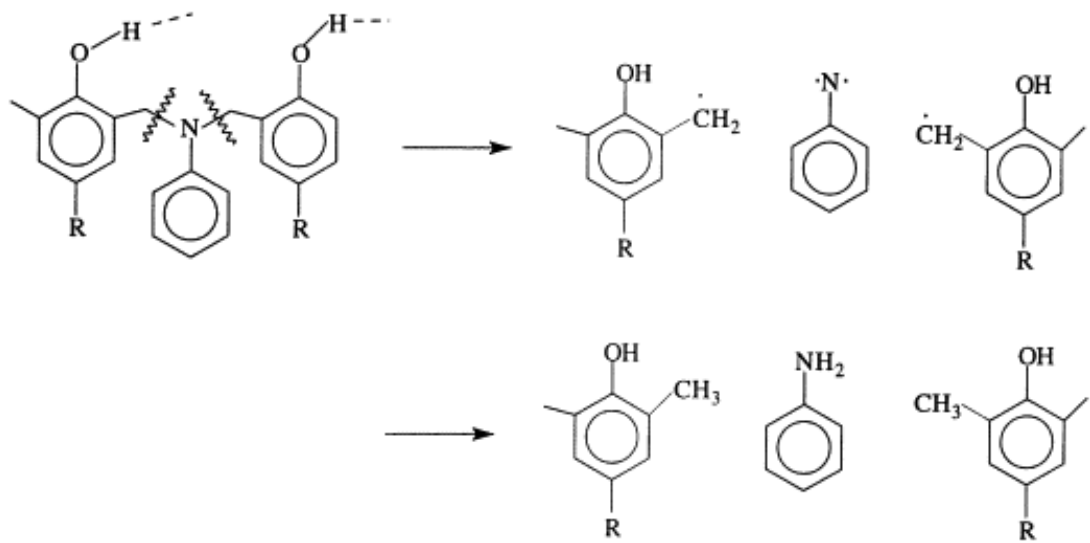


Figure 4.1.7 The degradation mechanism of monomer of polybenzoxazine resin [6]

The degradation mechanism of the resin can be explained with the mechanism of the Mannich base cleavage, which is the structure presumed characteristics of polybenzoxazines [6]. Since the bond energy of C-N is lower than the bond energy of C-aromatics [7], the C-N bonds were broken to give aniline and intermediates with phenyl functional groups. From the decomposition of the intermediates, phenol and phenolic compounds were produced. In Figure 4.1.7, the possible degradation mechanism for the aniline and intermediates release from the benzoxazine monomer is shown.

#### 4.1.4 Analysis of Recovered Carbon Fibre

Table 4.1.5 shows that the hydrothermal process led to a reduction of the critical mechanical properties of the recovered fibre at the conditions when the best resin removal efficiency (92.6%) was achieved. This can possibly be attributed to the increase in the elongation of individual fibres by about 36% after the degradation process. This agrees with the work of Bai et al. [8], who found loss of mechanical properties as a result of carbon fibre oxidation by the applied oxygen.

Table 4.1.5 Mechanical properties of virgin carbon fibre and recovered carbon fibre

	<i>Tensile Strength Analysis</i>		
	Virgin CF	Recovered CF <sup>1</sup>	Recovered CF <sup>2</sup>
Breaking Force [N]	0.135	0.118	0.105
Elongation [mm]	0.3	0.370	0.408
Tensile Strength [GPa]	3.5	2.7	2.73
Young Modulus	233	146.1	133.8

1 Recovered at 420°C, with KOH

2 Recovered at 420°C with KOH and 10 wt% H<sub>2</sub>O<sub>2</sub>

Figure 4.1.8 presents the SEM micrograms of virgin fibre and recovered fibres from waste CFRP at 420 °C in the presence of KOH and 10 wt% H<sub>2</sub>O<sub>2</sub>. There were a clear difference between SEM images of the virgin carbon fibre and the recovered carbon fibre, due to oxidation on the surface, the recovered carbon fibre appears even cleaner.

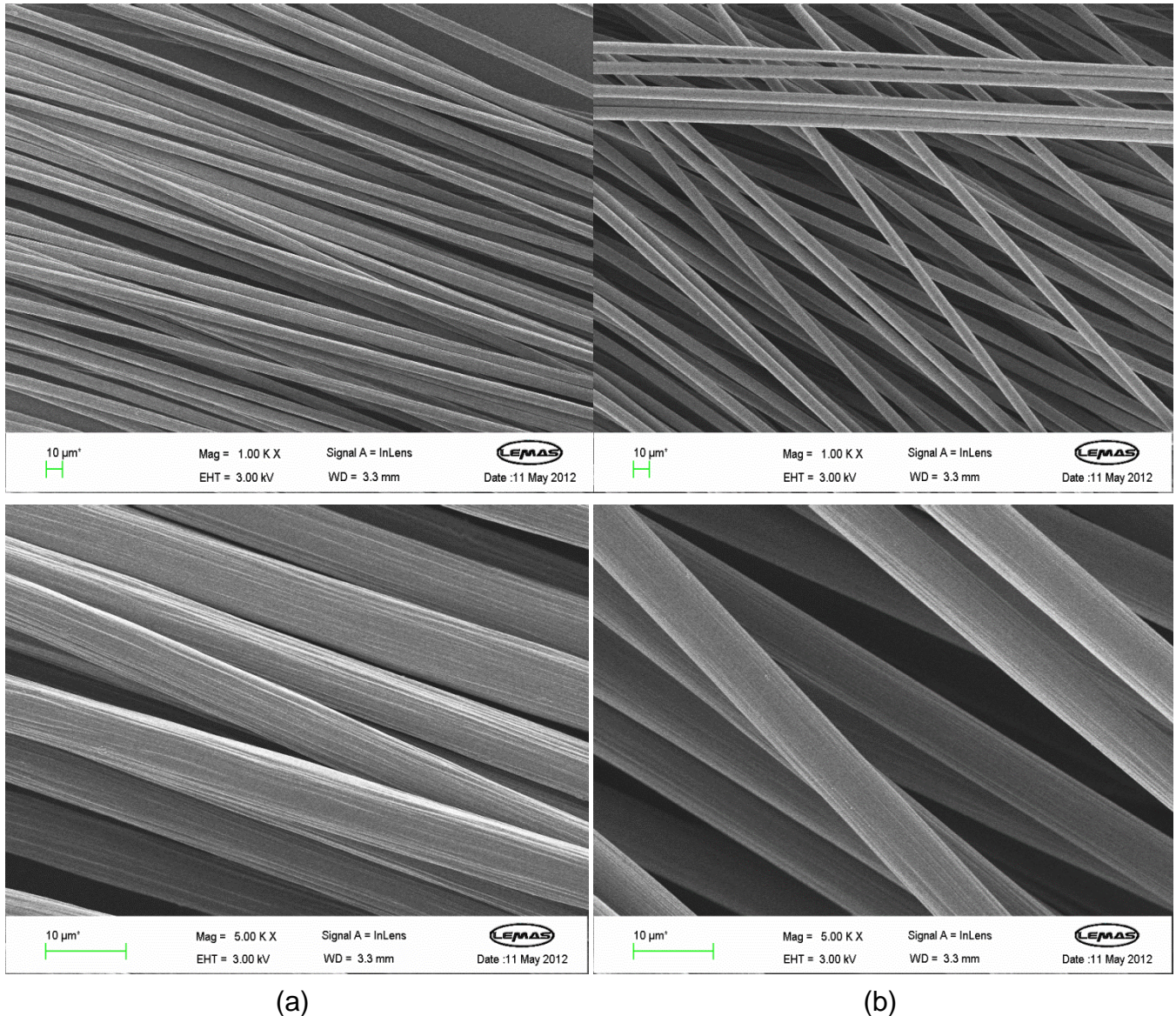


Figure 4.1.8 SEM images of (a) Virgin carbon fibres, (b) Recovered carbon fibres at different magnitudes

#### 4.1.5 Summary

In this section of the work, depolymerisation of carbon fibre reinforced plastic waste was carried out in sub and supercritical water. The effects of temperature, additives ( $\text{CaO}$ ,  $\text{Na}_2\text{CO}_3$ ,  $\text{NaOH}$ ,  $\text{KOH}$ ,  $\text{H}_2\text{O}_2$ ) and reaction time on the depolymerisation rate was investigated. The properties of the liquid effluent were also investigated by GC/MS/MS analyses. The mechanical properties of the recovered carbon fibre were tested to compare with the properties of virgin carbon fibre.

Water alone was able to remove only 55% of the resin fraction from the carbon fibre reinforced plastic waste during the hydrothermal depolymerisation. This removal was further improved with the addition of NaOH, and reached around 85% at 420°C and zero residence time.

Water at supercritical conditions was able to remove almost 93% of the resin from the CFRP waste, with KOH and 10 wt% H<sub>2</sub>O<sub>2</sub> at zero residence time. While the resin was converted into gas and liquid the carbon fibre was recovered by preserving 78% of its tensile strength due to the loss in the mechanical properties as a result of oxidation on the carbon fibre surface.

The main organic compounds detected in the liquid were phenol and aniline. Apart from them, organic compounds containing an oxazolidine ring, methyl phenols, methyl aniline and dimethyl benzenamine were detected, clearly the products from the degradation of polybenzoxazine resin was based on aniline and phenol.

## **4.2 Recovery of Carbon Fibres and Production of High Quality Fuel Gas from the Chemical Recycling of Carbon Fibre Reinforced Plastic Wastes**

In this section, degradation of carbon fibre reinforced plastic waste with ethylene glycol and ethylene glycol/water mixtures has been carried out at sub- and supercritical conditions. Detailed analyses of all the reaction products including gas, liquid and solid have been carried out for better understanding of the process. Also in this study, two processes were investigated to determine an appropriate use for the liquid products after carbon fibre recovery; (1) isolation of the reaction products by liquid–liquid extraction and (2) catalytic supercritical water gasification of the liquid products to produce a syngas rich in hydrogen or methane.

### **4.2.1 Influence of Reaction Conditions on Carbon Fibre Recovery**

The resin removal efficiencies with respect to reaction temperature and time are shown in Table 4.2.1 for depolymerisation of the carbon fibre reinforced plastic waste in ethylene glycol and Table 4.2.2 for that of the ethylene glycol/water mixture. The experiments on the decomposition of waste carbon fibre reinforced plastic in ethylene glycol were carried out at four different temperatures and at 0 and 10 min of reaction times to monitor the effect of time on resin removal. At temperatures of 300 and 360°C, the resin removal was not significant, however as the temperature was increased, removal increased to 92.1% at 400°C. The influence of time on the degree of depolymerisation of the resin was investigated at 380°C. At this temperature, resin removal increased from 79.3% to 89.7%, when the residence time was increased from 0 to 10 min. In reported studies with thermoplastics, the main drawback to depolymerisation in ethylene glycol was the very long reaction times of up to 8 h [9].

Table 4.2.1 Resin removal during depolymerisation of carbon fibre reinforced plastics in ethylene glycol (EG)

$V_{EG}$ [ml]	$T$ [°C]	Time [min]	Resin Removal [%]
60	300	0	13.2
60	360	0	26.6
60	380	0	79.3
60	400	0	92.1
60	380	10	89.7

In the experiments with ethylene glycol at a temperature of 380°C, the corresponding pressure was recorded as 4.2 MPa, therefore the reaction was conducted near the critical point of ethylene glycol ( $T_c = 447$  °C,  $P_c = 8.2$  MPa). Therefore, operating near the supercritical conditions of ethylene glycol enabled more resin to be depolymerised in very short reaction times even for a thermosetting (phenolic) plastic. The solubility of ethylene glycol in water and its decomposition during the reaction meant that it was impossible to measure separately the carbon of the resin degradation products in the liquid and gaseous products. Hence, it was difficult to construct a carbon balance for the carbon fibre reinforced plastics degradation in this work.

The effect of water addition as a modifier to the process was investigated at a temperature range of 380 to 420°C and at zero residence time. Resin removal increased with increasing ethylene glycol/water ratio (up to an ethylene glycol/water ratio of 5:1). In the present study, the highest resin removal of 97.6% was reached when the ethylene glycol/water ratio was 5 at 400°C. However, when the temperature was increased to 420°C, resin removal decreased significantly to 90.4% at the same ethylene glycol/water ratio. The same decrease was observed when the ethylene glycol/water ratio was 3. This might have been due to an increase in the

weight of recovered fibre due to char deposition at the higher temperature of 420°C, resulting in an erroneous decrease in resin removal.

Table 4.2.2 Resin removal during depolymerisation of carbon fibre reinforced plastics in ethylene glycol (EG)/water mixture

$V_{EG}/V_{water}$ [ml]	$T$ [°C]	Resin Removal [%]
5	380	94.2
5	400	97.6
5	420	90.4
3	400	95.2
3	420	90.4
1	400	73.8
1	420	75.2
0.33	420	66.5
0.2	420	67.3

It has been reported in the literature that at higher depolymerisation temperatures, re-polymerization of degradation products could occur leading to char formation. According to the studies on cellulose by Kruse and Dinjus [3], the decomposition path in supercritical water is from phenols to different short chain polymers due to poly-condensation reactions. From these intermediates, gases and coke formation occurs. The same reaction pathway has been suggested even for very short residence times (0–100 s) by Yong and Matsumura [10], under sub and supercritical conditions. They stated that phenols react with water at near critical conditions to produce gas and char, the char formation was doubled with a 30 °C increase in temperature as the reaction conditions approached supercritical



conditions. The carbon fibre reinforced plastic waste sample used in this study consisted of phenolic resin (polybenzoxazine resin based on phenol and aniline), re-polymerization of phenolic degradation products could produce char that remained on the recovered carbon fibre surface after cooling. Since, the extent of carbon fibre recovery was obtained by gravimetric measurements of solids; it was difficult to distinguish between char and carbon fibre. However, this problem could be addressed by carefully controlling the reaction conditions of temperature and time to minimize char formation. Char deposition on the recovered carbon fibre can be removed by moderate temperature oxidation; however, as mentioned earlier this can add to process cost as well as cause a decline in the mechanical properties of the recovered carbon fibre.

## **4.2.2 Processing of the Residual Liquid Product**

### **4.2.2.1 Liquid-Liquid Extraction Results**

The residual liquid product was analysed to determine whether the liquid could be used as a source of chemicals, either to recover the resin monomer or other high concentration/high value compounds. Therefore, liquid products obtained from the depolymerisation of the carbon fibre reinforced plastics were analysed to determine their composition using GC/MS/MS analysis. For the GC/MS/MS analyses, extraction with dichloromethane with the necessary pH adjustments as described in Section 4.1.3, was applied to separate the water fraction from the organic fraction.

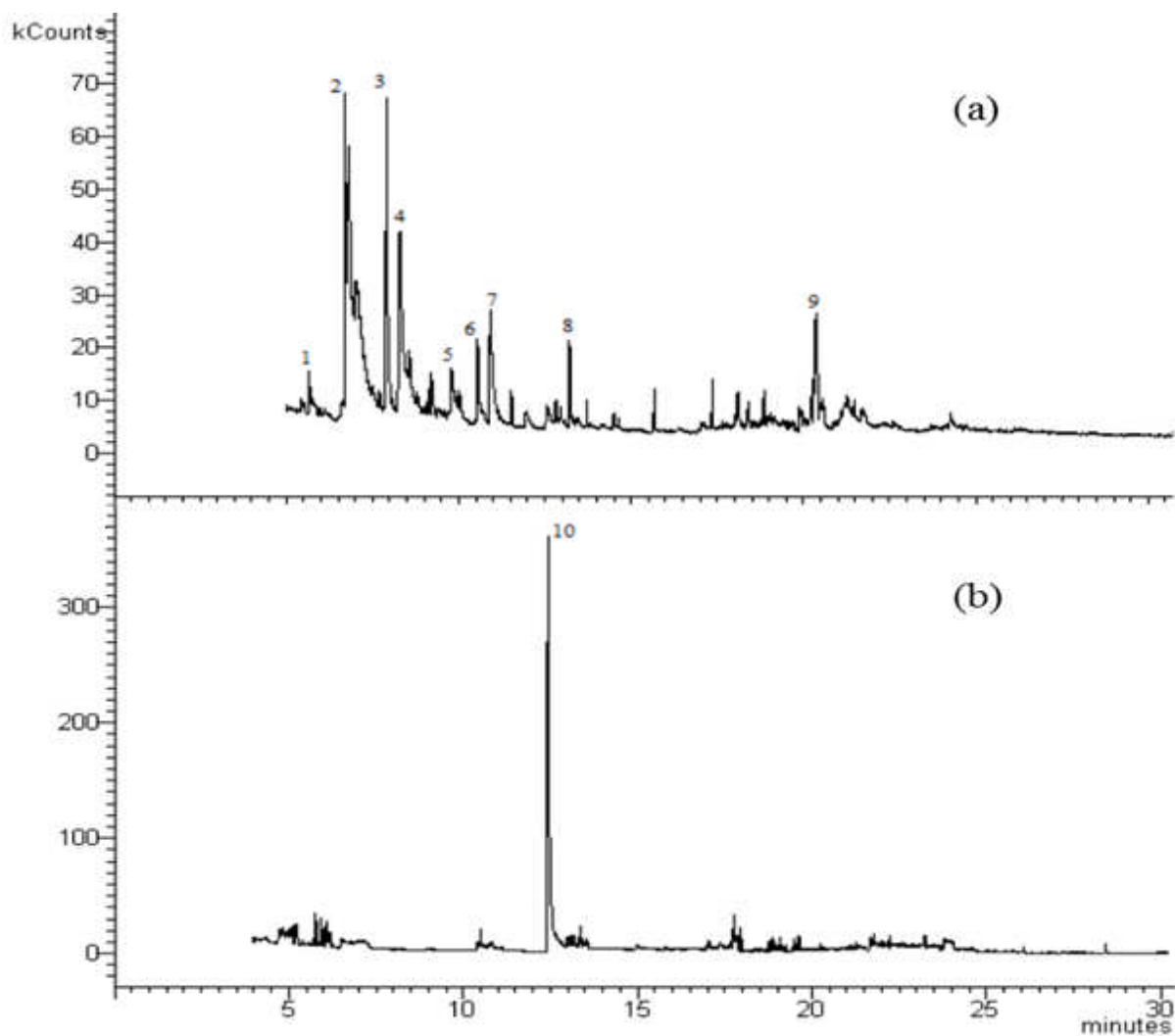


Figure 4.2.1 GC/MS/MS chromatograms of extracts from the residual liquid products obtained during carbon fibre reinforced plastics depolymerisation at 400°C with water only; (a) alkaline extraction (b) acidic extraction

The GC/MS/MS chromatograms obtained from the analysis of the alkaline and acidic extracts of the residual liquid products using water only as solvent at 400°C, are shown in Figure 4.2.1 (a) and (b), respectively. The alkaline extract contained aniline, methyl aniline, quinoline and phenyloxazole, apparently from the decomposition of the polybenzoxazine resin, whereas the acidic extract showed mainly the presence of phenol and methyl phenols.

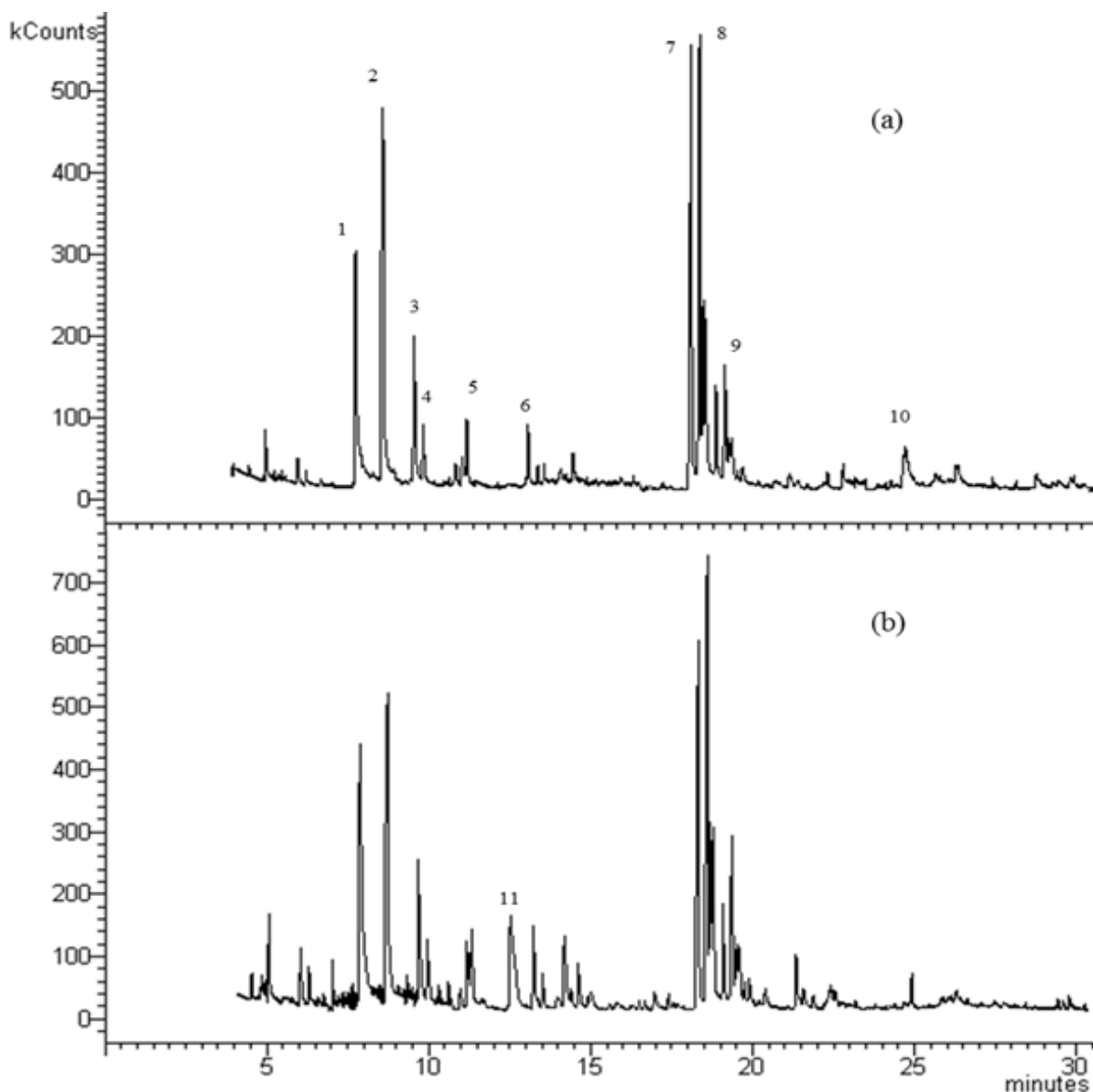


Figure 4.2.2 GC/MS/MS chromatograms of extracts from liquid residuals obtained during carbon fibre reinforced plastics depolymerisation at 400 °C with ethylene glycol only; (a) alkaline extraction (b) acidic extraction.

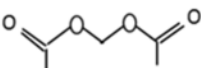
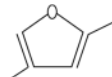
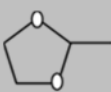
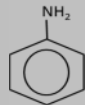
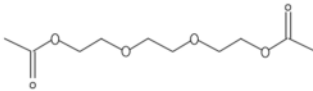
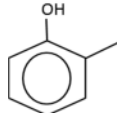
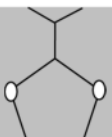
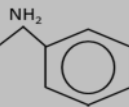
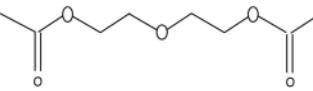
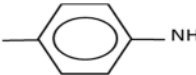
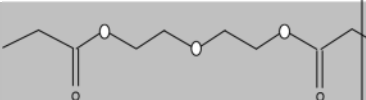
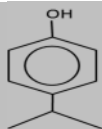
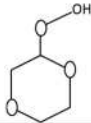
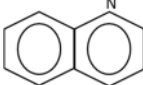
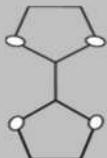
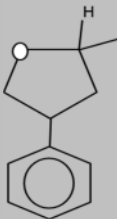
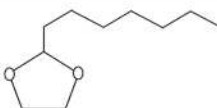
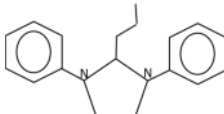
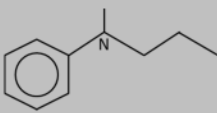
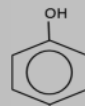
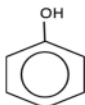
However, when ethylene glycol was used, it was a significant challenge to separate the organic compounds from the water soluble products with liquid–liquid extraction by using the same method; due to the miscibility of ethylene glycol and water; as well as the solubility of phenols and anilines, which were the main degradation products of the resin in both solvents. In the presence of ethylene glycol, the decomposition and polymerization of the ethylene glycol solvent occurred during the depolymerisation process as

confirmed by the GC/MS/MS chromatograms shown in Figure 4.2.2 (a) and (b).

Although the same acid and alkaline extraction method was applied, total recovery of the organic compounds could not be achieved, as only a small peak corresponding to phenol was found in the acidic extraction while no aniline was detected in the alkaline extract. Instead, products due to the reaction (including polymerization) of the ethylene glycol were obtained. Table 4.2.1 presents a list of compounds detected from the chromatograms in Figure 4.2.1 and Figure 4.2.2. The identified organic compounds in the liquid obtained from depolymerisation of CFRP with ethylene glycol were found from the NIST database available in the software with a degree of certainty higher than 75%. From this Table it can clearly be seen that compounds formed from ethylene glycol dominated the DCM extracts of the residual liquid product from ethylene glycol-treated carbon fibre reinforced plastics. While dioxolanes, dioxanes and diacetates were detected, which are the main organic compounds produced from the cyclization and poly-condensation reactions of ethylene glycol, phenols and anilines were the major products when only water was introduced into the reaction. The apparent increased solubility of phenols and anilines in ethylene glycol meant that only a small proportion of phenol was extracted into DCM, while no anilines could be extracted.

In addition, there was experimental evidence of the decomposition of ethylene glycol into gas as determined from the product gas analysis results. There was an increase in the yield of ethene in the gas products from ethylene glycol treatment compared to the experiments with water. For instance, the yield of ethene in the gas when the water alone was used for the depolymerisation, was only 0.4 mol%; while in the experiment with ethylene glycol and water mixture at a ratio of 5, it was 48.3 mol%.

Table 4.2.1 Main organic compounds detected in the liquid obtained from carbon fibre reinforced plastics depolymerisation at 400 °C, using ethylene glycol and water as separate solvents.

S/ N	Organic compounds detected with ethylene glycol as solvent		Organic compounds detected with water as solvent	
	Compound	Structure	Compound	Structure
1	1,1-Ethanediol diacetate		2,4-Dimethylfuran	
2	2-Methyl-1,3-Dioxolane		Aniline	
3	Ethanol, 2,2'-[1,2-ethanediylbis(oxy)] bis, diacetate		2-Methyl phenol,	
4	2-(1-Methylethyl)-1,3-Dioxolane,		N-Methyl, aniline	
5	Ethanol, 2,2'-oxybis-, diacetate		N,4-Dimethyl Benzenamine,	
6	Ethanol, 2,2'-oxybis-, dipropanoate		4-(1-Methylethyl) phenol	
7	Hydroperoxide, 1,4-dioxan-2-yl		Quinoline	
8	2,2'-Bi -1,3-dioxolane		5-Methyl-3-phenyl-1,3 oxazolidine	
9	2-Heptyl -1,3-dioxolane,		1,3-Diphenyl-2-propyl Imidazolidine,	
10	N-(2-Hydroxyethyl)-N-methyl aniline		Phenol	
11	Phenol		-	-

#### 4.2.2.2 Catalytic Supercritical Water Gasification of Liquid Products

The use of ethylene glycol as a solvent for the removal of resin from carbon fibre reinforced plastic waste resulted in high resin removal and the recovery of clean, mechanically well-preserved carbon fibres. However, the reaction of ethylene glycol resulted in many organic compounds in the residual liquid product, and recovery of the resin monomers proved extremely difficult. Therefore, designing a process to use the liquid residual product as a source of chemical feedstock may not be cost-effective. In addition, disposal of the liquid residuals as a waste stream, will have both cost and environmental implications for the process. Also, due to its physical properties such as viscosity, and equal C/H/O ratio, EG has been considered as a model substance for pyrolysis oil from biomass to be used in gasifiers [11]. De Vlieger et. al., [12] stated that supercritical water gasification of EG is a promising technique to produce H<sub>2</sub> rich gas from EG with the help of Pt as catalyst. Therefore, the conversion of the residual liquid product into a useable form of energy for the process through hydrothermal gasification to produce hydrogen- and methane-rich fuel gas was investigated.

The liquid products were subjected to non-catalytic supercritical water gasification and also gasification in the presence of two different catalysts, sodium hydroxide and ruthenium on an  $\alpha$ -alumina support. For the experiments, the residual liquid product produced from the experiment which gave the highest resin removal was used, i.e., the 5:1 mixture of ethylene glycol/water. This sample was reacted in the presence of no catalysts and also with either NaOH or Ru/Al<sub>2</sub>O<sub>3</sub> in the 75 ml reactor at 500 °C for a hold time of 30 min.

The product distribution after gasification is shown in Figure 4.2.3 and gas compositions are shown in Figure 4.2.4. When no catalyst was present, 41 mol.% of H<sub>2</sub> yield was achieved. The remaining species in the gas were CO<sub>2</sub>, CO and CH<sub>4</sub> with compositions 17 mol.%, 23.7 mol.%, 11 mol.% respectively. The other hydrocarbon gases, which are defined in Figure 4.2.4 as C<sub>2</sub>-C<sub>4</sub> had a total of 7.40 mol.%. The high H<sub>2</sub> and CO content in the gas agrees with the work of de Vlieger et al. [12] who achieved 42% H<sub>2</sub> and

20% CO yield in the gas produced from 15 wt% pure ethylene glycol and water at supercritical conditions with the help of a Pt catalyst.

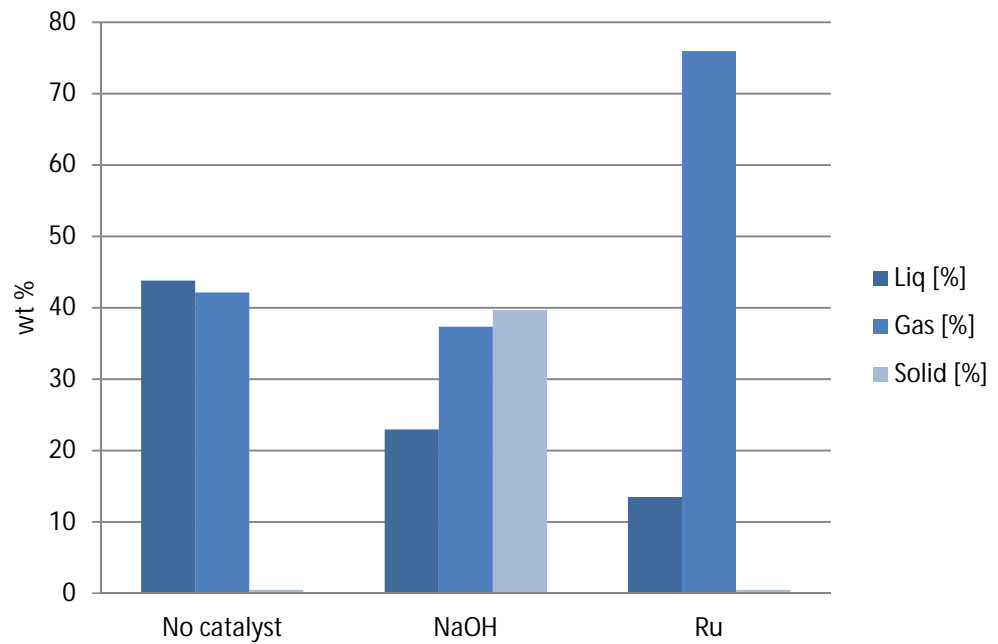


Figure 4.2.3 Product distribution after gasification of a sample of the residual liquid product.

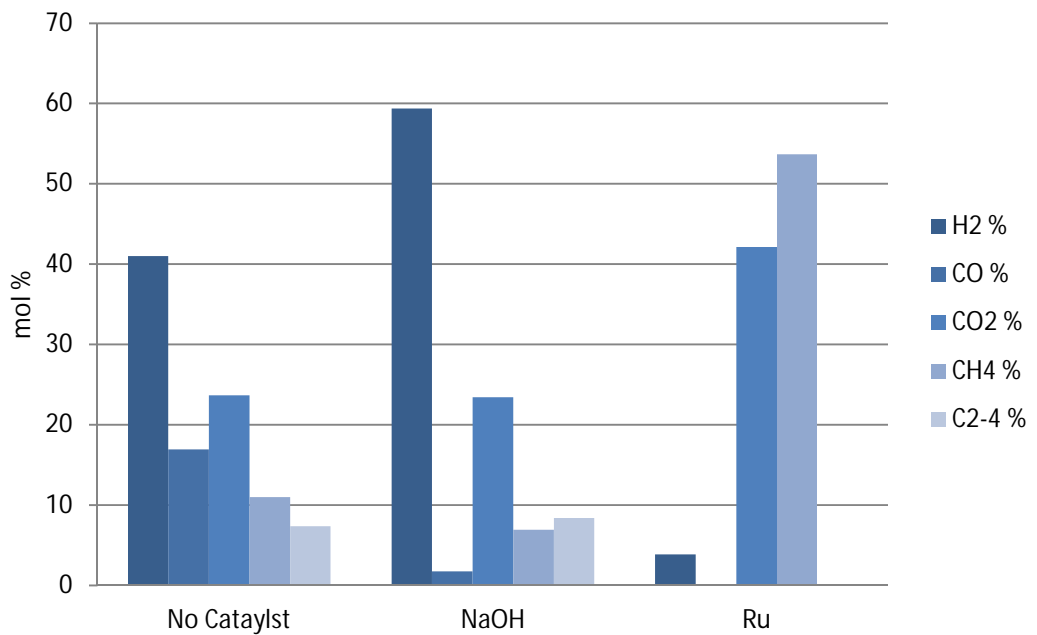


Figure 4.2.4 Gas composition after gasification of a sample of the residual liquid product.

With the addition of 1.0 g of NaOH as catalyst at the same reaction conditions, the carbon in the feed was captured as Na<sub>2</sub>CO<sub>3</sub>, so that the CO formation decreased to yield 1.77 mol.% in the gas. This is suggested to be due to the enhancement of the water–gas shift reaction, converting CO to hydrogen and CO<sub>2</sub>, which is captured as sodium carbonate [13].



Correspondingly, there is a large increase in the yield of hydrogen to nearly 60 mol% in the presence of the NaOH. The corresponding compositions of CO<sub>2</sub>, CH<sub>4</sub> and C<sub>2</sub>–C<sub>4</sub> hydrocarbons in the gas were 23.5 mol.%, 6.95 mol.% and 8.44 mol.%, respectively.

The effect of the presence of the Ru/Al<sub>2</sub>O<sub>3</sub> catalyst on gasification of the residual liquid product was also investigated. The results (Figure 4.2.3 and Figure 4.2.4) showed that the total gas yield was markedly increased in the presence of the Ru/Al<sub>2</sub>O<sub>3</sub> catalyst and that the CH<sub>4</sub> yield increased to 53.7 mol.% while that of CO and H<sub>2</sub> decreased dramatically. This could be the result of methanation reactions, promoted by the addition of Ru/Al<sub>2</sub>O<sub>3</sub> [14].



So if the aim is to produce CH<sub>4</sub> rich gas, Ru/Al<sub>2</sub>O<sub>3</sub> can be a good preference. In the cases where no catalyst and addition Ru/Al<sub>2</sub>O<sub>3</sub>, there was no char/solid formation, while in the presence of NaOH, because of the Na<sub>2</sub>CO<sub>3</sub> formation, there was solid formation.

Table 4.2.2 The produced mol gas per kg CFRP waste and the higher heating value of the product gas from the gasification experiments.

Sample No	Catalyst	H <sub>2</sub> [mol/kg]	CO [mol/kg]	CO <sub>2</sub> [mol/kg]	CH <sub>4</sub> [mol/kg]	C <sub>2-4</sub> [mol/kg]	HHV [MJ/Nm <sup>3</sup> ]
1	-	150.7	62.2	87.1	40.5	27.1	18.0
2	NaOH	250.3	7.5	98.8	29.3	35.6	17.3
3	Ru/Al <sub>2</sub> O <sub>3</sub>	18.8	0.5	203.8	259.4	0.8	22.0



In Table 4.2.2, yields of the product gases in moles per kg feed and the higher heating value of the gas produced are given. The highest HHV was obtained when Ru/Al<sub>2</sub>O<sub>3</sub> was used as a catalyst. The average HHV of gases produced from these experiments are similar to that of a typical gas produced from biomass via supercritical water gasification, which is around 20 MJ/Nm<sup>3</sup> [15].

#### 4.2.3 Mechanical Properties of the Recovered Carbon Fibre

The mechanical properties of the recovered carbon fibre were also tested, and the results are shown in Table 4.2.3. The results suggest that overall there was no decrease in the tensile strength of the fibres compared to that of virgin carbon fibre. In the previous section 4.1, carbon fibre from waste CFRP was recovered with supercritical water with the addition of hydrogen peroxide as an oxidant agent. Although high resin removal efficiencies were achieved, there was a significant decrease in the mechanical properties of the recovered fibres, apparently due to oxidation of the carbon fibre surface. Compared to the previous study with supercritical water, EG enabled almost all the resin from the waste to be removed, without using any other catalyst or reactive agent, thus preserving the mechanical properties of the carbon fibre.

Table 4.2.3 The mechanical properties of virgin and recovered carbon fibre.

	Virgin Fibre	Recovered Fibre	
		1*	2**
Breaking Force [N]	0.135	0.138	0.131
Elongation [mm]	0.3	0.282	0.427
Tensile Strength [GPa]	3.5	3.56	3.4
Youngs Modulus	233	254.32	159.44

\* Carbon fibre recovered during experiments at 400 °C in ethylene glycol

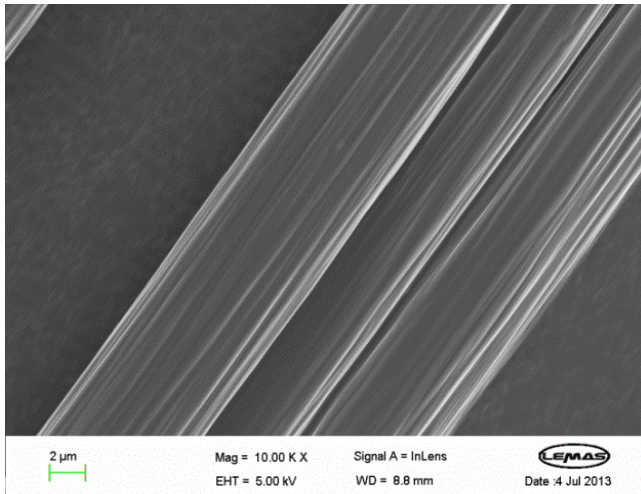
\*\* Carbon fibre recovered during experiments at 400 °C in ethylene glycol/water (ratio = 5)

When alcohols such as ethanol, methanol and 1-propanol were used, even at higher temperatures than 400°C, high resin removal could not be achieved, the addition of catalysts was required, as reported by Piñero-Hernanz et al. [1]. They used alkalis (KOH and CsOH) as catalyst and achieved 85% of resin removal when 1-propanol was used as solvent, in 15 min of reaction time. Also EG successfully depolymerised the resin at zero residence times, which is a further advantage in comparison to the alcohols.

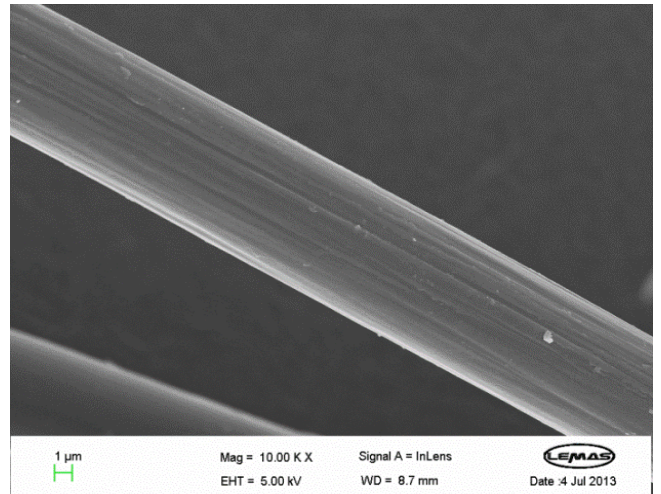
The recovered carbon fibres were analysed by scanning electron microscopy to compare the surface properties with the virgin carbon fibre (Figure 4.2.5). In Figure 4.2.5 (a), the virgin carbon fibre sample is shown and the image of the carbon fibre recovered from the treatment with ethylene glycol only at 400°C shown in Figure 4.2.5 (b), shows that the surface of the fibre is very similar to virgin fibre. The surface is almost resin free, and no cracks or fissures are observed on the recovered carbon fibre surface. When the reaction temperature was decreased to 380 °C, there was a decrease in resin removal as shown by some resin remaining on the carbon fibre surface as seen in Figure 4.2.5 (e). At the same temperature, when the reaction time was increased to 10 min, more resin was removed from the carbon fibre surface but still, it can be seen from Figure 4.2.5 (f) that on the recovered carbon fibre surface, some resin debris remained.

In Figure 4.2.5 (c) and (d), the images of carbon fibre reclaimed from the depolymerisation with the ethylene glycol/water mixture are shown. When the ethylene glycol/water ratio was 5, the recovered carbon fibre surface looked similar to that recovered with ethylene glycol alone at 400 °C. The mechanical properties of both reclaimed fibres are similar, with a slight decrease when the ethylene glycol/water mixture was used.

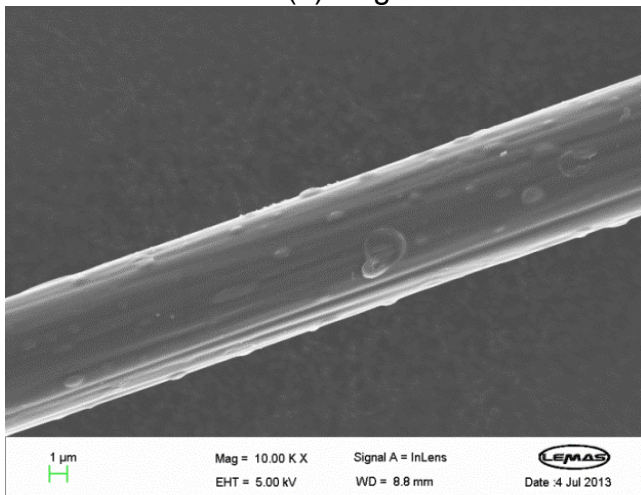
The FTIR analysis of the recovered carbon fibre at 400°C in EG/water mixture (EG/water ratio = 5) and the virgin fibre also show that the recovered carbon fibre surface has a similar structure, as given in Figure 4.2.6.



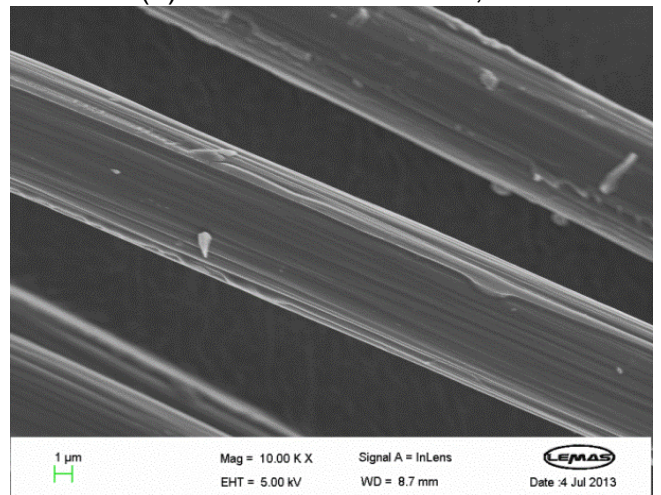
(a) Virgin



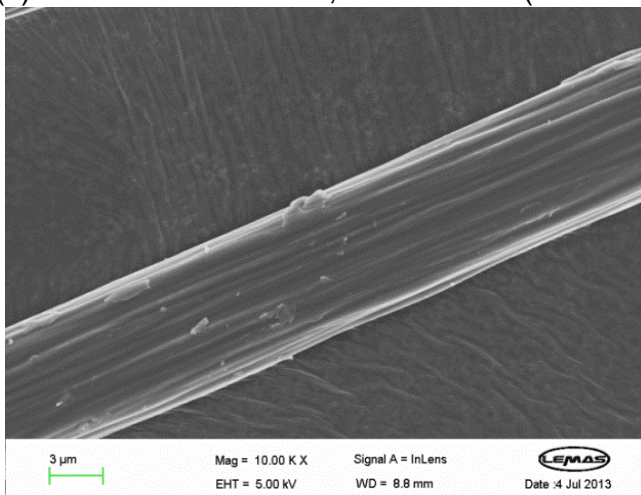
(b) Recovered at 400°C, in EG



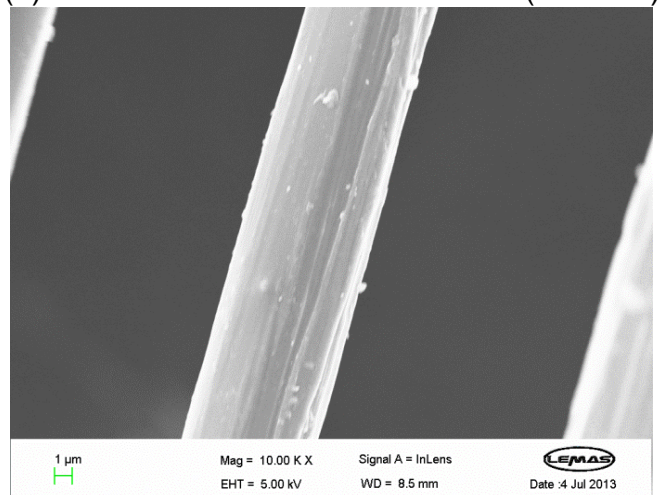
(c) Recovered at 400°C, in EG/water (ratio 5:1)



(d) Recovered at 400°C in EG/water (ratio 3:1)



(e) Recovered at 380°C, in EG (t = 0 min)



(f) Recovered at 380°C, in EG (t = 10)

Figure 4.2.5 SEM images of virgin and recovered carbon fibre samples in relation to treatment in ethylene glycol (EG) and EG/water mixtures

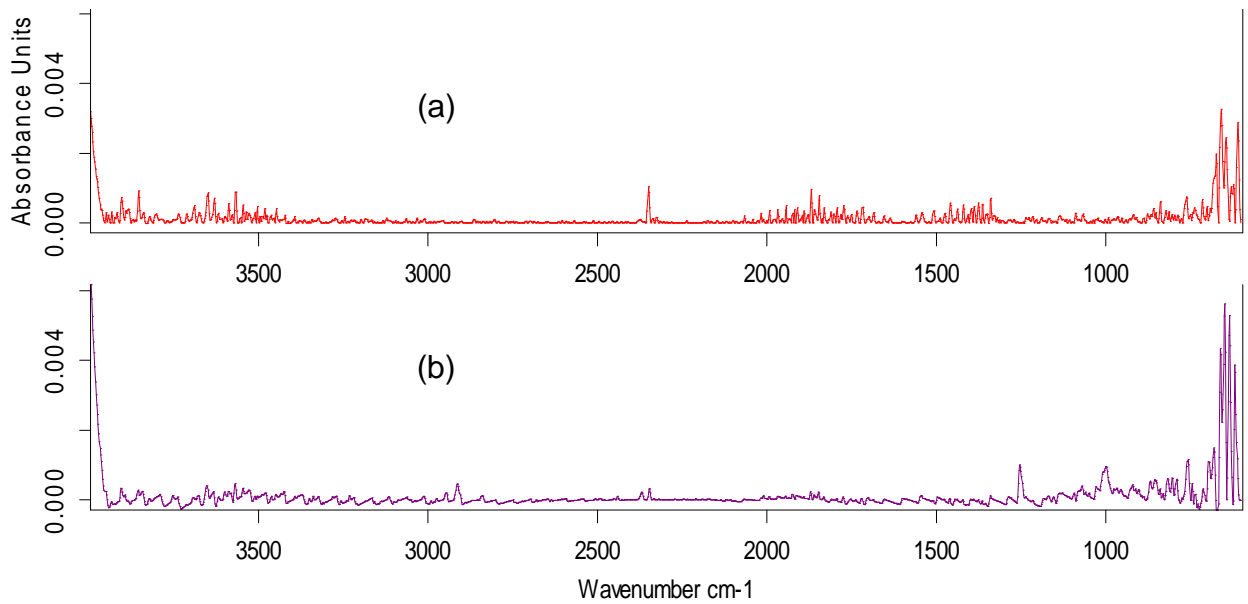


Figure 4.2.6 FTIR results (a) recovered carbon fibre at 400 °C in EG/water mixture (EG/water ratio = 5), (b) virgin carbon fibre.

#### 4.2.4 Summary

Depolymerisation of waste carbon fibre reinforced plastics in ethylene glycol at subcritical conditions achieved 92.1% resin removal at 400°C and also recovered the carbon fibres with similar mechanical properties to virgin carbon fibre. In the presence of water only, to achieve higher resin removal ratios, H<sub>2</sub>O<sub>2</sub> was introduced to the reaction at supercritical conditions, which resulted in a dramatic decrease in mechanical properties of the recovered fibre, whereas when EG used with water, the mechanical properties were preserved. Higher resin removal was achieved compared to previous work with water together with KOH and H<sub>2</sub>O<sub>2</sub>; at zero residence time, when mixtures of ethylene glycol and water were used as solvents without any addition of a catalyst, at high ethylene glycol/water ratios. However, increasing the reaction temperature to 420°C, resulted in char formation, which led to an apparent increase in the solid residue (char and carbon fibre) obtained. In addition, resin removal also decreased at lower ethylene glycol/water ratios.

It was difficult to extract carbon fibre reinforced plastics degradation products from the liquid residuals during ethylene glycol treatments, due to

their solubility and conversion of some of the ethylene glycol. An alternative treatment of the residual liquid product was via hydrothermal gasification at supercritical water conditions. It was shown that the residual liquid product could be gasified to produce either a hydrogen-rich fuel gas (60 mol.% of H<sub>2</sub>) or a methane-rich fuel gas (53.7 mol.% CH<sub>4</sub>), depending on whether a NaOH catalyst or Ru/Al<sub>2</sub>O<sub>3</sub> catalyst was used respectively.

### 4.3 Evaluating the Mechanical Properties of Reinforced LDPE Composites Made With Carbon Fibres Recovered via Hydrothermal Processing

In this section, the mechanical properties of fibre reinforced composites produced from recovered carbon fibres were tested. The recovered carbon fibres were produced via hydrothermal depolymerisation in ethylene glycol and water mixture as described in the previous section. The resin chosen for the production of the composites was low density polyethylene (LDPE) and four different coupling agents were added to the LDPE to see their effect on the mechanical properties of the product composite material. For comparison, composite materials were prepared with three different carbon fibres; virgin carbon fibre, recovered carbon fibre (non-oxidized) and recovered carbon fibre (oxidized).

The analysed mechanical properties were tensile, flexural and charpy impact strengths. The interactions between the matrix and the additives were described with the help of the Fourier Transform Infrared Spectrometry (FTIR) analyses.

#### 4.3.1 Properties of Recovered Carbon Fibres and Additives

The procedure for the recovery of the carbon fibres from the waste CFRP was previously described in section 4.2.

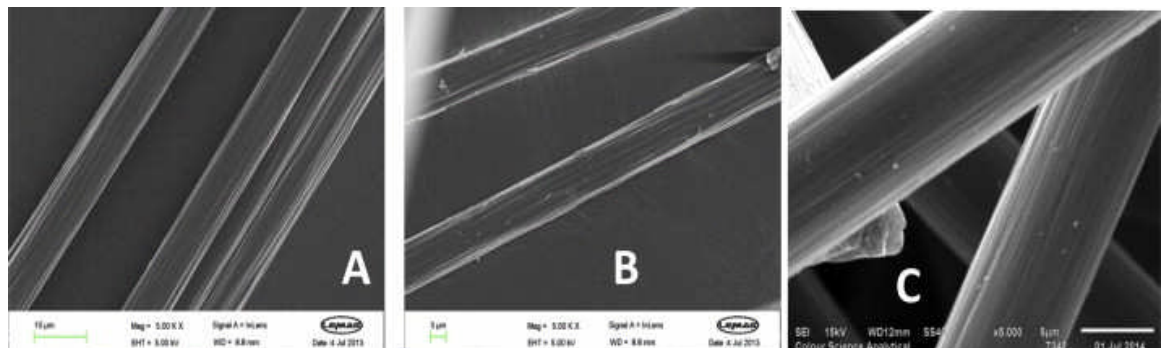


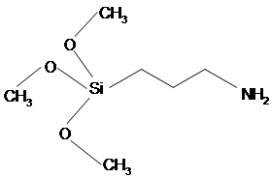
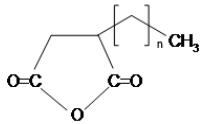
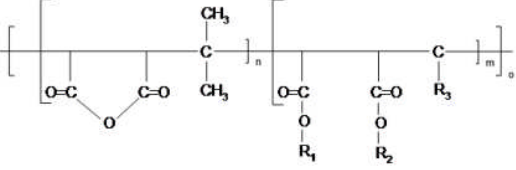
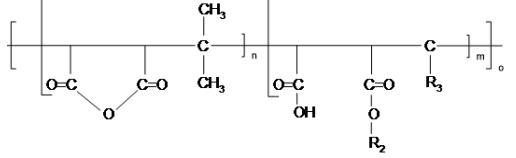
Figure 4.3.1 SEM images of (A) Virgin, (B) Recovered, (C) Oxidized recovered carbon fibres



For this study, the same method was applied, 10 g of the CFRP sample was loaded into a 500 ml capacity hydrothermal reactor, along with 50 ml ethylene glycol and 10 ml distilled water. This combination of water and ethylene glycol resulted in up to 96 wt% resin removal. Figure 4.3.1 shows the SEM images of the recovered carbon fibres. Oxidized recovered fibres were prepared by oxidizing the product fibres from the solvolysis process with air at 250°C for 1.5 h. SEM images show that the oxidized recovered carbon fibres had a cleaner surface than non-oxidized recovered carbon fibres.

A loading of 15 wt% carbon fibre were added into the LDPE matrix for each sample. Different surface modifying/coupling agents were tested to achieve stronger interfacial forces (and advanced mechanical properties) between the reinforcements and LDPE matrix. The main properties of the coupling agents/additives are summarized in Table 4.3.1

Table 4.3.1 The main properties of surface treating agents

Sample ID	Appearance	Chemical structure	$M_w^*/M_n^{**}$
CA-1	Transparent liquid		179
MA-g-HDPE	Solid, granulates		n.a.
CFA-1	Yellow, honey-like dense liquid		7150/6520
CFA-2	Yellow, solid		6345/5190

\* $M_w$ : Weight average molecular weight

\*\* $M_n$ : Number average molecular weight

Two commercial and two experimental coupling agents have been used. The two commercial additives were, the mostly used silane type (3-aminopropyl-trimethoxysilane, CA-1) and maleic anhydride-grafted-polymer (MA-g-HDPE), while the experimental additives CFA-1 and CFA-2 were polyalkenyl-polymaleic-anhydride derivatives, synthesized at the University of Pannonia, Hungary. The silane based coupling agents are well known with their ability to form a bond between the organic and inorganic materials [16]. The MA-g-HDPE was selected as the grafting improves the adhesion of the polyolefins to metals, fibres and other polymers [17]. The applied concentrations were 1 wt% for the commercial additive, and 2 wt% for the experimental additives based on cost considerations, as the 2 wt% concentration of experimental additives had been found to be more cost-effective than 1 wt% of the commercial additive [18].

For composite materials manufacturing, a laboratory two-roll mill (LabTech LRM-S-110/T3E, Labtech Ltd, Thailand) was used. 15 wt% carbon fibre was added into the raw LDPE in each case. The temperatures of the rolls were 180 °C (first roll,  $n = 20$  rpm) and 150 °C (second roll,  $n = 8$  rpm). Firstly, the LDPE was placed on the heated rolls and then the carbon fibre reinforcement was added together with additives to the molten polymer. Following the composite preparation, they were grounded into particles with dimensions up to 5 mm using a laboratory grinder. Then 100 mm × 10 mm sheets were press-moulded at a temperature and pressure of 180 °C and 34.5 MPa respectively. The product composite materials gained a rigid shape as shown in Figure 4.3.2. Finally, specimens with dimension of 1 mm × 10 mm × 100 mm were cut from the carbon fibre reinforced LDPE composite sheets for the mechanical properties analyses.



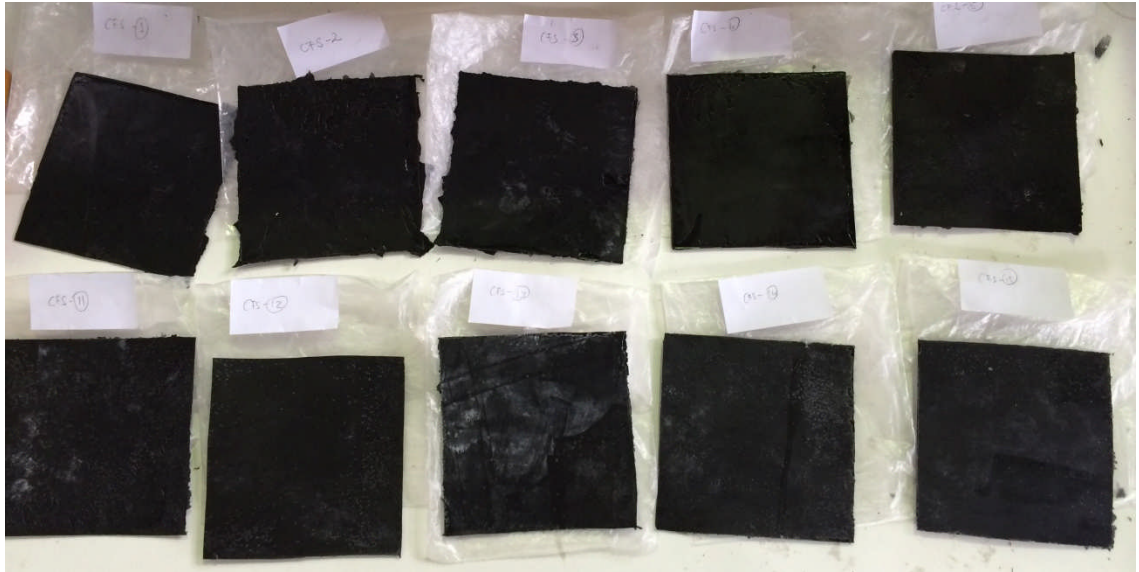


Figure 4.3.2 The carbon fibre reinforced LDPE composites, after press-moulding

Regarding the effect of the coupling agents and carbon fibres, the real fibre/ash content and its distribution inside the composite is a crucial parameter influencing properties. Therefore the fibre/ash content was measured by the standard MSZ EN ISO 3451-1:1999 method. In this method, the fibre/ash content of composite materials can be obtained by taking samples at nine independent points over the product composite materials and were oxidized at 500°C to determine the average fibre content of specimens. The results demonstrated that the average fibre/ash content of the reinforced composites was between 14.3% and 15.2%, while the deviation was between  $\pm 0.2\%$  and  $\pm 0.6\%$ . Thus, results confirmed that the uniform loading of 15 wt% carbon fibres in the LDPE matrix was accurate and successful.

## 4.3.2 Mechanical Properties of the Composites

### 4.3.2.1 Tensile and Flexural Strengths

Table 4.3.2 summarizes the tensile and flexural strengths of virgin carbon fibre, non-oxidized recovered and oxidized recovered carbon fibre reinforced LDPE composites. The mean values of the properties were

calculated based on five parallel measurements and the standard deviation was found to be no more than 10%.

In general, it can be seen that the virgin carbon fibre and recovered carbon fibre composites did not differ significantly in the absence of the additives (without any surface modifications): the tensile strength was between 12.7 MPa (virgin) and 17.4 MPa (oxidized), while the flexural strengths were 7.5 MPa (non-oxidized), 7.9 MPa (oxidized) and 8.0 MPa (virgin). It is important to note, that the raw LDPE matrix had 11.4 MPa and 7.5 MPa tensile and flexural strengths, respectively.

The results suggest that the tensile property could be improved by the application of non-surface modified carbon fibre and the best results were found by the application of commercial 3-aminopropyl-trimethoxysilane (CA-1). For instance, the tensile and flexural strength increased to 23.5 MPa and 16.7 MPa, respectively, using virgin carbon fibre. With respect to the two experimentally-synthesized additives, CFA-2 resulted in higher composite strengths than CFA-1. By reinforcing the LDPE with virgin carbon fibre, the tensile strength of the reinforced LDPE composite was 20.1 MPa with the CFA-2 coupling additive, while it was only 15.2 MPa with the CFA-1 additive.

In general, LDPE composites prepared with virgin fibres gave higher strength, than the other two kinds of recovered carbon fibre when the silane-type (CA-1) commercial additive was used. In other cases, the oxidized recovered carbon fibre appeared to give better performance than the virgin and the non-oxidized recovered carbon fibres. It is an important observation that neither tensile strength, nor flexural strength could be improved by chemical modification of the surface of the non-oxidized recovered carbon fibre. Indeed, the use of the additives (coupling agents) led to a lowering of both tensile and flexural strengths for the non-oxidized recovered carbon fibre compared to the properties of the oxidized recovered carbon fibre. The only exception was seen where the non-oxidized recovered carbon fibre gave higher tensile and flexural strengths compared to virgin carbon fibre in the presence of grafted-MA (MA-g-HDPE). This result could be attributed to favourable surface properties of recovered carbon fibre for anhydride or carboxyl groups present in grafted-MA.

Table 4.3.2 Tensile and flexural properties of composite materials

		<i>No additives</i>	<i>CA-1</i>	<i>MA-g-HDPE</i>	<i>CFA-1</i>	<i>CFA-2</i>
Tensile Strength, [MPa]	Virgin CF	12.7	23.5	13.2	15.2	20.1
	Recovered CF	16.5	9.9	14.7	7.7	8.1
	Oxidized Recovered CF	17.4	19.2	20.3	12.5	18.9
Tensile Modulus, [MPa]	Virgin CF	512	1150	541	451	971
	Recovered CF	571	479	549	410	484
	Oxidized Recovered CF	663	966	899	509	912
Flexural Strength, [MPa]	Virgin CF	8.0	16.7	6.2	6.5	11.9
	Recovered CF	7.5	8.9	7.0	4.3	4.6
	Oxidized Recovered CF	7.9	15.4	11.7	6.1	15.8
Flexural Modulus, [MPa]	Virgin CF	681	1415	724	648	1118
	Recovered CF	769	543	591	499	621
	Oxidized Recovered CF	755	1511	1015	647	1442

It is also clear from the results in Table 4.3.2 that the surface properties of recovered carbon fibres could be significantly improved by oxidation at low temperature (250°C). The improvement might be due to combustion of the char particles on the recovered carbon fibres surface as recovered

carbon fibres were generally covered with small char particles after recovery [19]. In the previous chapter, although it was found that the recovered carbon fibres via hydrothermal depolymerisation had enhanced mechanical properties without an oxidizing agent (or oxidation process), the chemical activity of the fibres' surface reduced due to char particles acting as a barrier, as a result giving weak interactions between the fibre surface and the LDPE matrix.

Depending on the raw material used (pitch based, rayon or polyacrylonitrile based) and production conditions, carbon fibres gain a resistance to oxidation temperatures differing from 400°C to 500°C. The mechanical properties of carbon fibre can be reduced with the exposure to oxidative atmosphere at these temperatures [20-22]. Therefore by oxidizing at low temperature, the negative effect of oxidization at high temperatures on the carbon fibre's mechanical properties was reduced, and the chemical activeness of the surface improved.

As a result, the composite material manufactured with oxidized recovered carbon fibres had better chemical and/or physical linkage established between the oxidized recovered carbon fibres and the LDPE matrix with the addition of the coupling agents, compared to the composites with non-oxidized recovered carbon fibres. For instance, after oxidation, the tensile strength increased by 94%, 38%, 62% and 135% by the application of oxidized recovered CF compared to non-oxidized CF after the application of 3-aminopropyl-trimethoxysilane, grafted-MA, CFA-1 and CFA-2, additives respectively.

Table 4.3.2 also summarizes the tensile and flexural modulus of the composite specimens. The modulus is a widely used parameter for constructional material characterization, because it refers to the stiffness of material. According the results, the LDPE composites with virgin carbon fibre gave the highest modulus values and better results were obtained from the recovered carbon fibres after oxidizing.

### 4.3.2.2 Elongation at Break

The elongation at break also called fracture strain is the ratio between the changed length and initial length after the breakage of the specimen. It represents the resistance of the material against the changes in its shape without any crack formation [23]. Three specimens with dimension of 1 mm × 10 mm × 100 mm for each sample were used and their average were calculated, and the standard deviation was found to be no more than 10%. The results for the carbon fibre reinforced LDPE composites shown in Table 4.3.3 demonstrated that the presence of carbon fibres significantly decreased the elongations, for example the raw matrix LDPE had 155% relative tensile elongation at break, which decreased to between 2.37–6.72% for the virgin carbon fibre reinforced composites. Therefore the data show that the reinforced composites were much more rigid, than the raw LDPE matrix. Virgin carbon fibres, non-oxidized carbon fibres and oxidized recovered carbon fibres had 3.22%, 4.07% and 4.10% relative elongation at break. Similar results were obtained by the application of 3-aminopropyl-trimethoxysilane (2.37–4.01%) and grafted-MA (3.64–4.52%).

Table 4.3.3 Elongation at break, [%]

<i>Sample</i>	<i>No additives</i>	<i>CA-1</i>	<i>MA-g-HDPE</i>	<i>CFA-1</i>	<i>CFA-2</i>
Virgin CF	3.2	4.0	3.6	4.0	4.9
Recovered CF	4.1	2.4	4.5	6.7	6.7
Oxidized Recovered CF	4.1	3.1	4.4	6.6	6.4

Interestingly, the virgin carbon fibres coupled with the two experimental additives had elongations of 4.04% and 4.88%, while considerably higher values resulted in the case of both recovered carbon fibre samples with the same additives (6.43–6.72%). Furthermore, the non-oxidized recovered carbon fibres containing LDPE composites had a little higher relative elongation than that of oxidized recovered carbon fibres.

In general, carbon fibre reinforcement decreased the elongation, as it was 155% in case of raw LDPE matrix. The product composite materials gained more rigid and stable structure.

#### 4.3.2.3 Charpy Impact Strengths

The impact strength describes the ability of a material to absorb shock and impact energy without breaking. The amount of energy absorbed by the specimen shows the toughness of the material [23]. Besides the tensile and flexural properties discussed above, the resistance against dynamic stress is one of the most important mechanical properties of polymers. Generally, impact strength can give some predictions regarding specimen resistance against dynamic load. In charpy impact strength test, three specimens with dimension of 1 mm × 10 mm × 100 mm from each sample were tested. Table 4.3.4 shows the charpy impact strength of carbon fibre reinforced LDPE composites with a standard deviation less than 10%. According to the earlier results, the matrix LDPE had 18.2 kJ m<sup>-2</sup> Charpy impact strength without reinforcement, which increased to 19.9, 23.0 and 26.7 kJ m<sup>-2</sup> using the virgin carbon fibres, non-oxidized recovered carbon fibres and oxidized recovered carbon fibres, respectively without any surface modification. Additives were favourable only in the case of the virgin carbon fibres, because the impact strength of the LDPE composites containing virgin carbon fibres changed from 22.9 kJ m<sup>-2</sup> (CFA-1) to 32.6 J m<sup>-2</sup> (3-aminopropyl-trimethoxysilane).

Table 4.3.4 Charpy Impact Strength, [kJ/m<sup>2</sup>]

<i>Sample</i>	<i>No additives</i>	<i>CA-1</i>	<i>MA-g-HDPE</i>	<i>CFA-1</i>	<i>CFA-2</i>
Virgin CF	19.9	32.6	23.2	22.9	26.6
Recovered CF	23.1	21.2	20.8	22.2	24.2
Oxidized Recovered CF	26.7	28.2	21.7	16.3	25.7

The application of recovered carbon fibres to the composite resulted in better impact properties than that of virgin carbon fibre composites without additives, whereas when coupling agents were used the LDPE composites with virgin carbon fibres gave the highest impact strength. The tested coupling additives notably increased the impact strength of virgin carbon fibre reinforced composites, more than recovered carbon fibres (both oxidized and non-oxidized). The impact strength of composites without coupling additives could be increased only in two cases: applying commercial 3-aminopropyl-trimethoxysilane in the case of oxidized recovered carbon fibres and CFA-2 experimental additive in the case of non-oxidized recovered carbon fibres.

#### **4.3.2.4 LDPE-Additive-Carbon Fibre Ester Linkage Mechanism**

In order to investigate the theoretical coupling reactions, the manufactured carbon fibre reinforced LDPE composites were also analysed by attenuated total reflectance Fourier transform infrared spectroscopy ATR-FTIR. The spectrum of each sample shows many similarities between samples (Figure 4.3.3). For example, typical infrared spectral bands were found between 3000 and 2800  $\text{cm}^{-1}$ , where symmetric and asymmetric vibrations of both methyl and methylene groups gave sharp and intensive absorption bands according to Table 4.3.5

The symmetrical and asymmetrical stretching vibrations of methyl groups are due to the changes in the interatomic distance along the axis of the bond [24]. The next significant signals occurred at 1465  $\text{cm}^{-1}$  and 1260  $\text{cm}^{-1}$ . According to literature data, the peak at 1465  $\text{cm}^{-1}$  was likely caused by C–O–H bending vibration of carboxylic acid and its derivatives, while the infrared signal at 1260  $\text{cm}^{-1}$  referred to the presence of C–O–C chemical linkage [25].

Similar sharp, well isolated infrared bands were recorded at 1100  $\text{cm}^{-1}$  and 1015  $\text{cm}^{-1}$ . It is also well known that both infrared absorption bands should be attributed to the presence of ester or even ether groups [25]. In addition, the very sharp and strong absorption band at 720  $\text{cm}^{-1}$  showed  $\beta(\text{CH}_2)$  vibration.

Table 4.3.5 Saturated aliphatic group frequencies adapted from Coates et. al. [25]

<i>Group Frequency [cm<sup>-1</sup>]</i>	<i>Functional Group/Assignment</i>
2970-2950/2880-2860	Methyl (-CH <sub>3</sub> ) C-H asym.*/sym.** stretch
2935-2915/2865-2845	Methylene (>CH <sub>2</sub> ) C-H asym./sym. stretch
2900-2880	Methyne (>CH-) C-H stretch
2850-2815	Methoxy, methyl ether O-CH <sub>3</sub> , C-H stretch

\*asymmetrical

\*\*symmetrical

The coupling effects of the silane-based and MA-grafted polymer type compatibilizers are well known as mentioned in the previous sections. It was reported that 3-aminopropyl-trimethoxysilane can link to the –OH groups on the carbon fibre surface via the Si–O–fibre chain [26, 27]. It was suggested that the two other Si–O–CH<sub>3</sub> and Si–(CH<sub>2</sub>)<sub>3</sub>–NH<sub>2</sub> chains are free, and can participate in strong chemical linkage with the LDPE matrix. In fact, the carboxyl groups of MA-g-polymer type compatibilizers are able to chemically link to the –OH groups on the carbon fibre surface, while the long polymer side chain can physically interact with the non-polar LDPE matrix. The two experimental additives can evolve a similar coupling mechanism. The applied experimental additives were low molecular weight polymers, with average molecular weights of 3000–5000 g mol<sup>-1</sup>.



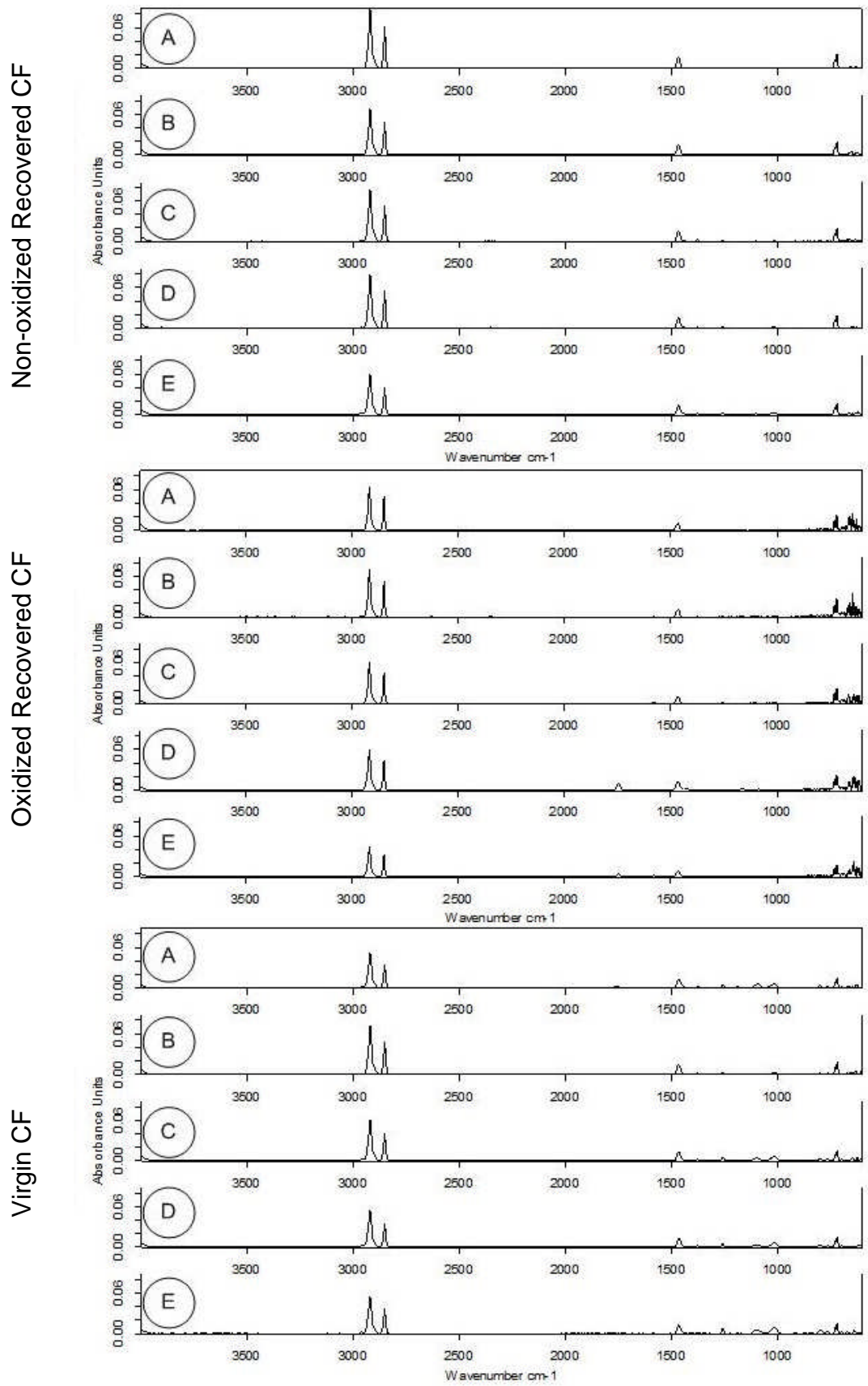


Figure 4.3.3 FTIR spectra of manufactured composites (A: without additive, B: CA-1, C: MA-g-HDPE, D: CFA-1, E: CFA-2).

Based on the infrared results, the proposed reaction scheme of coupling is summarized in Figure 4.3.4. In the structure of the compatibilizers, each monomer unit contains an anhydride ring with  $-\text{CO}-\text{O}-\text{CO}-$  chemical linkage. Another anhydride ring can react to produce an ester or half ester-type structure. The  $-\text{CO}-\text{O}-\text{CO}-$  chemical bonds were able to function as carboxylic acids. The possible chemical reactions between the experimental additive and carbon fibre should be through the reactions of the aforementioned  $-\text{COOH}$  groups of compatibilizers and the  $-\text{OH}$  groups of the carbon fibre surface. However, the most likely interaction between the two experimental coupling additives and the LDPE matrix was physical.

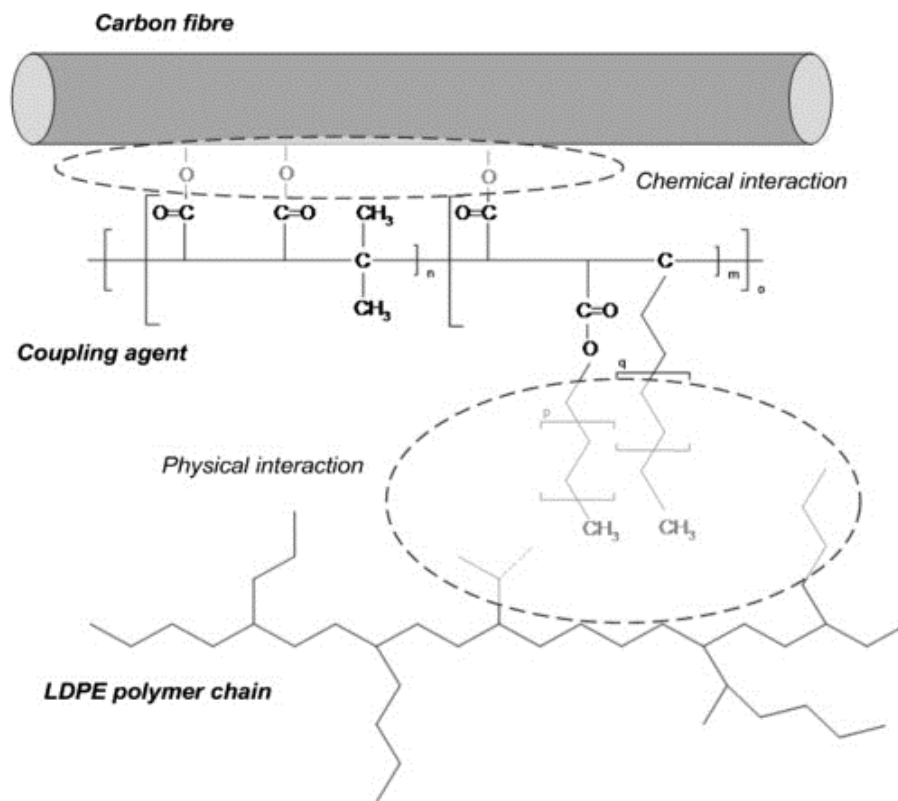


Figure 4.3.4 The proposed reaction scheme of coupling between carbon fibre and commercial LDPE matrix.

As shown in Table 4.3.1, owing to the half ester structure of CFA-2 experimental coupling agent, it could contain more carboxylic groups than the CFA-1 additives. This could be the reason that the CFA-2 additive could establish more chemical bonds with the carbon fibre than the CFA-1 additive, as demonstrated by the mechanical tests in this study.

The better performance of the oxidized recovered carbon fibre reinforced LDPE than non-oxidized one was explained as the less chemical activity of the non-oxidized recovered carbon fibres due to char particles on the surface prevented the chemical interaction between the carbon fibres and the coupling agents in the previous sections. This was confirmed with the attenuated total reflectance Fourier transform infrared spectroscopy (ATR-FTIR) analyses of the three carbon fibre samples as shown in Figure 4.3.5.

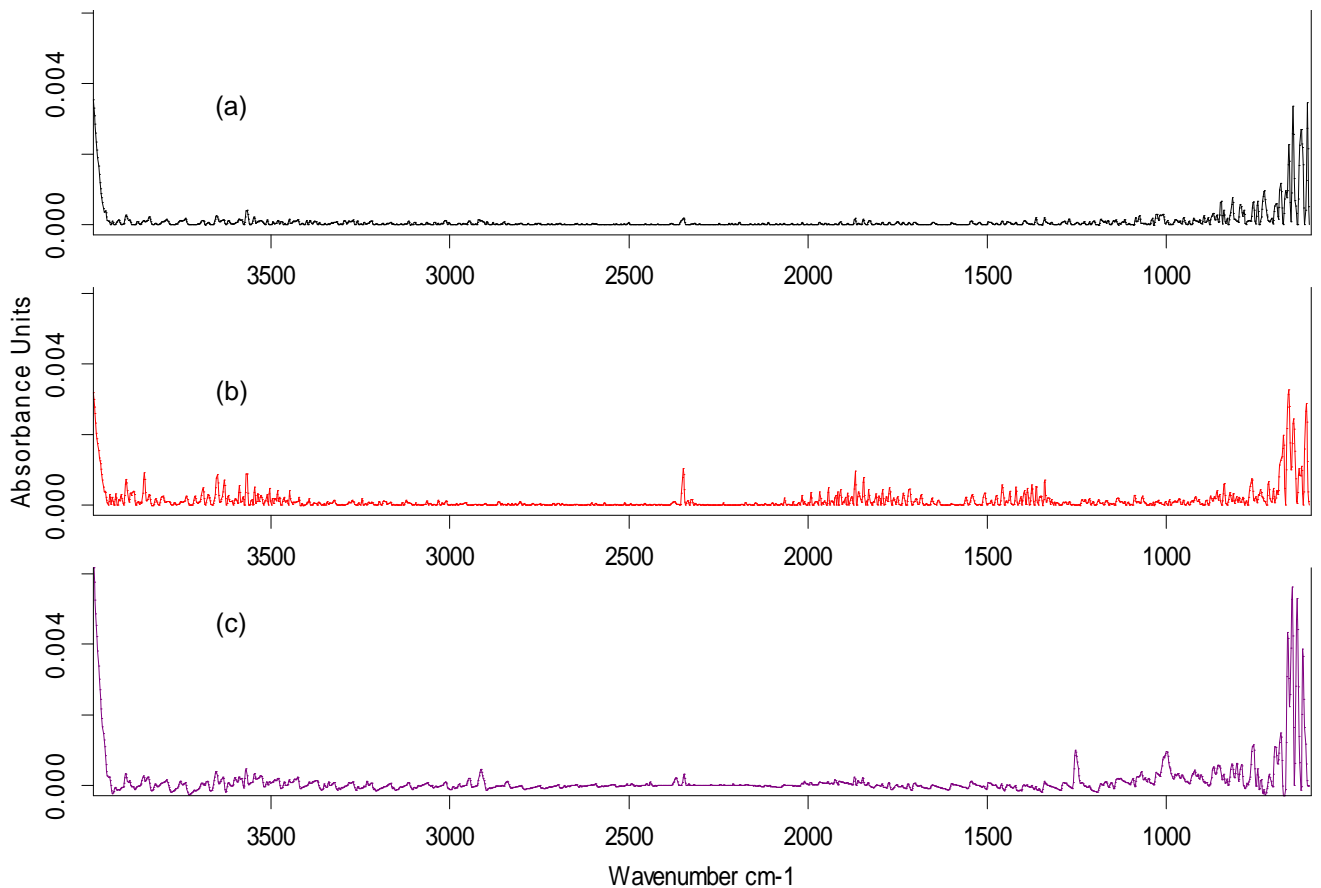


Figure 4.3.5 FTIR results of (a) Oxidized recovered carbon fibre, (b) Non-oxidized recovered carbon fibre and (c) virgin carbon fibre

While the virgin carbon fibre and the oxidized recovered carbon fibre had similar spectrums, non-oxidized recovered carbon fibre had small peaks between the wavelengths 2100 and 1350  $\text{cm}^{-1}$ . This also proved that char particles remained after hydrothermal processing with ethylene glycol and water. As a result, owing to having a cleaner surface, oxidized recovered carbon fibre became more chemically active and the product composite

material showed better tensile and flexural properties compared to composites reinforced by non-oxidized carbon fibre.

### **4.3.3 Summary**

The carbon fibres recovered via hydrothermal depolymerisation in ethylene glycol/water mixture were used to produce new composite materials with LDPE as matrix. The manufactured composite was then tested to determine the mechanical properties and were compared to composite reinforced with virgin carbon fibre. The recovered carbon fibres were also separated into two groups as oxidized and non-oxidized to compare the oxidation effect on the recovered carbon fibre. It can be concluded that the oxidized carbon fibres showed better strength properties than the original non-oxidized sample. The surfaces of the recovered carbon fibre were modified by different chemicals, and the most advanced properties were found when commercial silane-based and CFA-2 experimental additives were used. Essentially, the tensile properties of the composites could be improved by the two aforementioned additives. Based on infrared analysis, chemical reactions between the experimental additives and carbon fibre are proposed to be through the reactions of the  $-COOH$  groups of compatibilizers and the  $-OH$  groups on carbon fibre surface.

As a result, the recovered carbon fibres can be used to produce new composite materials with enhanced mechanical properties, by applying oxidation at low temperatures. Hydrothermal depolymerisation was able to recover the carbon fibre by preserving the mechanical properties, and also the resin fraction was converted into fuel gas with gasification of the liquid produced during depolymerisation, as described in the previous chapter.

## References

1. Pinero-Hernanz, R., et al., *Chemical recycling of carbon fibre composites using alcohols under subcritical and supercritical conditions*. Journal of Supercritical Fluids, 2008. **46**(1): p. 83-92.
2. Lee, G., et al., *Comparison of the effects of the addition of NaOH on the decomposition of 2-chlorophenol and phenol in supercritical water and under supercritical water oxidation conditions*. The Journal of Supercritical Fluids, 2002. **24**(3): p. 239-250.
3. Kruse, A. and E. Dinjus, *Hot compressed water as reaction medium and reactant: 2. Degradation reactions*. The Journal of Supercritical Fluids, 2007. **41**(3): p. 361-379.
4. Macko, J. and H. Ishida, *Structural effects of amines on the photooxidative degradation of polybenzoxazines*. Polymer, 2001. **42**(15): p. 6371-6383.
5. Low, H.Y. and H. Ishida, *Mechanistic study on the thermal decomposition of polybenzoxazines: effects of aliphatic amines*. Journal of Polymer Science-B-Polymer Physics Edition, 1998. **36**(11): p. 1935-1946.
6. Yee Low, H. and H. Ishida, *Structural effects of phenols on the thermal and thermo-oxidative degradation of polybenzoxazines*. Polymer, 1999. **40**(15): p. 4365-4376.
7. Pauling, L., *The nature of the chemical bond and the structure of molecules and crystals: an introduction to modern structural chemistry*. Vol. 18. 1960: Cornell University Press.
8. Bai, Y., Z. Wang, and L. Feng, *Chemical recycling of carbon fibers reinforced epoxy resin composites in oxygen in supercritical water*. Materials & Design, 2010. **31**(2): p. 999-1002.
9. Karayannidis, G.P. and D.S. Achilias, *Chemical Recycling of Poly(ethylene terephthalate)*. Macromolecular Materials and Engineering, 2007. **292**(2): p. 128-146.
10. Yong, T.L.-K. and Y. Matsumura, *Reaction Pathways of Phenol and Benzene Decomposition in Supercritical Water Gasification*. Journal of the Japan Petroleum Institute, 2013. **56**(5): p. 331-343.
11. Hafner, S., et al., *A detailed chemical kinetic model of high-temperature ethylene glycol gasification*. Combustion Theory and Modelling, 2011. **15**(4): p. 517-535.
12. de Vlieger, D.J.M., et al., *Hydrogen from ethylene glycol by supercritical water reforming using noble and base metal catalysts*. Applied Catalysis B-Environmental, 2012. **111**: p. 536-544.

13. Onwudili, J.A. and P.T. Williams, *Role of sodium hydroxide in the production of hydrogen gas from the hydrothermal gasification of biomass*. International Journal of Hydrogen Energy, 2009. **34**(14): p. 5645-5656.
14. Kwak, J.H., L. Kovarik, and J. Szanyi, *CO<sub>2</sub> Reduction on Supported Ru/Al<sub>2</sub>O<sub>3</sub> Catalysts: Cluster Size Dependence of Product Selectivity*. ACS Catalysis, 2013. **3**(11): p. 2449-2455.
15. Matsumura, Y., *Evaluation of supercritical water gasification and biomethanation for wet biomass utilization in Japan*. Energy Conversion and Management, 2002. **43**(9–12): p. 1301-1310.
16. Arkles, B., *Silane coupling agents: connecting across boundaries*. Morrisville: Gelest, 2004: p. 1-5.
17. Ganzeveld, K.J. and L.P.B.M. Janssen, *The grafting of maleic anhydride on high density polyethylene in an extruder*. Polymer Engineering & Science, 1992. **32**(7): p. 467-474.
18. Miskolczi, N., et al., *Production of Acrylonitrile Butadiene Styrene/High-Density Polyethylene Composites from Waste Sources by Using Coupling Agents*. Mechanics of composite materials, 2014. **50**(3): p. 377-386.
19. Żenkiewicz, M., et al., *Effects of electron-beam irradiation on surface oxidation of polymer composites*. Applied Surface Science, 2007. **253**(22): p. 8992-8999.
20. Peters, S.T., *Handbook of composites*. 2013: Springer Science & Business Media.
21. Westwood, M.E., et al., *Oxidation protection for carbon fibre composites*. Journal of Materials Science, 1996. **31**(6): p. 1389-1397.
22. Lamouroux, F., et al., *Oxidation-resistant carbon-fiber-reinforced ceramic-matrix composites*. Composites Science and Technology, 1999. **59**(7): p. 1073-1085.
23. Ensinger. *Technical Information on Properties of Plastics, Mechanical Properties, Elongation at Break*. Available from: <http://www.ensinger-online.com/en/technical-information/properties-of-plastics/mechanical-properties/elongation-at-break/>.
24. Lee, M. and J. Jeffers, *Identifying an Unknown Compound by Infrared Spectroscopy*. 1997: Chemical Education Resources, Incorporated.
25. Coates, J., *Interpretation of infrared spectra, a practical approach*. Encyclopedia of analytical chemistry, 2000.
26. Park, S.-J. and J.-S. Jin, *Effect of silane coupling agent on interphase and performance of glass fibers/unsaturated polyester composites*. Journal of Colloid and Interface Science, 2001. **242**(1): p. 174-179.

27. Yu, B., et al., *Enhanced interphase between epoxy matrix and carbon fiber with carbon nanotube-modified silane coating*. *Composites Science and Technology*, 2014. **99**: p. 131-140.

## **Chapter 5**

### **Chemical Recycling of Printed Circuit Board Waste via Depolymerisation in Sub- and Supercritical Solvents**

In chapter 5, the hydrothermal processing of polybenzoxazine resin was studied, and the results showed the applicability of this method on the thermosetting resins. In this chapter, the hydrothermal depolymerisation of the waste printed circuit boards obtained from desktop computer liquid crystal display (LCD) monitors was carried out by using different solvents. The printed circuit board sample in this study contains phenolic type brominated resin which has a similar structure to polybenzoxazine resin.

Water, ethanol and acetone were used between 300 - 400°C to investigate the effect of the solvent type. Alkalis (NaOH, KOH) and acetic acid were used as additives to promote the removal of the resin fraction of the printed circuit board as recycled chemical feedstock from the waste.

The liquid effluent was first extracted with a solvent and the organic phase was analysed via GC/MS/MS to detect the organic compounds produced after degradation of the resin. The aqueous phase was analysed via ion chromatography for any bromine content.



## 5.1 The Effect of Solvent on Resin Removal

Ethanol as a solvent was proven to be effective in depolymerisation of thermoplastics, as in the literature there are a number of studies especially with PET giving promising results. Also in recent studies, the possible usage in the depolymerisation of thermosetting plastics was investigated [1, 2].

Table 5.1.1 The effect of temperature on depolymerisation of printed circuit board in Ethanol

<i>Solvent</i>	<i>Temperature [°C]</i>	<i>Time [min]</i>	<i>Resin Removal [%]</i>
Ethanol	200	180	17.3
Ethanol	250	180	45.2
Ethanol	250	360	43.3
Ethanol	300	180	55.9
Ethanol	400	180	50.3

Ethanol was used in this study as well to depolymerize the waste printed circuit board (PCB) sample at a temperature range from 200 to 400°C; the results are given in Table 5.1.1. The resin removals were calculated according to the equation 5.1.1 as shown below;

$$R = \frac{F-X}{F_R} * 100 \quad \text{Equation 5.1.1}$$

R stands for resin removal [%]; F is the amount of the printed circuit board added to the reactor.  $F_R$  defines the amount of the resin in the raw printed circuit board waste, which was found to be 62 wt% according to the thermogravimetric and ash analyses as described in Section 3.1.2. X is the amount of the solid residue, after the hydrothermal depolymerisation.

Below the critical point (241°C, 6.14 MPa) of ethanol, the resin removal was very low after three hours reaction time. As the temperature was increased up to 300°C, the resin removal was improved; however, it was not more than 56 %. The further increase in the temperature to 400 °C did not affect the resin removal; however, the gas yield increased to give almost 10 times higher production than that found at 300°C (see Table 5.1.2), as the

ethanol itself decomposed to produce more H<sub>2</sub>, CO and CH<sub>4</sub> at 400°C, as shown in Figure 5.1.1.

Table 5.1.2 The gas yield after depolymerisation of printed circuit board in Ethanol

<i>Solvent</i>	<i>Temperature [°C]</i>	<i>Time [min]</i>	<i>Gas Produced [g/g waste]</i>
Ethanol	300	180	0.24
Ethanol	400	180	2.82

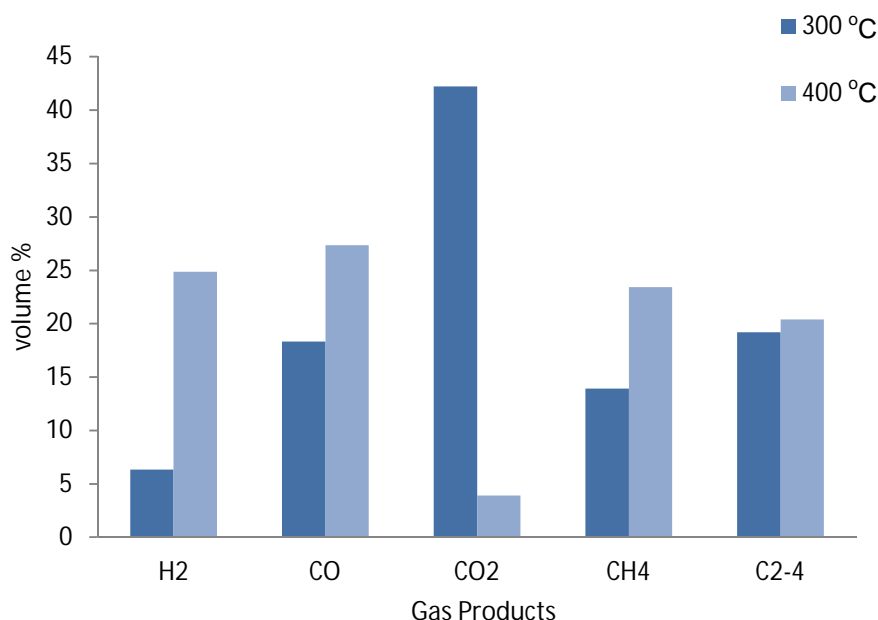


Figure 5.1.1 The gas composition after degradation of printed circuit board at 400°C in Ethanol

The effect of reaction time was also tested in the case of ethanol as the solvent; at 250°C there was no significant change in the resin removal when the reaction time was increased from 3 to 6 hours.

Table 5.1.3 The effect of acetone as solvent on depolymerisation of printed circuit board in the absence of any addition

<i>Solvent</i>	<i>Temperature [°C]</i>	<i>Time [min]</i>	<i>Resin Removal [%]</i>
Ethanol	300	180	55.9
Acetone	300	180	36.7

When acetone was introduced as the solvent, its resin depolymerisation ability compared to ethanol was much worse at the same reaction conditions. At 300°C, after 3 hours reaction time, the resin removal was low; most of the polymer did not react and only 36.7 % of it was removed (Table 5.1.3).

Table 5.1.4 The effect of water as solvent on depolymerisation of printed circuit board in the absence of any addition

<i>Solvent</i>	<i>Temperature [°C]</i>	<i>Time [min]</i>	<i>Resin Removal [%]</i>
Ethanol	360	0	59.1
Water	360	0	74.6

When water is used as a solvent, at zero residence time, almost 75% of the resin was removed, whereas ethanol was able to reach a resin removal of only 59% at 360°C as seen in Table 5.1.4.

Table 5.1.5 The effect of temperature on depolymerisation of printed circuit board in water in the absence of any addition

<i>Solvent</i>	<i>Temperature [°C]</i>	<i>Time [min]</i>	<i>Resin Removal [%]</i>
Water	360	0	74.6
Water	380	0	76.3
Water	400	0	81.0
Water	420	0	85.4

At its critical point, water experiences unique changes in its properties such as decrease in dielectric constant, density, ion product, and it becomes a good solvent for organic materials [3]. Xing et, al,. [4] suggested that the main polymer degradation mechanism in supercritical fluids is via free radicals reaction. At high temperatures, sufficient energy to break the bonds within the polymer to form free radicals was supplied by the reaction medium. Therefore, even in short residence times, high resin removals up to 85 % were achieved as the temperature increased as shown in Table 6.1.5. To increase the depolymerisation efficiency, some additives were tested to determine their effect on the resin removal. Alkalis (NaOH, KOH) and acetic acid were added to the reactor and depolymerisation took place at 400°C. While acetic acid had no significant effect, with the addition of alkalis, resin removal increased by 13% compared to water alone and reached 94% as shown in Table 5.1.6.

Table 5.1.6 The effect of additives on depolymerisation of printed circuit board in water

<i>Solvent</i>	<i>Additives</i>	<i>Temperature [°C]</i>	<i>Time [min]</i>	<i>Resin Removal [%]</i>
Water	-	400	0	81.0
Water	Acetic acid	400	0	81.9
Water	KOH	400	0	93.6
Water	NaOH	400	0	94.1

## 5.2 Product Distribution

Amongst all the solvents used in this study, only water was able to reach high resin removal efficiencies, especially in the presence of alkalis. Mainly, the resin was converted into liquid products, as around 85 wt% of the organics was detected in the liquid effluent when KOH was used as the additive. The GC-FID and GC-TCD analysis showed (Table 5.2.1) that the major composition of the gas products consists of H<sub>2</sub> and CO<sub>2</sub> as alkalis

promote the production of H<sub>2</sub> in supercritical water by promoting the water gas shift reaction (equation 5.2.1), while CO was high when water only was used as the solvent.



The gas composition and the total grams of gas produced per gram of waste are listed in Table 5.2.1.

Table 5.2.1 Gas Compositions during depolymerisation of printed circuit board in water, in the presence of (a) NaOH (b) KOH (c) no additives

Gas Component	Yields		
	(a)	(b)	(c)
H <sub>2</sub> [vol. %]	35.2	28.3	7.1
CO [vol. %]	3.3	1.1	13.9
CO <sub>2</sub> [vol. %]	58.4	68.4	77.1
CH <sub>4</sub> [vol. %]	2.2	1.7	1.4
C <sub>2-4</sub> [vol. %]	1.4	0.5	0.5
<b>Total produced gas [g/g waste]</b>	<b>0.31</b>	<b>0.34</b>	<b>0.28</b>

The presence of alkalis affected not only the gas composition but also the organic content of the liquid obtained was highly influenced by the introduction of KOH and NaOH into the reaction. As described in Chapter 3 (Section 3.5), the liquid effluent first underwent an extraction process with dichloromethane as solvent, to separate the organic phase from the aqueous phase. When alkalis were used as the additives, the major organic compounds detected in the GC/MS were phenol and phenolic compounds as shown in Figure 5.2.1. Phenol, amongst the other chemicals has the largest portion in the liquid effluent, at 62 wt%, which was six times higher compared to that when water alone was used. When NaOH was added with water, 80% of the resin was converted into liquid and this was additionally improved to a value of 86% in the presence of KOH.

At lower temperatures, the depolymerisation of the resin starts with free radical reaction following with chain initiation, growth and termination leading to the formation of intermediates (oligomers) [5]. With the increasing temperature, molecules with stronger bonds break down to give smaller molecules. With the addition of alkalis, the rate of hydrolysis reactions taking place increases as a result of hydroxide ions release.

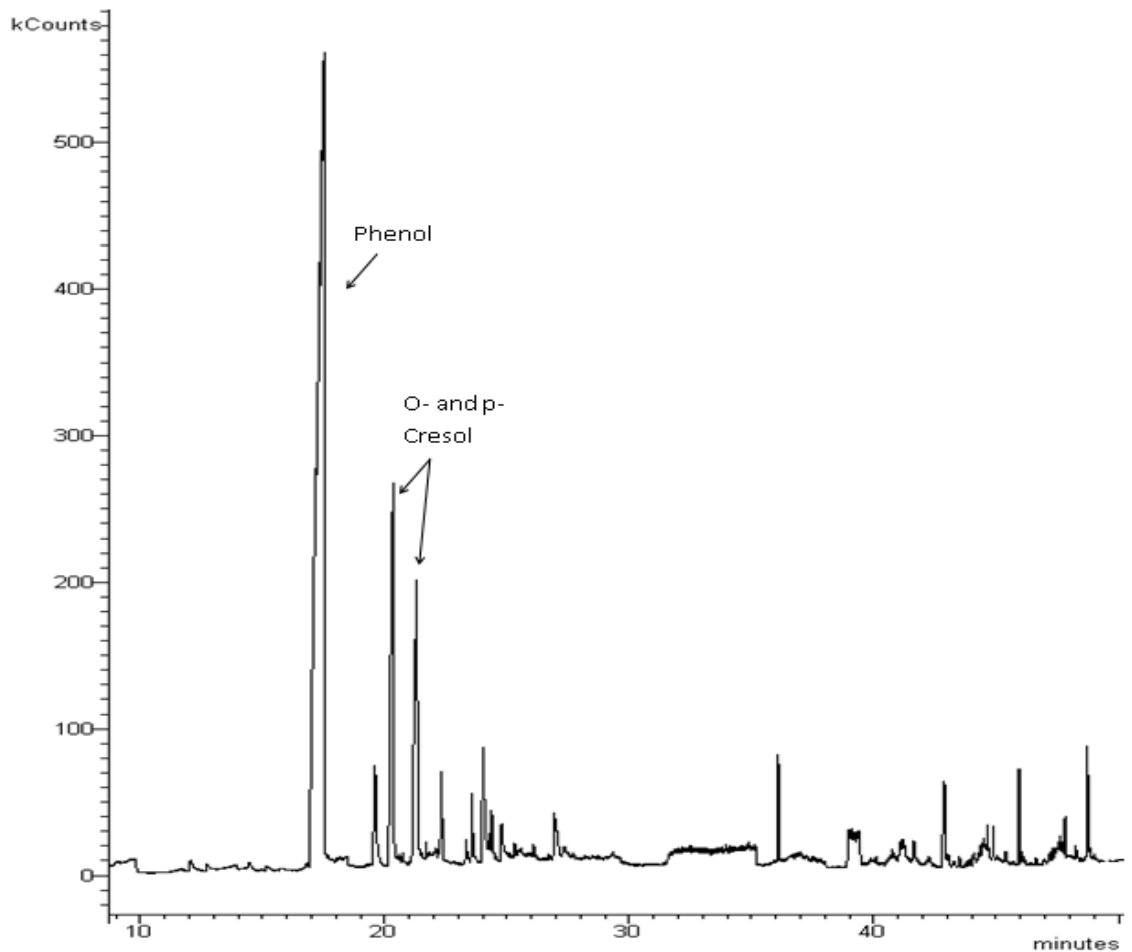


Figure 5.2.1 GC/MS result of the liquid from the experiment with water when NaOH was used as the additive, at 400°C

After depolymerisation in water at 400°C, with alkali addition, the liquid products mostly consisted of phenol, methyl-phenols (*o*-cresol, *p*-cresol, 2,4,6-trimethylphenol), and ethyl-phenols, as a result of the degradation of phenolic (epoxy) thermosetting resin. Tagaya et. al., [6] studied the thermal decomposition of moulding epoxy resin at 430°C. They reported that the resin degraded into phenol and phenolic compounds such as cresols, dimethylphenols. The addition of Na<sub>2</sub>CO<sub>3</sub> promoted the decomposition of the

resin. They concluded that supercritical water was a suitable medium for the waste plastics containing aromatic methylene, ether and carbonyl bridges, as they decomposed to their monomers such as phenol and alkyl phenol. The results of quantification analysis for the peaks detected during GC/MS analyses are listed in Table 5.2.2 in terms of mg organic produced per gram waste PCBs and the weight compositions.

Table 5.2.2 Organic composition of the liquid produced from depolymerisation at 400 °C with water (a) in the presence of NaOH (b) in the presence of KOH as catalyst (c) without any additives

<i>Sample</i>	<i>Yields [mg organic/g PCB]</i>			<i>Compositions [wt.%]</i>		
	(a)	(b)	(c)	(a)	(b)	(c)
Phenol	387.2	386.0	68.7	62.4	62.2	11.1
o-Cresol (2-methylphenol)	50.9	69.3	22.1	8.2	11.2	3.6
p-Cresol (4-methylphenol)	40.7	48.8	9.0	6.6	7.9	1.5
4-ethylphenol	6.9	14.0	5.9	1.1	2.3	1.0
2-ethylphenol	3.7	5.7	1.5	0.6	0.9	0.2
4-isopropylphenol	2.1	4.6	7.4	0.3	0.7	1.2
2,4,6-trimethylphenol	0.3	1.4	0.4	0.1	0.2	0.1
Dimethylanisole	0.9	-	0.5	0.1	-	0.1
2-methylbenzofuran	0.2	0.3	0.1	0.1	0.04	0.05
<b>Total</b>	<b>493.6</b>	<b>530.2</b>	<b>116.1</b>	<b>79.5</b>	<b>85.4</b>	<b>18.7</b>

Similar organic compounds were detected in the oil after pyrolysis of waste printed circuit boards. In the work of others [7], pyrolysis of printed circuit boards extracted from computers, televisions and mobile phones was investigated. The pyrolysis took place at 800°C in a fixed bed reactor. The major organic compounds detected in the oil were phenol, methyl and ethyl phenols, bisphenol A and methylethylphenol. Apart from the phenol and

phenolic compounds, brominated and phosphated compounds were detected in the oil as well, such as dibromophenol, triphenyl phosphate and cresyl phosphate. It was reported that the bisphenol A epoxy resin did not decomposed completely as bisphenol A and hydroxyldiphenyl were detected in the oil after the pyrolysis of all waste samples. Also the compositions of the oil were highly dependent on the type of the PCB from which it was extracted. For example, the phenol yields were 25.23, 10.06 and 38.49 wt% after pyrolysis of the printed circuit board obtained from computers, television and mobile phone, respectively [7, 8].

While no bromine was detected in the gas phase after the hydrothermal degradation of waste PCB sample; trace amounts in the form of bromophenol was detected in the organic phase, the amount was found to be no more than 0.03 ppm. However, when the aqueous phase was analysed, around 60 mg bromine per gram waste was detected, according to the ion chromatography results. This might be due to the high reaction temperature used, as it was reported that at temperatures around 300°C, high proportions of brominated compounds were found during the hydrothermal degradation of brominated epoxy resin. But with the increasing temperature, the brominated compounds further broke down and debromination occurred [5].

Also this shows that the bromine compounds were dissolved in the water after the hydrothermal treatment, which results in producing clean, almost bromine-free oil. These results confirm the work of others with brominated acrylonitrile–styrene–butadiene (Br-ABS) and brominated high impact polystyrene (Br-HIPS), stating that bromine content of brominated plastics ended up mostly in the aqueous phase due to dissolution in the water medium after degradation in supercritical water (450 °C, 31 MPa). The bromine species detected in the aqueous phase were HBr for Br-HIPS and NH<sub>4</sub>Br for Br-ABS. Also the addition of NaOH increased the debromination rate, 99 wt% of bromine atoms in the plastics collected in the aqueous phase as NaBr or NH<sub>4</sub>Br, depending on the reaction conditions [9]. The same affect could be observed in the presence of KOH, as potassium metal is reactive with the halogens to form potassium halides such as KF, KBr, KCl; however



no report was found in the literature about the mechanism in the supercritical water during the decomposition of printed circuit boards containing brominated flame retardants. Xing et. al., [4] studied the degradation of brominated epoxy resin from printed circuit board of waste desktop computers in sub and supercritical water. When the resin decomposed into oil at 400°C, 97.8 wt% of the bromine in the sample was dissolved aqueous phase after processing in the supercritical water, while at 250°C the only 31.25 wt% of bromine was collected in the aqueous phase. As a result, the oil contained 2-bromophenol.

Apart from bromine, trace amounts of chloride were detected in the water, possibly due to decomposition of chlorinated fire retardants or polyvinyl chloride (PVC) in the PCB.

The possible degradation pathway of the resin is shown in Figure 5.2.2, as suggested by Borojovich et. al., [10]. They also reported that the stability of the bromophenol was low during the thermal degradation, so the bromine in the resin tended to remain in the char or was released as HBr in the gas phase which means degradation of brominated epoxy resin starts with the decomposition of the brominated flame retardant [10, 11].

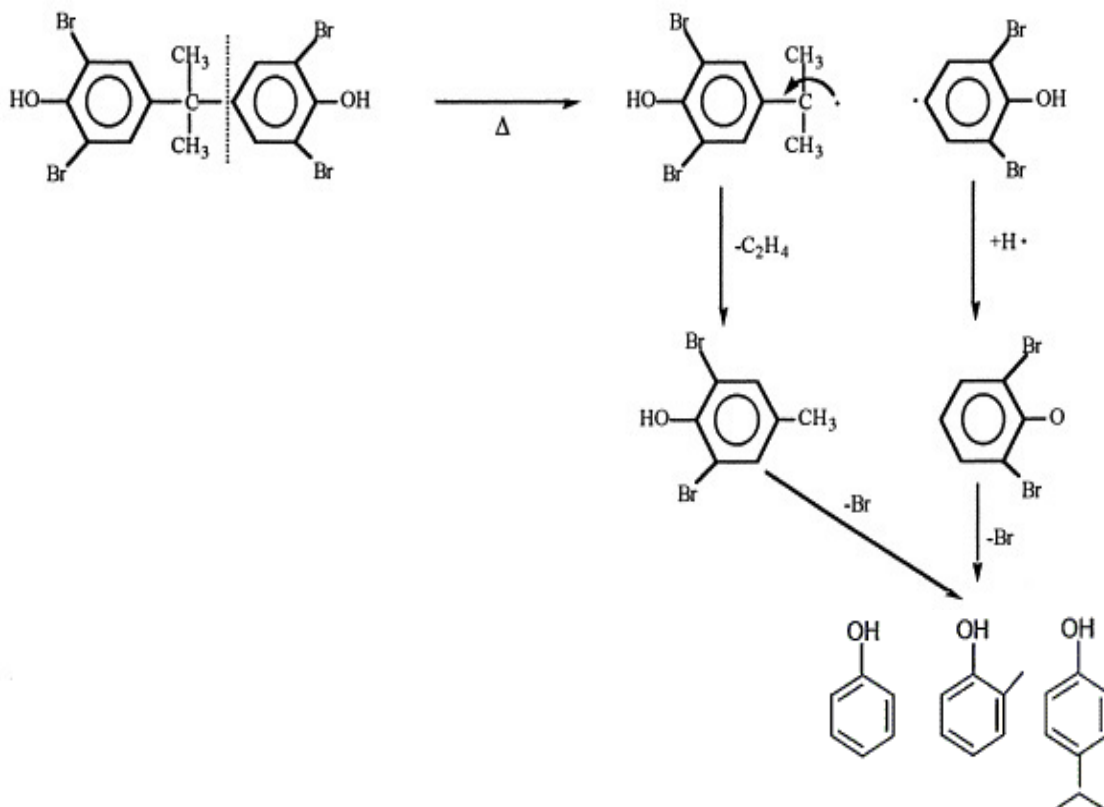


Figure 5.2.2 The degradation mechanism of the resin [10]

It was reported that in hydrothermal medium, hydrobromic acid formation is observed with the dissolution of HBr in water. Also it was stated that the 90% of bromine content was recovered in subcritical conditions [12]. Therefore, after hydrothermal depolymerisation of waste PCB, while the brominated resin was decomposed to give phenol and phenolic compounds, bromide ions were detected in the aqueous phase by ion chromatography. As a result, bromine free oil was formed which mostly consisted of phenol, o-Cresol, p-Cresol, ethylphenol and isopropylphenol.

The existence of isopropylphenol in the liquid effluent might also suggest that at first, resin was decomposed into bisphenol A. According to Hunter et. al., [13] isopropylphenol can be synthesized via hydrothermal cleavage of bisphenol A. So the resin might be decomposed to give first bisphenol A at low temperatures. With the increasing temperature, the resin further decomposed to give phenol, isopropylphenol, and other methyl and ethyl phenols when the supercritical conditions were reached.

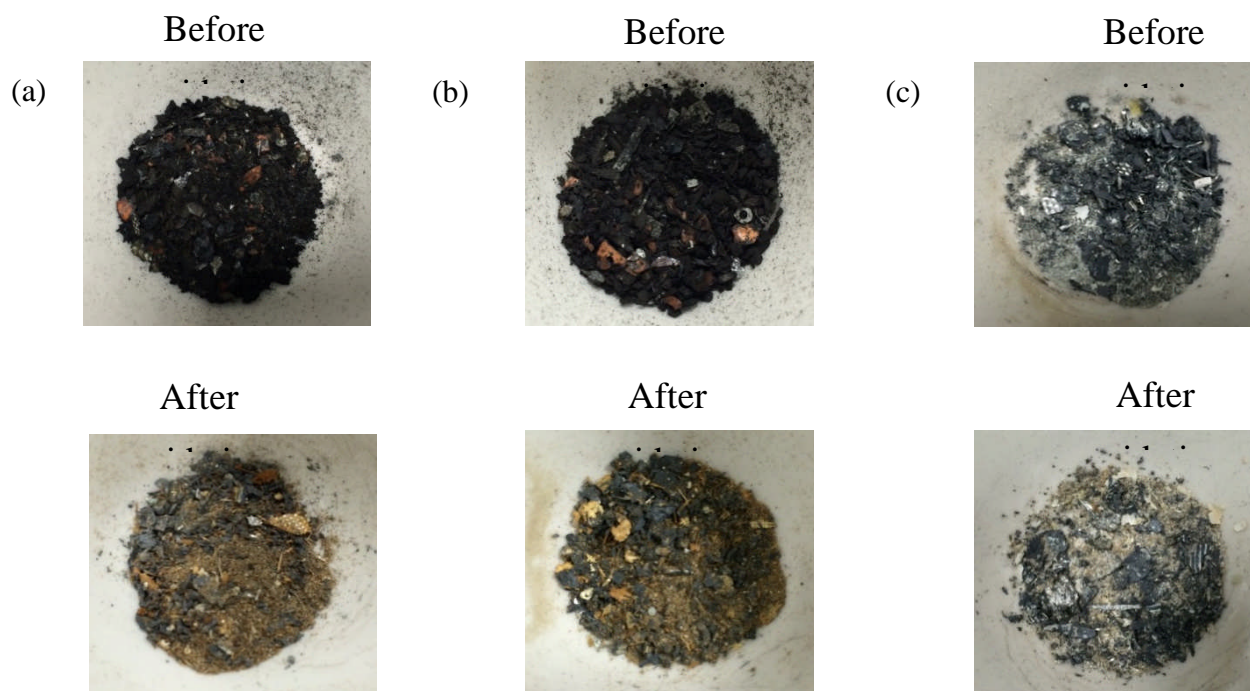


Figure 5.2.3 Solid residues after drying, before and after oxidation; samples from depolymerisation (a) via ethanol at 400 °C (b) via water at 400 °C (c) via water and NaOH at 400 °C

To determine the organic degradation products of the residues recovered after the hydrothermal treatment, oxidation was applied after drying and weighing the solid products. When the resin removal efficiency was low as in the case of depolymerisation with ethanol, there was a large difference in the amount of residue before and after the oxidation process, while there was no significant change in the presence of water with alkali, as shown in Figure 5.2.3. The clean residue can be further processed for recovery of valuable metals, such as copper, silver, gold, palladium, etc.

### 5.3 Summary

The hydrothermal depolymerisation of printed circuit board waste obtained from desktop computer liquid crystal display (LCD) monitors was investigated, to remove the resin fraction from the waste in order to recover metals, and also to recycle the resin as a chemical feedstock. At a reaction temperature of 400 °C, 81 % of resin removal was achieved when water alone was used as the reaction medium, and this was further improved in the presence of NaOH and KOH, which led to 94 % resin removal. However,

acetone and ethanol were not able to depolymerize the waste completely; only up to 56 % resin removal was achieved at 300 °C after 3 h reaction in ethanol. Further increase in the temperature caused ethanol to decompose to produce H<sub>2</sub> and CH<sub>4</sub> rich gas, while it had no effect on the resin removal. The liquid produced after hydrothermal processing was mainly composed of phenol, and phenolic compounds, which are the precursors of the original thermosetting resin. Most of the bromine content was found in aqueous phase, which results in oil recovery with near-zero bromine content. Addition of alkalis increased the phenol yield up to 62.5 wt%, and the residues were recovered in a clean state, ready for metal separation.

## References

1. de Castro, R.E.N., et al., *Depolymerization of poly(ethylene terephthalate) wastes using ethanol and ethanol/water in supercritical conditions*. Journal of Applied Polymer Science, 2006. **101**(3): p. 2009-2016.
2. Motonobu, G., *Chemical recycling of plastics using sub- and supercritical fluids*. The Journal of Supercritical Fluids, 2009. **47**(3): p. 500-507.
3. Kruse, A. and E. Dinjus, *Hot compressed water as reaction medium and reactant: Properties and synthesis reactions*. The Journal of Supercritical Fluids, 2007. **39**(3): p. 362-380.
4. Xing, M. and F.-S. Zhang, *Degradation of brominated epoxy resin and metal recovery from waste printed circuit boards through batch sub/supercritical water treatments*. Chemical Engineering Journal, 2013. **219**(0): p. 131-136.
5. Yin, J., et al., *Hydrothermal decomposition of brominated epoxy resin in waste printed circuit boards*. Journal of Analytical and Applied Pyrolysis, 2011. **92**(1): p. 131-136.
6. Tagaya, H., et al., *Decomposition reactions of epoxy resin and polyetheretherketone resin in sub-and supercritical water*. Journal of Material Cycles and Waste Management, 2004. **6**(1): p. 1-5.
7. Hall, W.J. and P.T. Williams, *Separation and recovery of materials from scrap printed circuit boards*. Resources, Conservation and Recycling, 2007. **51**(3): p. 691-709.
8. Williams, P., *Valorization of Printed Circuit Boards from Waste Electrical and Electronic Equipment by Pyrolysis*. Waste and Biomass Valorization, 2010. **1**(1): p. 107-120.
9. Onwudili, J.A. and P.T. Williams, *Role of sodium hydroxide in the production of hydrogen gas from the hydrothermal gasification of biomass*. International Journal of Hydrogen Energy, 2009. **34**(14): p. 5645-5656.
10. Borojovich, E.J.C. and Z. Aizenshtat, *Thermal behavior of brominated and polybrominated compounds I: closed vessel conditions*. Journal of Analytical and Applied Pyrolysis, 2002. **63**(1): p. 105-128.
11. Luijk, R., et al., *Thermal degradation characteristics of high impact polystyrene/decabromodiphenylether/antimony oxide studied by derivative thermogravimetry and temperature resolved pyrolysis—mass spectrometry: formation of polybrominated dibenzofurans, antimony (oxy)bromides and brominated styrene oligomers*. Journal of Analytical and Applied Pyrolysis, 1991. **20**: p. 303-319.

12. Brebu, M., et al., *Alkaline hydrothermal treatment of brominated high impact polystyrene (HIPS-Br) for bromine and bromine-free plastic recovery*. Chemosphere, 2006. **64**(6): p. 1021-1025.
13. Hunter, S.E. and P.E. Savage, *Kinetics and mechanism of p-isopropenylphenol synthesis via hydrothermal cleavage of bisphenol A*. The Journal of organic chemistry, 2004. **69**(14): p. 4724-4731.

## **CHAPTER 6**

### **HYDROTHERMAL PROCESSING OF REFUSE DERIVED FUELS**

This chapter contains research carried out on refuse derived fuels (RDF). RDF represents a processed form of municipal solid waste (MSW) which is a highly heterogeneous mix of components. RDF comprises mostly the combustible fractions of MSW including paper, cardboards, textiles, wood and plastics. Arising from MSW, RDF also contains appreciable amounts of ash.

RDF is a very complex mixture of municipal solid wastes which can contain paper, plastic, garden trimmings, leather, rubber, textiles etc. wastes and the composition is highly dependent on the geographical area that the waste was collected. Literature studies can give a general idea about the compositions. Chang et. al., [1] compared the properties of MSW and RDF samples prepared for waste incineration in Tainan County, Chania and the results are shown in Table 6.1 Thermal processing though incineration can yield toxic organic and inorganic materials which can cause serious problems to the environment. Gasification of MSW can be difficult due to the heterogeneous nature of the waste and also the MSW can have very high moisture content. Hydrothermal gasification of RDF could be a better solution to produce a clean fuel gas.

It is interesting to investigate whether the hydrothermal process can be applied to a very heterogeneous waste material for the recovery of syngas and/or chemicals. In addition, municipal solid wastes can have very high moisture contents of over 50 wt%, due to the high moisture content of the waste and also if the waste is collected in a wet climate. The high moisture content then opens the potential for hydrothermal processing as conventional gasification would require the waste feedstock to be dried, adding considerable costs to the process. The hydrothermal process was applied to the RDF sample to produce fuel gas with high heating value. For

this purpose,  $\text{RuO}_2/\gamma\text{-Al}_2\text{O}_3$  and NaOH were tested as catalysts, and their effect on gasification yields was investigated.

Table 6.1 The average of the sample property of MSW and RDF adapted from [1]

	MSW	RDF	
		25-100 mm	> 100 mm
Bulk density (kg/m <sup>3</sup> )	289.9	334.8	179.1
Paper (%)	28.62	8.08	5.70
Plastics (%)	26.33	29.15	57.81
Garden trimmings (%)	4.05	4.60	4.21
Textiles (%)	9.03	7.43	18.23
Food waste (%)	14.04	0.00	0.00
Leather/rubber (%)	0.58	1.13	1.48
Metal (%)	6.99	1.09	0.03
Glass (%)	7.26	0.00	0.00
Ceramics and china	0.47	0.00	0.00
<5 mm (%)	1.59	16.15	8.89
>5 mm (%)	1.04	32.36	3.65

The hydrothermal gasification experiments were conducted at 500°C. The effect of residence time (0, 30 and 60 min) and different ruthenium loadings (5, 10, 20 wt %  $\text{RuO}_2/\gamma\text{-Al}_2\text{O}_3$ ) were investigated. Also low temperature hydrothermal treatment of RDF was carried out in water and a water/methanol mixture at a temperature range of 300 to 400°C.

The liquid effluent produced from low temperature hydrothermal treatment was analysed with the help of GC/MS to determine if any valuable chemicals could be extracted. The TGA analysis of RDF were carried out to



characterize the thermal degradation behaviour, and also to determine the ash content of the RDF.

## 6.1 Low Temperature Hydrothermal Processing of RDF

At temperatures of 300 and 400°C, RDF underwent hydrothermal processing and the effect of additives (methanol, sodium hydroxide) was investigated. The reaction time was zero minutes in all experiments, and in the experiments with methanol, the water:methanol ratio was 3:1. The product distribution was calculated as wt.% and the results are shown in Table 6.1.1.

Table 6.1.1 Product distribution after low temperature hydrothermal processing of RDF

Additive	Temperature [°C]	Gas [wt%]	Liquid* [wt%]	Residue [wt%]
-	300	29.9	37.4	32.7
-	400	41.3	31.8	26.9
Methanol	300	19.1	49.0	31.9
Methanol	400	30.9	41.3	27.8
NaOH	300	28.3	49.3	22.3
NaOH	400	34.1	45.5	20.5

\* Calculated by difference

Around 75 wt% of the RDF was either converted to gas or liquid in all cases. At 400 °C, when no additives were presented, 41.3 wt% of RDF decomposed to yield gas which represented the highest conversion to gaseous products. The addition of methanol and sodium hydroxide increased the yields of liquid. The main gas product was carbon dioxide in

both the experiments carried out at temperatures of 300°C and 400°C in the absence of any additives. Methanol addition increased the hydrogen and carbon monoxide yields, while the addition of sodium hydroxide only increased hydrogen yield at the reaction temperature of 400°C. The results of gas product compositions after the hydrothermal processing of RDF are shown in Figure 6.1.1.

TOC analyses were performed to determine the amount of the organic carbon in the liquid effluent. In the absence of any catalysts, 18.4 wt% of the carbon in the raw RDF was detected in the liquid phase at 300°C and this amount increased to 26.8 wt% when the temperature was increased to 400°C. The addition of sodium hydroxide increased the organic carbon amounts in the liquid phase, especially at 300°C, it was 55.4 wt%. However, when the temperature was increased to 400°C, 29.8 wt% of the organic carbon in the raw RDF was detected in the liquid effluent. This might be due to carbon fixation by sodium hydroxide at corresponding temperature, while the amount of the gas products was increased, the composition of carbon dioxide was decreased when the temperature was increased from 300°C to 400°C. The high amount of the inorganic carbon detected in the liquid effluent can be a proof, as no inorganic carbon was detected in the absence of sodium hydroxide, while 39.6 mg and 75.4 mg inorganic carbon per gram RDF was detected in the presence of sodium hydroxide at 300°C and 400°C, respectively.

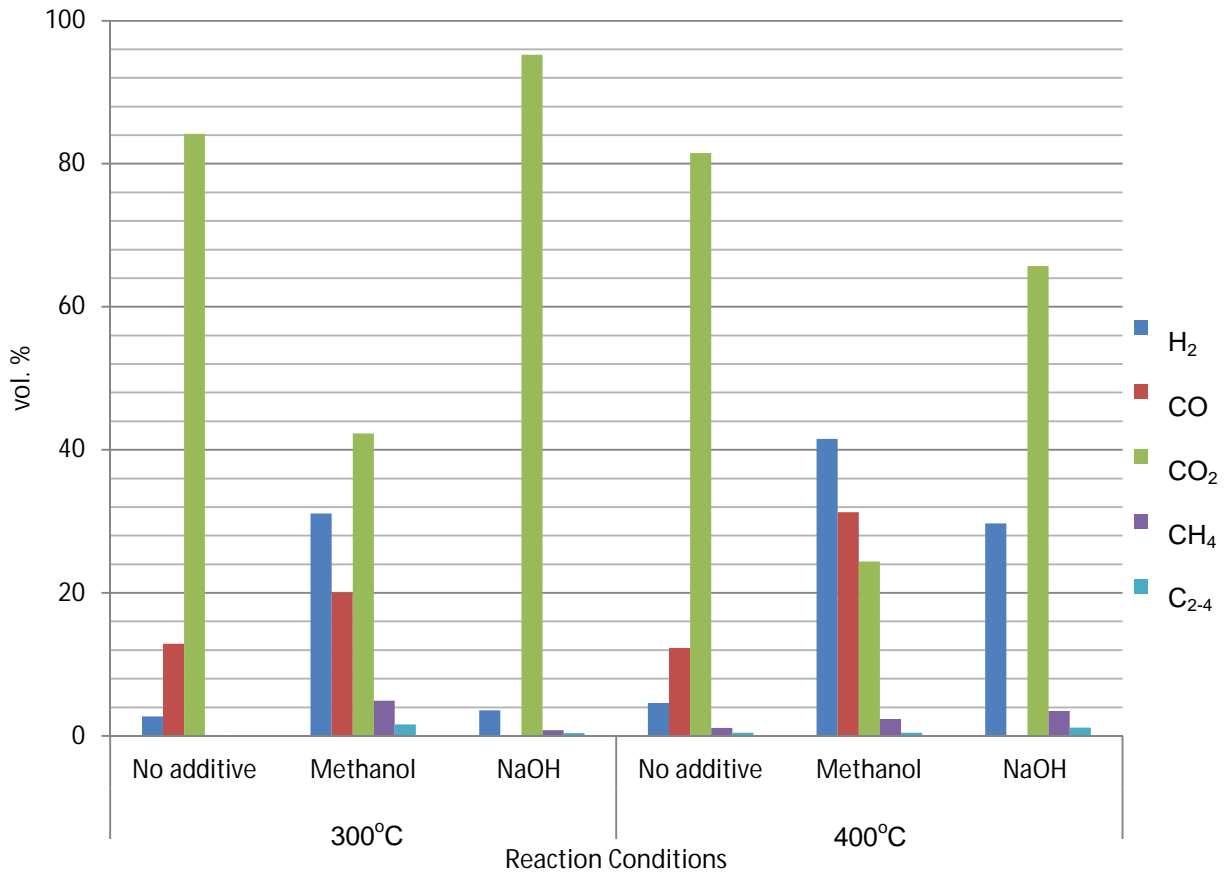


Figure 6.1.1 Gas composition after low temperature hydrothermal processing of RDF

The liquid effluent was also analysed with GC/MS. For the analysis, the liquid effluent was extracted with DCM with the method described in Chapter 3 in Section 3.5. When water alone was used, organic compounds with higher molecular weight were detected in the liquid effluent. At 300°C, small peaks on the GC/MS ion chromatogram were produced from the analysis of the liquid effluent, when temperature was increased to 400°C; cycloalkanes with ethyl- and methyl- groups were the main components together with ethyl- and methyl phenols. However, it was difficult to comment in detail in relation to the organic compounds degrading from RDF decomposition, as RDF represents a complex mixture of organic components and compounds.

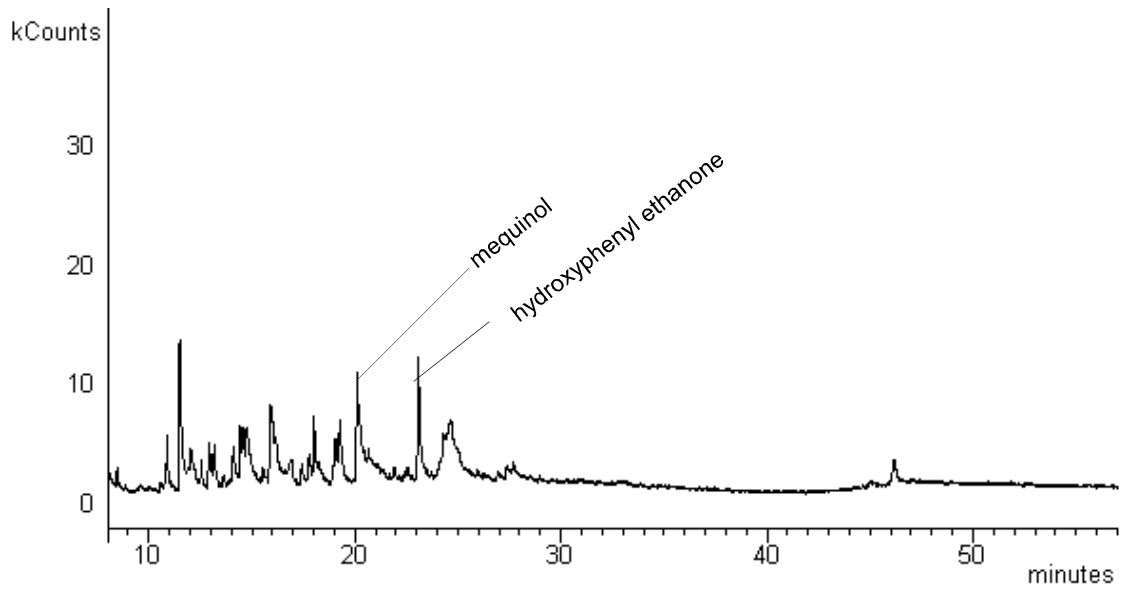


Figure 6.1.2 GC/MS outline of liquid residuals showing important compounds at 400°C when water alone was used

Addition of methanol and sodium hydroxide increased the organic content in the liquid, so that more complex materials such as furans, carboxylic compounds were detected, as shown in Figure 6.1.3.

Low temperature hydrothermal processing of RDF resulted in a liquid mixture containing a wide range of chemicals, due to the complex nature of RDF itself.

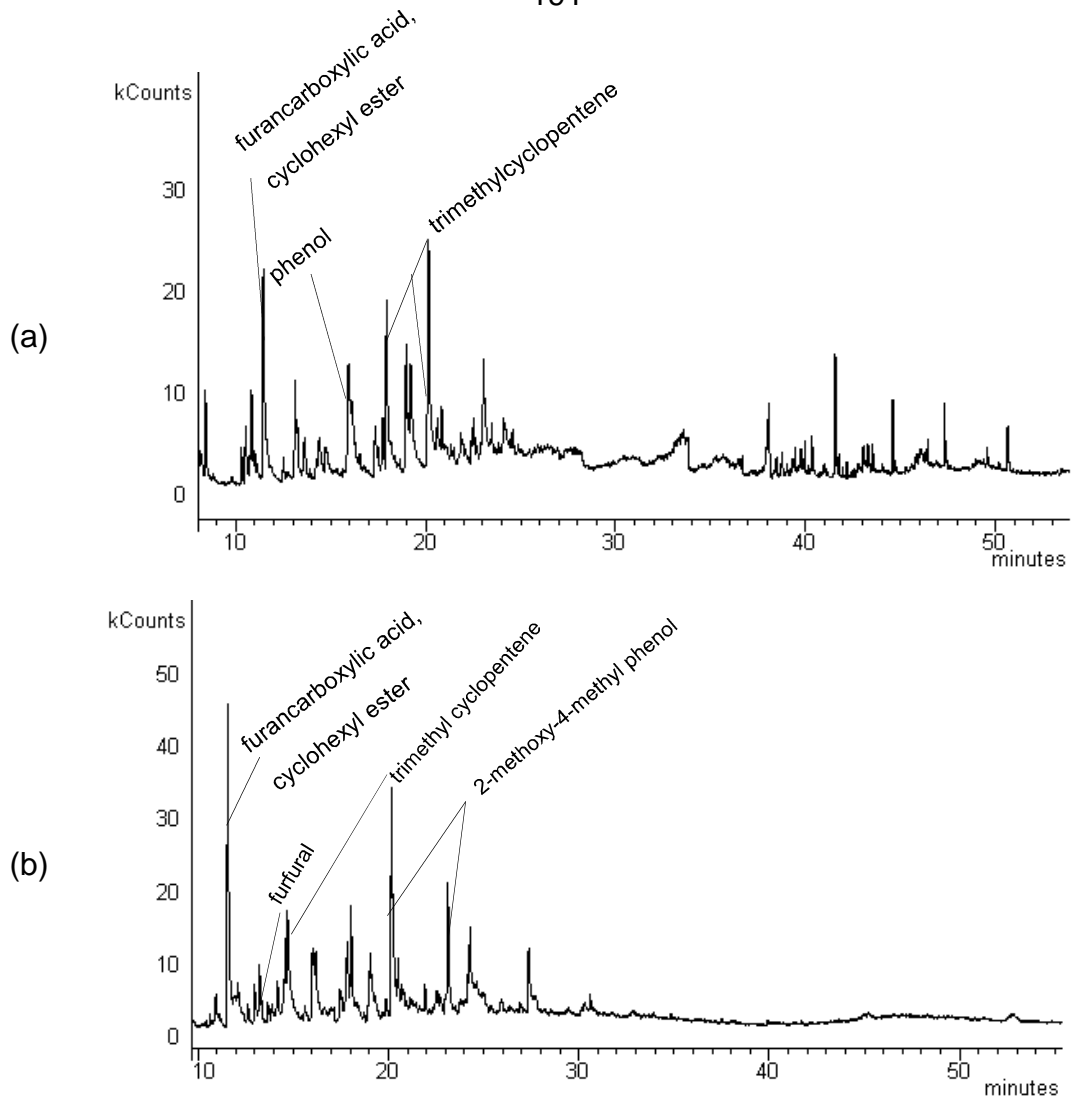


Figure 6.1.3 GC/MS chromatograms of liquid residuals obtained at 400°C showing important compounds (a) sodium hydroxide (b) methanol were used

## 6.2 Hydrothermal Gasification of RDF

The hydrothermal gasification of RDF was carried out at 500°C, and the effect of time, catalyst and different catalyst loadings were studied. For this purpose, NaOH and 5, 10, 20 wt% RuO<sub>2</sub>/γ-Al<sub>2</sub>O<sub>3</sub> catalysts were investigated at reactor residence time variations of 0, 30 and 60 minutes. The conversion to gas products was evaluated as “Carbon Gasification Efficiency (CGE)” which was defined with the formula shown in Equation 6.2.1.

$$CGE, \% = \frac{\text{Amount of carbon in gas phase [g]}}{\text{Amount of carbon in RDF [g]}} \times 100 \quad \text{Equation 6.2.1}$$

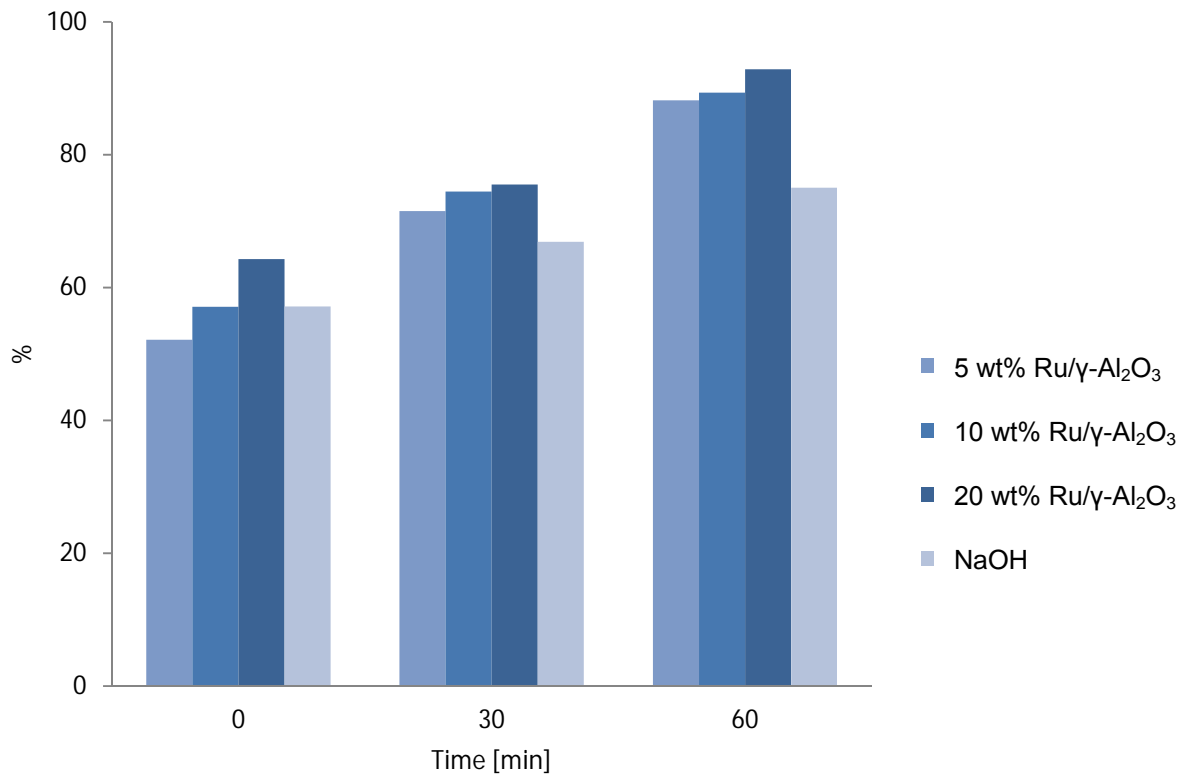


Figure 6.2.1 Carbon gasification efficiencies in relation to reaction time and catalysts

Almost 93% of the carbon present in the RDF was converted to gas after 60 min reaction together with 20 wt% RuO<sub>2</sub>/γ-Al<sub>2</sub>O<sub>3</sub> as catalyst as shown in Figure 6.2.1. The gasification rate was highly affected by the reaction time and the catalyst loading. The lowest carbon conversion with ruthenium catalyst was observed at 5 wt% RuO<sub>2</sub>/γ-Al<sub>2</sub>O<sub>3</sub> and zero minute reaction time, as 52% of the carbon in RDF was detected in the gas phase. In the presence of sodium hydroxide, 75 % of the carbon in RDF was converted to the gas phase at 60 minutes reaction time.

The carbon conversion to the gas phase was around 40% in the absence of any catalyst. The hydrothermal gasification of RDF in the presence of RuO<sub>2</sub>/γ-Al<sub>2</sub>O<sub>3</sub> catalyst led to conversion of the organic compounds in the waste into a fuel gas. The addition of NaOH gave lower carbon gasification efficiency. This might be due to the CO<sub>2</sub> fixation ability of NaOH, resulting in sodium salt production, which yielded less carbon dioxide

in the gas phase. The gas composition after the hydrothermal gasification was also affected by the catalyst type, catalyst loading and the reaction time. The effects of catalyst loading and reaction time on gas composition were investigated and the results are given in mol of gas produced per kg RDF.

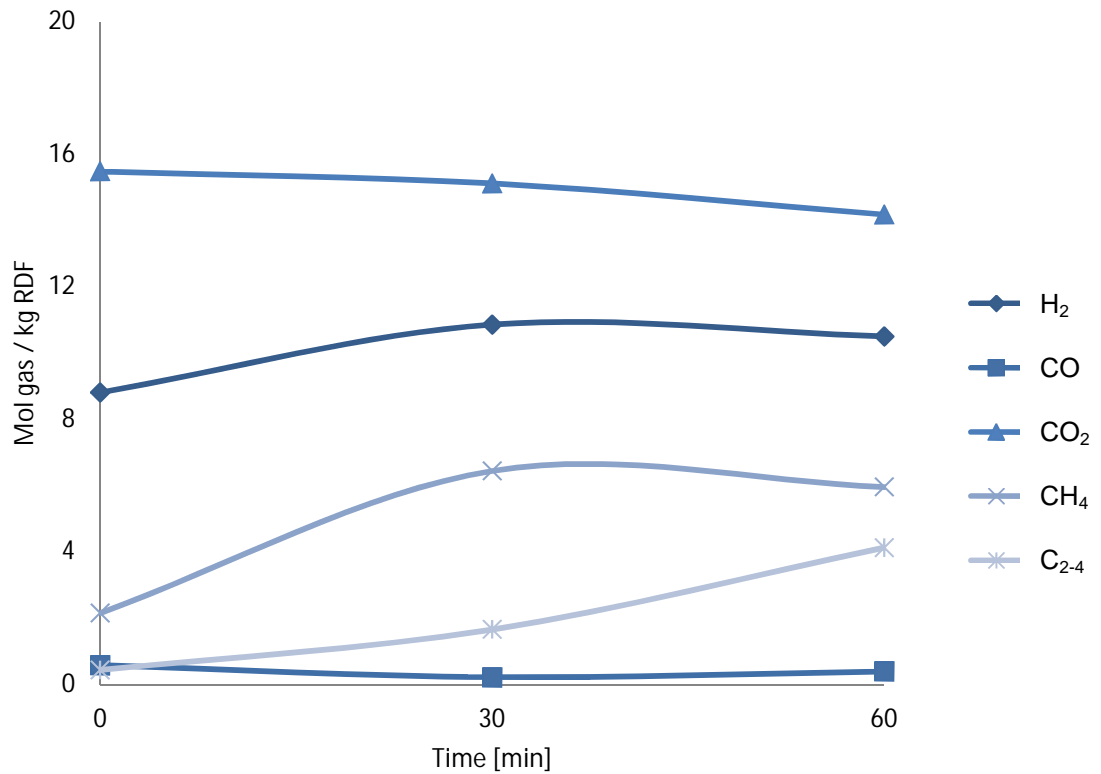


Figure 6.2.2 Gas composition after hydrothermal gasification of RDF with 5 wt% RuO<sub>2</sub>/γ-Al<sub>2</sub>O<sub>3</sub> at 500°C

When 5 wt% RuO<sub>2</sub>/γ-Al<sub>2</sub>O<sub>3</sub> catalyst was used, the main gases produced were CO<sub>2</sub>, H<sub>2</sub>, and CH<sub>4</sub> as shown in Figure 6.2.2. In the absence of any catalyst, the gas composition after the hydrothermal gasification of RDF resulted in lower amounts of gases for example, 3.3 mol H<sub>2</sub>, 1.5 mol CH<sub>4</sub>, 0.5 mol CO, 8.1 mol CO<sub>2</sub> and 1.7 mol hydrocarbon gases (C<sub>2-4</sub>) per kg of RDF. The compositions of all the gas components increased when the reaction time was increased from 0 to 30 minutes except for CO. However, a small reduction was observed when the reaction time was 60 minutes. Almost 11 mol H<sub>2</sub> and 6.5 mol CH<sub>4</sub> per kg RDF was produced at 30 minutes and these amounts stayed fairly stable when the reaction time was increased to 60 minutes.

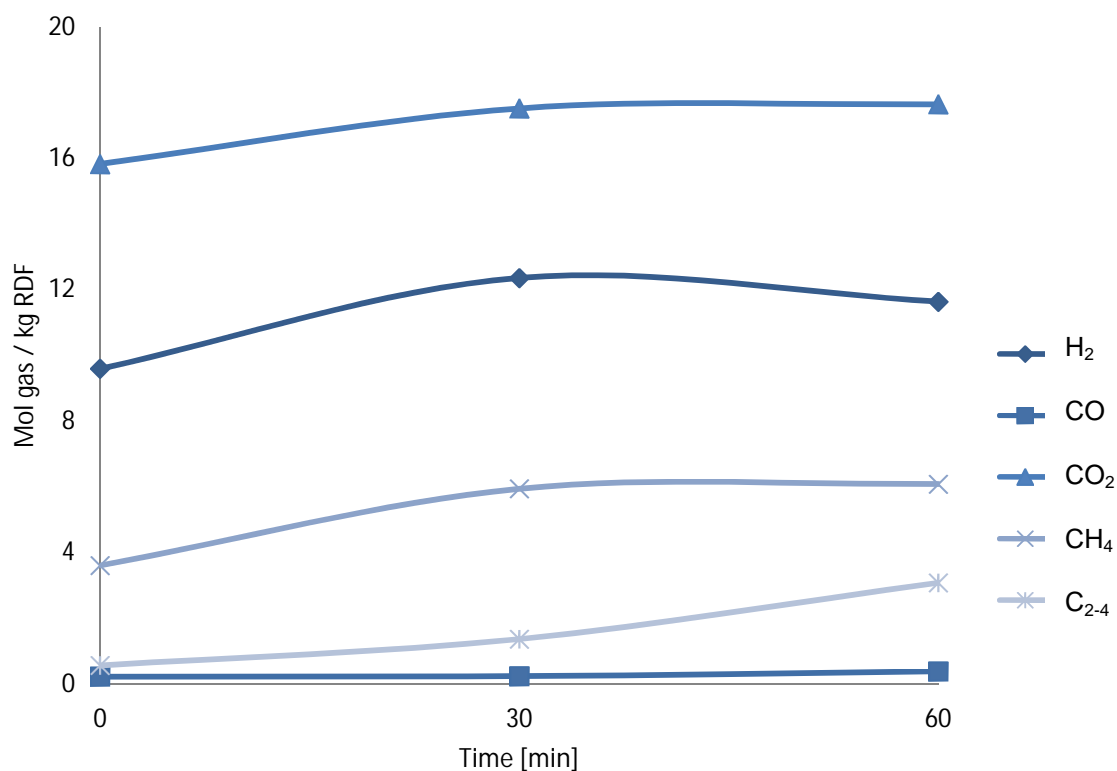


Figure 6.2.3 Gas composition after hydrothermal gasification of RDF with 10 wt% RuO<sub>2</sub>/γ-Al<sub>2</sub>O<sub>3</sub> at 500°C

The increase in the loading of ruthenium oxide in the catalyst yielded an increase in the gas compositions, especially in carbon dioxide. Except for hydrogen and CO, all the gas compositions were increased with the increasing reaction time. Figures 6.2.3 and 6.2.4 show the gas compositions after hydrothermal gasification of RDF with 10 wt% RuO<sub>2</sub>/γ-Al<sub>2</sub>O<sub>3</sub> and 20 wt% RuO<sub>2</sub>/γ-Al<sub>2</sub>O<sub>3</sub>, respectively.



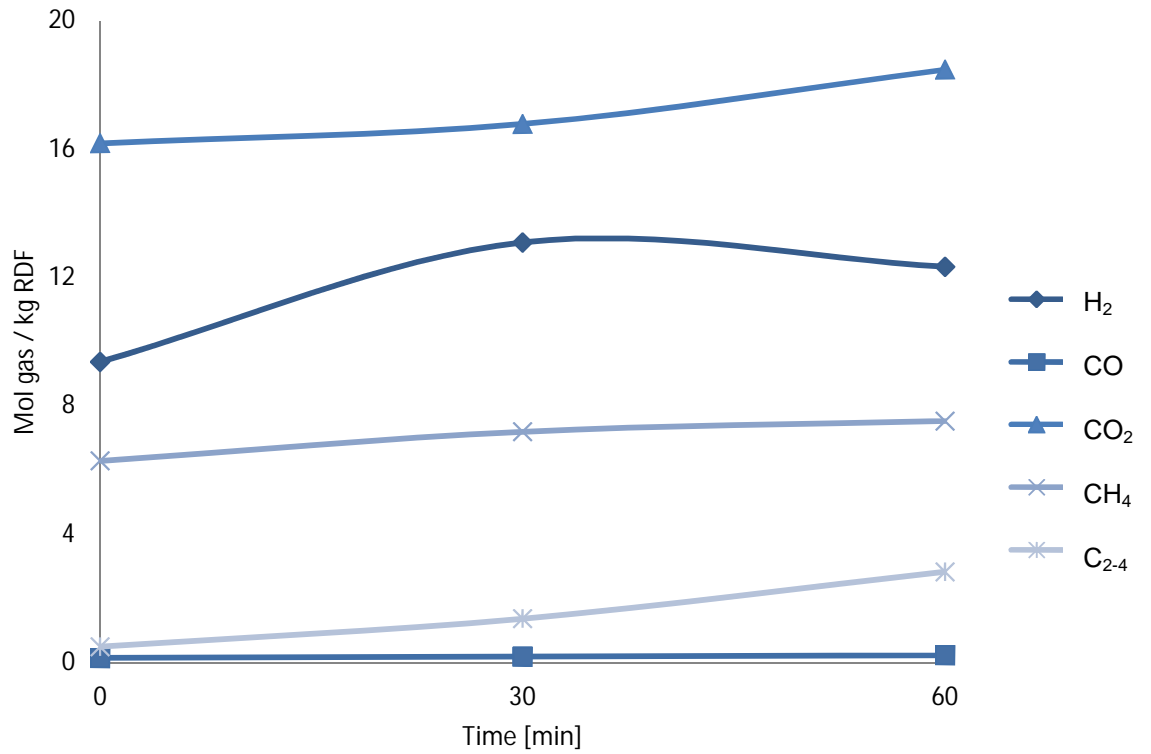


Figure 6.2.4 Gas composition after hydrothermal gasification of RDF with 20 wt% RuO<sub>2</sub>/γ-Al<sub>2</sub>O<sub>3</sub> at 500°C

The highest hydrogen yields were observed at 30 minutes reaction time with 10 wt% and 20 wt% ruthenium oxide loadings at 12.4 mol and 13.1 mol H<sub>2</sub> per kg RDF, respectively. When the reaction time was increased to 60 minutes, the hydrogen yield decreased while methane and carbon dioxide yields were increased. For better comparison of the catalyst loadings, the gas compositions at 60 minutes reaction time after hydrothermal gasification of RDF are shown in Figure 6.2.5. Since gases with highest heating values were obtained after 60 minutes reaction time, the comparisons between the catalyst loadings were made at this reaction time.

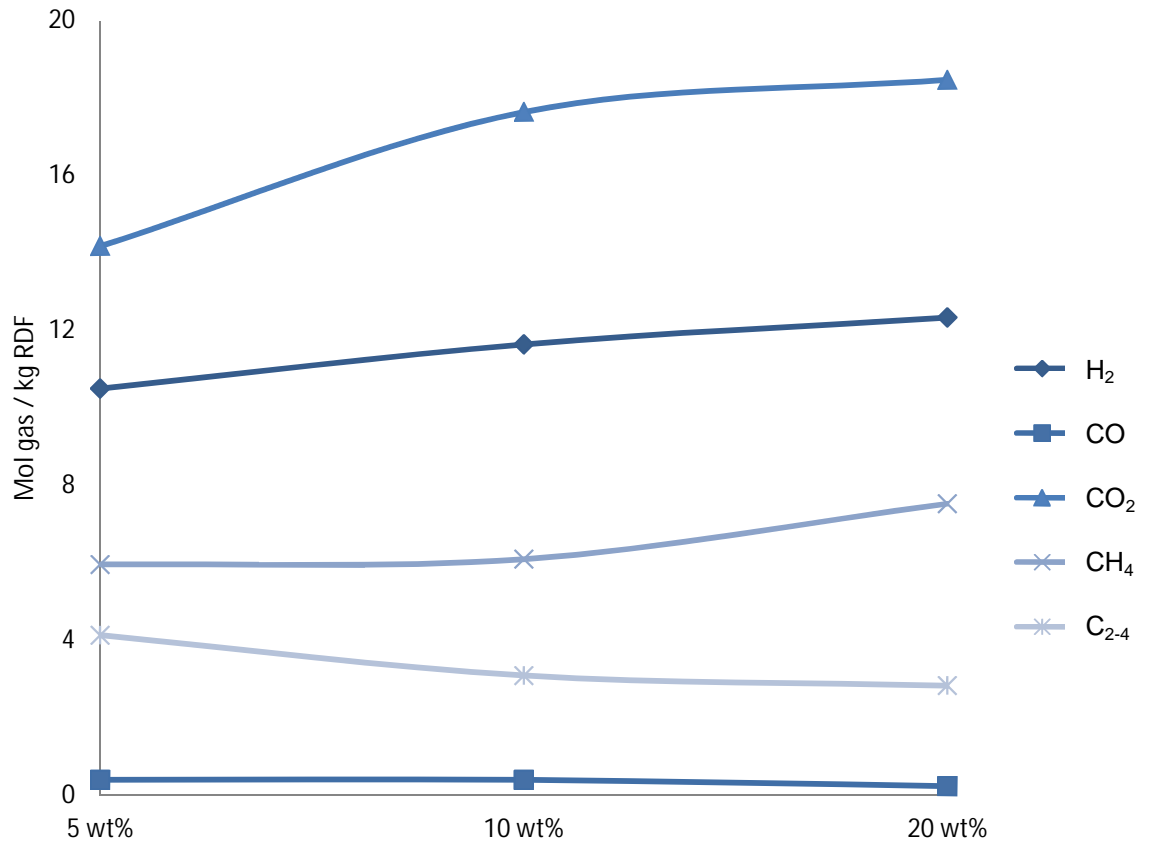


Figure 6.2.5 Gas composition after hydrothermal gasification of RDF at 500°C and 60 minutes reaction time with various RuO<sub>2</sub> loadings

The higher catalyst loading yielded more carbon dioxide, hydrogen and methane formation. The composition of hydrocarbon gases (C<sub>2</sub>-C<sub>4</sub>) and carbon monoxide decreased with the increasing RuO<sub>2</sub> wt% in the catalysts. The carbon gasification efficiencies were also increased with the increasing catalyst loading, as 88.2%, 89.3% and 92.8% of the carbon initially fed was detected in the gas phase after the hydrothermal gasification with 5 wt%, 10 wt% and 20 wt% RuO<sub>2</sub>/γ-Al<sub>2</sub>O<sub>3</sub> catalysts, respectively.

Similar gas compositions were obtained with gasification of biomass and plastic wastes with ruthenium as catalyst [2, 3]. For instance, low concentrations of biomass samples (glucose, cellulose and heterocyclic compounds), paper sludge and sewage sludge were gasified by Yamamura in supercritical water at 500°C in the presence of ruthenium as catalyst and produced hydrogen, methane and carbon dioxide as major products in the gas phase. Also it was reported that complete gasification of cellulose and

glucose was observed, together with high yields of N- and S-heterocyclic compounds [2].

In the hydrothermal medium, bonds between the carbon atoms would break and formation of short-chain products and intermediates occurs. From these intermediates and short-chain organic compounds, gasification reactions become favourable [4]. Therefore, it could be suggested that the ruthenium catalyst was able to increase the carbon-carbon bond cleavage and gasification efficiency. According to Sato et. al., [5] mainly methane, carbon dioxide and hydrogen were obtained in the gas phase after the hydrothermal gasification of alkylphenols at 400°C. They stated that the Ru/ $\gamma$ -alumina as catalyst gave the best results, compared to the other catalysts investigated Ru/carbon, Rh/carbon, Pt/ $\gamma$ -alumina, Pd/carbon and Pd/ $\gamma$ -alumina.

The gas compositions in terms of volume percent were also calculated and the results of hydrothermal gasification of the RDF with 5, 10 and 20 wt% RuO<sub>2</sub>/ $\gamma$ -Al<sub>2</sub>O<sub>3</sub> are shown in Figures 6.2.6, 6.2.7 and 6.2.8, respectively.

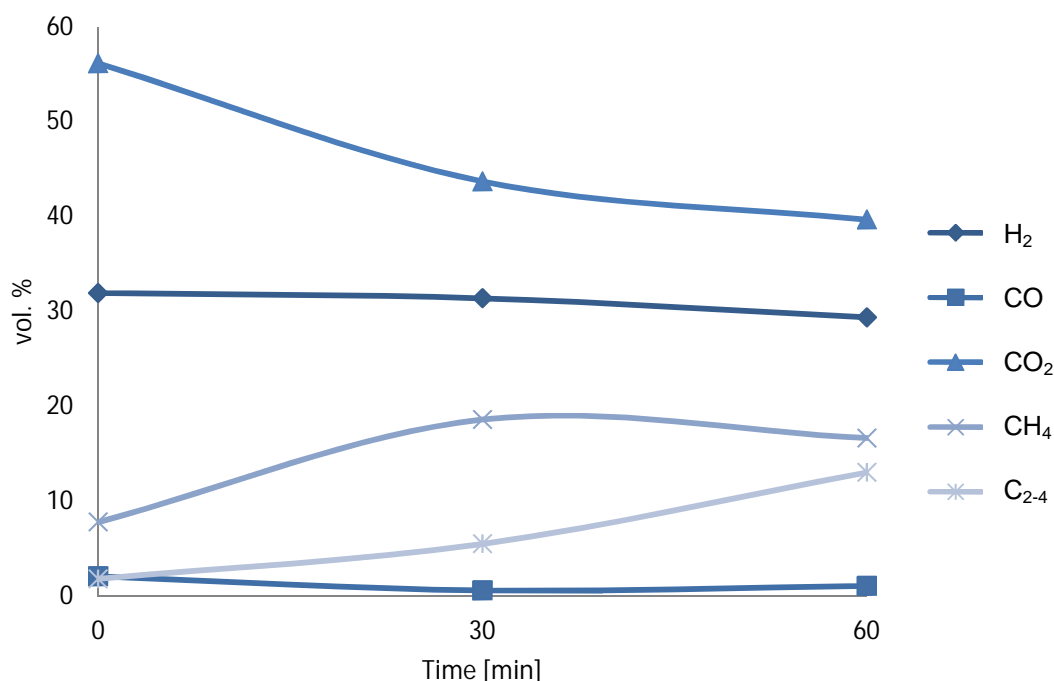


Figure 6.2.6 Gas compositions in vol. % after hydrothermal treatment of RDF at 500°C with 5 wt% RuO<sub>2</sub>/ $\gamma$ -Al<sub>2</sub>O<sub>3</sub>

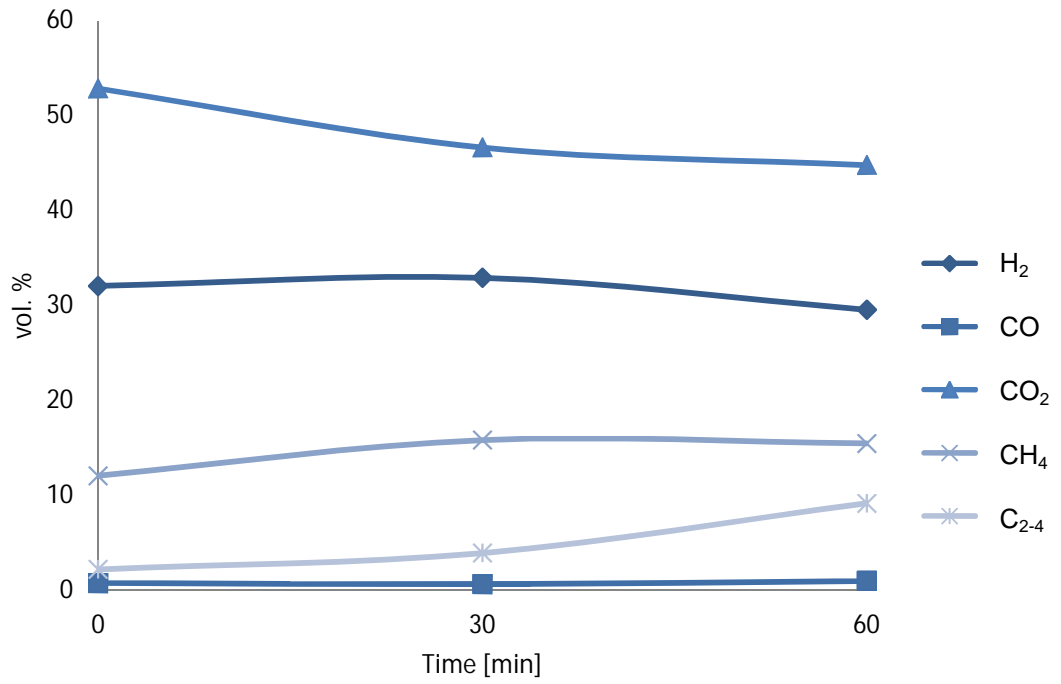


Figure 6.2.7 Gas compositions in vol. % after hydrothermal treatment of RDF at 500°C with 10 wt% RuO<sub>2</sub>/γ-Al<sub>2</sub>O<sub>3</sub>

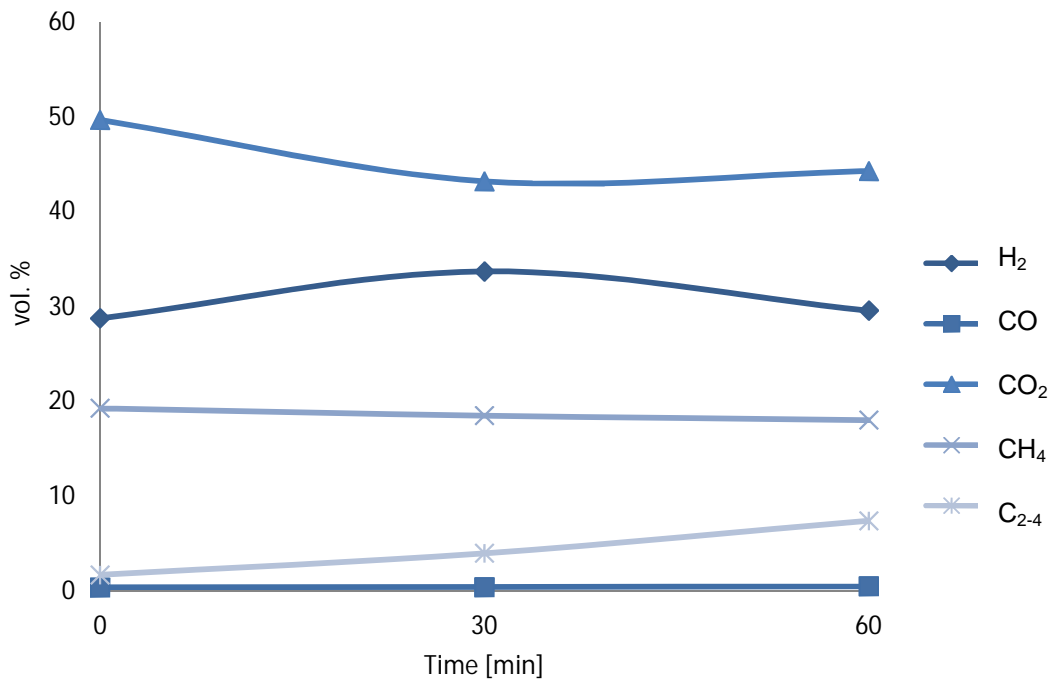


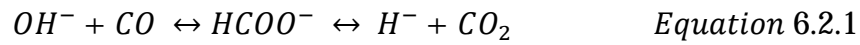
Figure 6.2.8 Gas compositions in vol. % after hydrothermal treatment of RDF at 500°C with 20 wt% RuO<sub>2</sub>/γ-Al<sub>2</sub>O<sub>3</sub>

The results clearly showed that the carbon dioxide was the major component in the gas phase, followed by hydrogen and methane. In the case of all the catalyst loadings, the composition of carbon dioxide decreased with the increasing reaction time, for example CO<sub>2</sub> was 56.2 vol% after zero min reaction time, and decreased to 39.7 vol% after 60 minutes reaction time, in the presence of the 5 wt% ruthenium catalyst. When no catalyst was present, around 22 vol% of hydrogen and 10 vol % of methane was produced, while with the addition of ruthenium catalyst, the hydrogen composition was in the range of 29 – 33 vol% in all experiments.

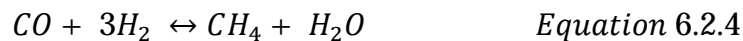
Methane yield was also increased in the presence of the ruthenium catalyst; however, the concentration was less than hydrogen in all experiments. In the studies with biomass model compounds, ruthenium catalyst was likely to suppress the reactions producing hydrogen, rather than methane. Byrd et. al., [6] detected higher yields of hydrogen in their research with gasification of glucose in supercritical water. They conducted the experiments at a temperature range of 700 – 800°C and a pressure of 25 MPa. When Ru/Al<sub>2</sub>O<sub>3</sub> was used as catalyst, almost 12 mol of hydrogen was produced from 1 mol glucose, which is the maximum theoretical amount that can be produced. They suggested that the glucose underwent dehydrogenation on the catalyst surface to give intermediates, before the cleavage of C-C bonds and/or C-O bonds. The breakage of C-C bonds yielded CO and H<sub>2</sub>, and with the help of water-gas shift reaction, formation of CO<sub>2</sub> and H<sub>2</sub> was observed. In this study, carbon monoxide composition was in the range of 0.4 – 2 vol.%, which agreed with the work of Byrd, suggesting that the water-gas shift reaction occurred during the hydrothermal gasification of RDF resulting in higher yields of hydrogen [6, 7].

At supercritical conditions, water dissociates into its ions and this self-dissociation is increased with the presence of metals [8]. The high hydrogen yields obtained suggested that the water gas shift reaction could be initiated with the interaction of CO with OH<sup>-</sup>, which was formed from water as described in the work of Byrd et. al. [6]. According to their report, with the self-dissociation of water on the metal surface, OH<sup>-</sup> ions were formed and reacted with CO, producing formate ion. Then the formate ion decomposed

into hydride anion and CO<sub>2</sub>. And by electron transfer, hydride anion reacted with water to form H<sub>2</sub> and OH<sup>-</sup>. They suggested the following reactions;



However, the high yield of hydrogen and domination of the water-gas shift reaction might be due to high temperature in which typical experiments are carried out (700 - 800°C). In this work, hydrothermal gasification of RDF was carried out at 500°C. Also in the literature data, there are reports indicating that methanation reactions become dominant in the presence of ruthenium catalyst. The mechanisms have been reported to involve the following; first hydrogenation of carbon dioxide occurs, then to carbon monoxide and finally to methane as in Equations 6.2.3 and 6.2.4 [9, 10].



According to the reactions shown in Equations 6.2.3 and 6.2.4, the concentrations of hydrogen and carbon dioxide are very important for the selectivity of methane. At the supercritical point, water becomes a reactant, as well as a solvent and a catalyst. . In this work, it was likely that water became a reactant and due to the presence of a large amount of water, the selectivity of the reactions was determined by the partial pressure of water, producing mainly carbon dioxide and hydrogen via water-gas shift reaction pathway.

To sum up, while hydrothermal gasification of RDF in the absence of any catalyst at 500°C produced a carbon gasification efficiency of 40.7%, and with a gas composition of 22 vol.% hydrogen, 3.4 vol.% carbon monoxide, 53.1 vol.% carbon dioxide, 9.9 vol.% methane and 11.7 vol.% hydrocarbon gases (C<sub>2-4</sub>). The presence of RuO<sub>2</sub>/γ-Al<sub>2</sub>O<sub>3</sub> increased the gasification efficiency and the gas yields. The highest carbon gasification efficiency was observed as 92.8% when 20 wt% RuO<sub>2</sub>/γ-Al<sub>2</sub>O<sub>3</sub> catalyst was used at 500°C after 60 minutes reaction time. Carbon dioxide, hydrogen and

methane were the main components in the gas phase. There was evidence that water-gas shift reaction and methanation reactions occurred during the gasification. However, the former appeared to more favoured, with selectivity to carbon dioxide and hydrogen, resulting in high yields of these two gases.

Apart from  $\text{RuO}_2/\gamma\text{-Al}_2\text{O}_3$  catalyst, sodium hydroxide was also investigated as a catalyst at different reaction times. The carbon gas efficiency and the gas composition after hydrothermal gasification of RDF in the presence of NaOH are shown in Figure 6.2.9.

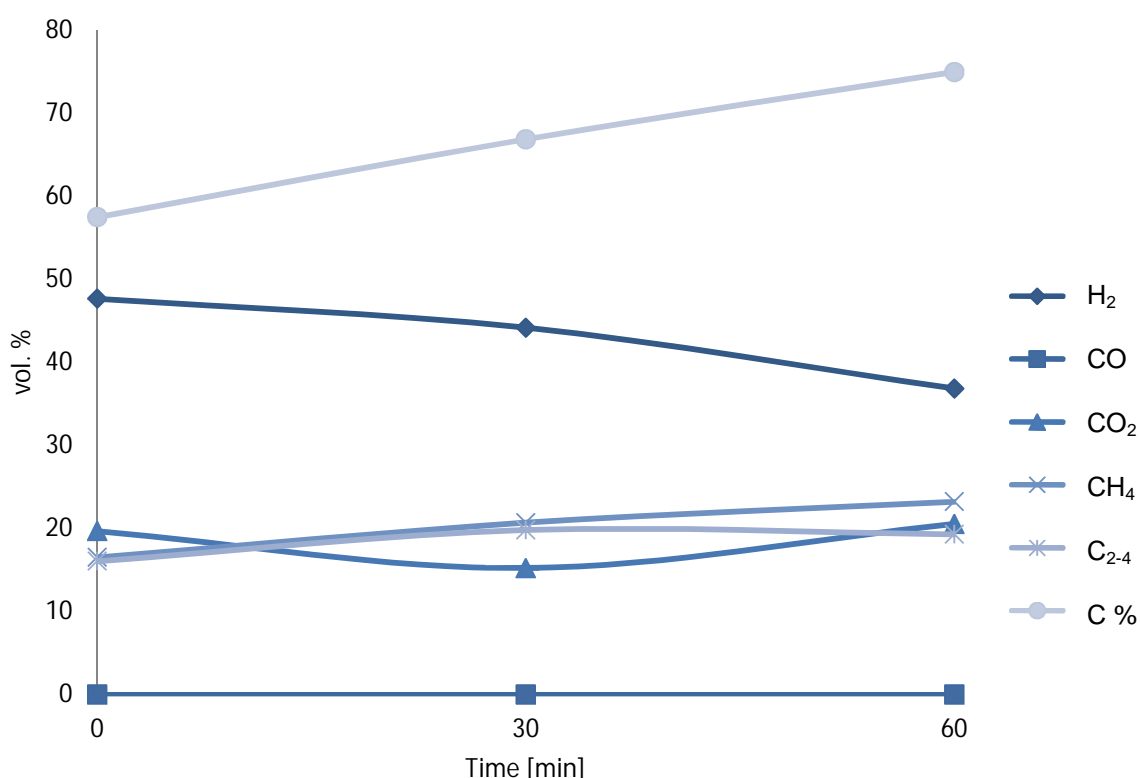


Figure 6.2.9 Gas compositions and carbon gasification efficiency after hydrothermal gasification of RDF with NaOH at 500°C at different time variations

When the gas compositions compared in the presence and absence of sodium hydroxide, it can be said that the presence of sodium hydroxide increased the carbon gasification efficiency, as it was 40.7% in the absence of any catalyst, and increased to 57.5% with NaOH. With the increasing reaction time, it reached to 75 % at 60 minutes reaction time. The gas compositions were highly influenced by the addition of NaOH. When no

sodium hydroxide was present, carbon dioxide was the main gas component at 53.1 vol.%, and decreased to a range of 16 – 23 vol.% with the addition of NaOH. This was due to the effect of sodium hydroxide which is the ability to promote the capture of carbon dioxide and consumption of carbon monoxide [11]. For all reaction times, the composition of carbon monoxide was zero, which supports the idea of promoting carbon monoxide consumption by sodium hydroxide.

Hydrogen concentration in the product gases was the highest amongst the other gas components, followed by carbon dioxide and methane. Interestingly, hydrocarbon gases ( $C_{2-4}$ ) composition increased from 11 vol.% to a range of 16 – 20 vol.% in the presence of NaOH, resulting in an increase in the heating value of the product gas. The increase in the time decreased the hydrogen composition while methane and hydrocarbon gases composition increased. At 500°C, after 60 minutes of reaction time, hydrothermal gasification of RDF yielded 36.9 vol.% hydrogen, 23.2 vol.% methane, 20.6 vol.% carbon dioxide and 19.3 vol.% hydrocarbon gases ( $C_{2-4}$ ).

The effect of sodium hydroxide might be through stabilization of the organic material in the RDF and sodium in the aqueous medium, which then resulted in the formation of intermediates with multiple functional groups such as hydroxylated ketones, aldehydes and acids that can gasify easily [11]. It has been reported [11] that with the presence of sodium hydroxide, these compounds would exist as their sodium carboxylate salts and decarbonylation reactions would occur. They reported that with the decarbonylation of the hydroxylated compounds that would produce carboxylic acids such as formic acid and acetic acid in the form of sodium salts due to the presence of sodium hydroxide. The increase in the amount of the inorganic carbon in the liquid effluent might be due to this salt formation, as after the hydrothermal gasification, they were dissolved in the aqueous phase. The results of the TOC analyses and the distribution of carbon are shown in Table 6.2.1. For example, sodium formates could react with water to yield sodium bicarbonate and hydrogen as shown in Equation 6.2.5 [12, 13].





From the decarbonylation reactions, carbon monoxide formation occurs and due to promotion of the water-gas shift reaction by the presence of sodium hydroxide, carbon dioxide and hydrogen yields increase [11, 14].

Table 6.2.1 Distribution of RDF-carbon after catalytic hydrothermal gasification

<i>Catalyst</i>	<i>Time [min]</i>	<i>TOC [g C/g C in RDF]</i>	<i>IC [g C/g C in RDF]</i>	<i>Gas [C wt%]</i>	<i>Liquid [C wt%]</i>	<i>Solid [C wt%]*</i>
Ru 5 wt%	0	0.10	0	52.1	21.3	26.6
Ru 10 wt%		0.08	0	57.1	17.0	25.9
Ru 20 wt%		0.05	0	64.3	12.0	23.7
NaOH		0.08	0.08	57.5	18.4	24.0
Ru 5 wt%	30	0.04	0	71.5	8.1	20.4
Ru 10 wt%		0.03	0	74.4	7.7	17.9
Ru 20 wt%		0.03	0	75.5	5.6	18.9
NaOH		0.07	0.11	66.9	15.7	17.4
Ru 5 wt%	60	0.04	0	88.2	9.2	2.7
Ru 10 wt%		0.04	0	89.3	8.0	2.7
Ru 20 wt%		0.02	0	92.8	5.1	2.1
NaOH		0.07	0.09	75.0	15.1	9.9

\* Calculated by difference

The comparison of the different types of catalysts with different ruthenium loadings was also investigated in relation to the hydrothermal gasification of RDF and the results are shown in Figure 6.2.10. The highest

carbon gasification efficiency was observed in the presence of 20 wt% RuO<sub>2</sub>/γ-Al<sub>2</sub>O<sub>3</sub> catalyst, which was 92.8 %.

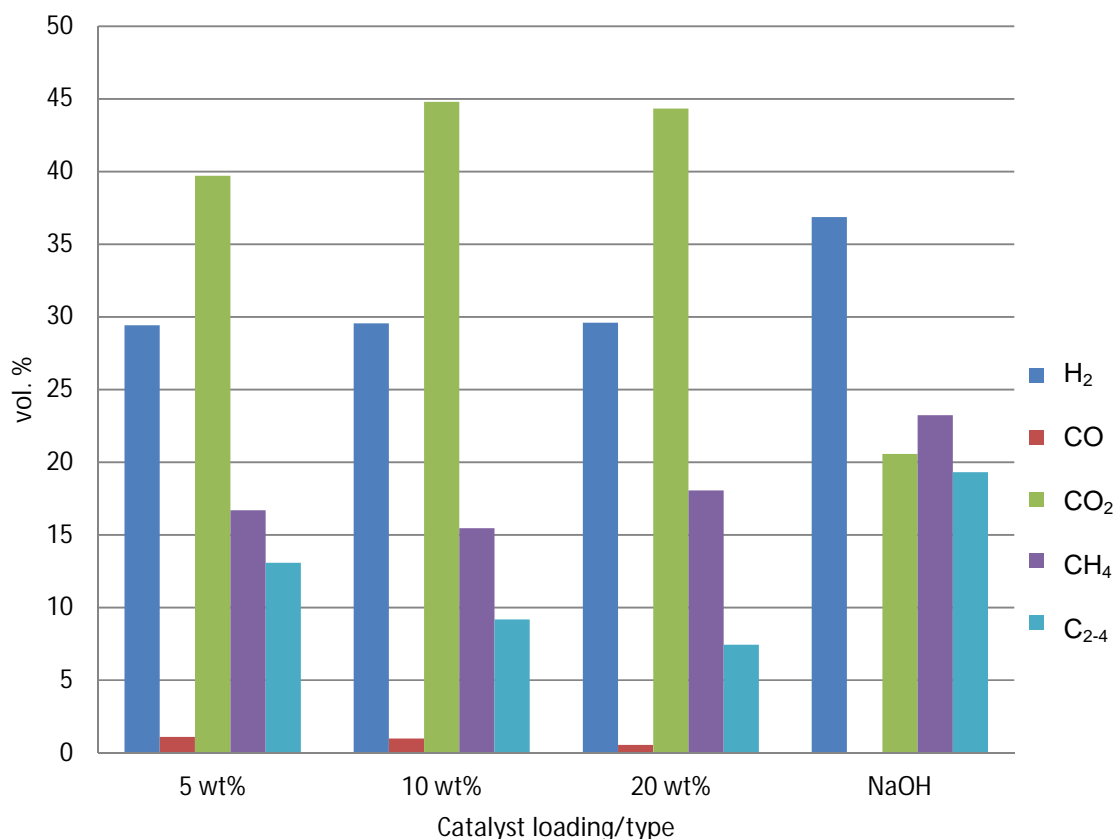


Figure 6.2.10 Gas composition (vol%) after hydrothermal gasification of RDF with different catalysts and catalyst loadings at 500°C and 60 minutes reaction time

Carbon gasification efficiency was the lowest in the presence of sodium hydroxide, as it decreased to 75%. The composition of gases also changed dramatically with the change of the catalyst type. While hydrogen and methane were the main gas components after hydrothermal gasification of RDF; carbon dioxide and hydrogen were the main gases in the presence of ruthenium catalysts. Also, addition of sodium hydroxide increased the hydrocarbon gases (C<sub>2-4</sub>) concentration, as it was 19.3 vol.% with NaOH, but was only 7.5 vol.% in the presence of 20 wt% RuO<sub>2</sub>/γ-Al<sub>2</sub>O<sub>3</sub> catalyst. The high yield of hydrocarbon gases (C<sub>2-4</sub>) resulted in higher heating values for the product gas, as shown in Figure 6.2.11. In a report in the literature, a mixture of sodium hydroxide and ruthenium oxide catalysts were used for

hydrothermal gasification of glucose and the results showed that selectivity of methane and hydrogen increased while that of carbon dioxide decreased. At high sodium hydroxide concentrations (1.5 M NaOH), carbon dioxide and carbon monoxide were not detected in the product gas, while hydrogen and methane yields were 71.2 and 28.0 mol%, respectively. With the decreasing sodium hydroxide concentration (0.5 M NaOH), while the compositions of carbon dioxide and methane increased to 34.3 and 31.0 mol%, hydrogen yield decreased dramatically to 32.8 mol% [15]. These results suggests that combination of sodium hydroxide and ruthenium oxide as catalyst could increase the hydrogen and methane yields, however that also increases the cost as high concentration of sodium hydroxide is needed.

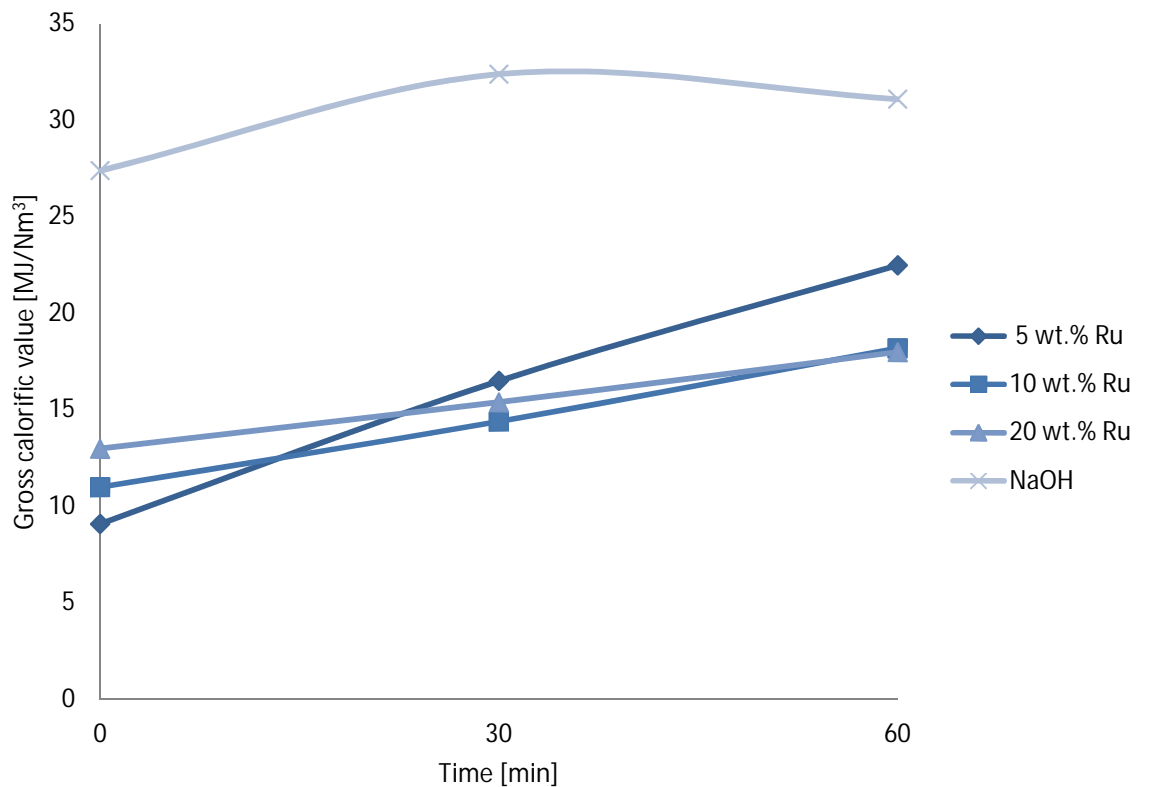


Figure 6.2.11 Gross calorific values of gas products in relation with temperature and catalyst loading/type

The gross calorific values were calculated based on equation 6.2.6

$$HHV = \sum_{i=1}^n X_i \cdot HHV_i \quad \text{Equation 6.2.6}$$

Where  $i \dots n$  = each combustible gas in the product mixture

$X_i$  = Volume fraction of each gas in the product mixture [vol/vol%]

$HHV_i$  = Calorific value of each gas in the product mixture [MJ/Nm<sup>3</sup>] (values were taken from ref [16])

In the presence of sodium hydroxide, a gas mixture with a higher calorific value was obtained which were in a range of 27.5 – 32.5 MJ/Nm<sup>3</sup>. The average gross calorific value of natural gas is around 38 MJ/Nm<sup>3</sup>, compared to this value; the gas produced with the addition of sodium hydroxide was very high. This was because the gas contained less carbon dioxide and much higher hydrocarbon gases (C<sub>2-4</sub>) in the product gas. However, the carbon gasification efficiencies were higher in the presence of the ruthenium catalysts. At 60 minutes reaction time, ruthenium catalysts produce gas mixtures having calorific value in a range of 18 – 22.5 MJ/Nm<sup>3</sup>.

To make a comparison of the calorific values of the gases produced and the raw RDF sample, the gross calorific values were calculated in the units of MJ/kg, based on the equation 6.2.7

$$HHV = \sum_{i=1}^n Y_i \cdot HHV_i \quad \text{Equation 6.2.7}$$

Where  $i \dots n$  = each combustible gas in the product mixture

$Y_i$  = Weight fraction of each gas in the product mixture [wt/wt%]

$HHV_i$  = Calorific value of each gas in the product mixture [MJ/kg] (values were taken from ref [16])

As mentioned in Chapter 3 (Section 3.1.3), the gross calorific value of RDF was 22 MJ/kg. In the presence of sodium hydroxide, a gas mixture with gross calorific value of 37.7 MJ/kg was produced, after hydrothermal gasification of RDF at 500°C and 30 minutes reaction time. In the presence of ruthenium catalyst, the maximum gross calorific value of the gas mixture was 18.9 MJ/kg, with 5 wt% RuO<sub>2</sub>/γ-Al<sub>2</sub>O<sub>3</sub> loading. Although carbon gasification efficiency was lower with the experiments in the presence of

sodium hydroxide, the product gas had a higher calorific value compared to reaction in the presence of the ruthenium catalysts. As a result, with ruthenium catalyst, a clean gas mixture with high calorific value was obtained, while with sodium hydroxide, higher calorific value gas was produced but at a lower amount, compared to reaction in the presence of the ruthenium catalysts.

## 6.4 Summary

As a representative complex mixture of wastes, RDF was processed using hydrothermal gasification with the aim to obtain valuable chemicals in the liquid phase and/or fuel gas. The low temperature hydrothermal processing of RDF yielded around 45 wt% liquid, however it was difficult to obtain a composition consisting of valuable chemicals.

Hydrothermal gasification of RDF gave promising results, as a clean fuel gas mixture was obtained in the presence of  $\text{RuO}_2/\gamma\text{-Al}_2\text{O}_3$  and sodium hydroxide as catalyst. Up to 93% carbon gasification efficiency was achieved in the presence of 5 wt% ruthenium catalyst, producing a fuel gas with a heating value of  $22.5 \text{ MJ/Nm}^3$ . The gross calorific value of the product gas increased to  $32.4 \text{ MJ/Nm}^3$  in the presence of sodium hydroxide, as a result of carbon dioxide fixation. Also, high yields of hydrogen were obtained in the presence of both the NaOH and ruthenium catalysts, as both promoted the water-gas shift reaction.

## References

1. Chang, Y.-H., W.C. Chen, and N.-B. Chang, *Comparative evaluation of RDF and MSW incineration*. Journal of Hazardous Materials, 1998. **58**(1–3): p. 33-45.
2. Yamamura, T., et al., *Ruthenium(IV) dioxide-catalyzed reductive gasification of intractable biomass including cellulose, heterocyclic compounds, and sludge in supercritical water*. The Journal of Supercritical Fluids, 2009. **51**(1): p. 43-49.
3. Matsumura, Y., et al., *Biomass gasification in near- and super-critical water: Status and prospects*. Biomass and Bioenergy, 2005. **29**(4): p. 269-292.
4. Onwudili, J.A. and P.T. Williams, *Catalytic conversion of bio-oil in supercritical water: Influence of RuO<sub>2</sub>/γ-Al<sub>2</sub>O<sub>3</sub> catalysts on gasification efficiencies and bio-methane production*. Applied Catalysis B: Environmental, 2016. **180**: p. 559-568.
5. Sato, T., et al., *Gasification of Alkylphenols with Supported Noble Metal Catalysts in Supercritical Water*. Industrial & Engineering Chemistry Research, 2003. **42**(19): p. 4277-4282.
6. Byrd, A.J., K.K. Pant, and R.B. Gupta, *Hydrogen Production from Glucose Using Ru/Al<sub>2</sub>O<sub>3</sub> Catalyst in Supercritical Water*. Industrial & Engineering Chemistry Research, 2007. **46**(11): p. 3574-3579.
7. Osada, M., et al., *Low-Temperature Catalytic Gasification of Lignin and Cellulose with a Ruthenium Catalyst in Supercritical Water*. Energy & Fuels, 2004. **18**(2): p. 327-333.
8. Kruse, A. and E. Dinjus, *Hot compressed water as reaction medium and reactant: Properties and synthesis reactions*. The Journal of Supercritical Fluids, 2007. **39**(3): p. 362-380.
9. Karn, F.S., J.F. Shultz, and R.B. Anderson, *Hydrogenation of Carbon Monoxide and Carbon Dioxide on Supported Ruthenium Catalysts at Moderate Pressures*. I&EC Product Research and Development, 1965. **4**(4): p. 265-269.
10. Lunde, P.J. and F.L. Kester, *Rates of methane formation from carbon dioxide and hydrogen over a ruthenium catalyst*. Journal of Catalysis, 1973. **30**(3): p. 423-429.
11. Onwudili, J.A. and P.T. Williams, *Role of sodium hydroxide in the production of hydrogen gas from the hydrothermal gasification of biomass*. International Journal of Hydrogen Energy, 2009. **34**(14): p. 5645-5656.
12. Sinač, A., A. Kruse, and J. Rathert, *Influence of the Heating Rate and the Type of Catalyst on the Formation of Key Intermediates and on*

*the Generation of Gases during Hydropyrolysis of Glucose in Supercritical Water in a Batch Reactor*. Industrial and Engineering Chemistry Research, 2004. **43**(2): p. 502-508.

13. Onsager, O.-T., M.S.A. Brownrigg, and R. Lødeng, *Hydrogen production from water and CO via alkali metal formate salts*. International Journal of Hydrogen Energy, 1996. **21**(10): p. 883-885.
14. Cortright, R.D., R.R. Davda, and J.A. Dumesic, *Hydrogen from catalytic reforming of biomass-derived hydrocarbons in liquid water*. Nature, 2002. **418**(6901): p. 964-967.
15. Onwudili, J.A. and P.T. Williams, *Hydrogen and methane selectivity during alkaline supercritical water gasification of biomass with ruthenium-alumina catalyst*. Applied Catalysis B: Environmental, 2013. **132–133**: p. 70-79.
16. Seader, J., J.J. Siirola, and S.D. Barnicki, *Perry's chemical engineer's handbook*. Perry's Chemical Engineers' Handbook, 1997.

## **Chapter 7**

### **Conclusions & Future Work**

The purpose of this study was to investigate the applicability of the hydrothermal processing for recycling of composite wastes. For this aim, waste carbon fibre reinforced plastic (CFRP) and printed circuit board (PCB) were selected as composite waste materials. The recovered carbon fibre was applied for the re-manufacture of new composite materials. In addition, refuse derived fuel (RDF) was chosen as a composite representative of municipal solid waste (MSW), to test the applicability of the hydrothermal process for the conversion of materials with different combustible fractions.

#### **7.1 Recycling of Carbon Fibre Reinforced Plastic Wastes via Hydrothermal Processing**

Waste carbon fibre reinforced plastic underwent hydrothermal processing for the recovery of the carbon fibre content of the material and recycling of the organic resin. Also the recovered carbon fibre was used in manufacturing of composite material, to determine the mechanical properties.

##### **7.1.1 Catalytic Hydrothermal Degradation of Carbon Fibre Reinforced Plastic Wastes**

Depolymerisation of carbon fibre reinforced plastic waste was carried out in sub and supercritical water. The sample used in this study was actual waste, consisting of ~60 wt% carbon fibre and ~40 wt% resin. Carbon fibre reinforced plastic waste was selected as one of the representative composite waste material in this research, as they have a strategic importance, and currently majority of carbon fibre reinforced plastic wastes are sent to landfill or incineration. The aim was to recycle the resin fraction by depolymerizing it into monomers or useful chemicals, and to recover the carbon fibres by preserving the mechanical properties. For this purpose, hydrothermal processing was applied, and the effects of temperature, additives (CaO, Na<sub>2</sub>CO<sub>3</sub>, NaOH, KOH, and H<sub>2</sub>O<sub>2</sub>) and reaction time on the



depolymerisation rate was investigated. The mechanical properties of the recovered carbon fibre were tested to compare with the properties of virgin carbon fibre.

Almost 93 % of the resin fraction of the carbon fibre reinforced plastic waste was successfully depolymerized in the presence of water at 420°C and 24 MPa as solvent with KOH and 10 wt% H<sub>2</sub>O<sub>2</sub> at zero residence time. The resin was converted into gas and liquid products; the main organic compounds detected in the liquid were phenol and aniline, and organic compounds containing an oxazolidine ring such as 5-Methyl-3-phenyl-1,3-oxazolidine and 1,3-Diphenyl-2-propyl imidazolidine, methyl phenols, methyl aniline and dimethyl benzenamine were other organic compounds contained in the liquid at lower concentrations. Clearly, these were the products from the degradation of polybenzoxazine resin used in the manufacture of the CFRP. The resin itself was found to be based on aniline and phenol skeletons.

The carbon fibre was recovered by preserving 78 % of its tensile strength due to the loss in the mechanical properties as a result of oxidation on the carbon fibre surface. Also this can possibly be attributed to the increase in the elongation of individual fibres by about 36 % after the degradation process. As a summary, due to the increase in the demand for carbon fibres in the global market and the increasing amount of carbon fibre composite wastes, it is essential to utilize a process for recycling. This study showed that water with the addition of alkalis was able to degrade the resin fraction from the CFRP waste, and recover the carbon fibres. Although the addition of hydrogen peroxide increased the resin removal, it caused a reduction in the mechanical properties of the recovered carbon fibres. However, the recovered carbon fibres can be used in many applications, such as in constructions of road as filler or in manufacturing suitable composites.

### **7.1.2 Recovery of Carbon Fibres and Production of High Quality Fuel Gas from the Chemical Recycling of Carbon Fibre Reinforced Plastic Wastes**

Depolymerisation of waste carbon fibre reinforced plastics in ethylene glycol at subcritical conditions achieved 92.1% resin removal at 400°C and also recovered the carbon fibres with similar mechanical properties to virgin carbon fibre. The resin removal was increased up to 97.6 %, when water and ethylene glycol mixture was used as solvent at 400°C.

However, substantial amounts of the ethylene glycol degraded during the process and so could not be recovered. Therefore, the resulting liquid effluent (comprising water, ethylene glycol and degradation products from ethylene glycol and resin) from the degradation of the organic resin in ethylene glycol water mixture was then subjected to hydrothermal gasification process, to produce fuel gas with high heating value. In the presence of ruthenium oxide catalyst, a gas mixture consisting of mostly hydrogen, methane and carbon dioxide was produced.

At 400°C, the corresponding pressure was around 8 MPa when water and ethylene glycol mixture was used as the solvent. At the same temperature, the corresponding pressure was around 20 MPa when water alone was used as the solvent. Without operating at higher pressures, ethylene glycol performed very efficiently and the two-stage process (depolymerisation with water and ethylene glycol mixture, and catalytic gasification of the liquid effluent from depolymerisation) offers great promise, as the carbon fibre was recovered with good mechanical properties, and the resin was converted into a fuel gas.

Compared to hydrothermal depolymerisation with water in the presence of alkali and hydrogen peroxide, depolymerisation with water and ethylene glycol mixture was proven to be better in terms of the mechanical properties of the recovered carbon fibre. While there was a reduction in the mechanical properties when hydrogen peroxide was used together with water and KOH, the mechanical properties of recovered carbon fibres were preserved after the hydrothermal depolymerisation with water and ethylene glycol. Also the

fuel gas with a heating value of 22 MJ/Nm<sup>3</sup> that was produced in the second stage of the process, can be utilized to supply energy for the whole process.

To sum up, hydrothermal depolymerisation of waste carbon fibre reinforced plastic via water and ethylene glycol mixture was successfully achieved. Operating at moderate pressures (~8 MPa) the resin fraction was converted into liquid mostly, and then with a separate gasification process, this liquid was converted into fuel gas to be used to supply energy for the process. The carbon fibres recovered by preserving the mechanical properties, so that they can be used for re-manufacturing new composite materials.

### **7.1.3 Evaluating the Mechanical Properties of Reinforced LDPE Composites Made With Carbon Fibres Recovered via Hydrothermal Processing**

The carbon fibres recovered via hydrothermal depolymerisation in ethylene glycol/water mixture was used to produce new composite materials with LDPE as matrix. A portion of the recovered fibre was used directly (non-oxidized) for the composite manufacture process, while a second portion was mildly oxidized at 250 °C for 1.5 h prior to composite manufacture. It was found that the oxidized carbon fibres showed better interfacial properties than the non-oxidized sample. Since the oxidation of carbon fibres was performed at low temperature, no reduction was observed in the mechanical properties of the recovered carbon fibre and also the chemical activity of the surface improved. The surfaces of the recovered carbon fibre were modified by different chemicals, and the most advanced properties were found when commercial silane-based and CFA-2 experimental additives were used.

Mechanical tests of the LDPE-based new composites showed that the resulting new material had enhanced mechanical properties. In the absence of any surface modifiers (additives), the tensile and flexural strengths of both oxidized and non-oxidized recovered carbon fibres were higher than the virgin carbon fibre composite's properties. However, when additives were used to increase the interaction between the matrix and the fibres, oxidized

recovered carbon fibre had higher tensile and flexural strengths than non-oxidized recovered carbon fibre. The better performance of the oxidized recovered carbon fibre reinforced LDPE than non-oxidized one was due to the less chemical activity of the non-oxidized recovered carbon fibres due to char particles on the surface, which prevented the chemical interaction between the carbon fibres and the coupling agents.

As a result, this study showed that the waste carbon fibre reinforced plastics can be recycled via hydrothermal processing by using water and ethylene glycol mixture or water with alkalis. The depolymerised resin fraction can be used as a chemical feedstock mostly consisting of phenol and aniline, or can be gasified to produce fuel gas to supply energy to the process. The recovered carbon fibres could be used for the manufacture of new composite materials, and the mechanical tests showed that the new composites with recovered carbon fibres had enhanced mechanical properties.

#### **7.1.4 Chemical Recycling of Printed Circuit Board Waste via Depolymerisation in Sub- and Supercritical Solvents**

The hydrothermal depolymerisation of printed circuit board waste was investigated, to remove the resin fraction from the waste in order to recover metals, and also to recycle the resin as a chemical feedstock. For this purpose, printed circuit board of a desktop computer liquid crystal display (LCD) monitor was recovered from an LG computer. The waste PCB consisted of ~62 wt% resin and ~38 wt% metals and ash. During this work, 81 % of resin removal was achieved when water alone was used as the reaction medium, and this was further improved in the presence of NaOH and KOH, which led to 94 % resin removal at 400°C. The liquid produced during the hydrothermal depolymerisation of printed circuit board waste was mainly composed of phenol, and phenolic compounds, which are the precursors of the original thermosetting resin. Most of the bromine content was found in aqueous phase, resulting in the recovery of an oil product with near-zero bromine content. Addition of alkalis increased the phenol yield up to 62.5 wt%, and the residues were recovered in a clean state, ready for metal separation.

Around 0.30 g gas per gram waste PCB was produced at 400°C. The gas composition was highly affected by the alkali addition, as carbon dioxide and carbon monoxide was 92 vol.% when only water was used as the solvent. The addition of sodium hydroxide and potassium hydroxide increased the hydrogen a yield, as 35.2 vol.% and 28.3 vol.% hydrogen was detected in the gas, respectively.

This study showed that hydrothermal treatment of waste printed circuit boards could be a good route for recycling as the water was used as a solvent which is cheap, benign and easy to access. Therefore, instead of combustion or acid leaching of waste printed circuit boards which are hazardous techniques for the environment, hydrothermal depolymerisation with water and alkalis can be applied to produce bromine free oil and solid residue consisting of valuable metals.

As two composite waste materials containing a phenolic type resin, carbon fibre reinforced plastics and printed circuit boards were successfully recycled via hydrothermal processing. Since actual real world waste samples were used, the outcomes of this study will contribute a great deal of data to the literature.

### **7.1.5 Hydrothermal Processing of Refuse Derived Fuels**

As a representative complex mixture of combustible wastes, RDF was processed using hydrothermal gasification with the aim to obtain fuel gas with high calorific value. The Hydrothermal gasification of RDF gave promising results, as a clean fuel gas mixture was obtained in the presence of  $\text{RuO}_2/\gamma\text{-Al}_2\text{O}_3$  and sodium hydroxide as catalyst. While a fuel gas with a heating value of 22.5 MJ/Nm<sup>3</sup> in the presence of 5 wt% ruthenium catalyst was produced, fuel gas with a heating value of 32.4 MJ/Nm<sup>3</sup> was produced in the presence of sodium hydroxide at 500°C and 60 minutes reaction time. High yields of hydrogen were obtained in the presence of both the NaOH and ruthenium catalysts, as both promoted the water-gas shift reaction. Also due to carbon dioxide fixation ability of sodium hydroxide and higher yields of hydrogen, affected the heating value of the product gas, as a result the

gas had much higher heating value compared to the gas produced in the presence of ruthenium oxide catalyst.

Almost 93 % of the carbon in the RDF was converted to gaseous products after hydrothermal treatment, in the presence of ruthenium oxide catalyst. This result indicates that RDF was upgraded to a clean mixture of fuel gases, as there were many impurities and contaminants in the raw RDF which limits its usage for energy production. Only drawback was the high carbon dioxide concentration in the gas, which decreases the heating value of the gas mixture. However, carbon dioxide can be removed from the gas mixture via known technologies such as pressure-swing absorption (PSA), leaving a fuel gas consisting of mostly hydrogen and methane. Also the high pressure of the product gas could be utilized so that the compression and pumping cost could be reduced, and the product gas could be used directly.

In the presence of NaOH, the product gas had much higher heating value (32.4 MJ/Nm<sup>3</sup>), however the carbon gasification efficiency was lower compared to the gas produced in the presence of ruthenium oxide. 75 % of the carbon in the RDF was detected in the gas phase after hydrothermal gasification in the presence of NaOH. The higher heating value of the gas was due to the ability of sodium hydroxide to fix carbon as carbonate salts. The gasification efficiencies were increased in the presence of ruthenium oxide catalysts, and almost 93 % of the carbon in the RDF was converted into gas phase. As a result, this study shows that the hydrothermal gasification of RDF produces a clean fuel gas mixture, mostly consisting of methane and hydrogen.

### **7.1.6 General Summary**

Hydrothermal processing of waste carbon fibre reinforced plastics and printed circuit boards to depolymerise their polymer (resin) fraction into valuable chemicals and fuel gas for recycling, and recovery of carbon fibres in CFRP waste and valuable metals in PCB waste were investigated. As a final step, the applicability of the hydrothermal process was tested on refuse derived fuel, as it is a good representative of municipal solid waste which is

a complex waste mixture consisting of plastics, other biodegradable materials and inorganic materials. Hydrothermal processing was proven to be an efficient process, since it was applied to real-world wastes. The unique properties of water at critical conditions make it a favourable solvent as it is the most abundant, non-hazardous and non-toxic substance in the world. The water becomes a solvent, reactant, catalyst and a product at the same time, during the hydrothermal processing of plastic wastes. For the wastes with high moisture content, complex structured and contaminated with hazardous or toxic materials, hydrothermal processing has a high tolerance, so that no pre-treatment or any separation processes are needed.

## **7.2 Future Work**

The outcomes of this research showed that the applicability of the hydrothermal process to the real-world wastes. The faster reaction times and high conversion yields in the studies with waste carbon fibre reinforced plastic and printed circuit board are useful to construct an industrial scheme semi-batch process. Especially in the case where ethylene glycol was used as solvent, due to the lower operating pressures, a two staged process can be envisioned; depolymerisation at moderate temperatures followed by a gasification process. Although the usage of ethylene glycol can be a drawback since it is a fossil fuel based solvent, this can be converted to an advantage. There are reports in the literature stating that PET can be decomposed into terephthalic acid and ethylene glycol in subcritical water as mentioned in Chapter 2. Therefore a complex mixture of plastics containing PET can undergo a hydrothermal process in the presence of water as solvent. This can be performed at moderate temperatures, and the production of ethylene glycol during the process can influence the depolymerisation rates of other composite materials.

In this study, the recovered carbon fibres were used for re-manufacturing of new composite materials and different coupling agents were tested to determine their effects on the mechanical properties of the new composite. For a better view, manufacturing of composites with recovered carbon fibres can be performed with different kind of matrices, so

that the interactions of the matrix and recovered carbon fibres can be researched in a wider extent.

RDF, as a more complex waste material sample, can be studied in more details to construct a process at lower temperatures with different catalysts. Hydrothermal gasification process was proven to be a good solution to produce fuel gas from RDF. Although the high gasification yields, due to high composition of carbon dioxide in the gas, the calorific value of gas decreased. The reduction of carbon dioxide composition can be investigated in the presence of different catalysts. Also lifecycle analyses of the catalysts should be investigated.

Catalysts in general are very important during the chemical reactions, as they affect the yields and selectivity. This work covers some catalysts and their effects on the hydrothermal process; however, different kinds of catalysts can be researched especially for the hydrothermal gasification process, to determine the best conditions for the desired products. The stability of catalysts is a major issue in hydrothermal catalysis due to the highly aggressive nature of water at elevated temperatures and pressures. This work has not involved detailed characterization of the used catalysts and their re-use. This will be of utmost importance for the commercialization of hydrothermal processing of complex waste materials. For instance, there could be inhibitive or synergistic effects between catalysts, catalyst supports and inorganic (ash) contents of the real-world wastes. This needs further investigation.

In general, there has been a rush towards adapting proven commercial reaction systems for hydrothermal processing, especially in the use of continuous systems. There have been numerous difficult problems encountered with continuous systems including reactor plugging, the need to use low concentration of feedstock, ash deposition etc. These problems are hardly encountered in batch systems. In fact, batch operations are simple and do not require the complexities involved in the use of external pressure sources since water can generate its own auto-genic pressure during batch processing. Although, batch systems are often less efficient than continuous systems in terms of cost and operation, but they appear to be suitable for



hydrothermal processing due to, especially when combined with energy recovery. Therefore, the nature of hydrothermal media could require a rethinking of the design of hydrothermal reaction systems. Future work could involve an investigation into developing hybrid reaction systems for hydrothermal processing, which combine the efficiency of continuous systems with the ease of operation of batch systems.

Currently application of supercritical water into continuous systems is possible, however there are still challenges to overcome. Especially to process the solids, the feeding systems are needed to be improved. Carbon fibre reinforced plastics and printed circuit board wastes can be pre-treated for size reduction, but feeding them into a high pressure reactor with the help of a conveyor is challenging. Scaling up to a batch process could prevent the feeding problem, however as mentioned earlier, for the ease of operation, continuous processes are more preferable.

Scaling up the process for an industrial application is crucial; however, more detailed research is needed to be conducted, such as energy and economics analyses. As a future work, an energy analyses can be performed, and also cost estimation should be carried out to check feasibility of the process. Utilization of energy is also another importing topic, as during depolymerisation in sub and supercritical water, high pressures and temperatures are achieved. The cost of the process can be reduced by utilizing this excess pressure and temperature, to supply energy to the process. Utilizing the excess pressure to produce energy has also challenges, as if the gasses at high pressure and temperature are to be passed through a turbine, coke formation could occur with the decreasing pressure and temperature. Therefore, the condensable organics from the gas stream should be separated by decreasing the temperature which will also decrease the pressure. Also the high pressure of the product gases can reduce the cost in transportation.

Apart from the energy analyses, further work is necessary to determine the kinetics of the reactions involved during the depolymerisation and gasification reactions. Rate constants, activation energies are to be calculated as well, in order to construct a commercial process. Also in this

research work, excess amount of water (or solvent) was used, for a more efficient and low cost process, material/solvent loading ratio should be optimized.

Another important parameter for scaling up for a commercial plant is the plant location, as in the case of MSW processing plant, the transportation of the feed would be a problem in terms of cost. The high moisture content (up to 50 wt%) increases the transportation costs. To prevent this cost, instead of building a high capacity plant, small scaled plants can be installed to the nearest locations where MSW is collected. In order to decide the modifications to the process, a pilot plant could be constructed at first, and with the further investigations, a scale-up process could be proposed.